CONCRETING AND HIGH PERFORMANCE CONCRETE IN HOT WEATHER

Proceedings of the

American Concrete Institute - Kuwait Chapter

First International Conference & Fourth Exhibition

September 29 - October 1, 2003

State of Kuwait

Edited by:

Naji M. Al-Mutairi
Moetaz M. El-Hawary
Khaldoun N. Rahal

aci
Kuwait Chapter

Proceeding of the ACI-KC First International Conference and Fourth Exhibition, September 29 – October 1, 2003, Kuwait.

CONCRETING AND HIGH PERFORMANCE CONCRETE IN HOT WEATHER

Edited by:

Naji M. Al-Mutairi
Moetaz M. El-Hawary
Khaldoun N. Rahal

Organized by:
American Concrete Institute – Kuwait Chapter (ACI-KC)

Sponsored by:
Kuwait Society of Engineers (KSE)
Kuwait Foundation for the Advancement of Sciences (KFAS)
American Concrete Institute – International

Co-sponsored by:
Gulf Consult, Kuwait
Kuwait Portland Cement Company

aci
Kuwait Chapter

Organizing Committee

Dr. Naji M. Al-Mutairi (Chairperson)
Dr. Moetaz El-Hawary
Dr. Khaldoun Rahal
Mr. Abdul Wahab Rumani
Eng. Amjad Saad

Scientific Committee

Dr. Moetaz El-Hawary
Dr. Khaldoun Rahal
Dr. Naji M. Al-Mutairi

ACI Kuwait Chapter

PO Box 12608, Shamiah 71657, Kuwait
Tel: 2448975 Ext. 312
Fax: 2428148 (Attn: ACI)

info@acikuwait.com
www.acikuwait.com

TABLE OF CONTENTS

Session 3

Session 4

Session 5

Session 6

Preface

Since its establishment in 1997, American Concrete Institute – Kuwait Chapter (ACI-KC) took on the responsibility to improve local concrete practices and spread awareness of the best techniques suitable to the local environment and quality of workforce. It promoted and encouraged technical forums that serve as a platform to exchange experiences and find sound engineering solutions to specific regional problems. ACI-KC maintained its duty to spread knowledge to improve concrete practice and serve the community.

During the past few years, ACI-KC conducted many technical activities. It organized three major exhibitions accompanied by a series of technical seminars, conducted many technical training courses, organized technical seminars, published technical documents, and participated in local and regional technical activities in addition to many other technical and social activities. The ACI Executive Vice President, Mr. James G. Toscus, stated that ACI-KC is the only international chapter that has published technical documents based on local experience (Guide to Damage Assessment and Repair of Concrete Structures, Guide to Proper Concreting Practices Part-I Mixing and Curing, Guide to Implementation of Concrete Repair, Guide to Proper Concreting Practices Part II Placement, Compaction and Finishing). Mr. William R. Folley, Senior Managing Director of ACI International has noted that ACI-KC is one of the most active and well-organized international chapters.

To continue this track record, the ACI-KC Board of Directors decided to organize its first international conference from September 29 to October 1, 2003. The theme of the conference was selected based on the most relevant topic to this region, *Concreting and High Performance Concrete in Hot Weather*. The topics covered by the conference include: new trends in construction materials, durability and deterioration, specifications and codes, repairs and retrofitting, quality assurance and control, and advanced construction technology. A total of 38 abstracts were received from 10 countries and twenty-five technical papers were finally accepted for this conference and are included in the proceedings.

ACI-KC hopes that this document adds to the technical knowledge in the theme of this conference. We look forward to the readers' constructive comments and feedback to improve our future activities.

Dr. Naji M. Al-Mutairi, Chairperson

ACI-KC First International Conference and Fourth Exhibition

Acknowledgement

The success of this conference is attributable to the organizing and scientific committees and the support of ACI-KC Board of Direction. To insure a successful event, members of the committees contributed enthusiastically to the various aspects of the organization of the conference activities for over fourteen months. Without their active participation, determination and dedication, it would not be possible to organize the conference.

ACI-KC highly appreciates the encouragement and help of the Kuwait Society of Engineers president Eng. Adel Al-Kharafee, past president Dr. Hasan Al-Sanad, General Manager Eng. Talal Al-Kahtanee, Eng. Tareq Al-Saqabee, Eng. Abdullah Al-Daajanee, and many more colleagues at the society.

The organizing committee expresses its deep appreciation to the keynote speakers, the chairpersons of the scientific sessions as well as the distinguished speakers and participants for the effort and contributions they made during the conference activities. Particular thanks are extended to Tin Cho Mohammed for his devotion to the conference administrative activities and for Tareq Abduljaleel, Melita Alvares, and Sheba Mathew for their help.

Finally, the organizing committee wishes to extend special thanks to the sponsors of this conference, Kuwait Society of Engineers, Kuwait Foundation for the Advancement of Sciences, and ACI-International. The support of the co-sponsors, Gulf Consult and Kuwait Portland Cement Company is also gratefully acknowledged.

Proceedings of the ACI-KC First International Conference & Fourth Exhibition. September 29-October 1, 2003, Kuwait — ***Concreting and High Performance Concrete in Hot Weather.***

ELECTROCHEMICAL SOLUTIONS FOR DURABLE CONCRETE REPAIRS

Haboubi, L., Fosroc International Ltd, Dubai, UAE

Davison, N., Fosroc Group Development, Tamworth, UK

Nemeth, M., Al Gurg Fosroc LLC, Dubai, UAE

ABSTRACT:

The understanding of the electrochemical nature of corrosion has led to the realization that durable repair of reinforced concrete entails more than simply replacing defective concrete and corroded reinforcing steel. Concrete Repair technology has developed in recent years and now employs the use of shrinkage controlled mortars; high fluidity micro-concrete; as well as nondestructive methods such as Electrochemical Chloride Extraction, Realkalization and more recently, internal galvanic anode technology. The availability of impressed current as well as galvanic techniques provides a 'third generation' approach to arresting the widespread problem of concrete deterioration.

The paper will elaborate on the importance of addressing the electrochemical activity relating to rebar corrosion, as well as discussing the various techniques available to address the root causes rather than just the symptoms; and hence provide long-term, durable concrete repair solutions. The application of such techniques to a range of situations ranging from small patch repairs to major rehabilitation of marine structures is examined.

Keywords:
Reinforcement corrosion, incipient anode effect, electrochemical techniques, chloride extraction, realkalisation, cathodic prevention, galvanic protection

1. INTRODUCTION

The corrosion of reinforcing steel in concrete is a problem which has been highlighted since the 1960's. As the Gulf region has rapidly developed over the past decades, the use of reinforced concrete has emerged as the most widely used construction material due to its versatility. However, it is not uncommon to see extensive corrosion of reinforcing steel in diverse structures including industrial & residential structures; ports and power & desalination plants; and which is caused by factors such as inadequate specifications, poor workmanship and/or contamination by deleterious elements, chlorides being foremost amongst these in the Gulf region.

The highly alkaline nature of concrete leads to the formation of a passive oxide layer on the surface of the reinforcing steel that reduces corrosion to negligible levels. However, the permeability of concrete can allow the ingress of chemical agents which lead to a breakdown in the protective passive layer and subsequent corrosion of reinforcing steel [ref.1]. The two most commonly encountered processes leading to rebar corrosion are (a) carbonation in which a pH reduction in the concrete pore solution is induced by the action of carbon dioxide and (b) chloride attack [ref. 2]. These processes lead to breakdown of the passive oxide layer and subsequent formation of expansive corrosion products, which can lead to cracking and spalling of the concrete surface.

Chloride attack on reinforcing steel can be as a result of chloride salts which have diffused in from the external surface, for example, wind-blown sea salt, or from cast-in chloride salts. Above a certain chloride level threshold [ref.3], steel corrosion is initiated. According to Tutti [ref.4], initiation is followed by a propagation period, which eventually leads to a cracking/spalling stage.

Many methods of concrete repair have been developed over the past few decades, however, it is now understood that in order to overcome the highly damaging effects of corrosion, the only durable course of action is to address the electrochemical nature of the problem. A variety of solutions to the problem of reinforcement corrosion exist which can be used to treat structures in the initiation/propagation phases or following failure [ref. 5]. In recent years, improved understanding of the corrosion process has led to the development of electrochemical techniques, which attempt to address the actual cause of the problem rather than just the symptoms.

Cathodic protection, a technique developed in the 19th century [ref. 6], is used extensively for galvanically protecting ships hulls and more recently offshore structures. In the 1970's, impressed current cathodic protection (ICCP) was first applied to a reinforced concrete structure [ref.7] and has since been applied to a number of structures suffering from chloride induced corrosion problems. In the Middle East alone, it is now estimated that over 500,000m^2 of reinforced concrete has been cathodically protected.

Another option is to use galvanic anodes to supply the required protection current to the steel, a technique that has been used preferentially in applications where the absence of an external power source is deemed advantageous. This paper describes a number of electrochemical treatments for protecting reinforced concrete structures, with examples of actual installations and supporting data obtained.

1.1 Concrete Repair Options

Understanding the cause and extent of reinforcement corrosion is the key to selecting an appropriate repair solution. A number of corrosion control techniques are now available to the building owner or engineer to prolong the life of the structure and minimize future maintenance. The solutions have been developed to meet the wide range of cost/lifetime requirements of building owner, and include Realkalization, Chloride Extraction, Impressed Current Cathodic Protection (ICCP), and Galvanic Protection. Some of these techniques may be used proactively to prevent corrosion damage from occurring; whilst others may be used to complement traditional structural concrete repairs in order to ensure durability.

2. TRADITIONAL PATCH REPAIR

The most common method of addressing spalling concrete on structures is reinstatement with a formulated repair mortar. This involves removal of loose concrete and breakout to and beyond steel, removal of steel corrosion products through mechanical cleaning, priming, and application of the repair mortar. More recent technical advances have led to the development of mortars with low shrinkage characteristics to improve patch longevity.

Such an approach is effective in aesthetically upgrading the structure in the short term but does not address the problem of on going corrosion due to existing carbonation or chloride contamination. This is attributable to the fact that this repair technique does not guarantee removal of chloride bearing concrete, which may remain in areas adjacent to the repair. There is a possibility that the differential in chloride concentration between patch and parent concrete can lead to the formation of an electrochemical corrosion cell. This can ultimately lead to failure at the periphery of a patch repair – a phenomenon commonly referred to as the 'incipient anode effect' [ref. 8] or 'corrosion ring'.

A potential solution is to break out all contaminated concrete. This is effective but expensive, dusty, noisy and disruptive and may necessitate temporary propping of the structure due to mass concrete removal.

In order to overcome this problem, a zinc-based galvanic sacrificial anode was developed [ref. 9]. This development has been described in more detail elsewhere [ref. 10], but has proved to be a practical and cost effective method of alleviating the issue of 'incipient anode' formation by restoring an electrochemical balance.

3. GALVANIC PROTECTION TECHNIQUES (SELF POWERED)

Galvanic protection using sacrificial anodes has been known for more than 150 years, but it is only recently that sacrificial anodes have been used for protecting reinforced concrete. This operates on the principle of a more reactive metal than steel (usually zinc), corroding preferentially to the steel as a result of a difference in potential between the two metals; and the resultant electromotive potential gives rise to a corrosion preventive current.

3. 1 Internal Discrete Galvanic Anodes

As discussed earlier (Section 2), 'incipient anodes' caused as a result of such patch repairs, can be neutralized using embedded sacrificial anodes tied to the steel at the edge of the repair One system (Galvashield XP™), comprising a zinc/active mortar composite, is attached to the reinforcing steel at the edge of the required patch repair to prevent the setting up of 'incipient anodes'. No external rectifier is required as the galvanic anodes are effectively self powered. The zinc anodes slowly corrode sacrificially over their life time and display intelligent

behavior by adjusting current output to reflect environmental conditions. Optional monitoring can provide the building owner or specifier with current output and polarization data if required. Table 1 shows typical current density results obtained from such data.

Table 1.- Typical Current Density outputs from monitored internal discrete galvanic anodes (ref. 19)

reading no.	temp (deg C)	current output A1 (mA/m^2 steel)	current output A2 (mA/m^2 steel)	current output A3 (mA/m^2 steel)	Avg individual current output A3 (mA/m^2 steel)
1	17	4.3	4.3	11.8	1.3
2	17	4	4	6.6	0.73
3	10	5.6	5.3	7.2	0.8
4	23	8.6	8.3	15.5	1.72
5	11	7	6	10	1
6	24	6.3	6.6	8.2	0.9
7	23	11	8.3	13.1	1.45
8	24	9	9	10	1.11
9	26	5.3	5.6	8.3	0.92
10	22	6.3	6.3	6.2	0.68
11	14	3.3	3.3	4.2	0.46
12	22	5	4.6	8	0.9
13	27	6	5.3	8.5	0.95
14	26	7.33	7.66	6.99	0.78
15	27	9.66	10.66	6.66	0.74
16	30	9.99	10.99	16.66	1.85
17	27	6.33	8.66	10.33	1.15
18	44	14.33	14.99	15.66	1.74
19	37	10.66	7.99	15.33	1.7
20	37	12.33	8.66	15.83	1.76
21	38	13.33	13.99	15.49	1.72
22	39	13.99	14.99	13.99	1.55
23		no reading	Monitoring unit connection problem suspected – then rectified		
24		no reading			
25	38	13.66	4.33	8.63	0.96
26	38	11.66	4.1	10.8	1.2
27	36	10.66	3.66	16.8	1.86
28	37	12.01	5.1	19.25	2.14
29	32	11.33	4.33	18.6	2.06
30	32	8.33	3.33	17.93	1.99
31	33	6.33	3.33	17.93	1.99
32	32	6	1.66	16.93	1.88
33	33	10.33	3.33	13.78	1.53
34	40	11.33	2.99	11.95	1.33
35	32	5.66	1	5.15	0.57
36	35	6.99	1.66	6.97	0.77
37	32	4.33	0.66	3.82	0.42
38	30	4.99	0.66	3.15	0.35
39	28	3.99	0.66	11.78	1.3
40	29	3.66	0.66	9.79	1.09

The 24 hour depolarizations taken vary from 30 to 100mV. This is what can be expected to achieve the level of protection required based on the background potentials of the areas outside of the zone of influence of the anodes.

A logical step is to extend the galvanic corrosion prevention to areas outside these repair patches. To this end, an enhanced sacrificial anode has been designed in a form which facilitates discrete installation into pre-drilled holes in reinforced concrete. This comprises cylindrical, mortar encased zinc anodes wired together in sequence and inserted into the pre-drilled holes in a grid configuration. When connected to the steel reinforcement the grid impresses a galvanic current through the steel reinforcement, suppressing anodic reactions and controlling corrosion. Such a system (Galvashield CC™) has been installed on a number of structures, suffering from chloride contamination, and trial data from a typical example is discussed below.

A19 Seaton Bridge trial

The current output data shows that all the anodes are providing good current output and the estimates of current density on the steel surface indicate that, according to the values in BSEN12696, should be capable of preventing pitting corrosion initiation and thus countering corrosion activity.

The magnitude of polarisation is such that it represents a significant reduction of the corrosion current and therefore corrosion rate.The trial has shown that this protection can be achieved on structures that are contaminated with chloride and at risk of corrosion.

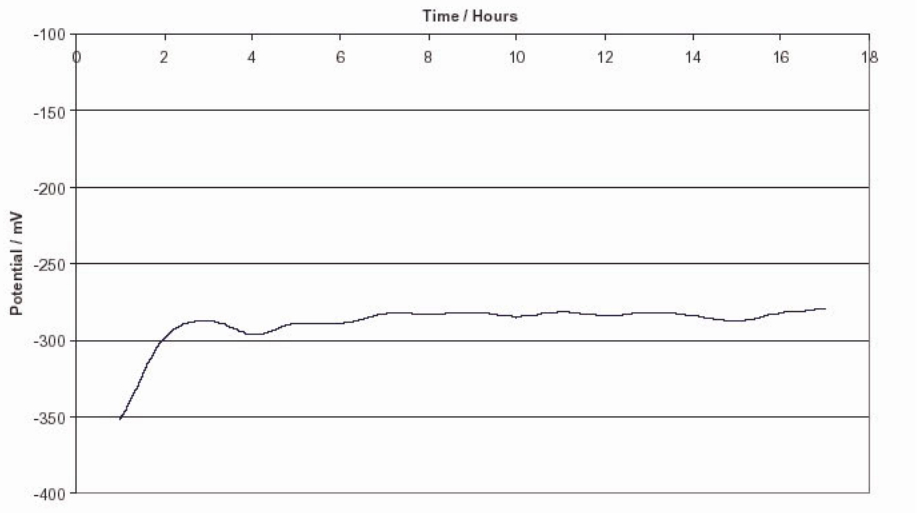

Figure 1 -Typical depolarization curve for reference electrode

The life of the anode system is directly related to the current output that is achieved and the results of the trial to date indicate that a typical anode life of 15 years can be achieved. [ref. 11]

This form of discrete galvanic protection system is a lower cost option than realkalization, desalination and ICCP. It can provide long-term, maintenance-free protection and is

particularly useful for those seeking an easy-to-install system with no ongoing monitoring costs. It is suitable for all types of structures including pre-stressed and post tensioned structures where ICCP, realkalization and desalination are often precluded due to potential hydrogen evolution and the associated risk of steel embrittlement.

3.2. Marine Galvanic Jacket Techniques

Studies conducted by the Florida Department of Transportation (FDOT) have shown that zinc anodes can provide long term cathodic protection in the tidal zone of steel reinforced concrete structures. Pile Jacket systems with an inbuilt zinc mesh anode can represent an attractive alternative to conventional impressed current CP based on their low installation and maintenance costs, simplicity and by their reliable, self-regulating performance [ref. 12].

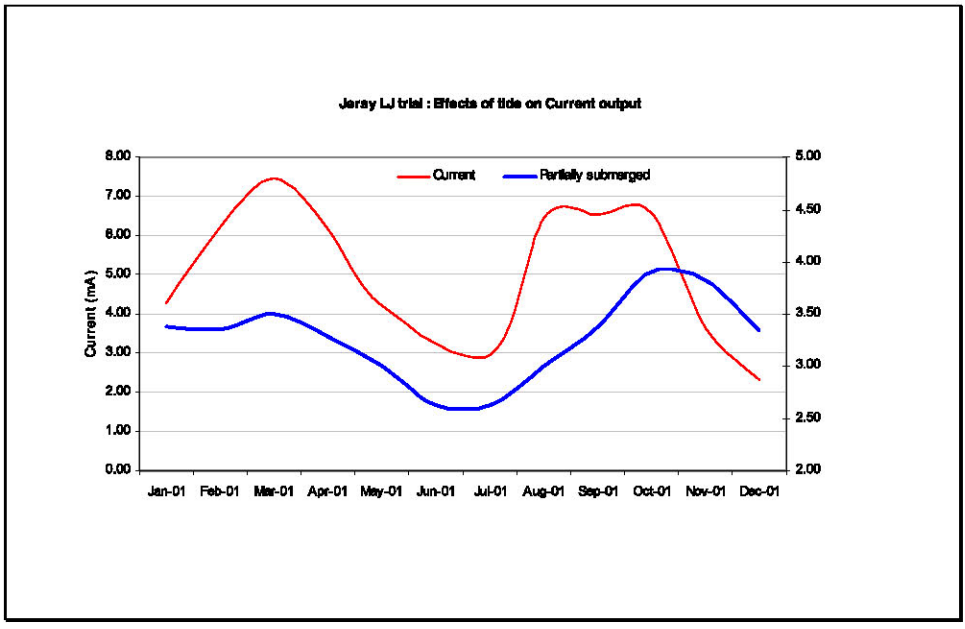

Figure 2 – Self – regulating current output vs. tide levels

The Zinc mesh pile jacket system amply satisfies the 100 mV polarization criterion, however due to the concrete remaining moist within the jacket cavity and the restriction of oxygen and chloride replenishment by the inert fiberglass form, the polarization decay criterion is not always satisfied at 4 hours, and the 24 hour value may be taken instead. The system would literally take months to fully depolarize if the wire connection became severed or disconnected (ref. 13).

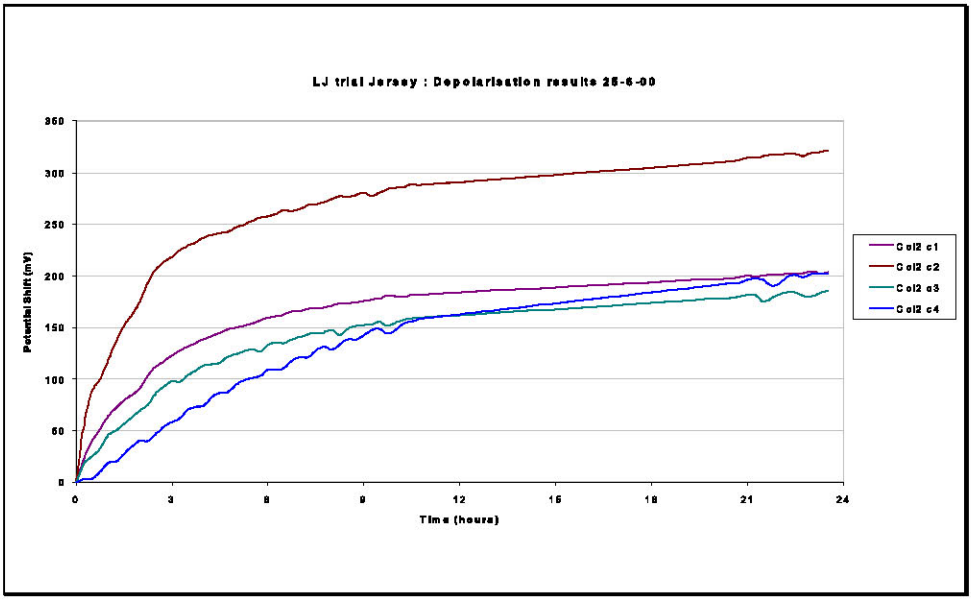

Figure 3 - Typical Depolarization vs. time curves for Galvanic Jackets

4. CHLORIDE EXTRACTION & REALKALISATION

In general, these nondestructive techniques are particularly appropriate in situations where condition surveys identify a significant risk of future corrosion; but in areas where the structure has not yet been affected by substantial delamination & spalling. Timely application of these techniques can thus avoid the need for costly & potentially disruptive patch repairs.

4.1 Electrochemical Chloride Extraction (ECE)

Sometimes also referred to as 'desalination', electrochemical chloride extraction [ref.14] is based on a process of reducing chloride ions from around the reinforcing steel in contaminated concrete down to a level below the corrosion threshold. This works on an induced current principle, whereby an externally mounted metallic anode (in this case a temporary one), is embedded into an electrolyte reservoir and a D.C current (typically in the range of 1 A/m^2 of concrete) is applied to the reinforcing steel which becomes a cathode. The (negatively) charged chloride ions are repelled away from the (negatively) charged reinforcing steel cathode and migrate towards the (positively) charged anodic mesh. Simultaneously, the electrolytic production of hydroxyl ions at the steel surface results also in the displacement of chloride ions and subsequent re-passivation of the steel with an effective buffer zone.

On delivery of the required no. of Amp/hours, the current is switched off, and the external anode, with its electrolyte reservoir is removed and discarded.

4.2. Electrochemical Realkalization (ERA)

Developed in the late 1980's to combat the growing carbonation problem in Scandanavia, ERA works on the basis of electro-osmosis and can be used to realkalize carbonated concrete by creating the existing reinforcement as the negative electrode, or cathode [ref.15]. As with ECE, a temporary external metallic anode mesh is installed and embedded in a disposable electrolytic mass containing an alkaline solution. Ionic migration occurs on applying a voltage between the two electrodes under the influence of current and electro-osmosis.

Over time (typically 4 to 8 days), the concrete is saturated to beyond the cover zone with the alkaline solution reinstating the pH level of the concrete to an initial level of 12, thereafter equalizing to around 10.8. When the entire cover concrete is impregnated, as evidenced by phenolpthalein indicator test, the current is switched off, and the external anode, with its electrolytic mass, is removed and discarded. A protective coating can then be applied to the surface of the structure to prevent further carbonation or chloride ingress.

5. IMPRESSED CURRENT CATHODIC PROTECTION (ICCP) (EXTERNALLY POWERED)

This is now the oldest of the electrochemical techniques and has been recommended for use on reinforced concrete structures since the 1970's. This technique involves the application of a low, direct current from a permanent anode to the reinforcing steel. Sufficient current is used (ranging from 0.25 to 25 mA/m^2 of steel) to prevent anodic reactions at the steel reinforcement and to maintain the reinforcing steel in a cathodic state thereby protecting it from further corrosion. One of the features of the system is the permanent requirement for a D.C power source (Rectifier unit) and a permanent anode system. In addition to the cost of initial installation, ICCP requires investment in periodic monitoring to ensure that the system is operating effectively.

Anodes for use in ICCP applications can take a variety of forms dependent on the type of structure to be protected and the practicalities of installation; and can utilize either discrete or external anode systems.

5.1 External Iccp Anodes

External systems can comprise either titanium mesh anodes overlaid by a thin layer of low resistivity mortar; titanium ribbon placed into slots in the concrete; or conductive paint systems.

MMO coated titanium wire mesh is commonly used to protect large flat areas of reinforced concrete. Installation of the mesh on the structure is followed by the application of a sprayed cementitious overlay, as described more fully elsewhere [ref.5], however, this technique may not be appropriate for every situation, where deadweight or appearance restrictions apply.

MMO coated titanium ribbon is applied into chases cut into the concrete surface at an approximate spacing of 300mm. The ~2cm width ribbon can be applied in either dimension and is then grouted using an appropriate material. The technique is generally applied to structures having a reasonable depth of cover, as this avoids potential electrical shorts.

Conductive paints/mortars can be applied to the surfaces of reinforced concrete structures and will behave as anodes provided continuity can be maintained between the concrete surface and the coating. These materials can prove cost effective on structures having relatively low steel densities, and where environmental conditions facilitate application.

5.2 Discrete Iccp Anodes

The facility to bury the discrete anodes within the concrete structure allows protection of deeply buried steel or multiple layers which may not be protected by a surface mounted system. In addition the applied system adds no weight loading to the structure, and can easily be applied to difficult geometry. Several units are linked together to the power supply, the density of units can be varied dependent on required steel current density

One type of a typical discrete system comprises cylindrical, mixed metal oxide (MMO) anodes connected by wire and grouted into drilled holes adjacent to the reinforcing steel.

An alternative discrete anode system (Ebonex) comprises a cylindrical material (~7-28mm diameter x 75-600mm length) formed from a patented electrically conductive ceramic tube. This material is highly corrosion resistant and as such is capable of withstanding high applied current densities required to protect adjacent reinforcing steel.

The Ebonex discrete anodes are installed into holes drilled into the concrete structure between reinforcing bars, an acid tolerant grout being used to fill the annulus.. Each discrete anode is equipped with a vent tube which allows discharge of gases formed at the anode surface during operation.

The operation of an anode in CP systems applied to reinforced concrete will result in the effective consumption of water and generation of oxygen and H+ ions, at the anode surface. It is important that the applied anode/mortar system is stable under these conditions, as acid etching can result in void formation around the anode, as has been observed previously in the case of mesh anodes. This will lead to steadily increasing circuit resistance and the formation of discontinuities, with ultimate failure of the system.

Trials have demonstrated that the high alkalinity of the Ebofix grout assists in neutralizing the acid generation, and the gas venting system allows dissipation of gaseous oxygen. The Ebonex anode/Ebofix mortar composite remained intact in full contact with the surrounding concrete matrix, even at exceedingly high current levels of ~900mA/sqm. In contrast an unvented titanium tubular anode demonstrated severe damage to the surrounding mortar, with substantial loss of cement binder [ref.16].

These results confirmed the hypothesis that both a formulated mortar of high alkali reserve and a gas venting mechanism should form an essential part of a discrete anode design, and with these items in place, long term performance of the Ebonex discrete anode system should be assured.

Site evaluation data of Ebonex discrete anodes in UAE.
Ebonex anodes were installed in a grid pattern, at locations between the two layers of reinforcing steel, with anode separations of 600mm and 1m. These units were powered up using a standard rectifier/control unit and half-cell potential measurements were taken at

various times using a copper/copper sulphate reference electrode, to determine the extent of protection offered by the CP system. Current output was 19mA/m^2 of steel.

Table 2 – 24 hour Depolarisation data from UAE Ebonex trial.

Ebonex Anode reference	Distance from Reference Electrode to Ebonex Anode (cm)	24 hour Depolarisation (mV)
A1	40	172
	50	163
	60	69
	70	89
A2	20	195
	50	119
	60	80
	65	79
A3	25	193
	45	102
	60	136
A4	10	158
	45	123
	50	111

The data in Table 2 clearly demonstrate that a significant level of polarization has been achieved, and in fact the criterion of 100mV depolarization detailed in NACE 0290-90 is achieved at a distance of over 50cm from the discrete anodes, suggesting cathodic protection has been conferred. It is also clear that the influence of the discrete anode unit on steel polarization decreases with distance as would be expected form the increasing contribution from the concrete resistivity.

6. CONCLUSIONS

Concrete repair can be an expensive business. It is labour intensive, access costs are often high, and there may be a consequential loss of income due to temporary closure of the structure.

By embracing the technologies described above, it is possible to offer the building owner or specifier a full range of repair and protection options to ensure that their concrete repair project addresses not only visible defects but the hidden corrosion that, if left unchecked, may incur even more costly and disruptive repair works in the future. These technologies are now gaining significant track record around the world, with meaningful data providing a high degree of confidence with a number of clients and specifiers.

REFERENCES

1. Bamforth, P.B (1996), "Definition of exposure classes and concrete mix requirements for chloride contaminated environments", 4th Int. Symp. 'Corrosion of Reinforcement in concrete construction', Cambridge, UK, 176-188.
2. Leek, D.S. (1991), "The passivity of steel in concrete", Q.J. Eng. Geol.,24, 55-66.
3. Building Research Establishment Digest 264, "The durability of steel in concrete: Part 2, Diagnosis and comment of corrosion-cracked concrete, Building Research Station, Garston, UK, 1982.
4. Tutti K (1980), "Service life of structure with regard to corrosion of embedded steel", Performance of concrete in marine environment, Publication SP-65, American Concrete Institute, Detroit, Michigan, pp 223 – 236.
5. Broomfield, J. P. (1997), "Corrosion of steel in concrete", E and FN Spon, London.
6. H. Davy (1824), "On the corrosion of copper sheathing in sea water and methods of preventing this effect", Phil Trans Royal Society, London, vol. 114, pp 151- 158.
7. Stratfull, R.F. (1974), "Experimental cathodic protection of a bridge deck", Transportation Research Record, 500, Transportation Research Board, Washington, DC.
8. Emmons, P.H.; Vaysburd, A.M. (1997), "Corrosion protection in concrete repair: Myth and reality", Conc. Int., March, 47-56.
9. Fosroc International Ltd., (1999), "Renderoc Galvashield XP Data sheet".
10. Sergi, G.; Page, C.L.(1999), "Sacrificial anodes for cathodic protection or reinforcing steel around patch repairs applied to chloride contaminated concrete", Eurocorr99, Aachen, topic 10, paper no.12.
11. Project report (2002) ''Galvashield CC sacrificial anode trial – summary report'', Arup Research & Development, Solihull, west Midlands
12. Leng, D, Haboubi, L.(2000), "The evolution of zinc based cathodic protection systems for reinforced concrete", 6th International Conference on Deterioration and Repair of Reinforced Concrete in the Arabian Gulf, Bahrain
13. Haboubi, L. (2002) The development and use of zinc based, sacrificial cathodic protection systems for reinforced concrete, 5th ICOPMAS conference, Tehran.
14. M.H. Decter, N. Davison (1999), "Electrochemical solutions for chloride contaminated reinforced concrete", in 'Creating with Concrete, Controlling Concrete degradation, 155-168', Dundee.
15. Miller, J.B. (1995), "Seven Years On: A review of the mechanisms and advantages of electrochemical repair", Construction Repair, vol 9, no 6.
16. Hayfield P.C.S., Hill A. (2000) : "Ebonex Discrete Anodes in the Cathodic Protection of Rebar in Concrete : Performance of Ebofix Grouts", Int. J. Rest. Build.,vol 6, no 6.

Proceedings of the ACI-KC First International Conference & Fourth Exhibition. September 29-October 1, 2003, Kuwait — ***Concreting and High Performance Concrete in Hot Weather.***

AC IMPEDANCE TECHNIQUE FOR CONCRETE DURABILITY AND CORROSION TESTING

Adel Husain, Suad Al-Bahar, and Safa Abdul-Salam

Kuwait Institute for Scientific Research
Department of Buildings and Energy Technologies
P.O Box 24885- Safat 13109, Kuwait Email:xhusain@yahoo.com

ABSTRACT

Corrosion of steel in concrete is one of the major problems with respect to the durability of reinforced concrete structures. Predictions concerning comparative performance of commercial quality mix design of ordinary Portland cement (NoCl-cast), chloride containing cement mortar (Cl-cast), calcium nitrite in mortar cement (CN-cast) and silica fume (SF) in mortar cement have been investigated.

The main objective of the investigation is to present comparative data on electrochemical impedance spectroscopy (EIS) for steel reinforcement in mortar cement with two different admixtures during the hydration process of cement (i.e. 28 days).

The Impedance behaviors of the small specimens are studied using a special corrosion cell designed to accommodate small test specimens of mortar cement. Thereafter, to qualitatively characterize the EIS spectrum for each system in terms of Nyquist and Bode plots, as well as in terms of the general equivalent circuit elements.

Results of examples from laboratory and site mixes are presented to illustrate the viability of EIS to be used as a diagnostic tool for characterizing the protective quality and behavior of the proposed mortar concrete mix design.

In this study EIS has been found to be rapid and accurate technique for measuring durability and more specifically corrosion rate of reinforced steel in concrete. Therefore, EIS has a great potential to be used very effectively to distinguish between acceptable and un-acceptable concrete mix design for field application practice.

Keywords: Electrochemical Impedance Spectroscopy (EIS), calcium nitrite, silica fume, and ordinary Portland cement.

INTRODUCTION

Electrochemical impedance spectroscopy (EIS) has been applied successfully to the study of corrosion systems for more than 20 years (Mansfeld 1982). The reason EIS has found increasing applications in corrosion research is because of the possibility of obtaining information about the chemical mechanism involved. An important advantage of EIS over other laboratory techniques is the possibility of using very small amplitude signals without disturbing the properties being measured. Another major quality of EIS is the possibility of working in low or variable conductivity environments. Thus EIS has been applied successfully to study the corrosion of Fe and carbon steels in neutral waters or deoxygenated formic acid (Zeller 1986).

The following points have been addressed on correlating the AC impedance measurement to the protection afforded by commercial quality admixture systems:

(i) To determine whether AC impedance test a reliable form of accelerated test for the smaller specimens, and how predictive can it be with the silica fume and calcium nitrite systems of commercial quality during dehydration process. (ii) Whether it is only useful as quality control or condition monitoring. The out put results from EIS behavior was examined and compared with respect to the lollipop specimens from previous experiments.

EXPERIMENTAL METHOD

The mortar mixture proportions of the samples prepared for this experiment were designed to yield a moderate range of transport properties and are based upon concrete mixture proportions from previous experiments. The cement was ASTM Type 1; the chemical composition of the mix proportion is given in Table 1. The pozzolanic mineral admixture was silica fume in slurry form. A chemical inhibitor in the form of Calcium Nitrite was used, as indicated in Table 1. The mixture proportion of the samples in this experiment for water cement ratio was a 75 % (by mass) aqueous solution. The chloride percentage by weight of the mixing water was 1.75 %.

Table 1. Laboratory-Prepared Concrete Mix Proportions

Specimen Type	Specimen Designation	Concrete Specifications
Plain Concrete	NoCl-cast	Type 1 ordinary Portland cement W/C 0.75
Plain Concrete with Cl	Cl-cast	Type 1 ordinary Portland W/C 0.75
Calcium Nitrite	CN-cast	Type 1 ordinary Portland W/C 0.75
Silica Fume	SF-cast	Type 1 ordinary Portland W/C 0.75

The mortar mixtures were prepared according to the procedures in ASTM C 109. The samples were cast in 100mm X 150mm molds made of Perspex materials, covered, and stored in a 100% relative humidity chamber. At 24 hours of age, the specimens were removed from the molds and stored in a humidity chamber until they were tested periodically at intervals of 28 days. Although no temperature controls were used, the laboratory temperature could be characterized by the interval 20± 2 ° C.

Each specimen was prepared for testing according to the specifications of the admixture proportion recommended by the suppliers of the materials. The present test cell and mold types were designed in order to have a small specimen of mortar cement concrete (10cmX15cm). The main advantage of this design is to study the response of the EIS spectrum on smaller sample and correlate it with the standard ASTM test specimen. The

specimen consisted of polished steel rebars approximately 6.9 mm in diameter as working electrode and two identical graphite electrode approximately 8 mm in diameter as auxiliary electrodes.
The purpose of using two embedded graphite electrodes was to verify the validity of the conductivity measurement for EIS technique and to reduce overestimated scattering in the signal noise. Conductivity, an intrinsic property, is independent of specimen geometry and size. A reliable technique for determining specimen conductivity should obtain equivalent results from replicate specimens with different lengths.
AC impedance measurement and data acquisition was controlled using Solartron Model 1287 Potentiostat/Galvanostat interfaced with Solartron Model 1260 Frequency Response Analyzer (FRA) to provide sweep frequency measurement. Both instruments were interfaced with computer for data logging, storage, and analysis. The applied potential amplitude was in the range of (10 - 100 mV) in the nominal frequency range of 100 kHz to 10 MHz. The AC impedance test data were obtained at the open circuit potential.
The impedance tests were performed using Solartron instruments with two and three electrode configuration:

(a) Auxiliary with two embedded graphite electrodes (as counter electrode).
(b) Saturated silver/silver chloride electrode as a reference electrode.
(c) Test specimen reinforced steel bar in mortar cement (10 cm X 15 cm)
(i.e. as working electrode).

The AC impedance test cell consisted of two plastic sheets made of Perspex. The plastic sheets were rested on the top and bottom of each sample, thus holding the sample, a wet filter paper saturated with 0.5M NaCl solution was rested on top of the specimen for potential measurement with reference electrode, whilst EIS measurement were made. Three identical test cells were designed and constructed for this study and the mortar steel specimen selected for test was mounted horizontally.

RESULTS AND DISCUSSIONS

Electrochemical impedance spectroscopy (EIS) have been utilized in this study to characterize four different compositions of duplicated cement concrete samples. Predictions concerning comparative performance of commercial quality mix design of ordinary Portland cement (NoCl-cast), chloride containing cement mortar (Cl-cast), calcium nitrite in mortar cement (CN-cast) and silica fume in mortar cement have been investigated. The evaluation has been attempted first, to examine the comparative ranking of EIS spectra obtained for each mix system when combined or superposed together in one impedance plot with respect to the corresponding corrosivity of each protection system. The second reason is to assess whether the early predictions made by ASTM corrosivity test and Electrochemical Impedance Spectroscopy (EIS) for selected materials of Lollipop samples are still valid.
The impedance results of Fig. 1 (a, b) to Fig. 4 (a, b) indicated impedance spectrum in the form of Nyquist and Bode plots for the plain concrete (NoCl-cast), chloride concrete (Cl-cast), calcium nitrite mortar cement (CN-cast), and silica fume (SF-cast).
Fig. 1, represent EIS measurement results in the form of Nyquist and Bode plots for the mortar cement specimens taken immediately after casting while Fig. 2, 3 and 4 represent the same test obtained after 3, 14, and 28 days respectively during dehydration process in the humidity curing chamber.
Qualitative analysis of the Nyquist impedance spectrums have indicated that the corrosion performance of the different concrete mixtures are in agreement with the ASTM test results of corrosion rate and potential values obtained in previous experiments. The impedance results have shown that the lab prepared ordinary Portland concrete structure during casting exhibited

the highest impedance and capacitance values among the rest of the specimens. This is shown clearly in Fig. 1 a, b and Fig, 2 a, b during casting and after 3 days exposure, respectively.
In other word the presence of a Warburg diffusion response indicated that the slow diffusion processes of the water species through porosity in the material and formation of passive film

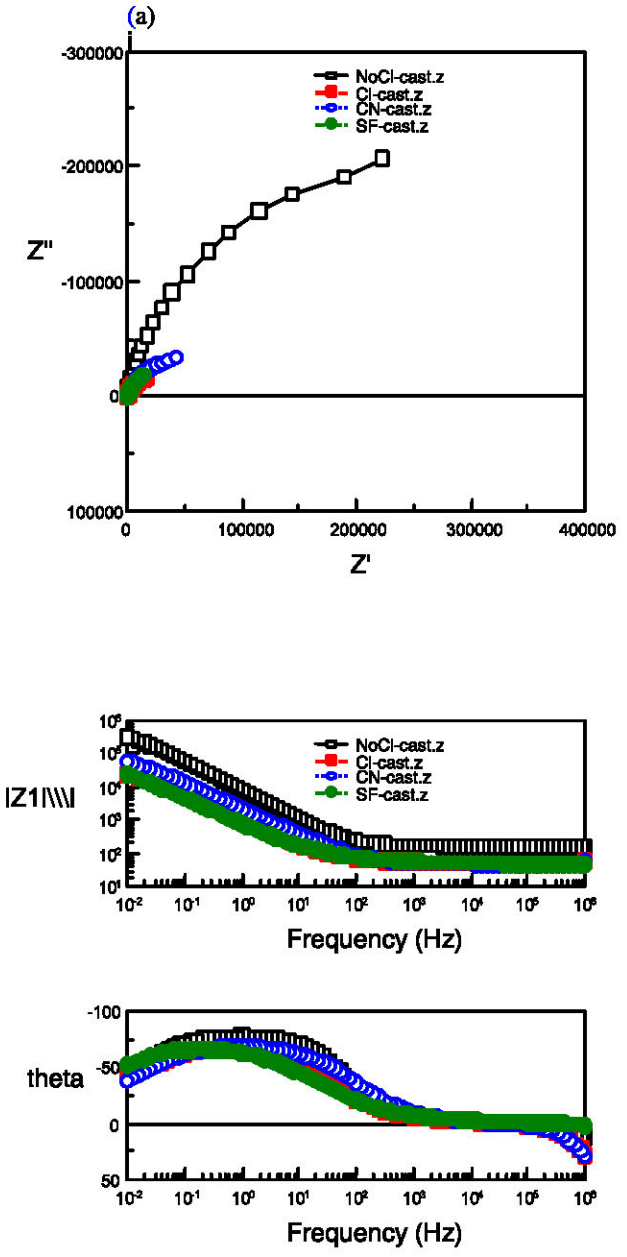

Figure 1. EIS Nyquist plot (a) and Bode plot (b) for the mortar specimens immediately after casting in the mold.

due to mortar alkalinity was the rate controlling factor for the mechanism of concrete corrosion protection at this stage
The natural process of alkaline passive formation and build up for this particular sample affects this process. Similarly water saturated concrete tends to show resistivities on the order of a few Kohm-cm, while oven-dried concrete can approach resistivity values typical of electrical insulator as it is reflected on the EIS spectrum taken before exposure for other concrete samples.
As it is expected from the protective nature of the silica fume mortar specimen (SF-cast), the dehydration process of SF concrete slowed down the diffusivity of the chloride species to reach the steel substrate. This is very much related to the mechanism of coalescence and interaction of the micro silica cement element in the pores structure of the concrete whilst in the dehydration process.

In contrast to the ordinary mortar concrete and silica fume mortar, the inhibited concrete (CN-cast) and chloride mix mortar cement (Cl-cast) concrete samples showed the lowest impedance and capacitive behavior. This is due to the high rate of permeability and adsorption of the chloride corrosive species to the steel substrate surface.

In the case of inhibited concrete sample, the attempt of studying such inhibitor with concrete is to show the viability of the EIS technique to be used as a tool for condition monitoring (Fig. 3 and 4). The EIS spectrum after 14 and 28 days is attributed to the improper application of inhibitor concentration and or due to under curing which may cause the corrosion process to become even worse than ordinary concrete cement without inhibitors (OPC).

The hypothesis behind the unexpected behavior of the inhibited concrete sample was more or less related to the improper film coverage and adsorption of the nitrite species to the passive oxide or hydroxide layer of steel surface with subsequent formation of unprotected micro-corrosion cells. If chloride ions arrive first as contaminant to the surface of the steel, the surface tends to become active when the molar ratio of Cl^- to Nitrite and hydroxyle ions in the pore solution reaches a critical value that exceeded 0.9. Microscopically, the concrete mix acts as a non-homogeneous electrolyte, which varies greatly with the overall moisture content, in addition to the rate and degree of diffusivity of corrosive species and inhibited ions such as oxygen, chloride and nitrite. This finding is in agreement with EIS spectrum previously obtained for the Lollipop ASTM samples.

In the case of the as-received specimen with no chloride addition an almost purely capacitive and diffusion response was observed during experimental testing. This effect has been reflected as straight spectra line in the Nyquist and Bode plot shown in the same figures (1 to 4) and even after 28 days of curing. There is little apparent change during this time, suggesting that the system is relatively stable and that there is no more water uptake and the material is acting as some sort a die-electric component.

In the case of the chloride contaminated concrete it is expected that Nyquist spectrum will reach its semi-circular shape and will become smaller and smaller with time. Similarly, the same EIS response would be expected from calcium nitrite specimen. Both specimens have shown a greater tendency toward reaching its charge transfer resistance and polarization resistance at a faster rate once exposed to the environment.

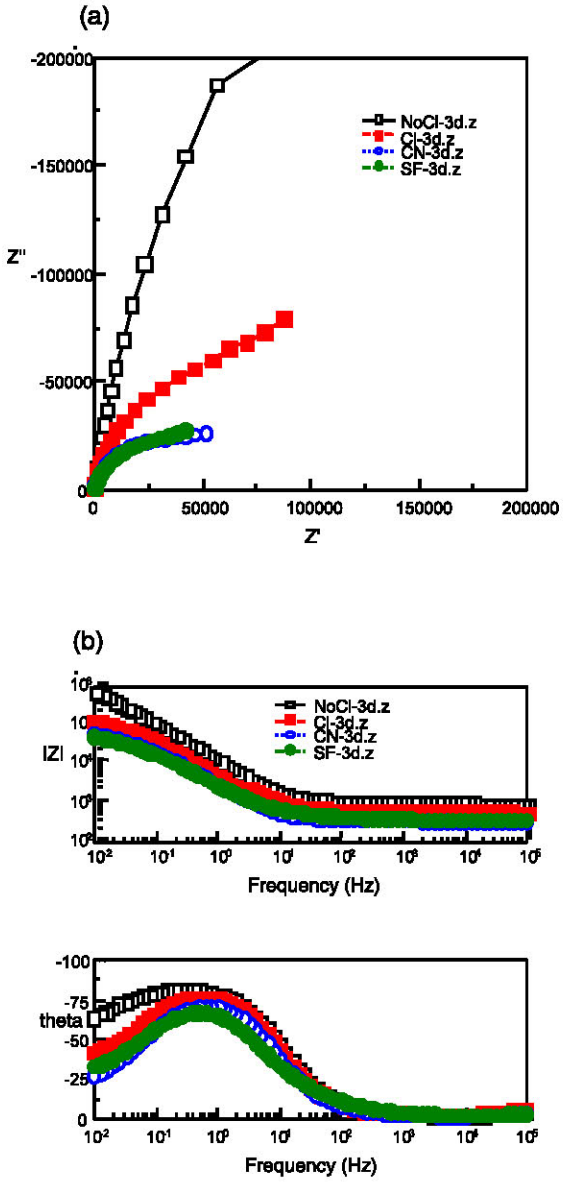

Fig. 2. EIS Nyquist plot (a) and Bode plot (b) for the mortar specimens immediately after 3 days of casting in the mold.

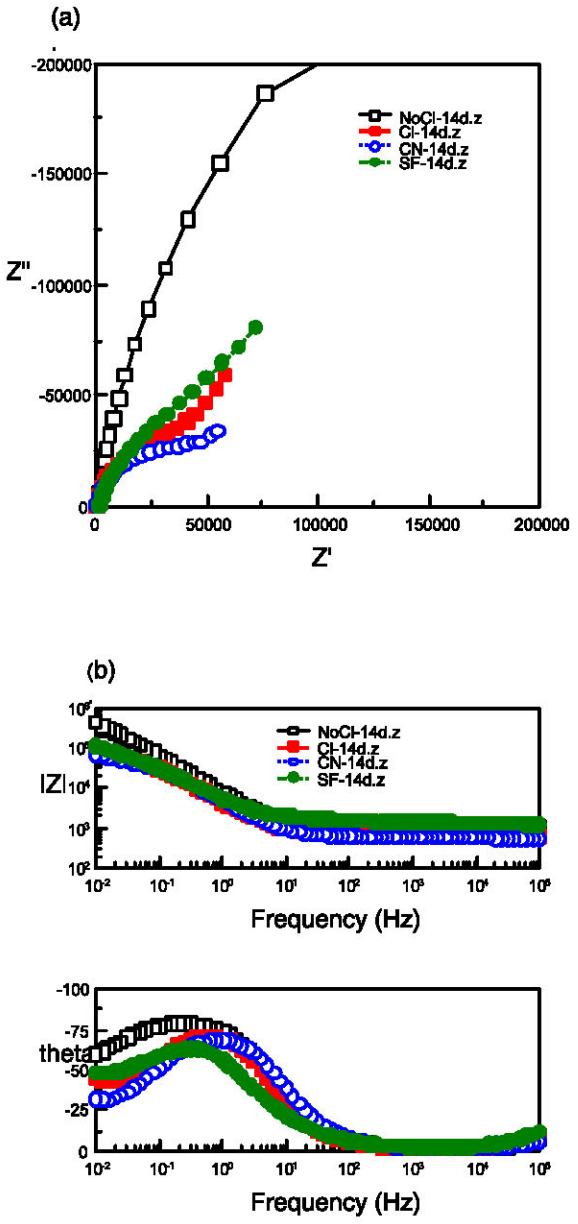

Fig. 3. EIS Nyquist plot (a) and Bode plot (b) for the mortar specimens after 14 days of casting in the mold.

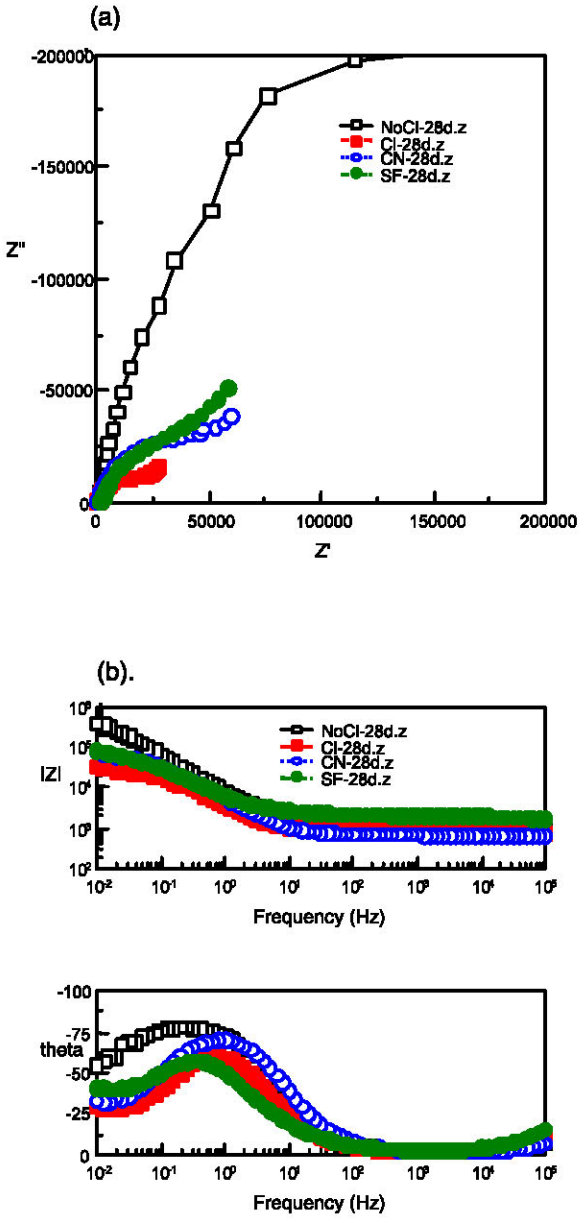

Fig. 4. EIS Nyquist plot (a) and Bode plot (b) for the mortar specimens after 28 days of casting in the mold.

EIS SPECTRUM ANALYSIS

The equivalent parallel R-C circuit in figure 5 explains and represents quite well the frequency impedance response of the concrete mix design systems used in this study.

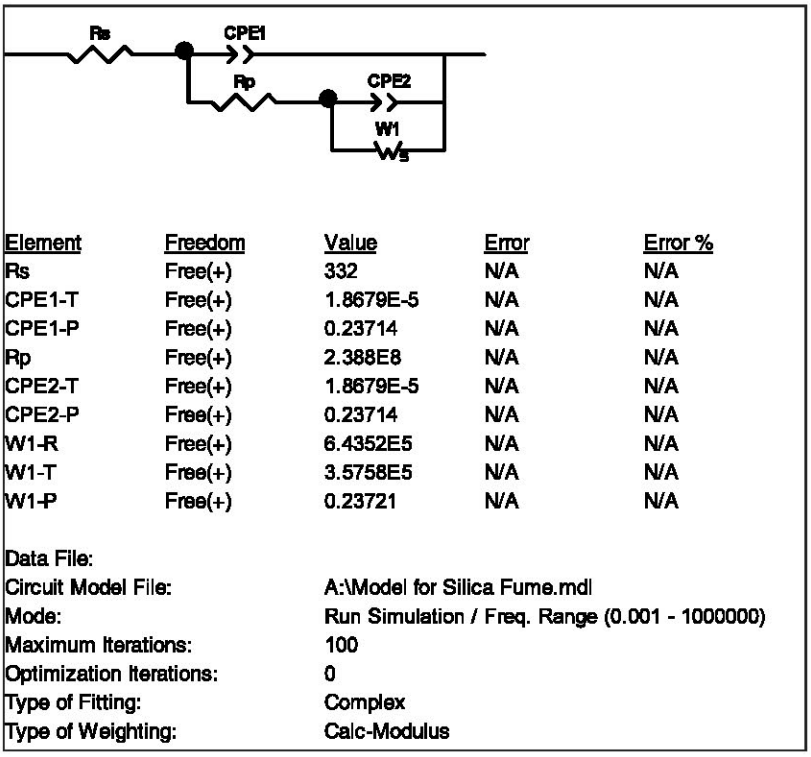

Element	Freedom	Value	Error	Error %
Rs	Free(+)	332	N/A	N/A
CPE1-T	Free(+)	1.8679E-5	N/A	N/A
CPE1-P	Free(+)	0.23714	N/A	N/A
Rp	Free(+)	2.388E8	N/A	N/A
CPE2-T	Free(+)	1.8679E-5	N/A	N/A
CPE2-P	Free(+)	0.23714	N/A	N/A
W1-R	Free(+)	6.4352E5	N/A	N/A
W1-T	Free(+)	3.5758E5	N/A	N/A
W1-P	Free(+)	0.23721	N/A	N/A

Data File:	
Circuit Model File:	A:\Model for Silica Fume.mdl
Mode:	Run Simulation / Freq. Range (0.001 - 1000000)
Maximum Iterations:	100
Optimization Iterations:	0
Type of Fitting:	Complex
Type of Weighting:	Calc-Modulus

Fig. 5. Example of equivalent circuit model with curve fitting analysis for capacitance and impedance elements for Silica Fume metal/solution interface under-study.

The real meaning of C (or CPE1) and Rp for the complex system metal/concrete/electrolyte in this study has now been very well established. In the author's view, at the beginning of the test C_c could be related to the capacitance of the concrete mortar cover film, acting as a dielectric material. Whereas (R_p) the ohmic electrical resistance of the mortar film or (pore resistance), acting as a barrier to the permeation of substances across it. With time, new electrochemical processes would take place and the equivalent circuit would consequently change, introducing now the double layer capacitance (C_{dl} or CPE2) prevalent at the substrate/cement interface and charge-transfer resistance (R_{ct}) that combined together with the Warburg diffusion impedance (Z_w or W1s). Thus, the high frequency semicircle is considered to represent information on the concrete or mortar layer (C_c, Rs, and R_{po}), whilst the semicircle at lower frequencies is thought to indicate the information on the metal substrate corrosion tendencies in conjunction with (C_{dl} & R_{ct}).

In this study, to explain the overall variation of R_{po} data with time for silica fume mix design, two phenomena are assumed to occur simultaneously but with variable rates depending on the exposure or hydration curing time:
(1) The increase in pore density, and (2) the partial sealing of the pores by cement hydration process or iron corrosion products and/or other types of protective micron size species that become more prominent over long immersion times. (Hepburn 1986) reported similar observations, which described the depression of the low frequency semi-circle (shown in the previous figures) to the presence of two distinct types of corrosion sites: sites that are initiating and sites that are becoming blocked by corrosion products and or protective elements. The value of C_c is generally considered to provide information on the degree of water penetration or diffusion through the concrete and in principle its value is expected to increase with time. This behavior can be qualitatively analyzed as functions of time on the Nyquist plot that form series of semi-circles with reduced/increased diameters. In this work there is little variation of C_c with testing time for the smaller plain concrete samples (NoCl) and silica fume (SF) may indicate a high rate of film stability and dehydration combined with oxygen diffusion through the concrete mortar system. The same effect of EIS behavior was observed for the ASTM specimens in previous experiments (Abdul Salam 2002). The relatively constant value of C_c during exposure time for sample of concrete with Cl and calcium nitrite in Figs. (2 and 4). Suggests that the values of capacitance of concrete cover film of the small pathways or pores are much less than the parallel capacitance of the remainder of the film which do not contribute significantly to the overall capacitance, even though the pathway controls the performance of the concrete composition. Another assumption may be attributed to the weakness of self-inhibition nature of the calcium nitrite and the high aggressive nature of the destructive chloride species in localized density on the steel substrate and particularly during the initiation of pores.

CONCLUSIONS

1. This work has shown the feasibility of using EIS as a monitoring tool for detecting corrosion processes on steel reinforcement in concrete with mix design technology.
2. EIS is considered to be a viable and accelerated diagnostic tool for the corrosion evaluation of the steel reinforcement in concrete mix design system for both smaller specimens and larger ASTM Lollipop specimens.
3. The prediction made by AC impedance, in this study with respect to material performance and environmental effect, is in agreement with the ASTM tests for concrete durability in terms of corrosion rates, corrosion potential and galvanic corrosion for previous exposures in laboratory and Kuwait environment.
4. For all concrete with NaCl addition, the reaction sequence would follow initially one of the diffusion controlled (passivation reactions) and changed to charge transfer control (polarization reactions). For concrete without the NaCl addition, the corrosion process is characterized by capacitive and diffusion controlled reaction sequence.

REFERENCES

Mansfeld, F., Kendig, Tsai, M., S. (1982), Corros. Sci. 22: p.455.
Zeller, R. L., Savinell, R. F. (1986), Corros. Sci. 26: p. 591
Hepburn, B. J., Gowers, K. R. and Scantlebury, J. D. (1986), British. Corros. J., Vol. 21, p. 105,
Abdul Salam S., Husain A., Al-Bahar, S. Al-Shamali, O. (2002), Proceeding of the 15th International Corrosion Congress /15th ICC 22-27 September 2002, Granada, Spain.

Proceedings of the ACI-KC First International Conference & Fourth Exhibition. September 29-October 1, 2003, Kuwait — ***Concreting and High Performance Concrete in Hot Weather.***

CORROSION PROTECTION SYSTEMS FOR IMPROVING CONCRETE PERFORMANCE IN ARID REGIONS

Suad Kh. Al-Bahar, Safaa M. Abdul Salam, Dr. Adel M. Husain, Hasan J. Karam
Kuwait Institute for Scientific Research
Building and Energy Technologies Department
P.O. Box 24885 Safat 13109 Kuwait, Email:sbahar@safat.kisr.edu.kw

ABSTRACT

Improving concrete performance and minimizing corrosion-induced deterioration of reinforced concrete structures are certainly required by the Building Codes and Specifications for arid regions such as the Arabian Gulf. Therefore using corrosion protection systems such as supplementary cementing "pozzolanic" materials, epoxy-coated rebars, and corrosion inhibiting admixtures, are becoming increasingly important for enhancing the quality of concrete and prolonging the life of reinforced concrete structures. Nevertheless, it is also important to examine these systems to evaluate their performance and to assess their impact on durability of the structures under the severe weather conditions of this region. At Kuwait Institute for Scientific Research, an experimental laboratory and field test program was implemented to identify and evaluate performance of some of the most suitable corrosion protection systems under the prevailing weather conditions in Kuwait. The study concluded that supplementary cementing materials contributed to improvement of concrete performance and its resistance to chloride diffusivity. Also, it concluded that epoxy-coated rebars are vurnable to corrosion pitting in saturated chloride environment, especially when the epoxy coating is damaged as received. As for the calcium nitrite corrosion inhibiting admixture, the study concluded that they are most effective when applied by the correct dose to compete with all available chloride ions, and when in combination with microsilica.

INTRODUCTION

It is becoming increasingly obvious that aggressive environment and severe conditions pose great threat to reinforced concrete structures in Arabian Gulf region. Whenever concrete deterioration is investigated in this region, it is rarely goes without mentioning corrosion–induced deterioration inflicted on structures integrity, and the premature damages and degradation taking place that trigger unplanned repair works which often ineffective, inadequate and repetitive. The region provides an extremely aggressive environment, which is characterized by high ambient temperature and humidity conditions, and severe ground and ambient salinity with high levels of chlorides and sulfates in the soil and groundwater. Structures exposed to the marine environment, groundwater conditions and industrial pollution have suffered the most. Concrete corrosion is becoming inescapable phenomenon in this region even to structures of high performance concrete, which are relatively new (10-15 years of construction age). Recent survey study that took place in 1997 on premature deteriorated structures (1), concluded that repair and rehabilitation cost are often expensive, not highly effective in arresting the corrosion processes, and would have to be repeated within few years. The study conducted in 1992 (2), on impact of metallic corrosion on Kuwait economy, showed that cost of direct and indirect corrosion was 5.2% of the gross national product (GDP), out of which 17.4% was an avoidable cost that could have been saved by application of corrosion control technologies. The economical impact was estimated to be KD. 266 millions paid as unrecoverable cost of unavoidable corrosion. The study concluded that cost of corrosion in the construction industry was 0.5% of the GDP. That had demonstrated clearly the economical consequences of the corrosion-induced deterioration of reinforced concrete structures.

Corrosion protection systems reduce the risk of corrosion in reinforced concrete structures in many parts of the world. The use of these systems though might increase the cost of construction; the increase is marginal compared with the cost for repair of the structure as a result of premature deterioration. It is estimated that when these protection systems are used, the increase in construction cost is typically only 10 % of the cost for repair of the premature corrosion-induced deterioration that occurs in the absence of the protection systems (3). As for the corrosion protection systems, such as supplementary cementing materials, corrosion inhibiting admixtures, and epoxy coated rebars, though they have been used for building constructions in very limited projects in the region, they have not been subscribed or standardized for in the national building code of practices in the region. This can be attributed to:

1. No serious attempts or collective well have been made to develop and update the national construction guidelines and code of practices to match the development in the concrete technology that suite the environmental conditions in the region.
2. Adopting foreign construction code of practices without paying attention to the specific nature of the construction materials and the environmental and service conditions prevailing in the region.
3. Adopting concrete construction practices that not necessary guarantee high performance and durability of the reinforced concrete structures under the aggressive, hot environmental conditions.
4. Lack of awareness and unfamiliarity with the use of these systems as well as the lack of comprehensive database on the long-term effectiveness of the systems under the environmental and service conditions prevailing in the region.

In 1997 Kuwait Institute for Scientific (KISR), supported by Kuwait Foundation for Advancement of Science (KFAS), and the major companies of material suppliers, ready mix concrete, and construction and consulting firms, have seized the opportunity to conduct this urgent study which aimed at identifying corrosion protection systems that are most suitable for application in reinforced concrete structures in Kuwait and to demonstrate enhancement achieved in concrete durability when these systems are used. Also among the main objectives are to establish performance data on the selected corrosion protection systems under typical local service conditions and to determine their economic benefits.

The corrosion protection systems that involved in the study are:

1. Epoxy coated reinforcing bar. Steel bars are protected with a coating of powdered epoxy that is fusion-bonded to the steel. The coating physically blocks chloride ions. Cracking and chipping of the coated bars may occur during transportation, storage and field handling, particularly where unskilled labors are used, as is prevalent in the Arabian Gulf region. Damages of such nature could be very detrimental to the integrity of these bars and the protection against corrosion (4).
2. Silica-fume (Microsilica) and Ground Granulated Blastfurnace Slag (ggbs). These are effective pozzolanic materials that significantly reduce concrete permeability and, thereby, reduce chloride ion ingress. The decreased permeability substantially increases resistance to chloride penetration and reduces the rate of steel corrosion and carbonation. Microsilica and ggbs concretes typically have low chloride diffusivity. On the other hand, though ggbs concrete has an early delay rate of hydration, it has lower heat of hydration and progressive compressive strength after 28 days, which superceded that of ordinary concrete and continue to rise after 56 days of curing(5). As for microsilica the concern includes the reduction in the pH value of the concrete which makes carbonation more likely and could cause bound chlorides to be liberated from the hydration products and reduction in the resistance of concrete to salt weathering which is caused by crystallization of salts in the concrete pores (6)
3. Calcium Nitrite Corrosion-Inhibiting Admixtures. It enhances the stability of the passivating layer on the surface of the reinforcing steel. In this concrete system chloride and nitrite ions compete for ferrous ions on the steel bar. If the chloride ion concentration is greater, the corrosion process will start. If, on the other hand, the nitrite ion concentration is greater, a passive layer will form to close off the iron surface. The effectiveness of the calcium nitrite admixture, therefore, is dependent on an accurate prediction of the chloride loading of the structure over its expected design life and, hence, on the selection of an appropriate dosage of the admixture (7).

TESTING PROGRAM

The testing program was designed to include standard and popular laboratory testing methods, accelerated and normal testing methods. The program also included field assessment studies, where specimens are prepared and placed in an exposure site of multiple conditions. The corrosion test program covered three different evaluations:

1. Strength development properties.
2. Corrosion activities-related tests.
3. Chloride ingress characteristics.

For specimen preparations local building materials were used such as Type I & Type V cements, sand, aggregates, and ordinary steel reinforcing bars. Chemical admixtures were provided by local suppliers, whereas local promenant construction companies provided the

research program with the required amounts of microsilica (from Elkem Microsilica), ggbs (from Falcon Cement), epoxy coated rebars (from Protech Dubai), and calcium nitrite (from Al-Gurg Fosroc Dubia). Table 1 presents test program summary designed for the study.

Table 1. Test Program Summary

Test	Specimen Size	Measurement
ASTM G-109	Beams: 279 x 152 x 114 mm	Macro-cell current Half-cell potential
Corrosion Rate (Lollipop)	Prism: 380 x 200 x 76 mm	Macro-cell current Half-cell potential
Time-to-Corrosion	Blocks : 300 x 300 x 200 mm	Corrosion rate Macro-cell current Half-cell potential
ASTM C-1202 (AASHTO T 277-86)	Cylinders: 100 x 200 mm	Total charge (conductivity)
AASHTO T 259-80	Slab: 300 x 300 x 75 mm	Chloride profile
Chloride Diffusivity	Cylinders: 100 x 50 mm	Chloride content
Outdoor Exposure	Beams: 120 x 120 x 350 mm With 2 bars With 1 bar Cylinders: 100 x 200 mm	Visual examination Half-cell potential Steel mass lost Chloride content

Strength Development Properties

This is presented in terms of compressive strength. Strength gain development is monitored and recorded at certain curing intervals. Any strength development with time can be related to change in permeability and chloride ingress characteristics. As hydration takes place and the curing process progresses, capillary pores are filled with hydration products. The capillary porosity of the paste depends on both w/c ratio of the mix and the degree of hydration. The type of cement influences the degree of hydration achieved at a given age. At a high water/cement (w/c), ratio the volume of the formed cement gel is not sufficient to fill the capillary pores, which are mainly responsible for permeability of hardened cement paste and its vulnerability to chloride ingress.

Corrosion Activities-related Tests

Time-to-Corrosion Initiation (Modified ASTM G-109). This is a stringent testing method that evaluates the effectiveness of concrete in protecting embedded steel bars from corrosion when salts are applied externally (8). The test requires 48 weekly test cycles to complete. Measurement proceeds after 96 h of salt-water ponding, followed by vacuum removal of the salt water and immediate freshwater rinse and vacuum removal again. This is followed by 72 h of air-drying. The weekly measurements involve readings of half-cell potential, corrosion

rate, and concrete resistivity, which are recorded with respect to a copper-copper sulfate reference electrode (CSE) of –350 mV.

Corrosion Rate Test (Lollipop Test). This is a popular laboratory test method, which demonstrates the effectiveness of corrosion protection systems exposed to the marine environment. The test takes its name from the shape of the test specimen. The test simulates the wicking of chlorides by concrete in seawater. The test studies the microcell corrosion current that occurs in a localized area on the steel rebar. Corrosion rate measurements are recorded every month, and involve half-cell potential and microcell corrosion current. This test takes at least one year for the initial results to appear. This test provides excellent chloride ingress profile indication, which qualifies the permeability characteristics of the different corrosion protection systems.

Chloride Ingress Characteristics Tests

The rate at which ions, particularly chloride ions, can diffuse through concrete is important with regard to possible corrosion of steel reinforcement. Ions diffuse through concrete due to differences in ion concentration, which are often independent of hydraulic pressure gradient. Ion diffusivity is generally determined by measuring the time for the concentration at a given point to reach a particular value. There are at least three test methods to determine ionic diffusion rates:

1. The first involves taking incremental samples at different depths by drilling and measuring the chloride content at each increment.
2. The second involves measurement of ionic diffusion by concentration difference between two sides of a specimen after ponding with a chloride solution at one side for certain period of time.
3. In the third method, ionic diffusion is measured by the change in electrical properties that results from changes in concentration.

Chloride Diffusivity. This is a popular long-term duration laboratory test method. This method is designed to assess the chloride ingress characteristics of cylindrical specimens; epoxy-coated on all surfaces, then cut at one end to expose the concrete The exposed concrete surface provides access for one-dimensional diffusion of chloride ions of 3% NaCl solution. Chloride concentration profiles are developed by periodical assessment of chloride concentration at certain depths (0-10 mm, 10-25 mm, 25-30 mm, and 30-50mm). For certain concentrations, at each depth, the time will be recorded and compared.

Electrical Indication of Concrete's Ability to Resist Chloride Ion Penetration ASTM C-1202-91). This is a standard test method designed to determine the electrical conductivity of concrete to provide a rapid indication of its resistance to the penetration of chloride ions (9). The test consists of monitoring the amount of electrical current passed through 100 mm diameter by 50 mm long cores when one end of the core is immersed in sodium chloride and a potential difference of 60 V dc is maintained across the specimen for 6 h. The total charge passed in coulombs is related to chloride permeability.

Resistance of Concrete to Chloride Ion Penetration (AASHTO T 259-80). This is a standard test method that evaluates the effect of variations in concrete properties on resistance to chloride ion penetration (10). The test results are correlated with findings of ASTM C1202 to confirm ionic diffusion by chloride ion concentration. Chloride diffusivity is measured by

assessment of chloride concentration at different depths, after 90 days ponding with 3% NaCl solution.

RESULTS AND DISCUSSION

In this paper results and performance of each corrosion protection system will be compared to performance of ordinary concrete and the ability to arrest the corrosion process and control the corrosion activities within each system.

Performance of GGBS Concrete

Table 2 presents the concrete mix proportions of the ordinary concrete and the ggbs concrete as 50 % of cement weight was replaced by ggbs. The water- to- cement ratio was selected to be relatively low to represent high performance concrete.

Table 2. Concrete Mix Proportions

Ingredients	Ordinary Concrete	GGBS Concrete
Water-to-cement Ratio	0.36	0.36
Cement type	I	I
Cement (kg/m^3)	472	236
GGBS (kg/m^3)	-	236
Sand (kg/m^3)	550	550
* Aggregate 20 mm (kg/m^3)	770	770
* Aggregate 10 mm (kg/m^3)	380	380
Water (l/ m^3)	170	170
** Chemical Admixture (Caplast NE/EDS) (l/m^3)	5.5-8.5	5.5-8.5

* SSD = Saturated surface Dry , ** Super plasticizer water reducer

Results shown in Table 3 indicates the improvments achieved in the compessive strength at 28 and 56 days in spite of the delay in maturity in the third and seventh day of the curing period. Improvements occurred as a result of 50 % replacement of cement weight by ggbs have affected positively the concrete resistivity to chloride ions penetration and the corrosion activities on the protected steel reinforcing bars. In Fig. 1, and according to ASTM C-876-91 (11) for corrosion risk assessment of half-cell potential of steel bars in concrete, the half cell potential of the steel bar protected by the ggbs concrete was less than –200 mV-CSE after 48 cycles of testing according to modified ASTM G-109, which indicates that steel bar condition in the region described as 90 % probability no corrosion activity occuring on the surface of the steel bar. This is incomparable to results of steel bars protected by ordinary concrete, when its corrosion potential recorded –215 mV after 35 cycles of testing, which describe the steel bar condition as in the region of uncertain corrosion risk area. After 40 cycles of testing and at 280 day the onset of corrosion activities occurs at half-potential of –240 mV-CSE.

Table 3. Improvements in Mechanical and Physical Properties of Ordinary Concrete as 50% of Cement Weight Replaced by GGBS

Properties / Concrete Type	Compressive Strength (kg/cm^2)				ASTM C-1202		AASHTO T-259 Percentage of chloride Absorption After 90 days	
	3 days	7 days	28 days	56 days	28 days	56 days	13 mm Depth	25 mm Depth
Ordinary Concrete Type I	443	490	579	600	2590	1713	0.120	0.052
GGBS Concrete	356	440	632	780	1220	636	0.034	0.021

Table 4 shows results of the corrosion activities for both concretes represented as time-to-corrosion initiation, magnitude of corrosion activities, corrosion current density, concrete electrical resistivity, and corrosion penetration rate. Corrosion rate determined by linear polarization and other electrochemical techniques, expressed in terms of corrosion current density (I_{corr}) can be converted into penetration rates by the following expressions based on Faraday's law (12):

$$\text{Corrosion penetration rate} = K \frac{ai}{nD} \quad (1)$$

where a = atomic weight of metal (55.8); i = current density,$\mu a/cm^2$; n = number of electrons lost, valence charge (2); D = density of steel, g/cm^3 (7.86); K = constant depending on the penetration rate desired with K = 0.129, mpy (mils penetration per year), K = 3.27 , mm/yr, and K = 0.00327 , m/yr

Table 4. Improvement in Concrete Permeability and Its Effect on Corrosion Activities on Steel bars

Properties / Concrete Type	Time–to Corrosion (Modified ASTM G-109) (days)	Magnitude of Corrosion Activities (μA. day)	Corrosion Current Density ($\mu A.cm^2$)	Corrosion Penetration Rate (μm/year)	Concrete Electrical Resistively ($k\Omega$. cm)
Ordinary concrete Type I	280	2081	0.166	1.927	70
GGBS Concrete	Corrosion Potential less than–200 mv	749	0.110	1.2	100

As results showed above there are significant improvements in concrete properties when 50% of cement replaced by ggbs, particularly with respect to chloride ions penetration and corrosion activities on steel bars, which qualify ggbs concrete for use in marine and off shore styructures.

Performance of Silica Fume Concrete in Comparison to Ordinary Concrete and Concrete with Calcium Nitrite

Results showed significant improvements in concrete properties with respect to chloride ions penetration, by 10% replacement of cement weight with microsilica, which had a direct effect on delaying the corrosion activities progress on steel reinforcement bars. According to AASHTO T-259 Table 5 presents results of chloride ions obsorption of concrete cover after 90 days of concrete surface ponding with 3% sodium chloride solution. Results showed substantial decrease in chloride ions obsorption that ranged from 60 – 80% depending on the variation in the water-to-cement ratio of the different concretes. The above results are in agreement with results

Table 5. Rate of Chloride Absorption at Different Depths of Concrete Surface

Concrete Code	Average Absorbed (%)		Maximum Absorbed (%)	
	1.6-13mm	13mm-25mm	1.6-13mm	13mm-25mm
* OU—50	0.161	0.118	0.186	0.177
**OUSF 50	0.089	0.049	0.111	0.111
*** OU –45	0.086	0.041	0.098	0.049
**** OUSF 45	0.069	0.006	0.096	0.009

* Ordinary Concrete: w/c =0.5, ** silica fume concrete: w/c = 0.5
*** Ordinary concrete: w/c = 0.45, **** silica fume concrete: w/c = 0.45

of ATSM C-1202 presented in Fig. 2 that indicate concrete resistivity to chloride ions penetration expressed as total charge passed through concrete in six hours. According to FHWA/RD-81-119 report (13) for chloride ion penetration as presented in Table 6,

Table 6. Chloride Permeability Based on Charge Passed

Charge Passed (Coulombs)*	Chloride Ion Penetrability	Typical of
> 4,000	High	High w/c (>0.6). Ordinary concrete
2,000 – 4,000	Moderate	Moderate w/c (0.4 – 0.5). Ordinary concrete
1,000 – 2,000	Low	Low w/c (>0.4). Ordinary concrete.
100 – 1,000	Very Low	Latex modified concrete Internally sealed concrete
< 100	Negligible	Polymer impregnated concrete. Polymer concrete.

*Reference 13

The concrete classification has changed from high chloride ions penetration (>4000 coulombs) to low chloride ions penetration (2000 coulombs) when 10% of cement weight replaced by microsilica. As for the effectiveness of silica fume concrete in protecting the steel reinforcement, Fig. 3 clearly shows that it proceeded the capability of ordinary concrete and the concrete with calcium nitrite. According to modify ASTM G-109 test and the interpretation given by ASTM C-876 for corrosion risk assessment, results of the corrosion potential of the steel bars protected by the different concretes, indicated that after 48 cycles of drying and wetting with 15% sodium chloride solution, silica fume concrete continued to provide protection to the reinforcement while those protected by calcium nitrite concrete exhibited uncertain corrosion activities on their surfaces.

Performance of Epoxy Coated Rebars

Results indicated in Figs. 4 and 5 show clearly that the effectiveness of the epoxy coated rebars is reliant on the quality of the concrete cover and the condition of the epoxy coating on the steel bar at the time of use. Fig. 4 shows the effect of steel bar coating condition on the corrosion potential of the steel bar. It is clearly evidant that the epoxy coating on the steel bar (OU-50C) has improverd corrosion activities resistance compared to uncoated bars (OU-50U). Also it shows the deterioration in the corrosion potential when the epoxy coating is damaged (OU-50D), it reveals the increased corrosion activities on the steel bar. Fig. 5 indicated the effectiveness of the silica fume concrete (OUSF50D) in delaying the penetration of the chloride ions and its attack on the damaged epoxy coating. It also shows the healing effect of the calcium nitrite when creating a passive layer on the damaged epoxy coated rebars to hinder chloride ions attack and hence corrosion activities from taking place. The discussion above has drawn the attention to the effectiveness of the epoxy coated rebars, nevertheless Fig. 6 is a cause for concern and second thought when epoxy coated rebars are used. It is quite often that the monitoring and the electrochemical measuring devices used for investigating the corrosion activities, will fail to detect any damages on the epoxy coated rebars and hence overlook any change in the corrosion potential readings unless the steel bars are physically removed and visually examined. That was the reason behind the sudden failure and the deterioration which took place on 1986 in the state of Floride in USA, when application of epoxy coated rebars became very popular and expansive without precautionary measures or previous knowledge of such danger.

SUMMARY AND CONCLUSIONS

As a summary to all above, its concluded that the supplementary cementing materials such as ggbs concrete and silica fume concrete when replace certain percentage of the cement weight in the concrete mixure, they have significant effect in enhancing concrete resistivity to chloride ions penetration and hence decrease the corrosion activities on steel bars protected by such concretes. As for the epoxy coated rebars results showed concerns related to the condition of the epoxy coating layer on the bar and to their application in high chloride laden environments. On the other hand it is proven that corrosion inhibiting admixures such as calcium nitrite are more effective when used with other protection systems such as ggbs and microsilica. Accordingly conclusions can be made as following:

1. Significant imrovements in concrete performance when suplementary cementing materials are used, especially with respect to resistivity to chloride ions petration and corrosion activities.
2. Corrosion protections systems satisfy durability requirements of reinforced conctere structures in marine environment.

3. Effectiveness of the epoxy coated rebars is reliant on the quality of the concrete cover and the condition of the epoxy coating on the steel bar at the time of use.
4. Effectivness of corrosion inhibiting admixtures such calcium nitrite is highly reliant on their concentration with respect to chloride ion concentration in the same environment. Any unaccounted for increase in the level of chlorides over the nitrite ions would lead to unexpected form of corrosion on the steel bars. That why such corrosion protection system would work better in multiprotection environment.
5. It is of great importance to conduct field research studies under the actual prevailing environmental to be able to conclude more realistic results that would make practical applications of such materials and systems more effective. Studies of that nature usually requires long time that spans to 5-10 years.

ACKNOWLEDGEMENT

Gratitude and appreciation are extended to Appleby Limited Company, Kuwait Foundation for Advancement of Science, and Kuwait Institute for Scientific Research for their financial support. Also recognition and gratitude go to all the firms and companies which contributed to the research by provision of materials and assistance when needed; these are: KBRC, FOSROC, Gulf Consult, Al-Bahar & Bardawil specialities.

REFERENCES

[1] Selected Corrosion Protection Systems for Reinforced Concrete Structures in Kuwait. Kuwait Institute for Scientific Research, Kuwait.

[2] Al-Matrouk, F.; Al-Hashem A.; Al-Kharafi F.M and El-Khafif M. (1996), "Impact of metallic corrosion on the Kuwait economy before and after the Iraqi invasion: A case study". *In Industrial corrosion and Corrosion Control Technology: Proceedings of the Second Arabian Corrosion Conference*, Kuwait: Kuwait Institute for Scientific Research, pp. 567-579.

[3] Berke, N.S., D.W. Pfeifer, and T.G. Weil. 1988. Protection against chloride-induced corrosion. *Concrete International* 10(12): 45-55.

[4] CSHRP. 1992. Effectiveness of epoxy-coated reinforcing steel. Canadian Strategic Highway Research Program, Final Report.

[5] Sharafi, A. A., Shahrour M. and Chetty S. M. K. (1993), "Short-and long-term effectiveness of rebar coating system in concrete exposed to aggressive environmental conditions in the United Arab Emirates". Presented at Kuwait Society of Engineers meeting, Kuwait City, Kuwait.

[6] Gjorv, O.E. (1995), "Effect of condensed silica fume on steel corrosion in concrete". *ACI Materials Journal*, 92(6): 591-598.

[7] Tourney, P., and N. Berke. 1993. A call for standardized tests for corrosion-inhibiting admixtures. *Concrete International* 15(4): 57-62.

[8] ASTM G 109. (1992), "Test method for determining the effects of chemical admixtures on the corrosion of embedded steel reinforcement in concrete exposed to chloride environments". American Society for Testing and Materials, Philadelphia, Pennsylvania.

[9] ASTM C 1202. 1991. Electrical indication of concrete's ability to resist chloride ion penetration. American Society for Testing and Materials, Philadelphia, Pennsylvania.

[10] AASHTO T- 259. 1993. Resistance of concrete to chloride ion penetration. In *Standard Specification for Transportation Materials and Methods of Sampling and Testing*, 14th Edition. Washington DC, USA: American Association of State Highway and Transportation Officials.

[11] ASTM C 876. (1991), "Standard test method for half-cell potentials of uncoated reinforcing steel in concrete". American Society for Testing and Materials, Philadelphia, Pennsylvania.

[12] Fontana, M.; and Greene N. (1978), "Corrosion Engineering", Second Edition. Chapter 12, Corrosion Rate Expressions, pp. 377-379.

[13] Whiting, D. (1981), "Rapid determination of chloride permeability of concrete". Report No. FHWA/RD-81-119, Federal Highway Administration, Washington, D.C., p. 174.

Proceedings of the ACI-KC First International Conference & Fourth Exhibition. September 29-October 1, 2003, Kuwait — ***Concreting and High Performance Concrete in Hot Weather.***

THE OPTIMAL FILLER CONTENT GIVING THE BEST PERFORMANCES OF CONCRETE

Dr. Guemmadi Z'hor, University Mentouri Constantine, Algeria
Dr. Toumi Belkacem, University Farhat Abbas Setif, Algeria
Dr. Houari Hacene, University Mentouri Constantine, Algeria

ABSTRACT:

Concrete producers are prompted to promote the utilization of the limestone based aggregates due to the limitation on extraction of alluvial materials in Constantine and the increased transportation costs. These fine aggregates constitute the principal deposits of Constantine.

The utilization of limestone-based aggregates for filler content has shown some discrepancies internationally. As the majority of our production units use excess of fine aggregate in their production, we attempted to undertake some tests on the influence of the filler content on concrete properties.

The basic parameters studied are: the variation of the fine content (0 to 24% with a step 6%), the provenance of the sands (two sites) and the granular distribution (continuous and discontinue).

Varying these three parameters, we have measured and observed various qualities of concrete consistency, mechanical strength, shrinkage and loss in weight.

In conclusion, significant results demonstrated that we could attain the best performances with 18% of fine content. For shrinkage we registered an acceptable behavior of almost 18% from the tests.

Keywords:
Aggregates, Fines, Concrete, Granular Classes, Sand, Limestone, Shrinkage

INTRODUCTION

Until recently, the aggregates supply has never been a source of major problem in most regions of Algeria. Since then several factors have developed and environmental and other factors can be held responsible for the lack of natural resources.

This state is due to the decrease of current deposits, especially problems linked either to the environment or exploitation of resources.

Moreover, the global changes in the cost of construction, transport and material have led to new initiatives to utilize available national materials. Chalky rocks have proven useful in Algeria, notably in regions where problems of aggregates supply are the most crucial. Similarly, Constantine, Mila, Oum El Bouaghi[1], can favourably respond to the problem of aggregate supply.

However, enterprises prefer the use of alluvial aggregates from hard rocks, showing reluctance to use crushed aggregates which seem to create several problems.

These problems are mainly linked to characteristics depending on type of the aggregates. There are important contents in fine elements (more than 10%), which imply that it is necessary to add more water than for rolled aggregates based concrete to obtain the same workability of concrete. This is detrimental to concrete qualities because the concrete placement is more delicate and its mechanical performances are notably reduced.

Several researches have been conducted in Spain, France, Morocco, Algeria and other countries on the use of chalky sand containing fillers in mortar and concrete confection[2]. The results obtained from these studies show that the tolerated limit of fillers contents vary from one country to another, as shown in Table 1.

The most important problem is to know the effects of these very fine products on the fresh and hardened concrete properties[3].

The objective of this research is to present the possibility of chalky crushed aggregates used in hydraulic concrete confection and also to determine the acceptable filler content limits in sands according to the petrographic nature of the original rocks[4].

In order to prove the influence of the filler presence on free concrete deformations, we have undertaken dimensional variation measurements on test tubes containing different filler rates and exposed to the free air by measuring the shrinkage and the loss in weight.

Table 1. Limits of filler contents authorized in different countries.

R.F.A.	Canada	Italy	U.S.A.	France	U.K
< à 4%	< 3 - 5 %	< 3 - 5%	< 7%	< 10 - 12%	< 16%

EXPERIMENTAL PROGRAM

Twenty concrete mixes containing different filler rates have been reviewed, based on the mineralogical nature of the aggregates as well as the granular skeleton of the concrete and their influence on rhiological properties of fresh concrete (slump, occluded air and density), and their mechanical properties (compressive and tensile strength) measured at the age of 7, 28 and 90 days. Shrinkage and weight loss measurements were undertaken since the moulds were removed until the age of 90 days.

The sand was fully washed and then reconstituted in large proportion of filler rates (0%, 6%, 12%, 18% and 24%). Two granular skeletons have been retained (Continuous and Discontinuous:8/15 grade suppressed). The cement content was kept constant (350 Kg / m3). Initially, the quantity of water was fixed to 182 l / m3 and then adjusted gradually in order to maintain a constant workability (8 to10cm), measured on ABRAMS cone. See Table 2.

Table 2. Identification of the twenty concrete studied

N°	Notation	Designation
1	AC0	Continues granular concrete; S1 Sand with 0 % de fillers
2	AC6	Continues granular concrete; S1 Sand with 6 % de fillers
3	AC12	Continues granular concrete; S1 Sand with 12 % de fillers
4	AC18	Continues granular concrete; S1 Sand with 18 % de fillers
5	AC24	Continues granular concrete; S1 Sand with 24 % de fillers
6	AD0	Discontinues granular concrete; S1 Sand with 0 % de fillers
7	AD6	Discontinues granular concrete; S1 Sand with 6 % de fillers
8	AD12	Discontinues granular concrete; S1 Sand with 12% de fillers
9	AD18	Discontinues granular concrete; S1 Sand with 18% de fillers
10	AD24	Discontinues granular concrete; S1 Sand with 24% de fillers
11	KC0	Continues granular concrete; S2 Sand with 0 % de fillers
12	KC6	Continues granular concrete; S2 Sand with 6 % de fillers
13	KC12	Continues granular concrete; S2 Sand with 12 % de fillers
14	KC18	Continues granular concrete; S2 Sand with 18 % de fillers
15	KC24	Continues granular concrete; S2 Sand with 24 % de fillers
16	KD0	Discontinues granular concrete; S2 Sand with 0 % de fillers
17	KD6	Discontinues granular concrete; S2 Sand with 6 % de fillers
18	KD12	Discontinues granular concrete; S2 Sand with12 % de fillers
19	KD18	Discontinues granular concrete; S2 Sand with18 % de fillers
20	KD24	Discontinues granular concrete;S2 Sand with 24 % de fillers

Characterization of Constituents

The Cement: The cement used for the concrete confection is the CPJ 45 accordingly to the Algerian norm NA 442. It comes from the cement factory ERCE (EL Hamma - Constantine). The chemical and mineralogical composition of the clinker is shown in Table 3.

Table 3. Portland clinker characteristics (%)

Mineralogical composition									
C_3S		C_2S		C_3A		C_4AF			
56.60		22.98		9.78		8.25			
Chemical Composition									
SiO_2	Al_2O_3	Fe_2O_3	CaO	MgO	SO_3	Na_2O	K_2O	other.	L.O.I
27.83	6.21	3.12	57.22	0.94	2.02	/	/	2.28	2.41

The Granulates: The specimen used comes from two different sites; the first one, "S1" which is found at 25 Km South/East of Constantine in the region of El Khroub, exploiting the deposit of Djebel Oum Setta. This site is composed of great extent of Cenomanienne rock of clear beige colour, safe, with 98% of very clean tender limestone. The second site, "S2" is situated at 20 Km South/West of Constantine in the region of Ain Smara, exploiting the deposit of Djebel Felten extending to Eocene rock white to greyish colour. The rock, fissured and altered with clays, composed of 85% of limestone and 8% of silica[5].

Gravels are industrial chalky crushed products of 3/8, 8/15 and 15/25. Physical, morphological and mechanical properties are found in Table 4.

Table 4. Aggregates properties

	S1	S2	Gravel		
Aggregates Grading	0/3	0/3	3/8	8/15	15/25
Physical Properties					
Density (Kg/m^3)					
▪ Absolute	2.73	2.65	2.57	2.58	2.60
▪ Apparent	1.44	1.46	1.36	1.35	1.34
Superficial tidiness (P)	-	-	1.50	1.28	0.56
Equivalent of sand	78.67	65	-	-	-
$CaCO_3$ (%)	86	98	85	83	84
Morphological Properties					
Flattening Coefficient	-	-	18	13	17
Mechanical Proprieties					
Los Angeles (LA)	-	-	20	23	22
Micro Deval (MDE)	-	-	16	17	-

The Fillers: We designate fillers with crushed elements that have not been subjected to any processing and having a granular grade of 0/d with d equal to 80 microns[6].

The fillers come from the chalky crushed sand dust. These fillers conform perfectly to the norm (NFP 18-501), their coefficient activity is in the order of 0.5. The chemical composition and the physical characteristics of the fillers are grouped in Table 5.

The filler content has an important role on the physical sand characteristics.

Table 5. Chemical composition of fillers

SIO_2	AL_2O_3	Fe_2O_3	$Ca\ CO_3$	MgO	SO_3	LOI	PH
0.06	0.09	0.02	99	0.01	0.01	43.8	9

Influence of Filler Rate on Physical Sand Properties

Apparent Density: We notice that the apparent density increases slightly for fillers with rates between 0 and 6%, then increases continually from 6 to 18% and it stabilizes over 18%, see Figure 1. The peak compactness is obtained between 18% and 24%. These two sands follow almost the same appearance. A light difference between these two sands is observed and it is due to this fact that the sand S2 always contained a small quantity of fillers after fully washing.

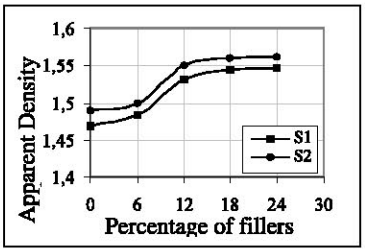

Fig.1 : Apparent Density versus fillers rate

Absolute Density: We observe that the absolute density increases rapidly for fillers with rate ranging from 0 to 12% and it increases very feebly between 12% and 18%. Then it stabilizes, as shown on Figure 2.

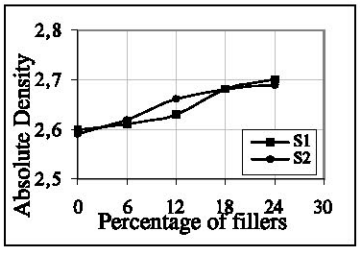

Fig.2 : Absolute Density versus fillers rate

Fineness Modulus: The fineness modulus (Fig.3) varies almost linearly with fillers rate and varies considerably between sand S1 and S2. The S1 sand is coarse and has FM equal to 3.2, adding fillers to this sand decreases FM to 75%. The FM of sand S2 varies from 2.6 to 2.3 considered proper sand according to specifications.

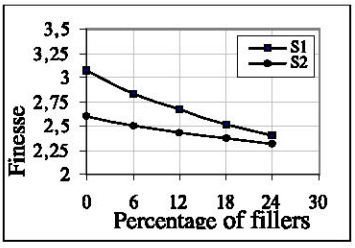

Fig.3 Finesse Modulus versus fillers rate

Piston Equivalent Of Sand: observation of Figure 4, leads us to imply that a correlation between the fillers percentage and the diminution of the equivalents of sand exists. We notice that the value of the equivalents remains superior to 65 in the interval 0 to 18% of fillers rate. For these two sands and according to the French standard the last value is the limit for the piston equivalent of sand. Over 18% of fillers rate, the value of sand equivalent decrease.

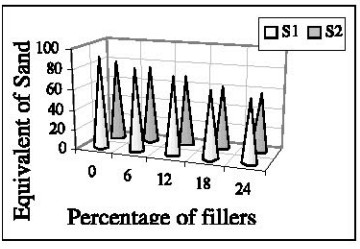

Fig.4 Piston equivalent of sand versus fillers rate

Concrete Mixture and Confection of Specimens

The method used for the concrete design is that of Dreux and Gorise[7]. Proportions of the different compositions are represented in Tables 7 and 8. Specimens have been made (mixing, placement in the moulds, tightening) according to Algerian standard[8], then conserved in water at 20°C after demoulding at the age of 24 h, until the time of the testing. The specimens destined for shrinkage and the weight loss measurements were conserved in the ambient air (60% HR, T=20°C).

RESULTS AND DISCUSSIONS:

Influence of Filler Rate on Fresh Concrete Properties

W/C: The fine elements play an important influence on the W/C. In reality, more the filler rate increases, more water is needed to keep a constant slump (see Figure 5). For a filler rate approximately equal to 18%, the demand for water becomes less important. This statement may be explained by the fact that fillers having a very important specific surface, form a colloidal microstructure that retains water until the value of approximately 18%. This observation remains valid for these two granular (continuous and discontinuous) skeletons, not taking into account the mineralogical nature of the sands.

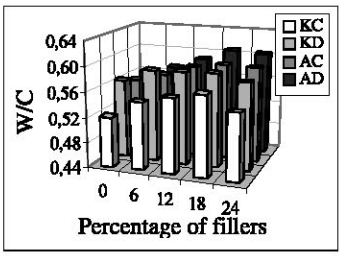

Fig.5 W/C versus fillers rate

At approximately 18% of filler rate, fillers behave as a fluidizer. According to R. Bertrandy[7] for a plastic consistency the optimal filler rate required seems to be between 8 and 12% of filler contents in the sand. In addition to this, it is necessary to consider a new parameter by allowing the fillers colloidal activity to intervene. As seen in these results:

- For a high coefficient of activity, the best workability is reached[6] with a filler rate of 8%.
- The wastage water becomes considerable for a higher coefficient of activity.

In our case (according to technical form) the coefficient of activity is equal to 0.5, which explains that we have gone until 18% to reach the optimum.

Real Density: Measures of real density in function of the fillers rate (Figure 6) show that these characteristics increase rapidly for filler rate rising from 0% to 12%. The optimal compactness is obtained between 12% and 18% of fillers where we have noticed the maximal value. Over this interval, a decrease is observed for all the curves which imply that limestone fillers have sometimes a positive and sometimes a negative influence on the density depending on their content. The different curves present a flatten bell with an optimum situated between 15% and 18% of fillers. The evolution of concrete densities based on aggregates issued from site S1 is better than those of site S2. The influence of fillers is much more steady on discontinuous aggregate concrete. This confirms the porosity effect in discontinuous granular skeleton.

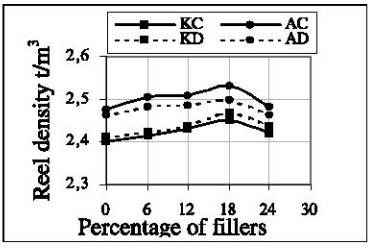

Fig. 6 Concrete reel density versus fillers rate

Occluded Air: Contrary to the variation of the real density and as shown in figure 7, the percentage of the occluded air decreases with respect to filler rate. We notice that the optimum is reached between 12 and 18% for the different curves. This verification is elsewhere confirmed by the preceding measurements of the density where we notice that in this interval, concrete structure is denser. We notice three zones:

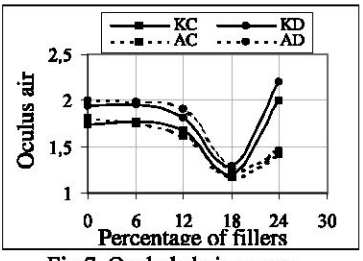

Fig.7 Occluded air versus filler rate

- From 0% to 12% of fillers, the curves are almost constant.
- From 12% to 17% of fillers, we observe an abrupt decrease.
- Over 17% of fillers, the curves increase for the site S2 in a rapid manner but for the site S1 they are slightly flat. In addition, we notice over the 18% stage there is a resumption of the occluded air. This resumption is apparently provoked by the interaction activity of cement-fillers-granulates, this statement need to be confirmed.

The Influence Of Fillers On Hardened Concrete Properties

Normalized mechanical tests have been conducted at the stages of 7, 28 and 90 days, to follow the progressive evolution of the compressive strength on cylinders 16x32cm and that of the bending traction prisms 7x7x28 cm.

Compressive Strength: The compressive strength evolution in function of the age (Figure 8) presents the same appearance for all filler rates. Globally, at 28 days the concrete compressive strength for 6%, 12% and 18% of fillers rate is superior to that of the concrete without fillers. On the other hand, for the content having 24% of fillers rate, the obtained resistance is always weaker for the two granular skeletons. Between 7 and 28 days, the increase of resistance in function of the age is appreciably linear. Over 28 days the filler effect tends to stabilise gradually until 90 days. This allows us to say, that at longer term, the contribution to the resistance becomes minimal.

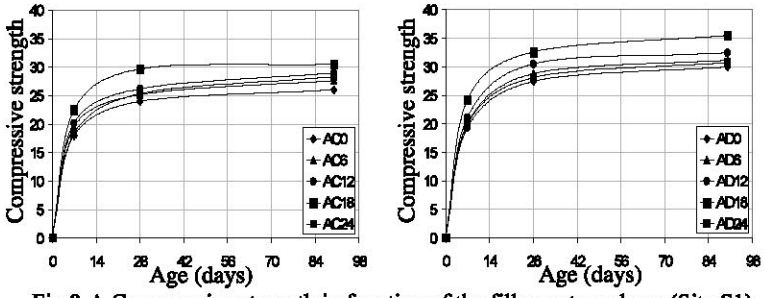

Fig.8-A Compressive strength in function of the fillers rate and age (Site S1)

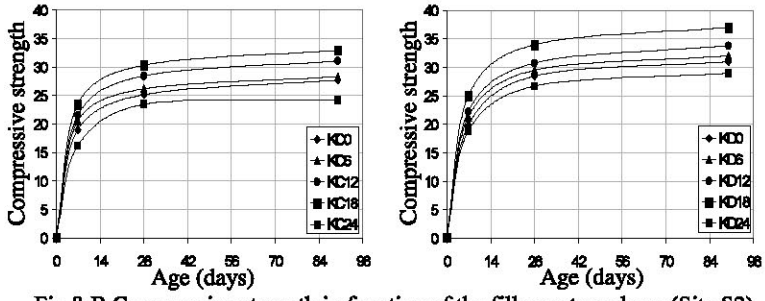

Fig.8-B Compressive strength in function of the fillers rate and age (Site S2)

The limestone fillers play, therefore, a beneficial role on the resistance until the content of 18% "the optimum value". The best compressive strength is obtained with the discontinuous granular skeleton of the site S1.

Tensile Strength: The observation of the presented values on figures 9 prompts us to deduce the same conclusion for the compressive strength. The best performance is obtained for the continuous granular skeleton of the site S2 with a filler rate of 18%, while the weakest acceptable performance is that of the concrete having 24% fillers rate.

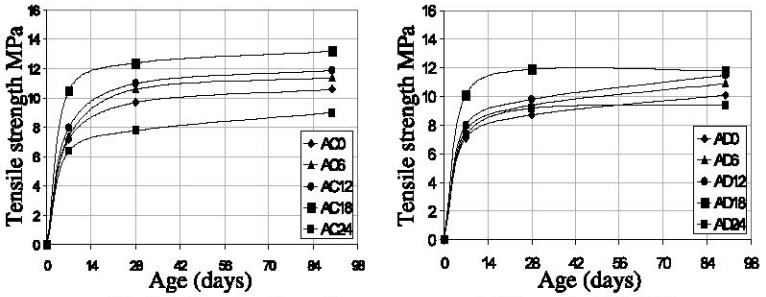

Fig.9-A Tensile strength versus age and fillers rate (Site S1)

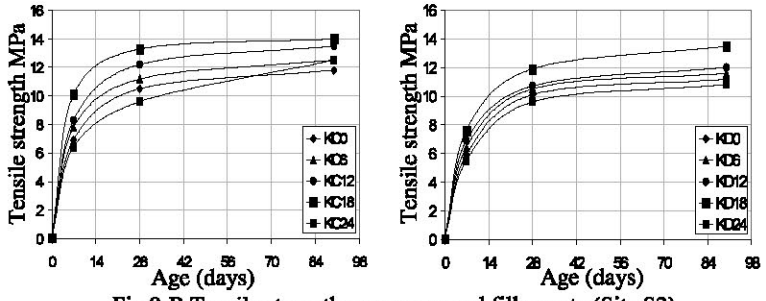

Fig.9-B Tensile strength versus age and fillers rate (Site S2)

Shrinkage And Weight Loss: We know that the shrinkage evaluation function of time, evaporation of water taken in concrete and by desiccation, by over 28 days evolution begins to stabilise. Globally, the totality representative curves obtained in our tests (figure 10), have an identical behaviour. Whereas, we notice that the withdrawal grows proportionally with the addition of the fillers. In the interval (0 to 6%) of fillers, the deformations due to the shrinkage grow in the same manner for the different curves during the first days. Over 5 days composition containing high filler percentage begins to plagiarize slowly from the weak content compositions. We have recorded that the shrinkage grows to an order of 50% from 1 day to 7 days, and 20% between 7 days to 28 days. We notice that sands with high content of fillers favour the shrinkage which is proportional to the weight loss (figure 11).

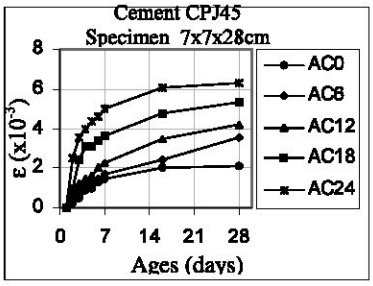

Fig.10-A Shrinkage versus the age and fillers rate (Site 1)

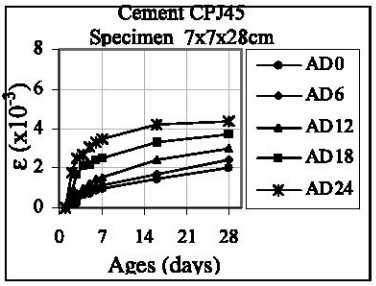

Fig.10-B Shrinkage versus the age and fillers rate (Site 1)

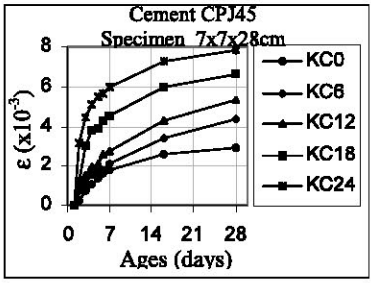

Fig.10-C Shrinkage versus the age and fillers rate (Site 2)

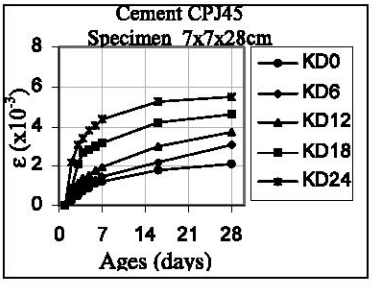

Fig.10-D Shrinkage versus the age and fillers rate (Site 2)

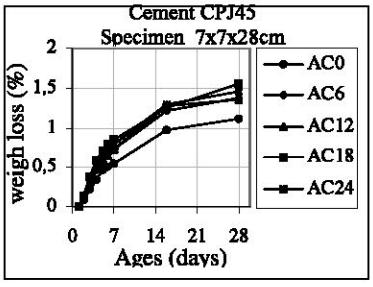

Fig.11-A Weight loss versus the age and fillers rate (Site 1)

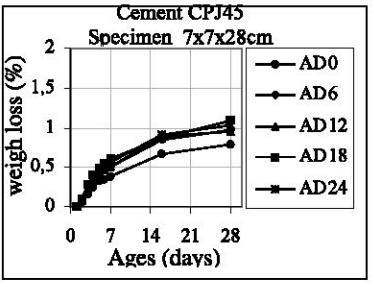

Fig.11-B Weight loss versus the age and fillers rate (Site 1)

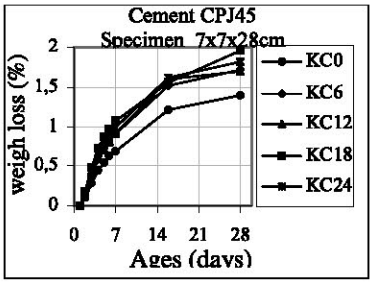

Fig.11-C Weight loss versus the age and fillers rate (Site 2)

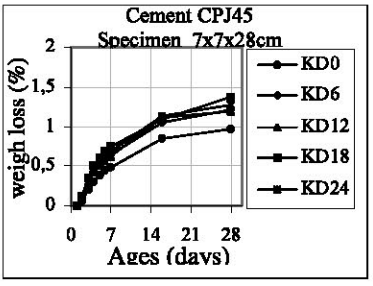

Fig.11-D Weight loss versus the age and fillers rate (Site 2)

CONCLUSION

Exploitable resources of limestone aggregates in Algeria are important. Intrinsic characteristics conform to specifications needed for hydraulic concrete. In all careers of Algeria, the fillers rate is too high (going until 30%) and dusting processing are inexistent; fully washing of sand may eliminate the fillers included in sands, which give poor resistance and reduces the concrete workability.

Mechanisms of limestone filler actions in the concrete are based on physical effects. Thus the filler particles grading of average dimensions, weaker than those of sand, contribute to identify the microstructure by reducing the matrix pore.

Fillers confer to the fresh concrete a power of water retention that allows it to resist the bleeding and provide a cohesion that maintains homogeneity (absence of segregation).

Fine grains slip between larger ones to increase the compactness and participate in the optimisation of the curve grading.

The fillers incorporation during crushing is beneficial for the concrete. The optimal content that allows obtaining the highest mechanical resistance, undertaken on a constant workability concrete, is in the order of 18% of fillers, whatever is the aggregate source and the granular skeleton. The demand for water decreases over 18% of filler rate and fillers begin to behave as a water reducing adjutant. The cement-fillers-aggregates interaction provokes a resumption of the occluded air when the filler rate is over 17%. Straight gains are linked to the improvement of the compactness obtained by the addition of fillers, and, on the other hand the straight decrease is due mainly to the increase of the W/C, the fillers effect tends to stabilise. The **optimal fillers content** that allows the obtaining of highest resistance is close to 18%.

REFERENCES

1. GUEMMADI Z., TOUMI B., HOUARI H., Enquêtes sur la maîtrise de la qualité du béton dans la région de Constantine, présenter au séminaire national de Génie Civil Sidi Bel Abbes 2001.
2. GUEMMADI Z., BENACHOUR Y., HOUARI H., Valorisation des sable de concassage, Colloque national de Génie Civil, Tlemcen, Octobre 1999.
3. GUEMMADI Z., Valorisation des granulats calcaire, contribution à l'étude du comportement du béton à base de sable calcaire à teneur en fillers variable conditions locales, thèse de Magister présenté à l'université de Constantine, Octobre 1999.
4. GLANGEAUD L., Etude géologique de la région littorale de la province d'Alger, bulletin de la carte géologique de l'Algérie 34.
4. BERTRANDY R., influence des fillers calcaires sur la maniabilité des bétons, Annales I.T.B.T.P. N° 328 Mai 75.
5. DREUX G., GORISSE F., Composition des bétons : méthode Dreux et Gorisse, Annales I.T.B.T.P. N° 414 Mai 83.
6. Normes Algériennes
7. BERTRANDY R.,Les granulats calcaires dans les mortiers et bétons, Revue scientifique et industrie pont de saint – Florent, le vieil N° 400 Juillet 68.
8. LECOMPTE A, Le couple calcaire-ciment influence de la nature du ciment sur les propriétés mécaniques de mortiers calcaires, Annales ITBTP N° 535 Juillet-Aout 95.
9. GUEMMADI Z., TOUMI B., HOUARI H., Etude du comportement du béton à base de sable calcaire à teneur en fillers variable, Colloque national de Génie Civil, Mostaganem, 13-14 novembre 2000.

Proceedings of the ACI-KC First International Conference & Fourth Exhibition. September 29-October 1, 2003, Kuwait — ***Concreting and High Performance Concrete in Hot Weather.***

DETERIORATION OF PLAIN AND BLENDED CEMENTS IN MARINE EXPOSURE

Omar Saeed Baghabra Al-Amoudi
Associate Professor
Department of Civil Engineering
King Fahd University of Petroleum and Minerals
Dhahran 31261, Saudi Arabia, (e-mail: amoudi@kfupm.edu.sa)

ABSTRACT

This study was conducted to investigate the sulfate resistance of two plain cements (Type I and Type V) and three blended cements made with fly ash, silica fume and blast furnace slag in marine environments. In addition to assessing the strength developments, the performance of these cements was evaluated by exposing the specimens to a "fresh" sea water for a period of two years and measuring the reduction in compressive strength and expansion of the mortar specimens; visual inspection, weight change of the concrete specimens; and mineralogical analysis using x-ray diffraction technique of cement paste specimens. The results of these tests indicated that deterioration due to sulfate attack was somewhat hindered on all plain and blended cements despite the high sulfate concentration in the sea water medium which is classified as "aggressive".

Keywords: Plain cements, blended cements, sulfate attack, sea water, marine exposures, performance.

1. INTRODUCTION

Deterioration of concrete in marine environments has been the subject of major concern and research since the invention of cement as a binding material [Al-Amoudi, 2002]. Due to the extensive spread of seas all over the world, as compared with the continental land available for human beings, marine structures and offshore oil facilities will grow and will continue to be made of concrete [Mehta, 1980; 1991] because concrete is not only the most economical structural material for construction of such structures, but also the most durable. The performance of concrete structures in sea water is of great importance because the durability of these structures is the most complicated system to investigate; where concrete deterioration is caused by a maze of interwoven mechanisms (i.e. chemical, physical and mechanical factors) [Al-Amoudi, 1992].

Research on durability of reinforced concrete in sea water is mostly concerned with two deteriorating actions; chloride-induced corrosion of reinforcing steel and sulfate attack on concrete [see the list of references]. The need for continued research on these aspects stems from the fact that there have been considerable changes in the physico-chemical characteristics of Portland cement in the past century, particularly in terms of C_3A and C_3S phases. Further, the addition of supplementary cementing materials, such as fly ash, silica fume and blast furnace slag, in Portland cement has significantly increased, particularly in the aggressive exposures of the Arabian Gulf. Moreover, the concentration of salts in marine exposures, particularly the sulfates and chlorides, may give the impression of a constant composition all over the world. However, Table 1 displays significant variation in the concentration of various salts, with the sea water in the Arabian Gulf being the most concentrated open sea [Al-Amoudi, 2002]. As part of a comprehensive research program initiated at KFUPM in the early 1990s to study the durability of plain and blended cements in high sulfate-chloride media [Al-Amoudi, 1992], this paper summarizes the investigation conducted to assess the sulfate attack on plain and blended cements exposed to marine environments.

Table 1: Concentration of Major Ions in Sea Water in Some Areas of the World [Al-Amoudi, 2002]

Major constituents	Concentration (mg/l) in								
	Black Sea [4]	Marmara Sea [4]	Mediterranean Sea [4]	North Sea [5]	Atlantic Ocean [5]	Baltic Sea [5]	Arabian Gulf [6]	BRE** Exposure	Red Sea
Sodium (Na^+)	4,900	8,100	12,400	12,200	11,100	2,190	20,700	9,740	11,350
Potassium (K^+)	230	340	500	500	400	70	730	400	1,350
Calcium (Ca^{++})	236	328	371	430	480	50	760	400	531
Magnesium (Mg^{++})	640	1,035	1,500	1,110	1,210	260	2,300	1,200	1,867
Chloride (Cl^-)	9,500	14,390	21,270	16,550	20,000	3,960	36,900	18,200	22,660
Sulfate (SO_4^{--})	1,362	2,034	2,596	2,220	2,180	580	5,120	2,600	3,050
Bicarbonate (HCO_3^-)	217	182	158	–*	–*	–*	128	–*	152
Total dissolved solids (TDS)	17,085	26,409	38,795	33,060	35,370	7,110	66,650	32,540	40,960
pH	7.4	7.9	8.0	–*	–*	–*	8.3	–*	6.3
Concentration ratio***	3.90	2.52	1.72	2.02	1.88	9.37	1.00	2.05	1.63

* Not reported
**Building Research Establishment, England
***Concentration of total dissolved solids compared to the Arabian Gulf sea water

2. EXPERIMENTAL PROGRAM

ASTM C 150 Type I and Type V Portland cements with a C_3A content of 8.5% and 3.5%, respectively, were used in preparing plain cement paste, mortar and concrete specimens. ASTM C 618 Class F fly ash (FA), silica fume (SF) and blast-furnace slag (BFS) were used at 20, 10 and 60% replacements by weight of Type I cement, respectively, to prepare FA, SF and BFS blended cements. An effective water to binder (w/b) ratio of 0.50 was kept invariant in all the paste, mortar and concrete specimens. In the mortar specimens, the sand to binder ratio was maintained at 2.75, while a binder content of 350 kg/m^3 and a coarse-to-fine aggregate ratio of 2.0 by weight were kept constant in all the concrete mixtures. The aggregates were 19-mm maximum size crushed limestone and dune sand from eastern Saudi Arabia.

After casting, all the specimens were covered with wet burlap in the moulds for 24 hours and, thereafter, cured in potable water for a further period of 14 days. They were then air-dried in the laboratory (23 ± 2°C) for one day before being placed in the sea water. The sea water was obtained from the Arabian Gulf beside KFUPM beach (see Table 1 for the concentration of various ions in the sea water) and was changed every month.

Cement paste specimens were used to study the effect of sulfate ions in sea water on the hydration products using X-ray diffraction (XRD) technique after 24 months of exposure to the marine environment.

Mortar specimens were used to determine the strength development in water and strength reduction and expansion due to exposure to sea water. The strength tests were conducted on 25-mm cube specimens according to ASTM C 39, while the expansion measurements were conducted on two 25×25×285 mm prismatic specimens as per ASTM C 441. Concrete cylinders, 76 mm in diameter and 152 mm high, were used to study the effect of sea water on the weight loss of concrete. See Al-Amoudi [2002] for further details on these tests.

3. RESULTS

The data on compressive strength development in all the plain and blended cement mortar specimens placed in water are depicted in Figures 1 and 2, respectively. All the cements exhibited somewhat similar strength after 14 days of curing, except the blast furnace slag (BFS) cement. After 180 days of curing, the maximum compressive strength was observed in the silica fume and fly ash cements. The strength development in BFS cement specimens, however, was the lowest at all curing periods due to the high quantity of BFS (60%) in this cement.

The reduction in strength in plain and blended cement mortar specimens exposed to sea water is plotted in Figures 3 and 4, respectively. The strength reduction was less than 20% in all types of cements after one year of exposure. After two years of exposure, the reduction in strength was in the range of 22 to 26% in all the cements except in the BFS cement which was 13%. The lowest reduction in strength in BFS cement may be attributed to their initially low strength, as was stated earlier.

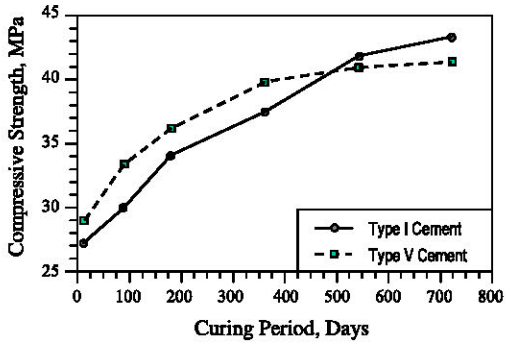

Figure 1: Strength Development of Plain Cements.

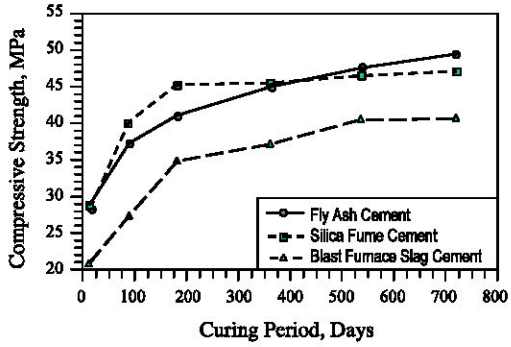

Figure 2: Strength Development of Blended Cements.

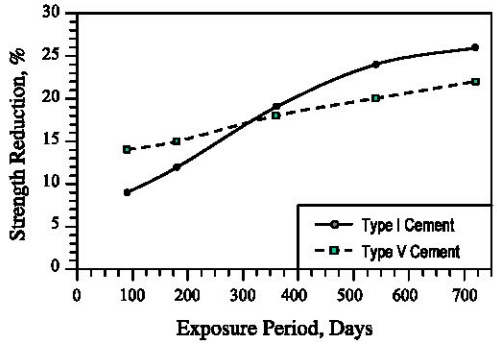

Figure 3: Reduction in Compressive Strength of Plain Cements.

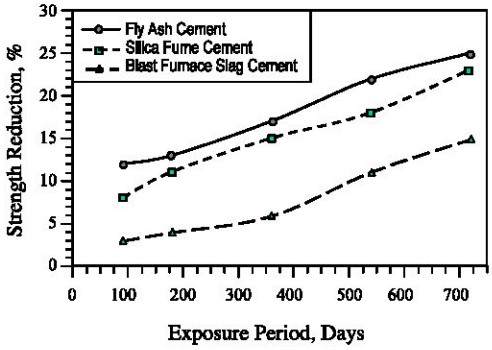

Figure 4: Reduction in Compressive Strength of Blended Cements.

The expansion data are presented in Figures 5 and 6 for plain and blended cement mortar specimens, respectively. After 540 days of exposure to the marine environment, the expansion in plain cements was more than that in all the blended cements. The better performance of blended cements could be ascribed to the dilution of the reactive cement phases (i.e., mainly C_3A and C_3S) in the parent cement due to its replacement by the pozzolanic materials [Al-Amoudi, 2002]. The maximum expansion of 0.08% was noted in

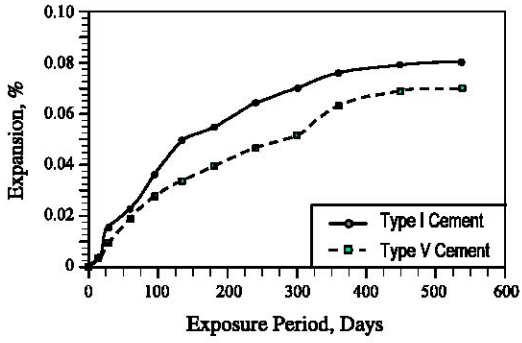

Figure 5: Expansion of Mortar Specimens Made with Plain Cements.

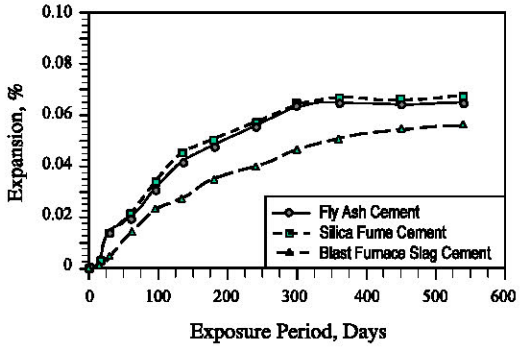

Figure 6: Expansion of Mortar Specimens Made with Blended Cements.

Type I cement after 18 months, followed by Type V cement, which had an expansion of 0.070%. The marginal improvement of Type V cement might be ascribed to its relatively lower C_3A. Among blended cements, BFS cement exhibited distinctly the lowest expansion of 0.056%. After 540 days, the expansion was about 0.067% in both FA and SF cements.

The data on weight change for the concrete specimens made with plain and blended cements are plotted in Figures 7 and 8, respectively. Surprisingly, an increase, rather than a decrease, in the weight was noted in all the concrete specimens, even after 24 months of exposure to the sea water. Visual inspection of these specimens did not reveal any type of "distinct" deterioration below or above the sea water level, as was observed in other aggressive exposures [Al-Amoudi, 1998; Al-Amoudi et al., 1994]. Only salt deposition was noted on the specimens in a way exactly similar to what has been observed on the specimens placed in sabkha (i.e., high sulfate-chloride) brines [Al-Amoudi, 1995]. The salt precipitation increased in proportion to the increase in weight. In fact, salt precipitation was noted even on the portions of the specimens above the sea water level though to a lesser extent.

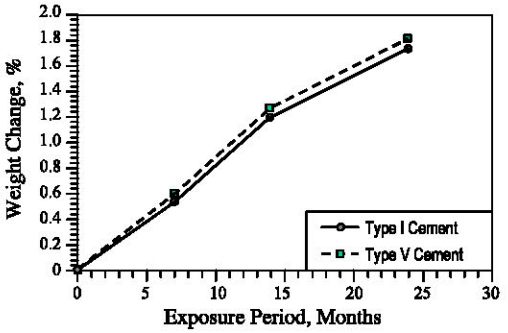

Figure 7: Changes in Weight of Concrete Specimens Made with Plain Cements.

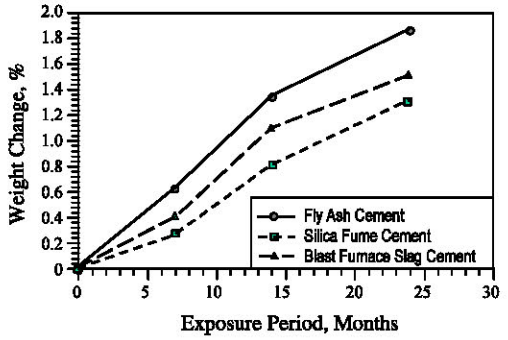

Figure 8: Changes in Weight of Concrete Specimens Made with Blended Cements.

The X-ray diffractograms (XRDs) for plain and blended cement pastes exposed to the sea water for a period of 24 months are presented elsewhere [Al-Amoudi, 2002]. The XRD data indicate that the portlandite peaks noted in the specimens cured in water were either totally

eliminated or significantly reduced when the specimens were exposed to the marine environment. Most of the peaks noted in the pastes exposed to sea water were very small; either the remnants of portlandite or gypsum or the calcium chloro-aluminate, known as Freidel's salt, or the magnesium hydroxide [Al-Amoudi, 1992]. These peaks were small and cannot be easily identified, as was noted previously in the case of the specimens exposed to a high sulfate-chloride environment [Al-Amoudi et al., 1994]. However, the formation of calcite, probably due to carbonation of cement, was noted in both the specimens cured in water and exposed to sea water.

4. DISCUSSION OF RESULTS

The data reported in this paper indicates that the maximum strength reduction noted in this investigation was about 25% in Type I and FA cements after two years of exposure to the marine media. Such a reduction can be considered as "small" for the following reasons: (i) the duration of exposure to the marine environment was relatively long (24 months); (ii) the specimen size was designed to be small (25 mm cubes) so as to accelerate the deterioration phenomena by the sulfate ions in the sea water; and (iii) the sea water had a sulfate (SO_4^{2-}) concentration of 5,120 ppm [Al-Amoudi, 2002], which is considered as severe, according to the Canadian Standard CAN3-A23.1-M77 [Mindness and Young, 1981] and ACI 318 [American Con., 1995]. The strength reduction in all the mortars was less than 30% that is generally considered as the threshold value for failure due to sulfate attack on small specimens similar to those utilized in this investigation [Al-Amoudi and Maslehuddin, 1996].

The expansion data also supports the results of strength reduction whereby the expansion of both plain and blended cements was vividly low. The expansion of all cements during the 18-month exposure to the marine environment did not exceed the 0.1% that is generally specified as the failure criterion for expansion [Al-Amoudi, 2002].

The relatively mild attack of sea water on all the cements used in this investigation is further supported by the weight change data generated by exposing the concrete specimens to sea water. As stated earlier, an increase in the weight of these specimens was noted thereby confirming the absence of noticeable concrete deterioration after two years of maritime exposure. The increase in weight was ascribed to salt penetration and precipitation that was visually noted on all the concrete specimens, both below and above the sea water level, as was discussed previously. Similar observation was noted when fifteen different concrete mixtures were exposed to a high chloride-sulfate "sabkha" solution [Al-Amoudi, 1995].

Literature review indicates that there are two forms of concrete deterioration that are ascribed to sulfate attack [Al-Amoudi, 1998]. The first mode of deterioration is akin to eating away of the hydrated cement paste and its progressive reduction to a cohesionless granular mass leaving the aggregate exposed and leading to loss of strength and reduction in weight. This mode is attributed mainly to the formation of gypsum and the non-cementitious magnesium silicate hydrate, and is known as the **acidic type** of sulfate attack. The second mode of deterioration, which is normally characterized by expansion and cracking, takes place when the reactive hydrated aluminate phases, present in sufficient quantities, are attacked by sulfate ions, thereby forming tricalciumsulfo-aluminate hydrate, also called ettringite or Candlot's salt. This **expansive type** of sulfate attack is ascribable to the formation of a colloidal form of ettringite in the presence of high concentrations of $Ca(OH)_2$ in the pore solution.

Visual inspection of the specimens exposed to sea water did not reveal any of the above two forms of deterioration during the two year exposure period. Previous studies in the 1950s and 1970s had reported excessive expansion and extensive deterioration in concrete structures exposed to sea water [Mehta and Haynes, 1975; Kalousek and Benton, 1970; Figg, 1979]. The reason for the increased proneness of old cements to expansion and spalling by sea water is probably ascribable to the high C_3A content of "old" Type I cements that were manufactured before 1950s. When the C_3A content is more than 11%, the susceptibility of concrete to expansion and cracking is significantly increased [Gjorv. 1971]. On the contrary, the present-day Type I cements often have a maximum C_3A content of about 9%. Accordingly, the expansion of Type I portland cement when exposed to sulfate media is much mitigated. The expansion characteristics are further reduced by the conjoint presence of chlorides with the sulfate salts in marine environments [Figg, 1979; Harrison, 1990]. Even if ettringite or gypsum is formed, the expansive stresses will be much reduced due to the concomitant presence of chloride ions [Lea, 1970; Al-Amoudi et al., 1994].

Considering the long-term (i.e., more than 20 years) performance of concrete, some researchers [Mehta and Haynes, 1975] reported that all Portland cements, including Type V cements with C_3A of up to 3%, will be significantly affected by sea water. The reason may be attributed to the first "acidic" type of sulfate attack, which is ascribable to the prevalence of portlandite produced by the hydration of C_3S and C_2S phases. In fact, the portlandite content is proportional to the C_3S to C_2S ratio of the cement and this ratio is responsible for the early strength development of the cement. Since the manufacturers of modern cements do care a lot about the high early strength only, they deliberately make the C_3S/C_2S ratio extremely high thereby increasing the portlandite content. Therefore, these cements will readily deteriorate after long exposure periods. The principal form of deterioration will be the gypsum "acidic" type, whereby the portlandite produced by the hydration of calcium silicate phases will react with the sulfate ions in sea water to produce gypsum according to the following reaction:

$$Ca(OH)_2 + SO_4^{2-} \xrightarrow{2H_2O} CaSO_4 \cdot 2H_2O + 2OH^-$$

To mitigate the inferior role of portlandite, it is recommended to use pozzolanic (i.e., mineral) admixtures to consume this portlandite as shown in the following "pozzolanic" reaction:

$$3Ca(OH)_2 + 2SiO_2 \longrightarrow 3CaO \cdot 2SiO_2 \cdot 3H_2O$$

In addition to consuming the portlandite, the pozzolanic reaction produces secondary C-S-H, which reduces the permeability of concrete thereby improving the sulfate resistance of blended cements. Therefore, the long-term performance of these cements, particularly those incorporating silica fume, is expected to be much better than plain portland cements exposed to marine environments, especially when the concrete mixture is to be prepared at a low water to binder ratio, similar to what is being currently used in offshore structures [Mehta, 1991].

5. CONCLUSIONS

Cement paste, mortar and concrete specimens prepared using Type I and Type V cements and Type I cement blended with fly ash (20%), silica fume (10%) and blast furnace slag (60%) were exposed to sea water for a period of 720 days. The performance of these cements was evaluated through visual inspection, measuring the reduction in compressive strength,

expansion and weight change. Based on the results developed in this investigation, the following conclusions can be drawn:

The reduction in compressive strength and expansion data indicated better performance by blended cements, particularly the BFS and SF cements. The performance of Type V cement was marginally better than that of Type I cement.

An increase, rather than a decrease, in weight was noted in all the concrete specimens. The lowest increase in weight of about 1.50% was noted in SF and BFS after two years of exposure. The weight change was 1.85% in plain and FA cements.

No signs of deterioration were observed on plain and blended cements, even though the sulfate concentration in the sea water was high. The weight loss, expansion and reduction in compressive strength were less than the threshold values reported in the literature to denote failure due to deterioration by sulfate attack, even after two years of exposure.

Considering the long-term durability performance of concrete in marine and offshore structures, SF or BFS cement can be used at a low water to binder ratio. To further enhance the resistance against deterioration by sulfate ions and/or salt crystallization, additional protective measures, such as the application of a water-resistant epoxy-based coating, may be considered.

ACKNOWLEDGEMENTS

The support provided by King Fahd University of Petroleum and Minerals is greatly appreciated. Mr. Efren Superales is acknowledged for typing the manuscript.

REFERENCES

Al-Amoudi, O.S.B. (1992), *Studies on Soil-Foundation Interaction in the Sabkha Environment of Eastern Province of Saudi Arabia*, Ph.D. Dissertation, King Fahd University of Petroleum & Minerals, Dhahran, Saudi Arabia.

Al-Amoudi, O.S.B. (1995), "Durability of reinforced concrete in aggressive sabkha environments," ACI Materials Journal, Vol. 92(3), 236-245.

Al-Amoudi, O.S.B. (1998), "Reinforcement corrosion and sulfate attack in concrete exposed to sulfate environment," Building and Environment, Vol. 33(1), 53-61.

Al-Amoudi, O.S.B. (2002), "Durability of plain and blended cements in marine environments," Advances in Cement Research, Vol. 14(3), July, 89-100..

Al-Amoudi, O.S.B. and Maslehuddin, M. (1996), "Concrete protection in aggressive media," A leader paper in: *Concrete in the Service of Mankind: Concrete Repair, Rehabilitation and Protection*, ed. R.K. Dhir and M.R. Jones. E&FN Spon, London, 139-154.

Al-Amoudi, O.S.B., Rasheeduzzafar, M., Maslehuddin, and Abduljauwad, S.N. (1994), "Influence of chloride ions on sulphate deterioration in plain and blended cements," Magazine of Concrete Research, Vol. 46(167), 113-123.

American Concrete Institute (1995), Building Code Requirements for Structural Concrete (ACI 318-95) and Commentary (ACI 318R-95), Farmington, USA.

Figg, J.W. (1979), "Chemical attack on hardened concrete, effect of sulphates and chlorides," Bulletin of the Institution of Corrosion Science and Technology, No. 75, 12-23.

Gjorv, O.E. (1971), "Long-time durability of concrete in sea water," ACI Journal Proceedings; Vol. 68, 60-67.

Harrison, W.H. (1990), "Effect of chloride in mix ingredients on sulphate resistance of concrete," Magazine of Concrete Research, Vol. 42(152), 113-126.

Kalousek, G.L. and Benton, E.J. (1970), "Mechanisms of sea water attack on cement pastes," ACI Journal, 187-192.

Lea, F.M. (1970), The Chemistry of Cement and Concrete, Edward Arnold Ltd., London, 3rd edition.

Mehta, P.K. (1980), "Durability of concrete in marine environment - A review," ACI SP-65, American Concrete Institute, Detroit; 1-20.

Mehta, P.K. (1991), Concrete in the Marine Environment, Elsevier Applied Science, London and New York.

Mehta, P.K. and Haynes, H.H. (1975), "Durability of *Concrete in Sea* water," ASCE Journal of the Structural Division, Vol. 101(ST8), 1679-1686.

Mindness, S. and Young, J.F. (1981), Concrete, Prentice-Hall, Inc., New Jersey.

Proceedings of the ACI-KC First International Conference & Fourth Exhibition. September 29-October 1, 2003, Kuwait — ***Concreting and High Performance Concrete in Hot Weather.***

ACHIEVING DURABLE CONCRETE SURFACES IN HOT CLIMATES BY THE USE OF ZEMDRAIN® CONTROLLED PERMEABILITY FORMWORK (CPF) LINERS

David Wilson, Max Frank GmbH, Germany
Shakeel Ahmad, Rezayat Trading Company Ltd., Kuwait

ABSTRACT

In hot aggressive environments improvements to concrete durability are still necessary in order to reduce annual multi-million dollar bills for concrete refurbishment and replacement. Research has resulted in new standards being developed which have involved the development of new exposure classifications with associated strength requirements, maximum w/c ratio and minimum cement content recommendations. These requirements can all be classed as "product" related. Ideally they should lead to a higher quality, more durable concrete, which will have the required design life for the prevailing exposure conditions.

Unfortunately, perfection is never achieved on site and every "process" problem that will arise, inevitably leads to significant reductions in the concrete's resistance to all aggressive elements. Hot climates exacerbate these problems. Thus, no matter what cement replacement or admixture is added to the mix, the outer 20mm of the surface will always be the worst concrete in the structure This paper reviews the problems arising from process and reviews how the use of CPF liners like Zemdrain® can offer a solution.

Keywords

Controlled permeability formwork, durability, curing, blemishes, cover, product, process, carbonation, chloride ingress, micro-organisms.

INTRODUCTION

The quality of the outer 20mm of the concrete cover zone is not determined by the cement content and w/c ratio of the mix, but is largely determined by:

- the use of impermeable formwork face contact materials which trap excess air and water at the formwork/concrete interface
- the use of release agents whose residues contaminate the concrete surface
- the quality of compaction
- the quality of curing
- the overall quality of workmanship

The above process problems are exacerbated in hot and aggressive environments due to:

- arid regions with bright sunshine and little cloud cover
- long spells of hot weather
- peak temperatures above 50^0C
- varying humidity levels and dry blistering winds with significant speed fluctuations

Reductions in surface quality due to the above can be quite significant and can have a dramatic influence on the theoretical design life of any structure. Detailed analysis of the problems arising from process demonstrates conclusively that the use of CPF improves the quality of the outer 20mm of the surface helping to overcome most of these problems.

EFFECTS OF PROCESS ON FINISHED CONCRETE SURFACES

The effects of a harsh environment combined with process problems can significantly effect the properties of the concrete surface up to a depth of 20mm. The use of oiled impermeable formwork face contact materials, such as plywood, steel and plastic, results in water gain, cement reduction and trapped air bubbles in this critical zone.

1. Surface Blemishes

Blemishes that can normally occur on a concrete surface, as a result of process problems have been well documented, (Monks 1981). Blemishes attributed to the excess air and water normally trapped at the concrete/formwork interface include: -

- blowholes and pinholes
- scouring, crazing and plastic cracking
- dusting, retardation and oil discolouration

Each of the above reduces surface quality and durability by making the concrete more susceptible to early age weathering and to the ingress of deleterious agents.

2. Contaminated Surfaces

Biological growth thrives on a porous surface with blowholes and contaminated with release agent residues. This is particularly the case in hot environments with cycles of wetting and drying. Independent research, (Franke 1993) has shown that residues of oil/release agents used with impermeable faced formwork can penetrate up to 5mm into such a concrete surface. These chemicals are not subject to UV degradation once they are away from the surface inside

the blowholes or pinholes. The residues of release agent not only provide nourishment for bacteria and fungi, but may also contaminate the water supply and affect the performance of applied coatings and surface penetrants, (Price 2000).

3. Surface Cement Content and Porosity

In the outer 20mm of the surface, the type of formwork face contact material used determines the porosity, w/c ratio and cement contents. A UK government sponsored research project; (Dhir 1999) involved laboratory plus in-situ testing on twelve construction sites. It was found that that surface cement content was typically reduced by up to 40 kg/m^3 below design values whilst porosity and w/c ratio were increased by up to 25%. This was irrespective of cement types (PC, GGBS, PFA, silica fume), the mix strength (25 to 60 N/mm^2) and the type of admixture (water reducers, superplasticisers, pore blockers, air entrainment) used and formwork orientation. The combination of reduced cement content and minimal surface blemishes leads to a surface with an increased porosity and reduced resistance to chloride ingress, expansive slats, chemical attack, abrasion and carbonation.

4. The Importance of Curing

The curing affected zone is judged to vary between 20 and 50mm depending upon the type and duration of curing employed. Adequate curing is, arguably, the most critical of all construction operations as regards concrete durability, unfortunately, as detailed in many learned journals it is rarely carried out effectively, (Price 1998). All the benefits of correct specification of materials and high standards of mix design and construction practice can be lost if curing is not properly carried out. The hot, dry and windy environment in the region necessitates the very highest standard of curing that can be obtained.

It is well known that good curing practice improves the performance of the concrete surface by reducing porosity and increasing resistance to carbonation, chloride ingress and abrasion. Curing is known to be particularly beneficial for concretes with cement replacements, including PFA, GGBS and Microsilica and in hot climates, (Walker 2002). The porous surface produced by conventional oiled formwork facilitates an immediate significant moisture loss upon formwork removal. The inevitable time delay between formwork removal and installing a curing regime result in less effective curing.

5. The Importance of Cover

The quality and depth of cover is always critical, but perhaps more so in aggressive environments. Surveys of in-situ structures in various areas across the world have revealed that it is almost impossible to consistently achieve the design cover, with shortfalls of 10 to 15mm below minimum common, (Slater 1999). This reduction in cover combined with the poor quality outer 20mm arising from process problems, results in premature reinforcement corrosion, even for well designed and placed mixes.

6. Summary

The majority of engineers make the erroneous assumption that the covercrete produced by conventional impermeable faced formwork will always be of the same durability and quality as the heartcrete. As the above has shown this is not the case, the worst concrete in any structure will always be at the surface, precisely the area where the best concrete is needed.

The only sector of the concrete industry to formally recognise this problem are the coating companies. Reference to their installation guidelines shows that they regard conventionally cast surfaces to be of low quality. They normally recommend that non-visible surface contaminants such as laitence, efflorescence, form release agents and curing agents must be removed prior to coating as part of normal surface preparation.

Damage to the long-term durability of concrete resulting from process problems should not be underestimated. However, in the main little attention is paid to process, this is remarkable since problems resulting from process are probably now the main factor in reducing concrete durability. Since water gain at the surface is primarily a function of the formwork type, we would appear to be wasting our time and money trying to solely treat the symptoms of poor durability, by improving the product, rather than one of the real causes namely process. The introduction of Controlled Permeability Formwork (CPF) liners like Zemdrain® is at last giving engineers the ability to address and overcome these process problems.

CONTROLLED PERMEABILITY FORMWORK (CPF)

CPF systems generally consist of a combined filter and drain supported by a rigid backing. Most currently available systems consist of a textile liner or a composite filter/net supported by conventional formwork. A more detailed explanation of the different types of CPF liner is contained in CIRIA Report C511, Controlled Permeability Formwork, (Price 2000).

1. What is Controlled Permeability Formwork?

A CPF liner is generally a one or two layer system composed of a specially engineered filter fabric laminated to a grid or drainage fabric. Product thickness is generally less than 2.5mm. The filter fabric should have a pore size of less than 0.050mm to help retain the majority of cement fines, whilst permitting the controlled removal of excess air and water from the concrete/formwork interface. Absorbency of liners should be minimal to prevent too much water being removed, which could be detrimental to the surface when using low w/c mixes. A maximum absorbency of 0.1 litres/m^2 for liners has been suggested. The purpose made CPF liners retain water within their structure to aid with early curing. These two aspects are important, as an absorbent dry liner would tend to suck water from the hydrating surface.

Liners are generally tensioned over conventional formwork surfaces using staples or other fixing devices. Release agents should never be used with CPF liners, either on the backing or on the liner itself. Once attached to the formwork, concreting is performed in accordance with local practice. The number of uses for a liner will depend upon the type of liner and the expected benefits. As an example from the CIRIA report it is recommended that Type II liners can be used once, whilst Type III liners can be used 2 to 3 times for durability applications.

2. The Benefits of Using CPF

During the compaction process, the CPF liner retains the majority of the cement fines, whilst allowing excess water and air to escape from the concrete/formwork interface. This avoids any water gain at the surface and results in a reduction in w/c ratio and an increase in cement content in the outer 20mm, (Figure 1). The removal of the air also virtually eliminates the formation of blowholes and pinholes. Some of the drained water also remains within the structure of the Zemdrain® and as long as it is in place the liner acts as a curing membrane.

The properties of the resulting concrete are significantly improved over those of a conventionally cast surface, (McCarthy 2002).

MINIMISING PROCESS PROBLEMS

Using a controlled permeability formwork liner such as Zemdrain® helps to overcome many of the process problems that can arise during construction resulting in:

- virtual elimination of blowholes and other surface blemishes
- no surface contamination as release agents are no longer required
- surface cement contents are increased and w/c ratio and porosity are reduced
- a well cured surface with the liner acting as a curing membrane
- improved durability properties equivalent to an extra 15 to 20mm of cover

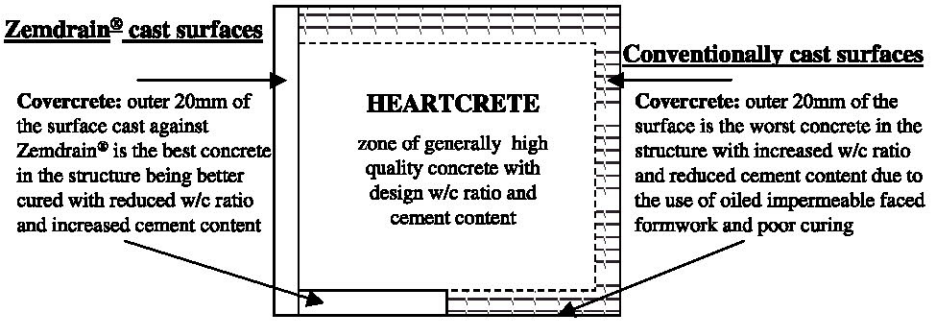

Figure 1. The benefits of using a CPF liner

1. Virtual elimination of Surface Blemishes

CPF liners permit the controlled removal of excess air and water that always accumulates at the interface between impermeable formwork face contact materials and the concrete. Hence, the blemishes that normally arise from air and water gain are largely for eliminated both vertical and top sloping formwork, (Monks 1999). An added benefit is that the absence of holes in the surface reduces the opportunities for expansive salts to gain entry. Examination of lightly sand blasted Zemdrain® cast surfaces show that proportionately fewer blowholes are revealed. Figure 2 shows the blowhole count for a typical C35 concrete, (Aitcin 1999).

Blowholes Size (mm)	Approximate number of blowholes per square metre			
	Vertical section		Negative slope section	
	Control	Zemdrain®	Control	Zemdrain®
> 10mm	-	-	-	-
5 to 10 mm	± 40	0	± 150	0
2 to 5 mm	± 200	± 2	± 200	± 2
< 2mm	± 100	0	± 100	0

Figure 2. Blowhole Count

2. No Surface Contamination

The use of release agent results in contamination of the concrete surface. The combined benefits arising from using Zemdrain®, including not using release agents, a low porosity surface with increased cement content and minimal blemishes, result in a surface, which reduces the risk of contamination by organic species, (Price 2000). This surface is hostile to bacterial growth in marine environments and in water retaining structures.

Inspection and testing of a 7 year old sea wall has shown that for the inter tidal and splash zones, algae growth on a Zemdrain® cast surface is minimal, whilst the conventionally cast surface has been heavily colonised, (McCarthy 2002). Several structures in water plants have been examined after 6 to 7 years in operation and they also show negligible algae growth in wet/dry environments on the Zemdrain® cast surfaces, which is not the case for surfaces cast against oiled steel or plywood faced formwork.

3. Porosity, cement content and w/c ratio

The capillary porosity of concrete from 10 sites was measured and is shown in Figure 3. These results cover a variety of mix strengths (35 to 60 N/mm^2) with cement replacements (GGBS, PFA and silica fume) and admixtures. The results show clearly the difference between the Zemdrain® and the control surface, up to 40% reduction, but also how the porosity is lower than in the centre. This reduction in porosity helps to further explain the increased resistance of the concrete surface to algae growth.

It has already been demonstrated that the outer 20mm of the surface cast against oiled impermeable faced formwork always shows a reduction in cement content and an increase in water/cement ratio for all conditions. These results are applicable irrespective of mix strengths (35 to 60 N/mm^2), cement replacements (GGBS, PFA and silica fume), admixtures used or formwork orientation. The reverse is true for surfaces cast against Zemdrain®; there is a gain in cement content and a reduction in water/cement ratio, (Dhir 1999). The nett increase in cement content over that for a surface cast against an impermeable face contact material is up to $100kg/m^3$, with reductions in w/c ratio of up to 45%. Figure 3 shows this effect for ten construction sites. Combined with the reduced porosity, the resulting surface has improved resistance to all forms of environmental attack, not only to ingress of aggressive elements but to the effect on surfaces of expansive salts.

Experiences in waste water treatment works, where conditions can be very aggressive, have shown that after 6 years exposure to an acid environment, a Zemdrain® cast surface remained largely unaffected, whilst the conventionally cast surface showed significant acid etching. In two covered potable water tanks, which have been in operation for 7 years, significant differences were noted between the columns cast with oiled steel and plywood formwork and the Zemdrain® cast walls. The walls remain unaffected, whilst for the columns, the blowholes have reopened and the surface is sandy and slimy to the touch due to soft water attack and the dirt adhering to the non Zemdrain® cast concrete. Thus demonstrating the difference in quality and durability of the two surfaces.

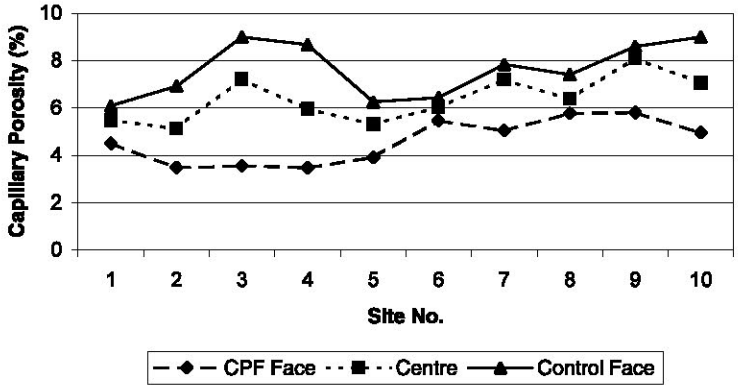

Figure 3. Capillary Porosity.

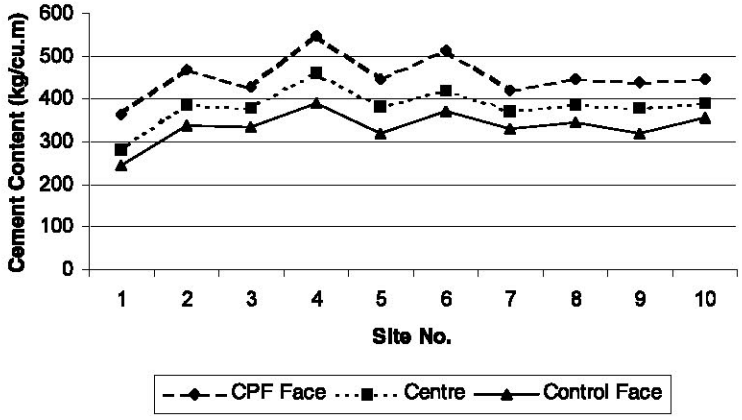

Figure 4. Cement Content.

4. Curing

It is to be expected that the highly porous surface produced by oiled steel or plywood faced formwork will result in a rapid loss of moisture upon formwork removal unless a curing regime is put in place immediately. As has been widely documented, this is very rarely, if ever achieved. The surface produced by Zemdrain® as shown in Figure 3 has a low porosity that ensures there is no rapid loss of moisture upon formwork removal. Even without additional traditional curing, the result is a well-cured surface.

In addition, some of the water drained from the concrete is retained within the liner. This water is then available to be reabsorbed by the hydrating concrete during the critical first 24 hours of the life of the structure. The benefits of the curing affect of Zemdrain® are shown in

Figure 5. Some researchers have stated that the effect is to largely desensitise the concrete to the effects of inadequate curing. These benefits are more obvious in harsher hotter climates. The recently published "Guide to the construction of reinforced concrete in the Arabian Peninsula" states that, "when CPF is used the resultant concrete surface is of a significantly higher quality than that produced by normal formwork and sensitivity to curing is reduced. It may, in future, be possible to use slightly shorter curing periods with CPF", (Walker 2002).

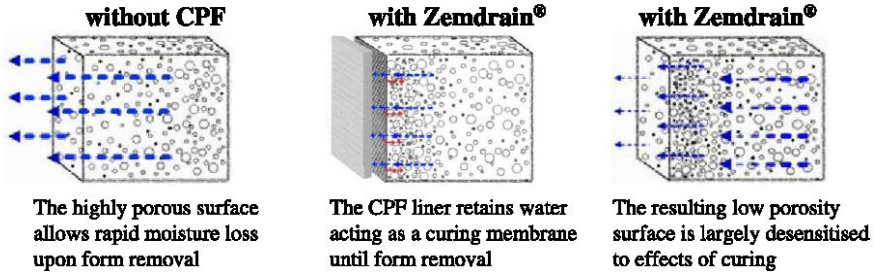

Figure 5. Curing - the Zemdrain® effect

5. Cover

The problem of achieving design cover is well documented. An acceptance that it occurs has been demonstrated by the increase in the depth of design cover with time. Despite the use of covermeters and better quality spacer blocks, it remains difficult to achieve the specified cover. Research on CPF at Dundee University has concluded that for chloride ingress, by using CPF, the equivalent benefit to the concrete is the same as an extra 15 to 20mm of cover or an increase in grade of approximately 15 kN/mm^2, (McCarthy 2001). Thus, CPF acts as an extra security that even if you fail to achieve design cover through process problems, the required level of durability will be maintained. The same report concluded that, other durability concerns are virtually eliminated by the use of Zemdrain® formwork liners.

6. Performance in Harsh Environments

Reinforced concrete structures in hot climates often deteriorate much more rapidly than structures in more temperate regions. In hot/wet and hot/dry environments the increased presence of chlorides in the atmosphere is particularly harmful to concrete. Laboratory work on simulated hot climate conditions has shown that for concrete cast against Zemdrain®, all measures of durability are improved, (Price 1992). The effective chloride diffusion coefficient is generally reduced by more than 50%.

Results from in-situ tests in the United Arab Emirates, (Wimpey 1995) have demonstrated the benefits of using Zemdrain® over a relatively short period of time. The concrete panels were composed of 50% PC / 50% GGBS, with a water/cement ratio of 0.4. Figure 6 illustrates the significant reductions in chloride levels with depth. The initial curing benefits of Zemdrain® tend to desensitise the concrete to the normally inadequately applied traditional curing. The reduced porosity surface that is produced means that Zemdrain® use will be of benefit irrespective of the type of mix, type of cement replacement or admixture that is used.

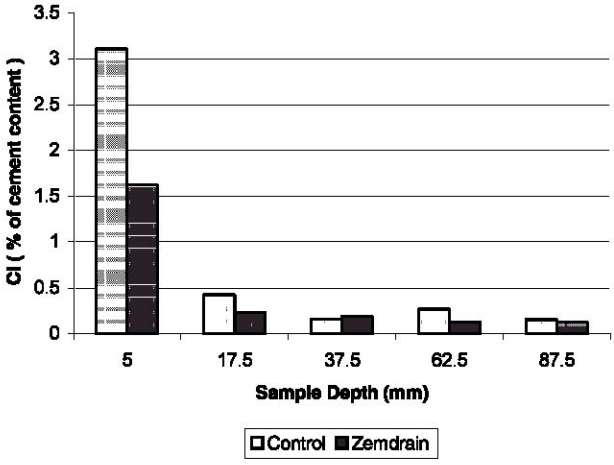

Figure 6 Chloride ingress under harsh conditions

7. Longer Term Performance

The oldest sites on which use was made of Zemdrain® in the concrete works have been in service for over 12 years. A variety of sites representing the main application areas have been revisited worldwide. Bridges, marine, water and wastewater structures have been visually inspected and in some cases in-situ testing performed.

- Bridge structure report: "The results of this investigation at the middle pier south face of Dock Street Bridge would suggest that, after 7 years in service the durability properties of concrete cast using Zemdrain® formwork lining remain considerably better than those of the concrete cast against normal plywood shuttering", (Rankin 1999).

- Sea wall report: "Marine growth was greatest on the reference (non CPF) concrete", (Dhir 1999). "The results showed that the use of CPF reduced chloride ingress by 40% at the surface to 80% at depth for both splash and inter tidal zones". "Comparisons with related laboratory data suggest that the benefits of CPF are maintained under aggressive exposure conditions and are equivalent to increasing cover depth by 15-20mm", (McCarthy 2002).

- Several potable water and wastewater structures were visually inspected after they had been in operation for up to 7 years. Inspection of structures in mild to medium aggressive conditions in several potable and water treatment plants, showed there was no visible degradation of the Zemdrain® cast surfaces which remained clean and intact. For traditionally cast surfaces, evidence of erosion was noticeable and strong algae growth was very pronounced in the wet/dry zones. The conditions prevalent in some wastewater and sewage applications can be very aggressive to concrete. At the sites investigated, both Zemdrain® and non CPF cast surfaces displayed erosion. However, the deterioration to the traditionally cast surface was at a much more advanced stage and indicated that the expected life of the Zemdrain® cast surface would be significantly longer, (Wilson 2002).

SUMMARY

It has been demonstrated that CPF use is effective in most concrete construction applications. Liner use is compatible with and complementary to cement replacements, admixtures, coatings and penetrants. In hot regions where climatic conditions are such that effective curing is often extremely difficult, the use of CPF also has significant practical advantages for producing durable reinforced concrete structures.

By negating many of the problems arising due to process, CPF gives the engineer working with concrete the opportunity to:-

- use inclined and vertical formwork, but still avoid virtually all surface blemishes
- minimise unsightly algae and micro-organism growth in wet/dry environments which affect all structures in water such as in inter-tidal zones and water holding tanks
- minimise the effects of expansive salts and acid attack in all structures reducing cleaning, maintenance and refurbishment costs
- ensure maximum resistance to aggressive elements (chlorides, carbonation, sulfates, etc.)
- ensure that surface penetrants are fully effective
- avoid the need for sand blasting and faring coats prior to coating application

The use of CPF is not the only method available for improving process. Other techniques can help, however, they only partially address individual problems and do not give the overall improvements to be expected from using CPF. Obviously using a CPF liner does not directly tackle problems arising from misplaced reinforcement and poor compaction. Design and workmanship issues not discussed above are not influenced by the use of a liner.

CONCLUSION

Deficiencies in the finished concrete surface are mainly due to process. Aggressive environmental agents can then more easily degrade surfaces. Using a CPF liner in place of conventional oiled impermeable faced formwork avoids process problems and improves the quality and durability of the concrete surface. The use of CPF is now included in national standards, (BSI 2002) and other publications, (BRE 2002). CPF has been described by a prominent engineer as possibly "the most significant step forward during the past 25 years in enhancing concrete durability", (Rostam 1995). When will industry take up this technology?

REFERENCES

Report: Aitcin, PC and Dallaire, E (1999). "Evaluation of Zemdrain MD formliner. Report from University of Sherbrooke, Canada, unpublished.
Digest: BRE, (2001), "Special Digest 1: Concrete in aggressive ground".
Standard: BSI, (2002), "BS8500-1:2002. Concrete Complementary British Standard to EN206
Report: Dhir, RK, McCarthy, MJ, and McKenna, PA (1999), "Total design using controlled permeability formworks". University of Dundee Report CTU 1399
Report: Franke, P, (1993), "Micro-organisms on concrete surfaces". LGA Nuremberg
Report: McCarthy, MJ, Giannakou, A and Jones, R. (2001), "Specifying concrete for chloride environments using CPF". Materials and Structures, Vol.34, November 2001
Article: McCarthy, MJ, Giannakou, A and Jones, R. (2002), "Tackling chloride ingress and corrosion: the role of CPF". Concrete Magazine, February 2002

Book: Monks,W.(1981). "Appearance Matters 3. Control of blemishes in concrete". BCA,
Book: Monks,W.(1999). "Plain formed concrete finishes". Concrete Society Report No. 52.
Proceedings: Price,WF and Widdows,SJ (1992). "Durability of concrete in hot climates: benefits from permeable formwork. Concrete in Hot Climates: Proc. Third RILEM Conference, Torquay 1992. London, E&FN Spon. pp.207-212.
Report: Price,WF (1998). Curing Concrete. Current Practice Sheet No.112. Concrete Society.
Book: Price,WF (2000). "Controlled Permeability Formwork". CIRIA C511.
Report: Rankin,GIB AND Cummings,SJ. "In-situ evaluation of surface properties of concrete cast using Zemdrain formwork liner". Dock Street Bridge, Belfast, 1999
Article: Rostam,S (1996). "High performance concrete cover". Construction and Building Materials, Vol. 10. No. 5. pp407-421, 1996
Proceedings: Slater,D and Sharp, BN (1999). "Specification for maritime structures". Controlling Concrete Degradation Conference, Dundee, Scotland, 1999.
Book: Walker,M (2002). "Guide to the construction of reinforced concrete in the Arabian Peninsula". CIRIA / Concrete Society publication
Proceedings: Wilson,DJ (2002). "Improving concrete quality and durability without using chemicals". WCCMS 2002, Kuala Lumpur, Malaysia
Report: Wimpey Al-Futtaim, (1995). "Zemdrain trials in the UAE, Reports 9035/9036",1995.

Proceedings of the ACI-KC First International Conference & Fourth Exhibition. September 29-October 1, 2003, Kuwait — ***Concreting and High Performance Concrete in Hot Weather.***

UNTREATED PHOSPHOGYPSUM AS A SET RETARDER FOR SLAG CEMENT PRODUCTION

Hamdy El. Didamony, Faculty of Science,
Zagazig University, Egypt
Saleh M. Abd El.Aleem, Faculty of Science,
Cairo University-Fayoum Branch, Egypt
Magdy A. Abd El.Aziz, Faculty of Engineering,
Cairo University-Fayoum Branch, Egypt

ABSTRACT

The utilization of large amounts of by-products and waste materials plays a very important role in solving ecological problems. Phosphogypsum is a waste product of the phosphoric acid. About to 200,000 tons of phosphogypum are annually produced in Egypt and cause serious storage and environmental problems. Phosphogysum is a rich source of calcium sulphate carrying impurities of phosphates and fluorides. This work aimed to evaluate the effect of substitution of natural gypsum by phosphogypsum on the hydration behavior as well as the physico-mechanical properties of slag cement. The natural gypsum was partially substituted by phosphogypsum in the ratios 2.0, 4.0 and 6.0 wt., %.

The different prepared mixes were hydrated up to 90 days. The hydration was followed and the physico-mechanical properties were estimated. The results revealed that, phosphgypsum accelerates the rate of hydration and enhances the mechanical properties of the investigated mixes, especially at later ages of hydration. It can be concluded that, phosphogypsum is more effective set retarder than natural gypsum and can be successfully used for slag cement.

Keywords :

Natural gypsum, phosphogypsum, hydration behavior, GBFSC, physico- mechanical characteristics.

1. INTRODUCTION

In the cement industry, gypsum is added into the clinker in order to delay the rapid reaction between C_3A and water. There is an optimum gypsum content which imparts the cement maximum strength and minimum shrinkage without excessive expansion. An excessive amount of gypsum will have an adverse effect on the mechanical properties of the cement due to the formation of ettringite in large amounts leading to internal cracking.

Conventionally, natural gypsum is used as a retarder, however, in some countries, because of the lack of natural gypsum or ecological necessities, new sources of gypsum , i.e., by-product gypsums are utilized in cement manufacture, such as phospho-, fluoro- boro-, titano-, tartaro-,citro- and desulpho gypsum[1]. Early hydration behavior of portland cement containing various chemical gypsums were investigated[2] . It was found that, more ettringite was formed on hydration with these gypsums and compressive strength development was satisfactory.

About 200000 tons of phosphogypsum as an industrial waste by-product of phosphoric acid manufacture are annually produced in Egypt and leading to serious storage and environmental problems. Phosphogypsum is a rich source of calcium sulphate carrying impurities of phosphates and fluorides[3].

Most of the researches have focused on the use of phosphogypsum in the manufacture of portland cement because it contains some impurities that may affect the setting properties of cement but does not change strength development[4]. Efforts have been made in several countries to use phosphogypsum in making cement[5], gypsum plasters[6], building products[7] and binders[8].

It was also proposed to add phosphogypsum directly into the raw mix of cement before clinkering to lower the temperature for clinker formation, as well as a retarding effect were reported[9]. The influence of phosphogypsum on the hydration of portland cement and trass cement was investigated[5]. It was concluded that, untreated phosphogypsum can be used as a retarder directly in trass cement, whereas portland cement requires purified phosphogypsum.

The granulated blast furnace slag is made by rapid quenching of molten slag formed during the manufacture of pig iron. The ground slag is capable of setting and hardening on its own with water but at a slow rate and therefore, it is used with portland cement for the production of portland slag cement. Granulated slag is hydraulically very weak due to its glassy structure. Therefore, a highly alkaline medium is required in order to disintegrate the silicate-aluminate network of the slag glass. Portland cement clinker is normally used to provide this alkalinity[10,11]. Also, the alkalinity can be provided by hemihydrate or phosphogypsum. The later activates the hydration of slag, because phosphogypsum contains phosphates and fluorides in addition to $Ca\,SO_4$.

The present work aims to study the effect of substitution of natural gypsum by untreated phosphogpsum on the hydration behavior as well as the physico- mechanical properties of ordinary portland and slag cements.

2. EXPERIMENTAL TECHNIQUES

The materials used in this investigation were ordinary portland cement clinker (OPCC), granulated blast furnace slag (GBFS), and natural gypsum (NG) provided from Beni Suef Cement Company. Also, phosphogypsum (PG) was used and provided from Abo-Zaabal Fertilizers and Chemical Industries company, Egypt. The surface area of the clinker and granulated slag were 3000 and 3050 cm^2/g respectively. The natural and phosphogypsum were sieved through 90-μm sieve. The chemical analysis of these materials is given in Table (1). The dry mixes were prepared as shown in Table (2).

The ingredients of each mix were homogenized on a mechanical roller in a porcelain ball mill for one hour to assure complete homogeneity. Each cement was continuously and vigorously mixed with water using ordinary gauging trowels on a steel plate for three minutes. The water demand for standard consistency and setting times were determined according to ASTM specifications[12,13]. The different mixes were mixed with water of consistency and pelletized for the determination of free as well as combined water, apparent porosity, bulk density and free lime. The compressive strength was measured on cement mortars according to ASTM specification[15] using 50 mm cubes. The specimens were cured in a humidity champer at 25 ± 2 °C for one day, then demolded and cured under tap water till the time of testing 3,7,28 and 90 days.

The bulk density of cement pastes, d_p, was determined through weighing the hardened paste, submerged in water(suspended weight) and in air (saturated weight) as follow:

$$\textit{Bulk density } (d_p) = \frac{\textit{Saturated weight}}{\textit{Saturated weight} - \textit{suspended weight}}$$

The apparent porosity, ε, was determined by the determination of bulk density, d_p, the evaporable and total water contents (W_e & W_t) of the hardened cement pastes as in the following equation[16]

$\varepsilon = 0.99\, W_e \times d_p \times 100 / (1+W_t)$, 0.99 is the specific volume of free water.

For estimation of free, combined and total water contents at any curing time, a weight of the saturated sample was ignited at 1000 °C for one hour to determine the total water content (W_t). At the same curing time, the hydration of another sample was stopped by pulverized 10 g of representative sample in a beaker containing methanol acetone mixture, then mechanically stirred for one hour. The mixture was filtered through a gooch crucible, G_4, and washed with ether[15]. The solid was then dried at 70 °C for one hour to complete evaporation of alcohol. The dried sample was put into an air tight container. The combined water content (W_n) was determined from the ignition loss of the dried cement paste on the ignited weight basis. The free water content, (W_e) was calculated as:

$$W_e, \% = (W_t - W_n), \%$$

The free lime content of each cement paste at any curing time was determined as described elsewhere[17].

3 RESULTS AND DISCUSSION

3.1 Optimization of natural gypsum

In order to determine the optimum amount of natural gypsum as set retarder for slag cement, different amounts of gypsum 2.0, 4.0, 6.0 and 8.0 wt, % were mixed with 60 % clinker and 40 % slag to produce GBFSC. The cement blends were mixed with the water of consistency and cured in tap water up to 90 days. The values of water of consistency and setting times of the investigated GBFSC pastes are presented in Fig. (1). It is clear that, the water of consistency increases and the setting is retarded with the gypsum content. The increase of water of consistency with the amount of gypsum is mainly due to the formation of calcium sulphoaluminate hydrates either ettringite or monosulphate which need more combined water than those of calcium aluminate hydrate. Also, the setting time is retarded by the increase of gypsum content due to the formation of calcium sulphoaluminate hydrates around the C_3A grains which retards the fast setting of C_3A [16].

The compressive strength of the cement mortars as a function of curing time is plotted in Fig. (2). The compressive strength of all cement mortars increases with curing time due to the formation of hydration products which fill some of the open pores of the cement mortars and then the strength increases. It is clear that, the compressive strength of the cement mortars increases with the gypsum content up to 6.0 %, especially at latter ages of hydration then decreases at 8.0 % gypsum. This is mainly due to the formation of increased amounts of sulphoalumonate hydrates which affect the mechanical properties. Samples with 2.0 % gypsum give higher compressive strength at 3 days due to the deficiency of the sulphoalumanite hydrates[17]. The results show that, 4.0 - 6.0 % gypsum is the optimum content which imparts the cement desirable compressive strength. Therefore, natural gypsum was substituted with 2.0, 4.0 and 6.0 % phosphogypsum.

3.2 Substitution of natural gypsum by phosphogypsum

Figure (3) shows the water of consistency and setting times of GBFSC pastes containing 2.0, 4.0 and 6.0 % phosphogypsum instead of natural gypsum. It can be seen that, the water of consistency decreases with the phosphogypsum content. The setting times behave in the same manner as the water of consistency. Phosphogypsum contains phosphate and fluoride impurities, which improve the workability of cement pastes. Therefore, the cement pastes containing phosphogypsum has lower water demand in comparison with those with normal gypsum alone. Also, the impurities of phosphogypsum accelerate the rate of hydration of cement clinker phases, consequently the setting times are shortened.

Some researchers concluded that, the use of phosphogypsum is associated with much longer setting time than that of natural gypsum[18,19]. On the other side, in a recent work the 4.0 % phosphogypsum gives lower setting time and while at 6.0 % the setting time is elongated[20]. This may be due to the presence of phosphates which act as retarders and fluorides as accelerators.

The hydration kinetics of the slag cement with phosphogypsum were studied by the determination of free lime and combined water contents up to 90 days. Figure (4) shows the variation of free lime contents of the investigated cement pastes cured up to 90 days. The results show that, the free lime content of the all hydrated pastes increases up to 7 days then decreases up to 90 days. The initial increase of free lime content up to 7 days is mainly due to

that, the rate of lime liberation from C_3S and ß-C_2S phases exceeds the rate of lime consumption by the pozzolanic reaction of slag. After 7 days, the rate of liberation of lime decreases, whereas the rate of its consumption increases due to the increase of slag hydration and its pozzolanic reaction with the liberated lime at later ages (7-90 days). At a given time of hydration, the free lime content of cement pastes containing phosphogypsum is higher than that containing normal gypsum alone. Also, as the phosphogypsum content increases, the free lime increases due to the important role of the fluoride impurities of phosphogypsum which increase the hydration rate of cement clinker minerals, especially ß-C_2S, C_3S[21].

The combined water contents of GBFSC pastes containing different phosphogypsum contents instead of natural gypsum and hydrated up to 90 days are graphically represented in Fig. (5). The combined water content increases with curing time for all hydrated cement pastes due to the continuous hydration of cement clinker phases and also, to the pozzolanic reaction of slag with the liberated lime. Both the two reactions increase the amount of hydrated products with large combined water content. At any time of hydration, the values of combined water of pastes containing phosphogypsum exceed those containing normal gypsum alone. Also, as the amount of phosphogypsum increases the combined water content enhances. This may be due to that, fluoride impurities of phosphogypsum accelerate the rate of hydration of silicate minerals, forming more hydrated products.

The change of bulk density and apparent porosity of GBFSC cement pastes containing different phosphogypsum contents with curing time are present in Fig. (6). As the hydration progresses, the hydration products fill a part of the available pore volume to form a more compact body. Therefore, the bulk density increases and apparent porosity is reduced with curing time for all hardened pastes. The rate of slag hydration increases with time, because at early ages of hydration, an acidic oxide film is formed and covers the slag grains. This film is broken in presence of $Ca(OH)_2$ and gypsum as alkaline sulphate activators. As the phosphogypsum content increases, the rate of hydration of clinker minerals increases and accordingly the amount of C-S-H increases[21]. The GBFSC pastes containing normal gypsum alone show the lowest bulk density and highest apparent porosity. This may be due to the highest water demand of the cement pastes with normal gypsum alone in comparison with those containing phosphogypsum.

The relationship between the compressive strength and curing time of cement mortars containing different phosphogypsum contents is illustrated in Fig. (7). The compressive strength increases with curing time as well as phosphogypsum content. Also, the mortars containing normal gypsum alone have lower values of compressive strength than those containing phosphogypsum. Also, fuloride impurities of phosphogypsum play an important role in the activation of both cement clinker and slag portions, leading to the formation of additional amounts of C-S-H gel which is the main cementing material. Therefore, as the amount of phosphogypsum in cement increases, the rate of hardening of cement mortar enhances especially at later ages[22].

CONCLUSIONS

1. The substitution of normal gypsum by untreated phosphogypsum improves the workability and slightly decreases the water of consistency as well as the setting times of GBFSC pastes.

2. The free lime and combined water contents increase with the substituted phosphogypsum up to 90 days. The fluoride impurities of phosphogypsum activate the hydration of portland cement clinker and slag portions.
3. As the amount of phosphogypsum increases, the apparent porosity decreases, bulk density and accordingly the compressive strength increase.
4. Phosphogypsum is more effective retarder than natural gypsum and can be successfully used for GBFSC production.

REFERENCES

(1) M. H. Ozkul (2000).,"Utilization of citro-and desulphogypsum as set retarder in portland cement" Cem. Concr. Res. ,30, PP. 1755-1758

(2) J. Bensted, (1980)." Early hydration behavior of portland cement ontaining boro-,citro-and desulphogypsum" Cem. Concr. Res.,10(2), PP. 165-171

(3) M.Singh and M. Garg" (2000) Making of anhydrite cement from waste gypsum" Cem. Concr. Res. ,30, PP. 571-577

(4) K. Murakami(1969). "Utilization of chemical gypsum for portland cement" The fifth Inter. Symp .chemistry of cement, IV, Cement Association of Japan , Tokyo, PP. 457–503

(5) H. Olmez and E. Erden, (1989) "The effect of phosphogypsum on the setting and mechanical properties of portland cement" Cem. Concr. Res. 19(3) PP. 377-384

(6) H .Badowska, E. Osiecka and B. Majewski, (1978) "Utilization of phosphogypsum wastes in plaster production" Colloq. Int. Sous. Prod.Dechets.Geenie.Civ. (C.R.) PP. 187-192

(7) M. Singh, (1988) "Utilization of by-product phosphogypsum for building materials" Build. Res. Note No. 9, CBRT Publication, Roorkee India

(8) M. Singh ,M. Garg, (1992) "Investigation of a durable gypsum binder for building materials" Constr. Build. Mater. ,6, PP. 52-56

(9) P.k. Mehta and J.R. Brady, (1977) "Utilization of phosphogypsum in portland cement industry" Cem. Concr. Res. 7(5) PP.537-543

(10) P.C , Hewlett, Lea's (1998) "Chemistry of cement and concrete", John Wiley & Sons Inc., New York

(11) J. Bijnen and E. Niel(1981) " Cem. Concr. Res.", 11, P. 307

(12) ASTM Standards (1992) "Standard Test Method for Normal Consistency of Hydraulic Cement". ASTM. , C 187- 83-195

(13) ASTM Standards, (1992). " Standard Test Method for Setting of Hydraulic Cement by Vicat Needle" , ASTM Designation, C 191-83, 208

(14) ASTM Standards (1992)" Standard Test Method for Compressive Strength of Hydraulic Cement Mortars", ASTM Designation, C 109 -92, 62

(15) El-Didamony, H., Haggag, M.Y. and Abo El-Enein, S.A ,.(1978)" Hydration kinetics,surface properties and microstructures" Cem. Concr. Res., 8, PP. 351-358

(16) S.A.S El- Hemaly, F.H.Mosalamy and H.El- Didamony ,(1985) " A hydraulic binder based on plaster of paris and granulated slag" Rev. Int. Hautes Temper. Refract. Fr, 22, PP. 162- 167

(17) Kondo, R., Abo El-Enein, S.A., and Daimon, M. (1975)" Kinetics and mechanisms of hydrothermal reaction of granulated blast furance slag" Bull. Chem. Soc., Japan, 48, PP. 222-226
(18) E.M. Lawson and P.J. Mixon. (1978). Brit. Res. Est. .Current Paper CP 50/78 , BRE , Carston . P.37,
(19) J. Bensted(1979) World Cem. Technol., 10(2), P.404
(20) H .El-Didamony, S.A.El-Alfi and M.M Elwan (2002)., "Sil. Ind.", 67(1-2), PP. 9-14
(21) I. Older, V. Duckstein and Th. Becker, (1978)" Cem. Concr .Res." 8(4), P. 469
(22) I. Soroka and M. Relis , (1983) Am. Ceram. Soc. Bull., 62(6), P. 695

ملخص العربى

نظرا للمشكلة التى تواجه العالم اليوم من زيادة نسبة تلوث البيئة ولاسيما من مخلفات الصناعة والتى تتراكم بكميات كبيرة فى معظم المصانع ومنها الجبس الفوسفاتى والذى ينتج ثانويا أثناء تصنيع الأسمدة الفوسفاتية بمعدل يفوق ٢٠٠٠٠٠ طن سنويا فى مصر وهو غنى بكبريتات الكالسيوم مع بعض الشوائب من الفوسفات والفلوريد.

تم فى هذا البحث دراسة مدى الاستفادة من استخدام هذا المنتج الثانوى كمهدئ لعملية الشك كبديل للجبس الطبيعى فى إنتاج الأسمنت الحديدي واحتوت الدراسة على استخدام نسب مختلفة من هذا المنتج مع كلنكر الأسمنت وخبث الحديد وتم إجراء اختبارات قياس نسبة ماء الخلط وزمن الشك الابتدائي والنهائى وتعيين الماء المتحد كيميائيا وكمية الجير الحر والكثافة الكلية والمسامية وقوى تحمل الضغط الميكانيكى وتوصلت الدراسة إلى أن الاستبدال الجزئي أو الكلى للجبس العادى بالجبس الفوسفاتى يعطى خواص ميكانيكية جيدة للأسمنت الحديدى ويحسن كذلك من عملية الهيدرة .

Table (1) : Chemical composition of the starting materials, Wt%

Material	SiO_2	Al_2O_3	Fe_2O_3	CaO	MgO	SO_3	P_2O_5	I.L
PC Clinker	21.26	5.53	3.60	64.70	1.25	0.75	-	0.53
BF Slag	36.25	12.87	0.80	40.00	2.54	0.36	-	0.27
N. gypsum	4.13	0.83	0.27	33.08	0.08	43.39	-	19.82
P. Gypsum	8.46	0.31	0.36	32.98	0.12	36.41	1.85	18.37

Table (2): Mix composition of the different cements , Wt. %

Mix No.	PC Clinker	BF Slag	N. gypsum	P. Gypsum
M_1	58.8	39.2	2	-
M_2	57.6	38.4	4	-
M_3	56.4	37.6	6	-
M_4	55.2	36.8	8	-
M_5	56.4	37.6	4	2
M_6	56.4	37.6	2	4
M_7	56.4	37.6	0	6

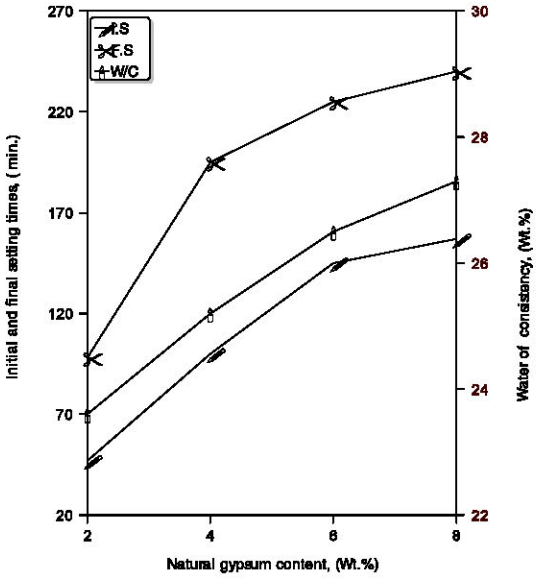

Fig. (1) : Water of consistency and setting times of GBFSC pastewith different amounts of natural gypsum.

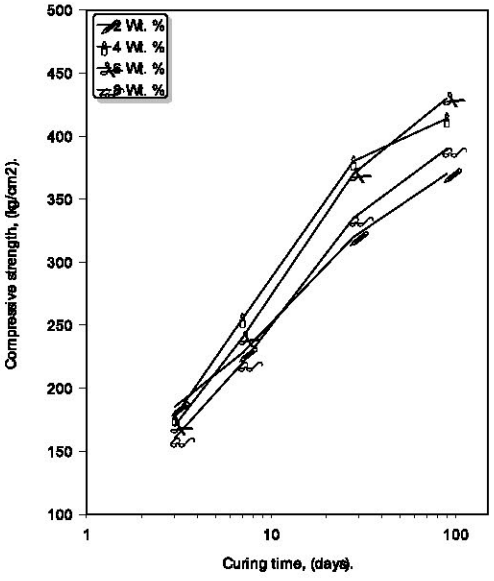

Fig. (2) : Compressive strength of GBFSC mortars with various proportions of natural gypsum up to 90 days.

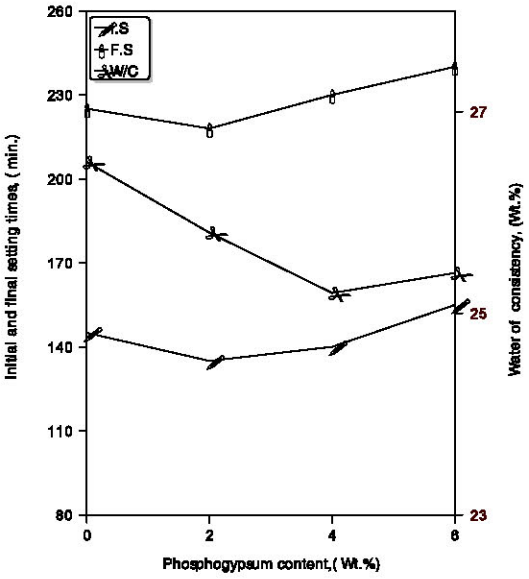

Fig. (3) : Water of consistency and setting times of GBFSC pastesas a function of phosphogypsum content.

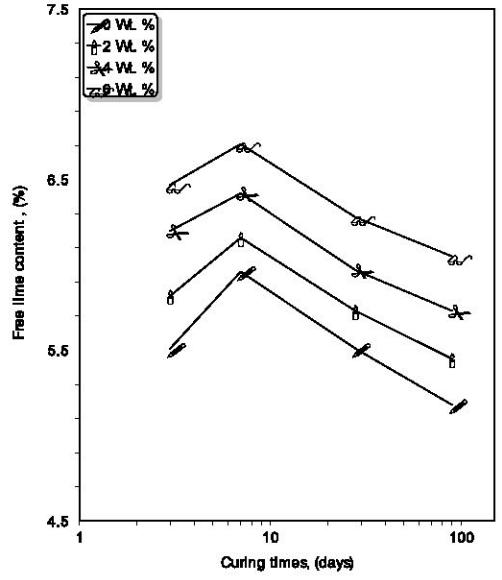

Fig. (4) : Free lime contents of GBFSC pastes as a function of phosphogypsum content as well as curing time.

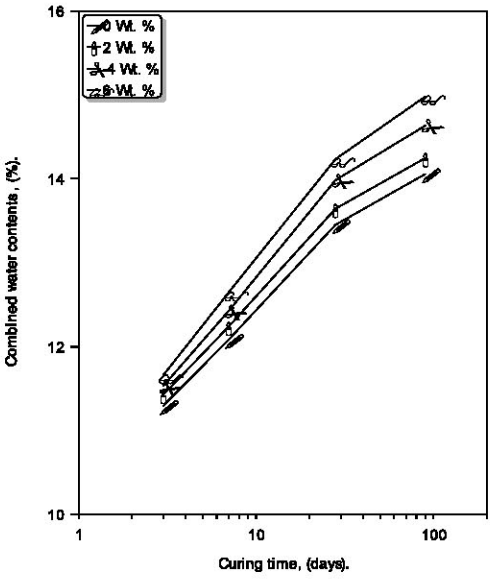

Fig. (5) : Combined water contents of GBFSC pastes containing various proportions of phosphogypsum with curing time.

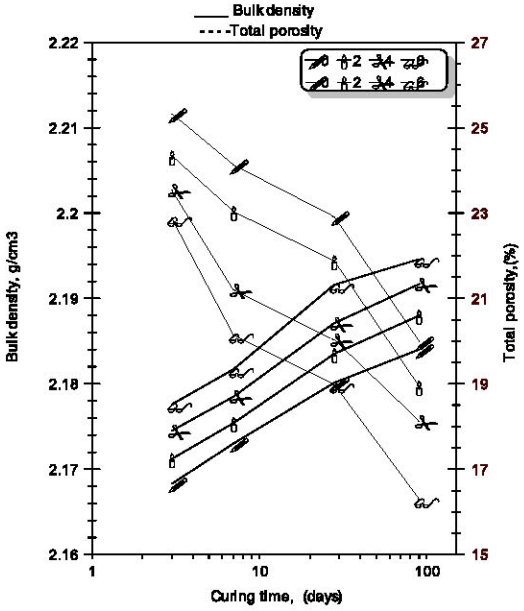

Fig. (6) : Bulk density and total porosity of GBFSC pastes in relation with phosphogypsum contents and curing time.

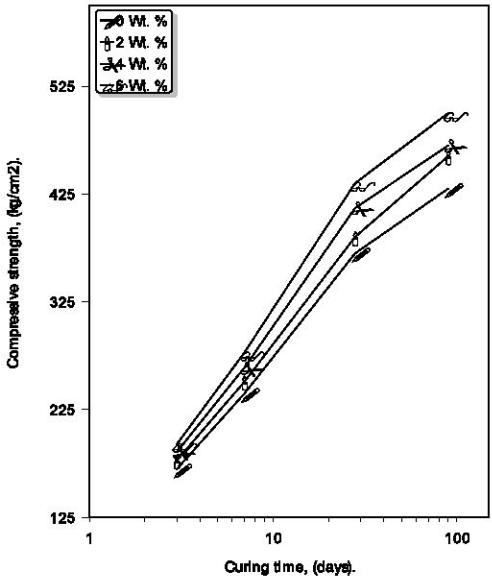

Fig. (7) : Compressive strength of BFSC mortars in relation with phosphogypsum content and curing time.

Proceedings of the ACI-KC First International Conference & Fourth Exhibition. September 29-October 1, 2003, Kuwait — ***Concreting and High Performance Concrete in Hot Weather.***

DESIGN OF CONCRETE STRUCTURES FOR TEMPERATURE LOADING

Dr. Mustafa Kamal Badrah, Department of Civil Engineering
University of Aleppo, Aleppo, Syria

Email: mkbadrah@popmail.com

ABSTRACT

The basic phenomenon of thermal movement applies on concrete framework. Restraining frame elements under temperature change results in deformations and thermal forces. Two types of thermal analysis are investigated: *Element temperature analysis* which assumes that the whole structure is subject to a temperature change; and the *gradient temperature analysis* which caters for temperature change between inside and outside the façade and roof elements. Designing structure elements anti-thermal are discussed; in addition to the ability to avoiding thermal loading by means of reducing the restraint of the structure.

BACKGROUND INFORMATION

When the temperature of a body is raised or lowered, the material is expanded or contracted according to the following equation:

$$\Delta L = \alpha TL \ldots\ldots\ldots\ldots\ldots\ldots\ldots\ldots\ldots\ldots\ldots\ldots\ldots(1)$$

Where L is the original length of the member, 'α' is the coefficient of linear expansion, 'T' is temperature change, ΔL is the member length increase or decrease. If this expansion or contraction is wholly or partially resisted, stresses are set up in the body. For a fully restrained element subjected to 'T' temperature increase, the thermal compression force is given by (Case, et al *1996*):

$$P = \alpha TEA \ldots\ldots\ldots\ldots\ldots\ldots\ldots\ldots\ldots\ldots\ldots\ldots\ldots\ldots\ldots(2)$$

Where, 'E' is Young's Modulus, 'A' is element area. As an example, for a concrete column of 40 x 40 cm and 4 m length the compression force under temperature change 'T = 25 C' is 1088.1 KN. If basic laws (e.g. Eqs. 1 and 2) are integrated into a finite element analysis program, deformations and actions under thermal effects in sophisticated structural models can be computed and then sections can be designed to cater for extra forces risen from temperature loading.

TYPES OF TEMPERATURE ANALYSIS

One type of temperature analysis is to investigate the effect of temperature increase or decrease on the structure as a whole. It is important then to determine the temperature change 'T' as referred to in the above equations. This may be taken as the difference between temperature of the concrete during casting and the extreme low or high temperature the structure may be subject to. 'T' is normally taken 20-30 C according to the geographical area. This type of analysis shows

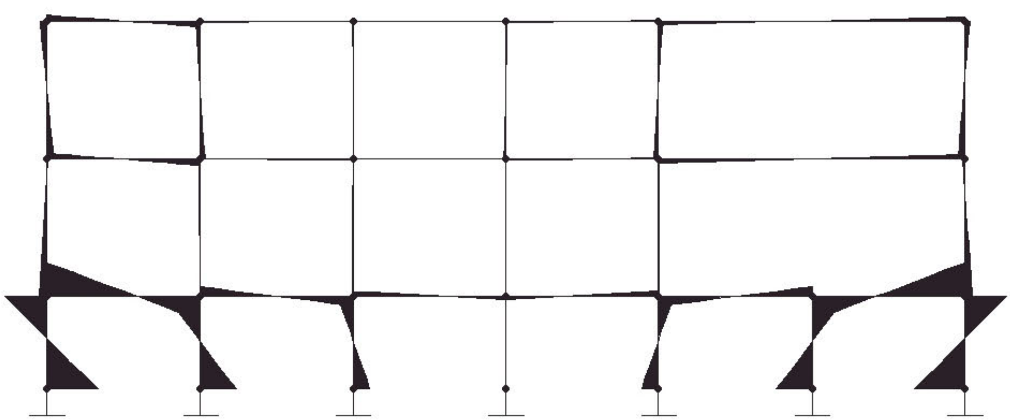

Figure 1: Bending moment diagram of a plane frame under element temperature loading

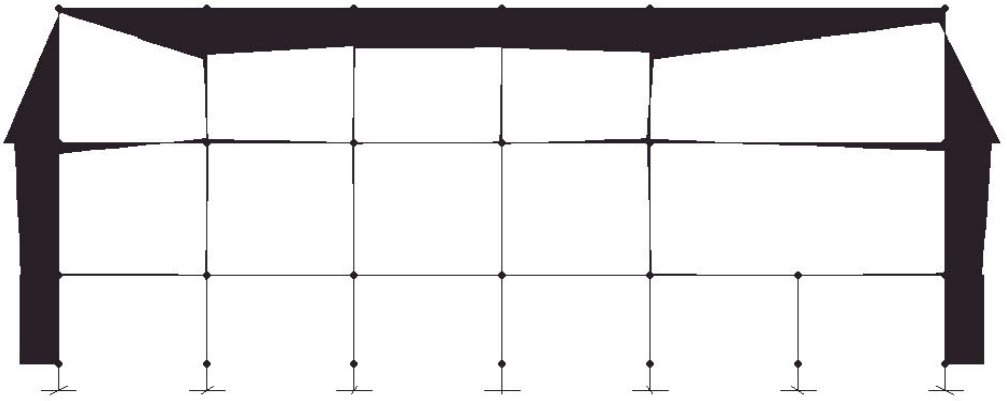

Figure 2: Bending moment diagram of a plane frame under gradient temperature loading

that lower stories of the structure will be subject to thermal forces more than other parts of the building (Badrah *2003*), see Fig. 1

Another type of temperature analysis is to investigate the effect of temperature change between inside and outside the structure; for example, temperature analysis of an office block structure equipped with air-conditioning and heating systems. In the latter, the temperature inside building rooms is around 20 C while outside the building; it could reach as high as 50 C during summer and as low as -20 C during winter. This results in temperature gradient between the outer side and the inner side of the façade and roof elements; and this causes rotations of sections of these elements; and produces thermal forces in the outer elements as shown in Fig. 2

DESIGN OF MEMBER SECTIONS

The bigger the section area of a member the higher thermal effects it will get. In relation to member type, generally, slabs show lesser thermal effects than beams and columns since they can expand or contract in two main directions. Large shell structures are usually subject to minimum stresses under gravity loading but they still need a least amount of reinforcement as a precaution measure against thermal effects (Chatterjee *1988*).

Beams, columns and foundations are the most thermally-affected members. They need to be designed for extra bending moments and axial forces especially in case of element temperature loading. In Fig 1, the side beam in the first storey was subject under temperature loading of T = 30 C to bending moment M = 182 KN.m and to axial force N = 174 KN. Side columns were also subject to M = 269.1 KN.m and N = 87 KN. These forces need to be resisted by adding extra reinforcement. Side bars usually supplied in high depth beams will absorb a part of these thermal forces in addition to extra top and bottom bars. Extra links are also needed for resisting thermal shear forces

In case of gradient temperature loading, thermal forces are less severe compared with the element temperature case. In Fig. 2, maximum bending moment in the top floor beams was

M = 41.22 KN.m under gradient temperature of 25 C. Maximum bending moment in side columns was M = 37.5 KN.m. These forces are negligible and can be resisted by normal practice of reinforcement detailing with reinforcement ratio more than minimum values usually stated in design standards.

AVOIDING THERMAL EFFECTS

Some design standards state lower limits for the structure dimensions not to be designed anti-thermal and upper limits for the structure dimensions to be acceptable provided that it is designed anti-thermal. Normally, the longer the structure is the larger thermal forces are set up in its members. Dividing the structure to several parts by using Expansion joints is a way to reduce thermal effects; although it may not be acceptable form aesthetic and functional point of view.

Another way to avoid thermal effects is by proper insulation of the building benefiting from emerging technologies in building materials. Although, absolutely eliminating thermal effects in structural members is impossible, however, they can be reduced to a large extent by using good insulation system and temperature-resisting building materials. On the other hand, controlling thermal movement in vulnerable finishes such as (brickwork, block work and glazing) is a key factor for avoiding thermal damages (Davison & Owens *2003*). Conventional guidance is followed in the movement provisions for these materials. This will reduce restraining the structure and consequently results in avoiding high thermal stresses.

But foundations and low level concrete framework will still severely restraint structures with large horizontal dimensions . Controlling erection of such structures by fixing foundation and low level concrete framework in median temperature condition (around 15-20 C) is helpful to reduce the temperature change 'T' and so reducing thermal forces.

CONCLUSIONS

Under temperature loading, high thermal forces are set up in lower stories of concrete frames. Extra reinforcement should be provided to absorb these forces unless measures of avoiding these forces are taken. Expansion joints, good insulation of the structure using temperature-resisting building materials, and controlling erection weather conditions are some means of eliminating thermal forces.

Only negligible thermal forces are set up in outer elements in case of gradient temperature loading. Normally these forces are absorbed by applying provisions of design standards regarding minimum reinforcement ratios and reinforcement detailing.

REFERENCES

Badrah, M.K. (2003), "Behavior of structures under thermal effects", accepted for publication in the Proceedings of the '9 ASEC' Conference, UAE

Case, J., Chilver, L. & Ross, C.T.F. (1996), Strength of materials and structures, Arnold, London, UK

Chatterjee, B.K. (1988), Theory and design of concrete shells, Oxford & IBH Publishing Co.

Davison, B. & Owens G. W., eds. (2003), Steel Designers' Manual, Blackwell Science, UK

Proceedings of the ACI-KC First International Conference & Fourth Exhibition. September 29-October 1, 2003, Kuwait — ***Concreting and High Performance Concrete in Hot Weather.***

HOW TEMPERATURE AFFECTS EARLY AGE CONCRETE BEHAVIOR UNDER LOCAL CONDITIONS

Dr. Toumi Belkacem, University Farhat Abbas Setif, Algeria
Dr. Guemmadi Z'hor, University Mentouri Constantine, Algeria
Dr. Houari Hacene, University Mentouri Constantine, Algeria

ABSTRACT:

This paper presents the evolution of compressive concrete strength at early age under local conditions. A large-scale test was conducted using concrete with type II cement for assessing the mechanical strength development in curing modes and temperature treatment under Algerian climatic conditions.

The different curing modes were saturated, without evaporation and ambient. The curing temperatures were 20°, 30° and 50°C successively. Measurements were taken at the ages of 0.42, 1, 2, 3, 7 and 28 days. Three other concrete mixes were used at water-cement ratio of 0.45, 0.55 and 0.65 to determine the temperature evolution in core of massive concrete elements that have volume-exposed surface ratio of 0.05, 0.10 and 0.15. The temperature evolution was continuously monitored from 24 hours and up to three days of concrete age.

Obtained results attest that, at early age, the compressive strength rate is affected by temperature, type of moulds and curing conditions. Tensile strength was affected as well as the compressive strength. The temperature in the core of testspecimens varied with the type of moulds (plastic, steel, cardboard), curing conditions and concrete massivity.

Keywords:

Concrete, Early age, Temperature, Curing, Mould, Massivity, Strength

INTRODUCTION

Early age concrete behavior is a major industrial problem and is a subject of great interest in concrete technology. The rate of construction that results from the great technical developments, economic considerations and environmental concerns is increasing. Concrete firms have begun considering how they can quickly achieve compressive strength of concrete in order to manipulate manufactured concrete elements without damaging their long-term properties. This objective is not only to get a proper understanding of concrete hardening process at early age, but also a computing method that can assess the concrete properties at any time.

Hydraulic concretes always need waiting time to acquire their final strength by natural hardening. This constitutes one of the major inconveniences during production. This waiting time is more and more mismatched with the productivity of concretes firms. In concrete industry, there are several ways for accelerating the process of concrete hardening. If the thermal treatment is the most efficient means to get the critical strength, it may be intensified by climatic conditions particularly in hot climate as the case of Algeria where mean temperature in summer is about 45°C and that may involve great thermal gradient inside and on the surface of the concrete. These thermal factors affect both concrete durability and mechanical properties. Consequently, mathematical models for concrete strength assessment must not neglect the temperature effect on thermo-mechanical concrete properties.

The object of this article is to present the concrete behaviour at early age and to put in evidence how concrete performances are influenced by mould nature, curing mode, curing temperature, W/C and the Volume to Surface ratio. So, a comprehensive experimental program was undertaken to follow-up the development of the mechanical strength under test-tube temperature environment at early age.

The obtained results provided much information on the early age of concrete behavior and demonstrate that the curing mode and temperature affect compressive strength and increase the tensile strength. The temperature within test-tube is affected by the type of mould, curing mode, W/C and also by the V/S ratio.

EXPERIMENTAL PROGRAM

The sample submitted for tests is an ordinary concrete. The gravel, sand, cement and water used for mixing were local products. All tests were conducted according to Algerian standard. The selected parameters were:

- Nature of the mould (steel, cardboard, plastic)
- Curing mode (ambient, saturated, without evaporation).
- Curing temperature (20°C, 30°C and 50°C).
- Water to cement ratio
- Volume to surface ratio.

Tests were organized under two categories of measurement:
The first test related to the assessment of the influence of the mould type, the curing mode and the curing temperatures on the compressive and tensile strength at the ages of 0.42, 1, 2, 3, 7 and 28 days.

The second test related to the measurement of test-tube temperature (continuously followed from 24 hours and up to three days of concrete age).

MATERIAL USED AND CONCRETE CONFECTION

Granulates: Granulates that form the skeleton of the concrete are from the career of Ain Smara. The granular classes used are 0/3, 3/8, 8/15 and 15/25.

Cement: The cement type is CPJ 45. It was procured from the ERCE factory and it conformed to the Algerian's norms (NA 442).

Concrete confection:
The formulation of the concrete mix is according Dreux and Gorisse's method. Three concrete mixes M1, M2 and M3 that differ only by the W/C ratio (W/C = 0.45; 0.55; 0.65 respectively) have been prepared. The dosages of the final constituent are reported in Table 1. The mixture M1 is expected to monitor the resistances and the temperature evolution within test-tubes under the influence of the mould type and the mode of conservation. For assessing the influence of the W/C and the Volume/Surface on the temperature evolution, the three mixes M1, M2 and M3 have been used.

Table 1. Dosages of concrete constituents

Constituents	Dosage en Kg/m^3		
	M1	M2	M3
Sable 0/3	435.9	418.7	449.2
Sable 3/8	133.2	127.9	137.2
Gravel 8/15	400.5	384.7	412.7
Gravel 15/25	805.3	773.5	829.8
Cement	350.0	426.7	295.4
water	192.0	192.0	192.0
W/C	0.55	0.45	0.65
Slump	11 cm	9 cm	13 cm

Results and discussion:
The concrete presents an evolutionary behaviour over a period of time. Its complex mechanical behaviour, deformation and mechanical effects often are irreversible. This behaviour is not manifested at the level of granulates that are considered inert by their nature but it is at the level the paste cement is formed. Undoubtedly, when cement and water are mixed, three major effects begin to develop at the level of the paste, mechanical strength, heat generation and volume reduction. These three effects are generally influenced by certain conditions.

Influence of the mould type:
The nature of the mould influences the compressive strength. Plastic moulds (Fig.1) provide better compressive strength than that obtained with steel moulds (Fig.2) and cardboard moulds (Fig.3) in curing mode. This gain in strength can be explained by the insulating nature (thermal insulation) of plastic moulds. A certain quantity of the heat generated by the hydration of the cement is kept by the mould; it confers on the concrete certain auto maturation that accelerates the process of the hardening.

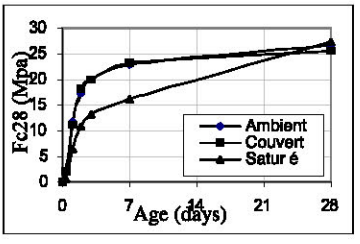

Fig.1 compressive strength versus age – steel moulds

This auto maturity is instigated by the temperatures in the centre of test-tubes caused by plastic moulds. Moulds made of steel generate lesser temperature than plastic during the curing modes.

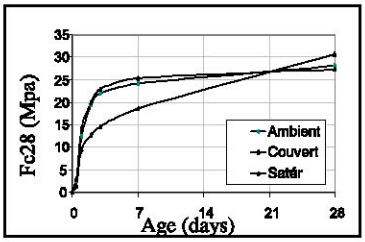

Fig.2 compressive strength versus age – plastic moulds

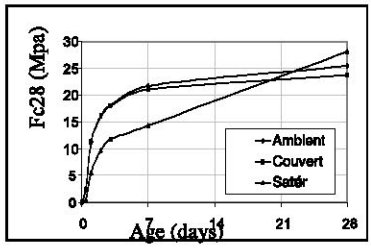

Fig.3 compressive strength versus age – Cardbord n moulds

This can be explained by the strong thermal conductivity of metal. Moulds in cardboard, although more insulating than moulds made of steel, give weaker strength compared to the other two moulds. This reduction can be owed to their rigidity (against moulds) and to the impact that appears in the microstructure of the concrete (inflation éttraingite, thermal expansion...). The nature of mould considerably influences the base of the concrete.

Influence of the fashion of conservation: at early age, the given strengths in curing mode 'saturated' are less important than those in curing mode, 'without evaporation and ambient'. Since the water consumed by the cement hydration is continually replaced by outside contribution and the pores are not empty by auto desiccation of the concrete. This saturation of water is noted at the time of the bruising of test-tubes at the age of 10 hours and 1 days as the test-tubes break themselves in the humid soil.

Test-tubes conserved in water for long time present superior resistance. This may be explained by the advanced hydration state because there is sufficient water quantity. The process of hydration contained is contrary to the other two present - lack of water by evaporation and by auto desiccation.

The strength by the ambient conservation and without evaporation modes are approximately identical for the same type of mould. Concrete strength are affected by the mode of conservation.

Influence of the treatment temperature: The results (Figs 4, 5 and 6) show that the strength, at early age, increases with the rise in temperature. But in the long term, the strong temperature treatment of the raw concrete, led to weakness in concrete strength. The results are reinforced by the bibliographic analysis that shows that several researchers have raised this point. The influence of the temperature is appreciable, considering that the kinetics of hydration laws obey Arhenius law.

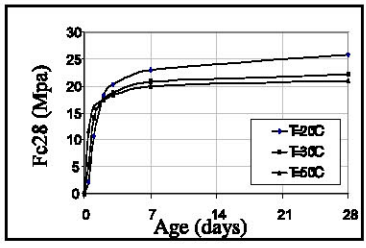

Fig.4 compressive strength versus age – steel moulds

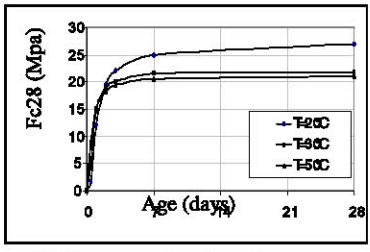

Fig.5 compressive strength versus age –Plastic moulds

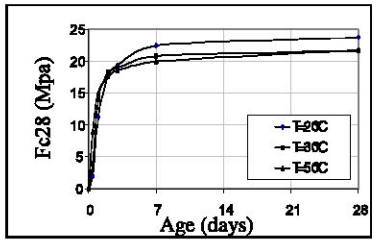

Fig.6 compressive strength versus age – cardboard moulds

The experimental results [1,2,3] analysis by the least square method, leads us to calculate the different constants of the three models (Tables 2 to 7).
Observing these results, it can be noted that for the three temperatures, the exponential model (Model 3) has a better interrelationship with the logarithmic model (Model 1) and hyperbolic model (Model 2). The logarithmic model under extreme strengths at early age and in extreme ulterior strengths, at later ages for all temperature, and final strength of treated concrete is less important than that of untreated concrete.

At relatively elevated temperatures, hyperbolic and exponential model, foresee final strength less important than those experimentally obtained. At early age, the exponential model converges very well with the experimental results. This model will therefore be preferred for software development to assess the mechanical strength at early age of the concrete.

Influence of the W/C ratio on the evolution of the temperature within concrete elements: the elevation of the temperature for a massive concrete element is inversely proportional to the W/C ratio, that is to say, that the elevation of the temperature within concrete is directly linked to the cement content. This observation is verified in this study for the three W/C ratio (Figs. 7, 8 and 9).

Influence of the V/S ratio on the temperature evolution within concrete elements:
The V/S ratio constitutes a balance between the generation of heat and its dispersion. The concrete is a material having a weak thermal conductivity, so the diffusion of the heat from the centre toward the outside is very weak: the more the V/S ratio is larger, the greater the value of the temperature in the centre. The V/S report can constitute a measure to predict the elevation of the temperature in the massive elements (ratio of heat generation laws to the heat dispersion). The influence of the V/S ratio is also seen the instant the heat is picked and in the phase of cooling. The three V/S show that the more this ratio increases, the temperature is much more and baffling.
Perhaps, due to this Bournazel reports that cracks to the thermal withdrawal appear in dams during the winter that follows their construction.

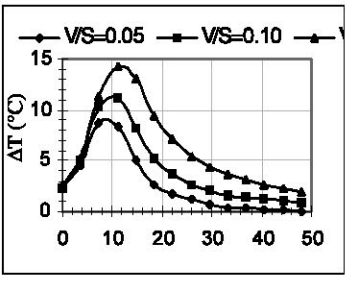

Fig.7 Evolution of température in fonction of rapport W/C (W/C=0.45)

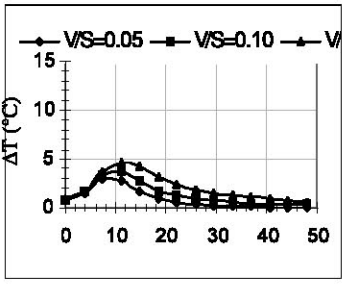

Fig.9 Evolution of température in function of rapport W/C (W/C=0.65)

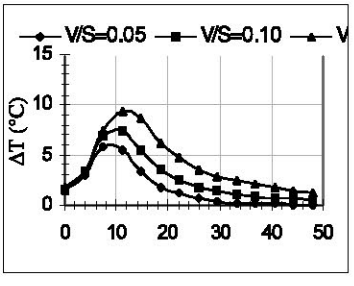

Fig.8 Evolution of température in function of rapport W/C (W/C=0.55)

T = 20°C

Table 2. Parameters of Models

Model	$R = a + b \log(t_e)$			$R = t_e /(a\, t_e + b)$			$R = a \exp(-b/t_e)$		
Parameters	a	b	VAR	a	b	VAR	a	b	VAR
	10,4628	7,6601	93.88%	0,0353	0,0538	93.53%	26,8654	0,9009	99.15%

Table 3. Observed values, Esteemed values and models curves (P = 95%)

Model	Age	Value Observed	Value Esteemed	Model Tendency Curve	observed Values versus predicted values (P = 95%)
$R = a + b \log(t_e)$	0,42	2,1	6,19	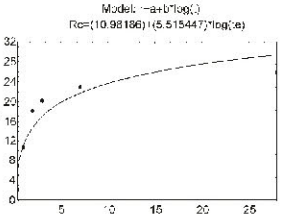	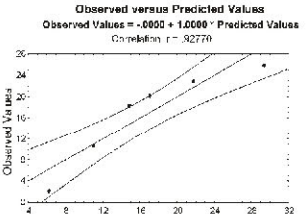
	1	10,7	10,98		
	2	18,3	14,80		
	3	20,3	17,04		
	7	22,9	21,71		
	28	25,8	29,36		
$R = t_e /(a\, t_e + b)$	0,42	2,1	6,10	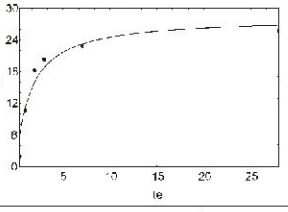	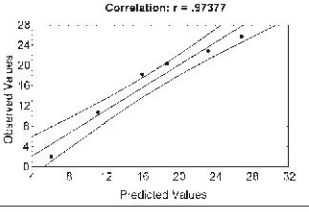
	1	10,7	11,20		
	2	18,3	16,05		
	3	20,3	18,75		
	7	22,9	23,22		
	28	25,8	26,82		
$R = a \exp(-b/t_e)$	0,42	2,1	3,14	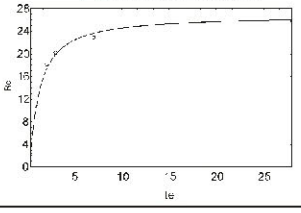	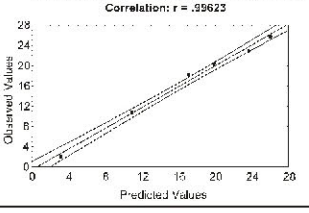
	1	10,7	10,91		
	2	18,3	17,12		
	3	20,3	19,89		
	7	22,9	23,62		
	28	25,8	26,01		

T = 30°C

Table 4. Parameters of Models

Model	$R = a + b \log(t_e)$			$R = t_e /(a\, t_e + b)$			$R = a \exp(-b/t_e)$		
Parameters	a	b	VAR	a	b	VAR	a	b	VAR
	12,6107	3,6817	80.12%	0,0426	0,0357	95.06%	22,6653	0,5447	99.17%

Table 5. Observed values, Esteemed values and models curves (P = 95%)

Model	Age	Value Observed	Value Esteemed	Model Tendency Curve	observed Values versus predicted values (P = 95%)
$R = a + b \log(t_e)$	0,42	5,4	9,41	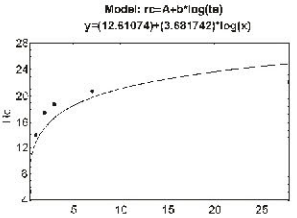	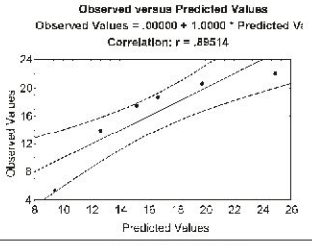
	1	14	12,61		
	2	17,5	15,16		
	3	18,8	16,65		
	7	20,7	19,77		
	28	22,1	24,87		
$R = t_e /(a\, t_e + b)$	0,42	5,4	7,83	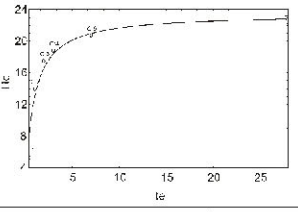	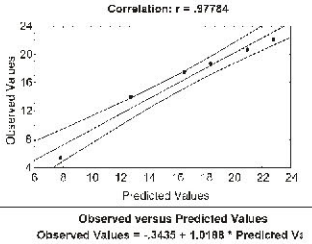
	1	14	12,76		
	2	17,5	16,53		
	3	18,8	18,34		
	7	20,7	20,95		
	28	22,1	22,78		
$R = a \exp(-b/t_e)$	0,42	5,4	6,195	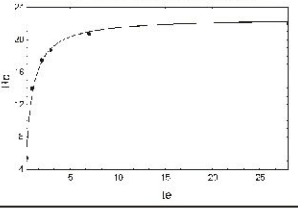	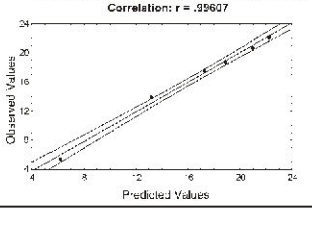
	1	14	13,14		
	2	17,5	17,26		
	3	18,8	18,90		
	7	20,7	20,96		
	28	22,1	22,22		

T = 50°C

Table 6. Parameters of Models

Model	$R = a + b \log(t_c)$			$R = t_c / (a\ t_c + b)$			$R = a \exp(-b/t_c)$		
Parameters	a	b	VAR	a	b	VAR	a	b	VAR
	15,2339	2,0954	87.90%	0,04803	0,01587	97.09%	20,4433	0,24450	98.30%

Table 7. Observed values, Esteemed values and models curves (P = 95%)

Model	Age	Value Observed	Valuc Esteemed	Model Tendency Curve	observed Values versus predicted values (P = 95%)
$R = a + b \log(t_c)$	0,42	11,7	13,41	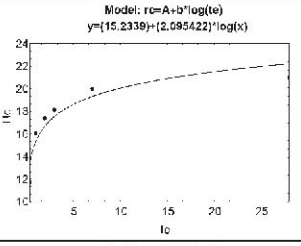	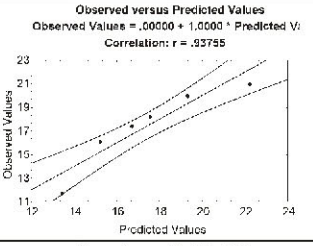
	1	16,1	15,23		
	2	17,4	16,68		
	3	18,2	17,53		
	7	20,0	19,31		
	28	21,0	22,21		
$R = t_c / (a\ t_c + b)$	0,42	11,7	11,65	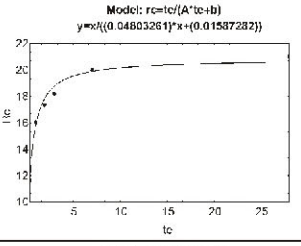	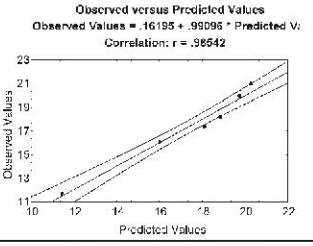
	1	16,1	15,64		
	2	17,4	17,86		
	3	18,2	18,75		
	7	20,0	19,88		
	28	21,0	20,57		
$R = a \exp(-b/t_c)$	0,42	11,7	11,42	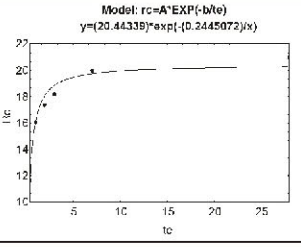	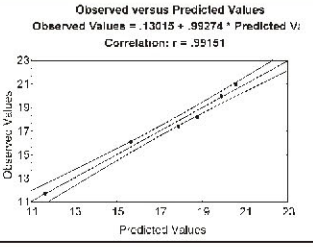
	1	16,1	16,00		
	2	17,4	18,09		
	3	18,2	18,84		
	7	20,0	19,74		
	28	21,0	20,26		

CONCLUSION:

Moulds influence the concrete resistance by their nature, their rigidities and their shape. For current curing mode, plastic moulds give the best strength in compression. The saturated curing mode, give the weakest strength at early age and the strongest at long-term. The tensile strength is affected by both conservation and temperature.

The high temperature of treatment gives the relatively larger strength at early age and the relatively weaker strength at long-term.

The equivalent age concept constitutes a convenient method permitting to predict concrete mechanical strength required in the establishment of concrete project scheduling for an optimal exploitation.

Since mechanical property evolution is strongly affected by temperature, and the advancement of hydration reactions obeys to the Arhenius law, maturity functions based on this law give realist predictions of those obtained in tests.

The cement content is directly linked to concrete pieces temperature elevations. The concrete is a bad conductor of the heat and the necessary time for cooling can be considerable for the massive pieces.

REFERENCES:

TOUMI B. *Contribution à l'étude du comportement du béton au jeune âge sous conditions locales.* Thèse de magister, Université Constantine 1999.

TOUMI B., GUEMMADI Z., HOUARI H., Effet de la température sur la résistance du béton au jeune âge. Séminaire national du Génie Civil, SNGC Sidi bel Abbes 15/16 mai 2001.

TOUMI B., GUEMMADI Z., HOUARI H., *Etude du caractère thermo-mécanique du béton au jeune âge Models de prévision de la résistance mécanique.*
Séminaire internationale sur la modélisation numérique en structure et géomatériaux SMNSG 2001, Batna, 22-24 Octobre 2001

GUO CHENGJU Maturity *of concrete : Method for Predicting Early Stage Strength.*
ACI Materials Journal Vol. 86 N°4 July-August 1989 P. 341-353

BYFORS J. *Plain concrete at early ages,* Stockholm : Swedish Cement and concrete Research institute, 1980, 345 P, Rapport N° Fo 3/80.

BOURNAZEL J. P., REGOURD M. M. *Matthematical Modeling of concrete Durability : The use of Thermodynamics Processes* Concrete durability Sp 144-12 PP 233-249

BRESON J. *Prediction of Strength of Concrete Products,* RILEM International Conferance on concrete at Early ages, Paris: Ecole National des Ponts et Chaussés 1982, vol. P111-115

PLOWMAN *Maturity and Stength of concrete* Magazine of Concrete Research 1958 Vol. 8 No. 22 PP 13-22

CARINO N. J., TANK R. C. *Maturity functions for concrete made with various cements and admixtures* ACI Materials Journal Vol. 92 N°2 March - April 1992 P. 188-196

CHANVILLARD, G. D'ALOÏA, L. *Concrete Strength Estimation at Early Age : Modification of the method of Equivalent Age.* ACI Materials Journal Vol. 94 N

Proceedings of the ACI-KC First International Conference & Fourth Exhibition. September 29-October 1, 2003, Kuwait — ***Concreting and High Performance Concrete in Hot Weather.***

READYMIXED AND SITEMIXED CONCRETE FOR VILLAS IN KUWAIT —A COMPARATIVE STUDY

M. N. Haque
Department Of Civil Engineering, University Of Kuwait,
P.O. Box 5969, Safat 13060, Kuwait.

ABSTRACT

Concrete is a main material of construction in Kuwait. The degradation of concrete structures in Kuwait can be attributed to the aggressive service environment, hot and dry climate that is characterized by high rates of water evaporation during the day, condensation in coastal areas at night, and salt-contaminated wind-borne dust and ground water. In addition, the locally available aggregates are contaminated with chlorides and sulfates. Lack of quality control often exacerbates the above effects.

It is very common in State of Kuwait that owners supervise their villas' construction. Most owners are somewhat uncertain about the method they should follow for concrete supply and mixing. Should they use the readymixed concrete (RMC) or sitemixed concrete (SMC)? Concrete mixing, production, placing and compaction are, of course, the initial and pivotal stages towards producing a durable structure. Accordingly, in this case study the focus was on the cost, strength development, permeability and the likely future performance of villas, made with RMC and SMC.

The results suggest that the quality of readymixed concrete is superior to that of sitemixed concrete. The paper concludes that RMC is a much better value for money because of its consistent quality and performance as indicated by the compressive strength and the permeability characteristics of the concretes tested.

INTRODUCTION

Concrete is a main material of construction in Kuwait, The degradation of concrete structures in Kuwait can be attributed to the aggressive service environment, hot and dry climate that is characterized by high rates of water evaporation during the day, condensation in coastal areas at night, and salt-contaminated wind-borne dust and ground water (Haque et al. 1997, Fookes 1993, 1995). In addition, the locally available aggregates are contaminated with chlorides and sulfates, Lack of quality control often exacerbates the above effects. Of course, the cost of maintenance, repair and rehabilitation of structures run annually into billion of dollars (Neville 1997).

Now it is very common in State of Kuwait that owners supervise their villas' construction. Most owners are somewhat uncertain about the method they should follow for concrete supply and mixing. Should they use the readymixed concrete (RMC) or sitemixed concrete (SMC)? Concrete mixing, production, placing and compaction are, of course, the initial and pivotal stages towards producing a durable structure. Accordingly, in this case study the focus is on the cost, strength development, permeability and the likely future performance of villas, made with RMC and SMC.

In a previous similar study, which was initiated in May 1996, in Kuwait summer, it was concluded "that the initial cost savings realized by employing on-site concrete making practices lead to a less durable concrete. If a comparable quality of site-mixed concrete is required, the savings in material cost would be nominal, if any" (Haque 2000). In order to be more definitive, the present study was undertaken in Kuwait winter to eliminate the initial effect of very hot/dry exposure conditions, if any.

In Nov./Dec. 1999, the average cost of 1 m^3 of ready mixed concrete was 20 Kuwaiti Dinar (KD) while that of the site mixed concrete, on average, was 14 KD. Accordingly, in a typical private villa, an owner can save an average of 1750 KD by using the SMC. But unfortunately not all owners are aware of the limitations of this type of concrete. A very obvious disadvantage is that construction with the SMC approximately takes four folds more time than that with RMC. Also, both strength development and durability characteristics of the two concretes have been reported to be different (Haque 2000). This study is a further endeavor to evaluate the short-term performance indicators of the two concretes.

TESTING PROGRAM

Six random sites, using ready mixed concrete (RMC) of K300 (~30 MPa), and 5 random sites using site mixed concrete (SMC), were selected for sampling and testing concrete. Table 1 includes the mix proportions of the two concretes. The comparative study consisted of measuring slump, strength and permeability of both RMC and SMC, respectively. Table 2 shows the location of various villas and the type of the concrete employed. The table also includes the slump and the temperature of the fresh concrete at the time of sampling. The sampling of concrete was undertaken in November 1999, the time of the year when temperate climatic conditions prevail in Kuwait:

Table 1. Mix Proportions of Ready Mixed and Site-Mixed Concrete (kg/m^3)

Concrete Constituent	RMC K300	SMC K300
Cement	390	450
Water (1)	200	227
Sand	685	720
Aggregate (18 mm)	500	1083 (all-inclusive)
Aggregate (13 mm)	300	
Aggregate (9 mm)	250	
Super Plasticizer	3	
Total Weight/Mix	2325	2480
W/C ratio	0.51	0.50

Table 2. Concrete Slump and Temperature

Id.*	Location	Slump (mm)	Temperature (^0C)
R1	South Surrah	95	27
R2	South Surrah	95	27
R3	Jahra	100	27
R4	Salmiya	85	26
R5	Yarmouk	105	27
R6	Fintas	105	27
S1	South Surrah	155	27
S2	South Surrah	140	27
S3	South Surrah	100	27
S4	Salwa	135	26
S5	Jabrieh	105	27

R*=Readymix concrete
S*=Sitemixed concrete

Concrete specimens cast for both strength and permeability for the RMC and SMC were stored, alongside the villa under construction, for the first 24 hours. These specimens were then transported to the concrete laboratory in Kuwait University, demoulded and subsequently stored in a water curing tank maintained at 27 ± 2^0C. The compressive strength values are the average of 3 whereas the permeability values are the average of 2 specimens. The indicative quality of a concrete as given by Autoclam index (1997) is given in Table 3. The strength and permeability results are included in Tables 4 and 5, respectively.

Table 3. Indicative value of concrete quality (Autoclam)

Clam Water Permeability Index ($m^3 \times 10^{-7}/min^{-0.5}$)	Protective Quality of Concrete
<3.7	Very Good
>=3.7 9.4	Good
>=9.4 13.8	Poor
=13.8	VeryPoor

Table 4. Concrete Compressive Strength (MPa)

Point Id.	7 Day	28 Day	90 Day
R1	24.5	34.5	36.5
R2	25.0	35.0	37.0
R3	24.0	34.5	37.0
R4	23.5	33.0	35.0
R5	24.0	34.0	36.5
R6	26.5	37.0	39.0
S1	17.5	22.0	22.5
S2	19.5	24.5	25.0
S3	22.0	27.5	28.0
S4	22.0	26.5	27.0
S5	23.0	29.5	30.0

Table 5. Concrete Water Permeability
(Using the "Autoclam" Permeability System — Mark III)

Point Id.	Clam Water Permeability Index ($m^3 \times 10^7/min.^{05}$)	Protective Quality of Concrete
RI	2.3	Very Good
R2	3.1	Very Good
R3	2.9	Very Good
R4	2.6	Very Good
R5s	3.1	Very Good
R6	2.6	Very Good
Si	9.8	Poor
52	8.9	Good
53	7.5	Good
S4	4.5	Good
S5	5.0	Good

DISCUSSION OF RESULTS

(i) Workability of the Concretes

It is clear that the workability of all ready mixed concretes is consistent and yielded a slump of 100 mm as specified. While for the site mixed concrete, the workability is much higher and it varied from 100 to 150 with an average value of 130 mm. This is because of the lack of quality control in the SMC since the proportioning of the mix is done manually and on a volume basis. In addition to that usually workers at site add more water to the mix to facilitate casting and compaction of the SMC. The temperature of all concretes, both RMC and SMC, were found to be almost equal to 26^0C.

(ii) Concrete Compressive Strength

As a result of the lack of quality control, volume batching and possible addition of more water during casting / finishing and personal errors due to manual proportioning in SMC, the compressive strength were mostly below the 28-day design strength and varied from 22.0 to 29.5 with an average value of 26 MPa. The compressive strength of the ready mixed concretes was much higher than those of site mixed concretes and gave an average value of 35 MPa at 28 days; about 35% higher than those of SMC. A somewhat similar trend in the strength development at 91 days can be seen in Fig. 1.

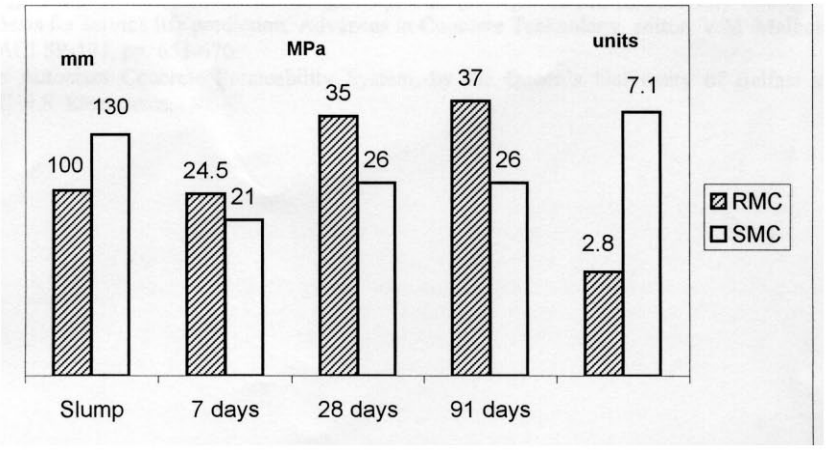

Fig. 1. Average value of the characteristics of the RMC and SMC tested

(iii) Water Permeability

According to clam indices, the quality of protective concrete cover in the ready mixed concretes were very good and much better than those of site mixed concretes which had, on the average, a permeability value of 3 fold than that of the RMC (See Fig. 1). This again can be attributed to the lack of quality control, volume batching, higher wlc ratio and personal errors due to manual proportioning of the SMC.

CONCLUSIONS

The results of this study suggest that the quality of the RMC is superior to that of the SMC. Whilst, the use of site mixed concrete could save some money on concreting of a villa, the use of ready mixed concrete gives better value for money invested due to its consistent quality and long-term better performance as indicated by the compressive strength and permeability characteristics of the concretes tested.

ACKNOWLEDGEMENT

The site and experimental work was undertaken, supervised and collated by Eng. Bader Al-Saqabi, Department of Civil Engineering, and the author is highly indebted to him.

REFERENCES

Fookes, P.O. (1993), "Concrete in the Middle East — past, present and future: A brief review. Concrete", vol. 27, 14-20.

Fookes, P.G. (1995), "Concrete in hot, dry, salty environments". Concrete 29: 34-39.

Haque, M.N. (2000), "Some concreting practices in Kuwait villas need improvement", Kuwait J. Sci., vol. 10(1), 77-82.

Haque, MN. & A1-Khaiat, H. (1997), "Durability survey in Kuwait" ACI Concrete International, vol. 19, 41-44.

Long, A.E.; Basheer, P.A.M. & Montgomery, F.R. (1997), "In-situ permeability testing — A basis for service life prediction, Advances in Concrete Technology, editor, V.M. Malhotra, ACI SP-171, pp. 65 1-670.

The Autoclam Concrete Permeability System, by the Queen's University of Belfast and C.N.S Electronics.

Proceedings of the ACI-KC First International Conference & Fourth Exhibition. September 29-October 1, 2003, Kuwait — ***Concreting and High Performance Concrete in Hot Weather.***

ASSESSMENT OF OVERDESIGNING OF KUWAITI RESIDENTIAL VILLAS

A.W. Sadek, S. Al-Fadala, N. Al-Mutairi
Kuwait Institute for Scientific Research

ABSTRACT

The present paper addresses the existing and pressing problem of inconsistent building designs in Kuwait and such a problem has led to the unjustified increase of the cost of typical residential buildings. For the purpose of the present study, six units of typical residential villas were selected as representative sample of Kuwaiti villas. Accurate design of these units was conducted according to ACI provisions.
In order to have a meaningful comparison, same concrete dimensions as per existing design were maintained in the accurate design and only reinforcement needed to be determined. Accurate and existing designs were compared for different members of the reinforced concrete skeleton of all units. A clear case of over design was indicated.

Keywords:

Structural design; Reinforced concrete; Kuwaiti villas; Reinforcement; Flexure; Shear; Columns.

INTRODUCTION

It is well known that construction activities, which can be chronologically classified as pre-construction (analysis and design), during construction and post-construction (usage and maintenance), have significant impact on the direct and indirect costs of construction. The present study addresses the impact of the pre-construction tasks, analysis and design, on the quality of design and cost functions of residential buildings in Kuwait.

In general, the significance of this study comes from the fact that the cost and safety of residential buildings affect almost every citizen in Kuwait. Moreover, with the absence of a uniform national building code, current practices of analysis and design of buildings involve inconsistencies and non-uniformities. First, it is up to the designer to select whatever foreign code to be followed in specifying the loads and designing structural members. Second, based on a preliminary review of existing design documents and personal contacts with several design offices it is found that it is common here in Kuwait to over-design structural members to allegedly provide safer buildings. It should be stated that every design code stipulates, explicitly or implicitly, certain factors of safety adequate for the local conditions. Over-designing beyond these limits is a waste of materials and money as it provides for unjustified levels of safety.

Reviewing the literature, it was concluded that the present paper is the first attempt to examine the impact of design practices on the quality and cost of residential buildings.

The presented work is part of a series of research programs conducted at Kuwait Institute for Scientific Research whose findings are expected to serve the immediate objective of providing recommendations on improving the quality of building designs and most important reducing the cost of buildings construction in Kuwait. On the other hand the findings of the present study will form the basis for a full scale endeavor leading to the development of the much needed National Building Code for Kuwait.

Focusing on Kuwaiti villas the objective of the study is set as to assess the current practices of structural design of residential buildings in Kuwait at the different stages of evaluation of loads, materials properties, analysis and design procedures, details and specifications. Further, the assessment of over-designing is limited to the super-structure, i.e. reinforced concrete skeleton members, namely slabs, beams and columns.

BUILDINGS SAMPLE

The buildings sample consists of six residential units of villa type, whose details are presented in Table 1 and the detailed design documents (Sadek et al., 2001) were compiled and reviewed as the existing design documents. All villas are of two to three stories, with or without basements, and the structural system is invariably of the reinforced concrete skeletal type that is most commonly used in construction. Date of construction of the selected units ranges from 1983 to 1998 and the locations of the units cover several districts within Kuwait City. Selected units are either government or private projects designed by either governmental or private design agencies. Different systems of framing plans are included in the sample, such as solid slabs, ribbed slabs, flat plates and their combinations. Hence, it is believed that the selected sample is representative of the residential Kuwaiti villas.

Table 1. Details of the Buildings Sample

Unit	1	2	3	4	5	6
Location	Coastal line-sector B1	Surra	Different Locations	Ardiyah	Hutein	Qurain
Project Type	Governmental	Private	Governmental	Governmental	Private	Private
Design Agency	Private	Private	Governmental (PHA)	Governmental (PHA)	Private	Private
No. of Floors	G+1	B+G+1+R	G+1	G+1	B+G+1+R	B+G+1+R
Built-up Area/Floor (m^2)	169	382	168	121	166	229
Type of Infill	Concrete blocks	Hebel blocks	Concrete blocks	Concrete blocks	Concrete blocks	Concrete blocks
Structural System	R.C. Skeleton	R.C. Skeleton	R.C. Skeleton	R.C. Skeleton	R.C. Skeleton	R.C. Skeleton
Framing Plan	Projecting Beams + Solid Slabs	Projecting Beams + Ribbed slab	Mixed Flat Plate/Projecting Beams + Solid Slabs	Projecting Beams + Solid Slabs	Solid Slabs	Solid slabs + Ribbed Slabs
Foundation Type	Isolated	Isolated	Isolated	Isolated	Isolated	Isolated

PHA: Public Housing Authority

B: Basement

G: Ground Floor

R: Roof

R.C. : Reinforced Concrete

ACCURATE DESIGN

Detailed computer-based structural analysis of the selected residential units was performed to find the straining actions in the resisting elements. For this purpose, the commercial software STAAD III (STAAD III, 1990) was employed.

The selected buildings were redesigned according to ACI-318 provisions (ACI, 1989) while considering the same concrete dimensions as stated in the existing design and hence the reinforcement was accurately found by the present redesign process. This approach of maintaining the existing concrete dimensions in the accurate design stage is essential to have a common reference between the existing and accurate design, and, hence a meaningful comparison is possible. One shortcoming of this approach is that, although in some cases, the existing statical systems and/or proportions might not be appropriate, no comments or alternative suggestions are made. This can be justified by the absence of all design documents and other practical considerations or constraints that possibly interfered in the selection of the existing system. The following design loads criteria were used in the analysis.

Dead Loads.

Density of structural concrete	=	2500 kg/m^3
False ceiling and ducts	=	100 kg/m^2
Flooring	=	150 kg/m^2
Roofing	=	250 kg/m^2
Ribbed one-way slabs (depth 35 cm)		
Uniform own weight	=	400 kg/m^2
Partitions		
Exterior concrete blocks wall (20 cm)	=	490 kg/m^2
Interior concrete blocks wall (15 cm)	=	435 kg/m^2
Aerated autoclaved concrete blocks (20 cm)	=	100 kg/m^2

Live Load.

Intensity on all floors	=	200 kg/m^2

Lateral Loads.

Wind loads	=	none
Earthquake loads	=	none

Material Properties

Concrete strength for typical construction was specified by cube strength f_{cu} = 25 MPa. In some buildings, concrete for columns was specified by f_{cu} = 30 MPa. Reinforcement minimum yield stress was taken as 420 MPa.

COMPARATIVE STUDY

Slabs

Solid Slabs

Main and secondary reinforcements in all solid slabs found in the buildings sample were accurately evaluated and compared with the corresponding values as per the existing design. A sample comparison of the reinforcement in the existing design and the accurate design of the solid slabs in one of the units, unit 6, is presented in Table 2. The reinforcement is shown for the maximum +ve moment (field moment) in both directions. It is clear from the table that the reinforcement used is ranging between 10-50% more than the required value.

Table 2. Comparison Between Existing and Accurate Bottom Reinforcement for Solid Slabs for Second Floor Roof of Unit 6

No	ts	Existing		Accurate		Increase
	(cm)	main	secondary	main	secondary	%
S1	12	Φ10/15	Φ10/15	Φ10/20	Φ10/20	40
S2	12	Φ10/15	Φ10/15	Φ10/20	Φ10/20	40
S3	12	Φ10/16.7	Φ10/20	Φ10/20	Φ10/20	12
S4	12	Φ10/16.7	Φ10/20	Φ10/20	Φ10/20	12
S5	12	Φ10/16.7	Φ10/20	Φ10/20	Φ10/20	12
S6	12	Φ10/15	Φ10/20	Φ10/20	Φ10/20	15
S7	16	Φ12/15	Φ12/16.7	Φ12/20	Φ10/20	53

Flat Slabs

Flat plates encountered in the sample were of irregular configurations (columns are not of equal spacing and not aligned), and hence the simplified code method for determining the straining action by dividing the plate into column strip and field strip was not applicable. Analysis may be performed by using the equivalent frame method, outlined in the ACI-318 (1989), or more accurately, using a three-dimensional finite element model utilizing plate elements to determine the straining actions. The latter approach was employed to model flat plates using the general-purpose finite element program SAP 2000 (1995). Shell elements were used to represent the flat plate and beam elements were used to represent the marginal/drop beams.

The flat slab thickness used was 18 cm and the concrete cover was assumed to be 1.5 cm for the purpose of design calculations. Maximum values for positive (field) bending moments were used to determine the required bottom reinforcement directly, whereas maximum values for negative reinforcement were averaged for a width of 50 cm for design purposes. This procedure is a common practice to avoid designing on a very local sharp peak that typically occurs at supports as a result of the finite element discretization. The high negative moment

value that is averaged is typically at limited locations that are already covered within the column cross section.

A sample comparison between the reinforcement for the flat slab system for unit 3 in the existing structure and the accurate design is given in Tables 3 and 4. The reinforcement is shown for the maximum field moment in two perpendicular directions for the first floor slab in Table 3, whereas the maximum -ve moment (on top of columns) in both directions is presented in Table 4. It is clear from the table that the percentage of increase in the reinforcement used ranges from 0 to 156% more than the required value based on the maximum moment at each strip/location.

Table 3. Comparison Between Existing and Accurate Bottom Reinforcement for Flat Slab (for +ve moment) in the Second Floor of Unit 3

Strip Location	**Direction 1**					**Direction 2**				
Col. Location	**A_s existing**		**A_s accurate**		**%**	**A_s existing**		**A_s accurate**		**%**
	Φ	**S**	**Φ**	**S**	**incr.**	**Φ**	**S**	**Φ**	**S**	**incr.**
1-2&جـ-د	12	20	10	20	44	10	20	10	20	0
3-6&جـ-د	14	20	12	20	36	16	20	12	20	78
1-2&د-هـ	14	20	12	20	36	10	20	10	20	0
3-6&د-هـ	16	20	12	20	78	12	20	10	20	44
1-2&هـ-ز	14	20	10	20	96	16	20	10	20	156

Table 4. Comparison Between Existing and Accurate Top Reinforcement for Flat Slab (for –ve moment) in the Second Floor of Unit 3

Strip Location	**Direction 1**					**Direction 2**				
Col. Location	**A_s existing**		**A_s accurate**		**%**	**A_s existing**		**A_s accurate**		**%**
	Φ	**S**	**Φ**	**S**	**incr.**	**Φ**	**S**	**Φ**	**S**	**incr.**
2&هـ	16	20	14	20	30	14	20	14	20	0
4&هـ	16	20	12	20	78	16	15	14	20	74
6&د	16	15	14	20	74	14	20	14	20	0
2&و	12	20	12	20	0	14	20	14	20	0
4&و	12	20	12	20	0	14	20	12	20	36

Beams

Flexure Reinforcement

Detailed comparison of the existing and accurate flexure reinforcements of beams in the six units was performed. Comparison was made in terms of the reinforcement ratio of the existing reinforcement to the accurate reinforcement determined assuming the same cross sections as per the existing drawings. To make the comparison more visible, the average values of the reinforcement ratio for the six units are shown in Fig. 1. Averaging is made over all beams and all floors for top and bottom reinforcement so that a single ratio can be obtained for each building as shown in Fig. 1. Overall average flexure reinforcement ratios range from 1.16 to 2.04, i.e. flexure reinforcement is over-designed on the average by as much as 15 to 100%. This is an alarming finding and current practices need improvement in order to achieve cost-effective designs.

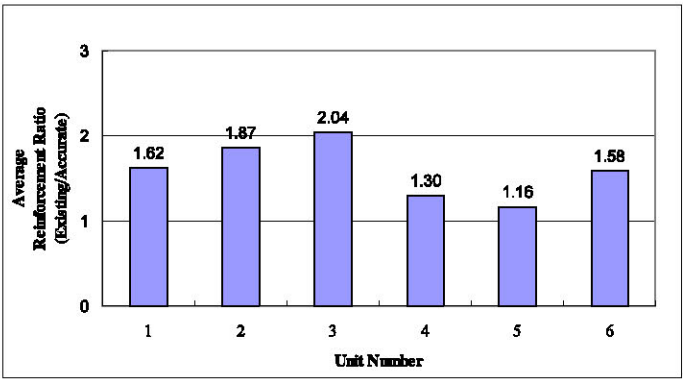

Fig. 1. Average flexure reinforcement ratios for the six units.

Shear Reinforcement

Shear reinforcement in beams is in the form of stirrups provided to resist shear stresses. Shear reinforcement ratios of existing to accurate reinforcements were calculated for all beams in each unit. Average ratios similar to the one presented for flexure reinforcement are shown in Fig. 2 for the six units. The average values are ranging between 1.08 and 2.05, i.e. shear reinforcement in beams are over-designed by as much as 8 to 100%.

Fig. 2. Average shear reinforcement ratios of the six units.

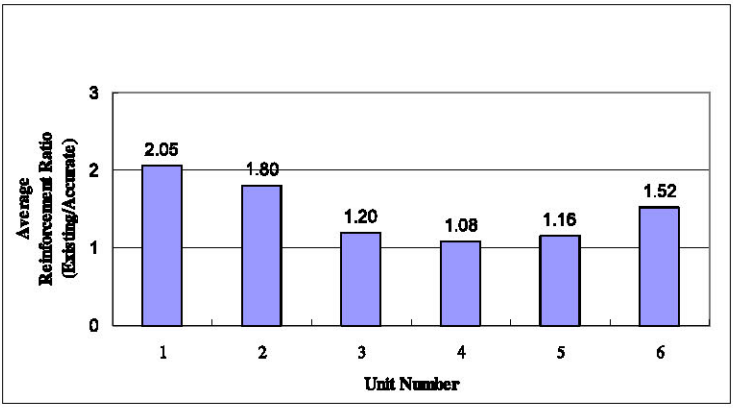

Columns

The design of columns was based on the ACI-318, assuming axial load with minimum eccentricity. Two approaches were used for the comparison of the accurate and existing designs. In both approaches, the concrete dimensions were fixed. The first approach assumed the minimum reinforcement necessary to sustain the given loads, given that the concrete dimensions are unchanged. It was noted that, even with the minimum reinforcement, the column capacities were much larger, indicating that the concrete dimensions chosen for the existing design are excessive. Average column reinforcement ratios of all units are shown in Fig. 3. Apart from units 1 and 4, ratios are rather low. A second approach was used by finding the capacity of the existing columns and ratios of the existing column capacity to the actual load acting on columns were calculated and found to be very high and can reach up to ten. This clearly indicates the oversizing of columns. Average ratios range from 2.8 to 4.3 as shown in Fig. 4.

Fig. 3. Average reinforcement ratio for columns in the six units.

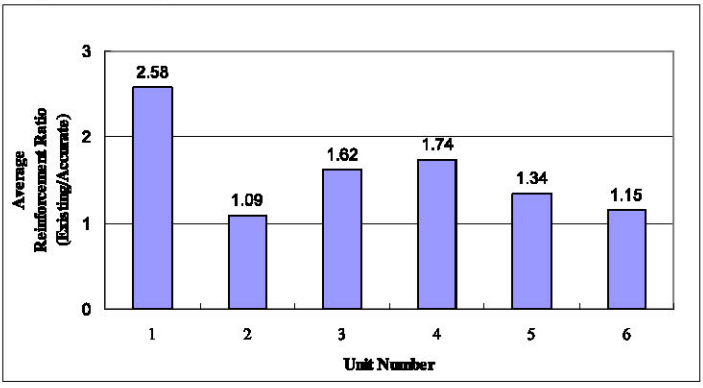

The large difference in the capacity versus load in small-sized columns is due to the minimum dimension of columns used (20 x 40 cm) in the existing design. This is an acceptable common practice to ensure proper column forming during construction. It is also possible that the increase in column size was due to architectural requirements.

Fig. 4 Average capacity-to-actual-load ratio of columns in the six units

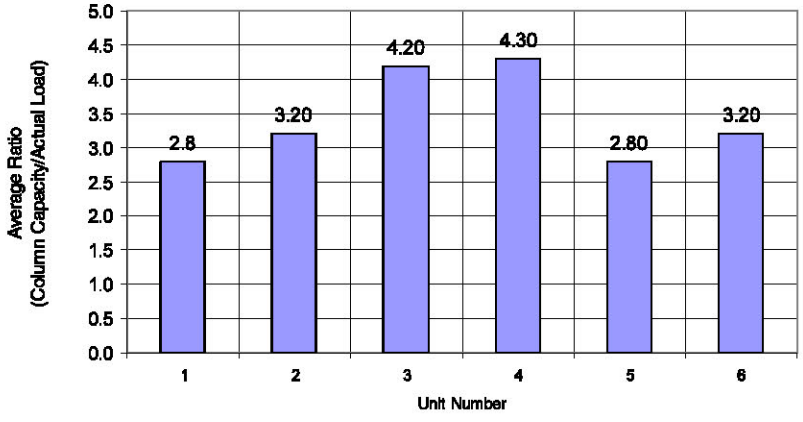

CONCLUSIONS

1. Based on the comparison of existing and accurate designs of the buildings sample, all structural members are invariably found to be highly over designed. Maintaining the same concrete dimensions as per the existing design, the reinforcement provided is found to be much higher than required and determined by the accurate design conducted in the present study. The average percentages, as obtained for the entire buildings sample, of increase of reinforcement are 30% for slabs, 60% for beams and 60% for columns.
2. Columns are substantially oversized in terms of concrete dimensions, the carrying capacity of these elements as per the existing design is found to be much higher than the actual applied loads by as much as 240% for columns, on the average.

REFERENCES

1. ACI-318. 1989. Building Code Requirements for Structural Concrete. American Concrete Institute, Detroit, Michigan, USA.
2. Sadek, A.W., Al-Mutairi, N., Al-Fadala, S., Karam, H. and El-Shinnawy, A. 2001. Cost and safety impact of current design practices of residential buildings in Kuwait. Kuwait Institute for Scientific Research, Report No. KISR 6020, Kuwait.
3. SAP 2000. 1995. General Purpose Finite Element Program. Computers and Structures Inc., California, USA.
4. STAAD III. 1990. Version 19.1, Structural Analysis and Design Software, Research Engineering International, California, USA.

Proceedings of the ACI-KC First International Conference & Fourth Exhibition. September 29-October 1, 2003, Kuwait — ***Concreting and High Performance Concrete in Hot Weather.***

A STUDY ON COST ESTIMATION OF STRUCTURAL CONCRETE FRAMING FOR RESIDENTIAL BUILDINGS IN KUWAIT

Hasan Kamal, Ph.D.
Kuwait Institute for Scientific Research, Building and Energy Technologies Department, PO Box 24885 Safat, 13109 Kuwait, Tel: (965) 4836100 Ex. 4561, Fax: (965) 4845763, hkamal@kisr.edu.kw

Khaled Al-Rasheed, Ph.D.
Kuwait University, Civil Engineering Department, PO Box 5969 Safat, 13060 Kuwait, Tel: (965) 4811188 Ex. 5742, Fax: (965) 4817524, khaled@civil.kuniv.edu.kw

ABSTRACT

Accurate estimate of the construction cost of buildings is extremely important to the contracting parties. Uncertainty in the final cost of a building is reduced by increasing the accuracy level in the cost estimation processes of the building that avoids the unexpected cost rise during construction. A study was recently conducted to analyze the construction costs related to twenty concrete residential buildings projects from different locations around Kuwait and having different built-up areas. Information and pertinent cost data of the concrete structural framing were only collected. The data included the Material and Labor costs.

The Material cost consists of the cost of re-bar steel, cement, aggregate, formwork and blocks. The Labor cost consists of the cost of excavation, carpentry, concrete, steel re-bar, blockwork and general labor. The data were analyzed and it was found that using the same contractor in the construction of these buildings contributed in the cost reduction of the buildings to certain extend. The Material cost of the buildings represented in average around 61.25% of the total cost of the concrete framing of the building while the Labor cost represented around 38.75%.

BACKGROUND

Owners, Consulting Engineers, and Contractors are highly interested in accurately estimating the cost of buildings. The cost of the buildings depends on the construction processes, duration and many other factors. Cost estimation is the process of establishing the expected cost required to complete a project in accordance to the design plans and specifications, prior to commencement of construction.

Cost estimation can be divided into two main types, preliminary estimation and final estimation. Owners are usually interested in the preliminary cost estimation of projects. This preliminary estimattion will provide a rough and approximate cost of the project. The final cost estimation provides detailed and comprehensive information about the project items and activities. Contractors and bidder are usually interested in the final cost estimations.

Absolute assurance of determining the cost of a project is hard to be achieved because incomplete information is acquired for the expected construction processes and unexpected obstacles of the project. Therefore, uncertainties exist in cost estimation of projects. Uncertainty arises in cost estimation of a project due to the highly variable nature of projects. The resources needed to complete project activities on schedule may have limited information that directly affects the project estimation cost.

Other factors are inherent in uncertainty of construction cost estimation of projects due to variability in manpower and material cost and quality, construction methods and etc. Hence, accuracy of an estimate is a key factor which will reduce uncertainty in the final cost estimation and avoid unexpected cost rise during construction. Probabilistic approaches can be used in cost estimation of projects as uncertainties exist in the cost estimation processes of projects. The probability of accurately estimating the cost of a project can be determined and the standard deviation of this probability can be used as a measure of variation of the estimated cost.

Cost of construction resources changes from time to time based on the market fluctuations. In this study, data were collected during a period of 5 years for the cost of several projects in different locations in Kuwait and having different build-up areas. The projects were residential concrete buildings and the cost included the concrete framing systems only. The cost analysis was carried out in two parts namely Material cost and Labor cost. Material cost included the cost of re-bar steel, cement, aggregates, formwork and blocks. Labor cost included cost for carrying out works such as excavation, carpentry, concrete, steel re-bar, blockwork and general labor.

OBJECTIVES

A study was conducted on cost estimation of concrete framing systems of residential buildings projects in Kuwait. Material and Labor costs were collected and analyzed for several projects. The main objectives of this paper are:

- To determine the contribution of both Material and Labor costs to the total cost of the concrete framing systems of projects. The average ratios between the Material cost and the Labor cost to the total cost of the concrete framing systems of the project are determined.
- To classify the percentage of contribution of each item considered to the Material and Labor costs of the projects to the group cost and to the total cost of the concrete framing system. The average estimated cost of each item in the Material and Labor costs is determined and sorted with respect to the total cost of the concrete framing cost of the projects.

A STUDY: STRUCTURAL COST ESTIMATING

Description

A study was recently conducted in Kuwait for analyzing the construction cost of concrete framing systems for residential buildings projects. The cost data for twenty residential buildings were collected in Kuwaiti Dinar (K.D.). The projects were located in different locations along the east cost of Kuwait and having different built-up areas ranging from 550 to 2800 m^2.

Information and pertinent cost data were collected from these projects for a period of 5 years, from 1996 to 2000, and included costs of structural concrete framing only. The collected data included the Material cost and Labor cost of the concrete framing systems of the projects. The cost analysis was carried out in two groups, Material cost and Labor cost, as follows:

1. Material cost included cost of re-bar steel, cement, aggregates, formwork and blocks.
2. Labor cost included cost for carrying out works of excavation, carpentry, concrete, steel re-bar, blockwork and general labor.

It is worth to note that the surveyed projects were constructed by the same contractor. Therefore, the same material and workmanship qualities were assumed for all projects and uncertainties due to workmanship quality are neglected.

Methodology of Cost Estimation Analysis

The cost of the above mentioned projects were collected from the market and tabulated in a spreadsheet. These projects were all constructed by one contractor. The same workmanship quality was used and building materials with similar performance were also used. The costs were classified into two groups, Material and Labor.

The Material group consisted of all the wood required for making the formworks, the re-bar steel for reinforcing the concrete structural elements, blocks for building the concrete frames, and the amount of cement, aggregate and sand required for the concrete mixes.

The Labor group consisted of the manpower required to accomplish the excavation work at the beginning of projects, carpentry work for making the forms, steel re-bar work for laying out the steel re-bars in concrete based on the drawings, concrete casting work, blocking work, and general labors used in other activities during building the concrete frame of the projects.

The cost of each item of the two groups was determined for the twenty projects. As the projects had different built-up areas, the costs were divided by the areas; therefore, the cost of each item per square meter was estimated. The average Material cost for the twenty projects was expressed as

$$\overline{MC} = \frac{\sum_{i=1}^{n} MC_i}{n} \tag{1}$$

where $\overline{MC}$ is the average Material cost for the projects, MC_i is Material cost for project i, and n is the number of projects. The average Labor cost of the projects was defined as

$$\overline{LC} = \frac{\sum_{i=1}^{n} LC_i}{n} \tag{2}$$

where $\overline{LC}$ is the average Labor cost for the projects, LC_i is Labor cost for project i, and n is the number of projects. The average cost of each item of the Material and labor was determined and used in another study for predicting the cost of concrete framing systems of residential buildings.

The partial percentages are the ratios of the estimated cost of the type of work mentioned in the group divided by the total cost of the group. The total percentages are the ratios of the estimated cost of the type of work to the total cost of the concrete framing cost of the projects.

Results and Discussions

The actual Material, Labor, and total costs were determined for each project separately. By considering the average cost of the twenty projects, it was found that the Material cost represented 61.25 % and the Labor cost comprised 38.75 % of the total cost of the concrete framing systems of the projects as shown in Figure 1. Table 1 lists the partial percentage contribution of each type of work to the Material group with respect to the group. The table also shows the total percentage contribution to the total cost of the cost of the concrete framing systems of the projects.

The re-bar steel estimated cost had the highest partial and total percentage with respect to the group and total costs of the framing of the projects, 32.97% and 20.19%, respectively. Cement consisted of 25.44% and 15.58%, respectively, of the group and total costs of the concrete framing of the projects.

The percentage of cost contributions to the group and total costs of the framing systems of the projects were then sequenced by block material, 16.98% and 10.40%, aggregate, 12.98% and 7.95%, formwork, 9.94% and 6.09%, and Sand, 1.69% and 1.03%, respectively. Therefore, within the Material group, re-bar steel had the highest cost followed by cement.

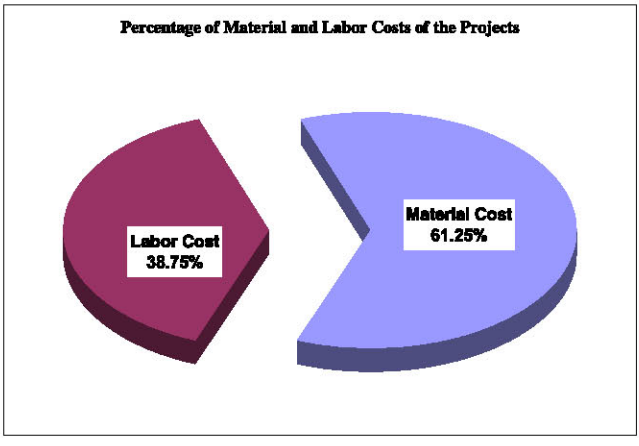

Figure 1. Percentage of Material and Labor Costs of The Projects.

Table 1. Cost Percentage of Material Group Works.

Material Cost Percentage to Total Cost of Project		61.25 %
Type of Work	Percentage of Work Type Cost to Material Cost (%)	Percentage of Type of Work Cost to Total Cost (%)
Formwork	9.94	6.09
Re-bar Steel	32.97	20.19
Cement	25.44	15.58
Aggregate	12.98	7.95
Sand	1.69	1.03
Block	16.98	10.40

The partial and total percentage contributions of each type of work in the Labor group with respect to the group and total costs of the concrete framing systems of the projects are listed in Table 2. Carpentry cost was the highest in this group as the percentage of the partial group cost was 39.91% and the percentage of the total project framing cost was 15.46%.

The partial and total percentages of the remaining works within Labor group were as follows: concrete casting, 18.04% and 6.99%, steel re-bar work, 16.19% and 6.28%, blocking labor, 15.36% and 5.95%, excavation, 5.98% and 2.32%, and general labor for other activities in the projects, 4.51% and 1.75%, respectively.

The partial percentages of the cost of items mentioned in both groups of work, Material and Labor are shown in Figures 2 and 3, respectively. The values in the Material cost are ranged from 1.69% to 32.97%. While the values in the Labor cost are ranged from 4.51% to 39.91%.

Table 2. Cost Percentage of Labor Group Works.

Labor Cost Percentage to Total Cost of Project		38.75 %
Type of Work	Percentage of Work Type Cost to Labor Cost (%)	Percentage of Type of Work Cost to Total Cost (%)
Excavation	5.98	2.32
Carpentry	39.91	15.46
Steel re-bar	16.19	6.28
Casting	18.04	6.99
Block Labor	15.36	5.95
General Labor	4.51	1.75

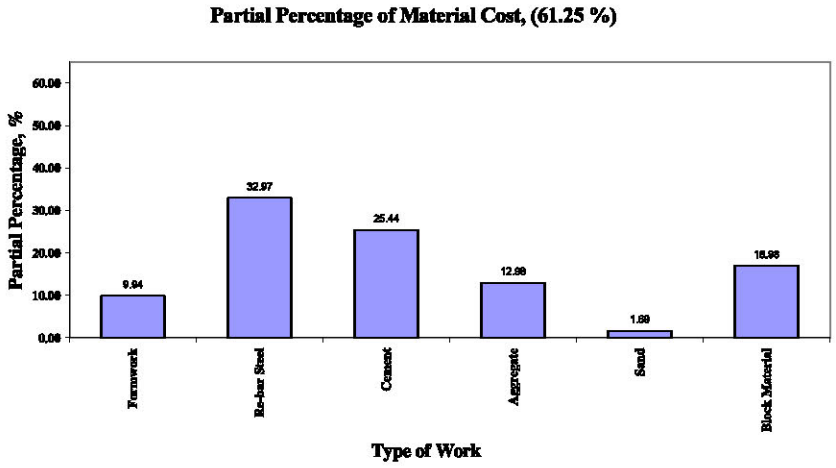

Figure 2. Partial Percentage of Material Cost with Respect to the Group.

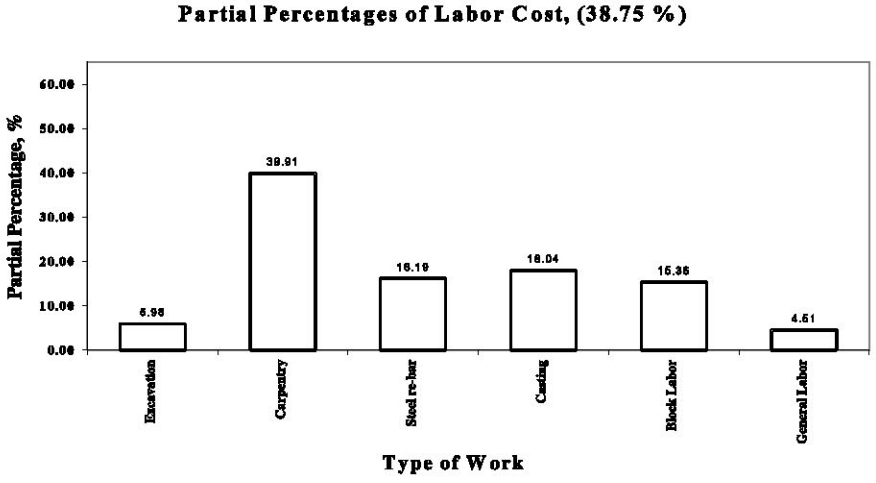

Figure 3. Partial Percentage of Labor Cost with Respect to the Group.

The contribution of the estimated cost of each item as a percentage cost with respect to the total cost of the concrete framing system of the projects is shown in Figure 4. The estimated costs are sorted from the left to the right of the figure. The re-bar steel, as a material, comprised about 20.19% of the total cost of the frames, in average. The estimated cost of cement and carpentry are almost the same around 15.58% and 15.46%, respectively.

The estimated cost of block material is next and around 14.40% of the total cost. The sequence of the estimated costs are then showed to be ordered as aggregate, concrete casting, formwork, steel re-bar work, blocking labor, excavation, general labor, and sand costs.

The estimated costs of the first three items, re-bar steel, cement, and carpentry comprised about 51.23% of the total cost of the framing systems. The remaining items comprised 48.77% of the total cost. The cost of a concrete framing system can be reduced to a significant level by finding a lower cost sources of materials, as the Material cost consist 61.25% of the total cost of the frames.

Reducing the Labor cost also contribute to some level to the reduction of the total cost of the concrete frame. Reducing the cost of the Labor group must be conditioned on the fact that the labors quality should meet a certain professionalism standard. Using bad quality labors for savings in the Labor cost may adversely affect the cost of the buildings. The affect may appear is the maintenance period of the buildings.

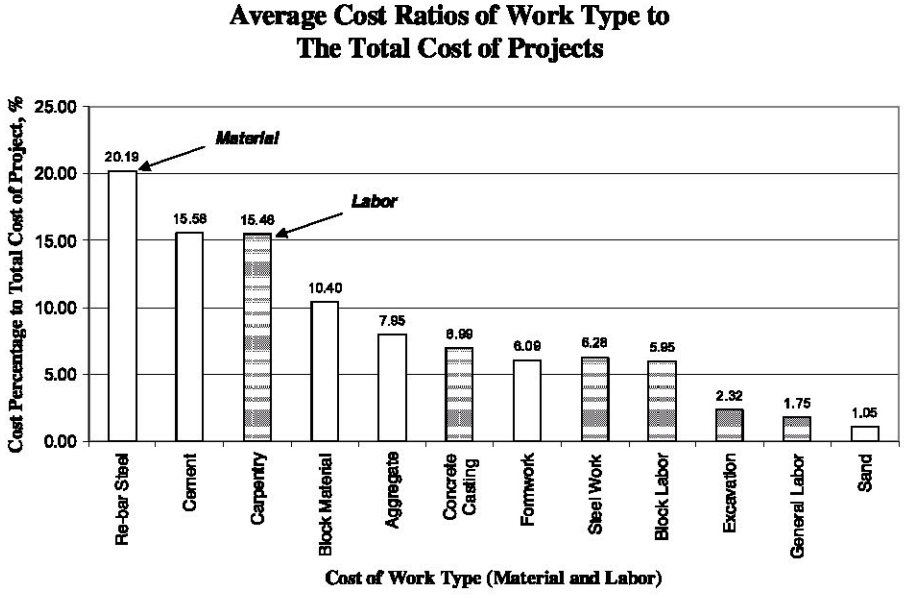

Figure 4. Percentages of Costs to the Total Cost of the Concrete Framings.

CONCLUSIONS

A study was conducted in Kuwait for determining the cost of the concrete framing systems of residential buildings. Two groups of estimated costs were collected and analyzed, Material cost and Labor cost. Each group consisted of several items. As a result of the analysis, it was found that the estimated Material cost comprised 61.25% and Labor estimated cost comprised 38.75% of the total structural framing cost. The contribution of each item of the two groups to the total cost of the framing systems of the structures was determined and sorted.

The re-bar steel, cement and carpentry costs comprised a significant percentage of the total cost of the concrete frames. It was found that by appointing the same contractor on several projects the cost of buildings could be reduced to a certain extent. This is due to the fact that the source of materials remains the same and re-locating them between the various

sites minimizes cost of resources like manpower and equipment. Also the overhead cost of the contractor is much less.

The analysis conducted in this study is useful for Owners, Consulting Offices and Contractors for precisely estimating the cost of their future projects. Another study is now in process as a continuation of this work for accurately estimating the cost of concrete framing systems using simulation methods.

REFERENCES

Adrian, J. J. (1982), Construction Estimating, Prentice-Hall, Virginia.

Ayyub, B. M. and Gupta, M. M. (1994), Uncertainty Modelling and Analysis: Theory and Applications, Elsevier Science B. V., Amsterdam, Netherlands.

Dagostino, R. F. (1993), Estimating in Building Construction, Prentice-Hall, NJ.

Kamal, H. A. (2001), Simulation-Based Reliability Assessment Methods of Structural Systems, Ph.D. Dissertation, University of Maryland at College Park, MD.

Shtub, A., Bard J. F. and Globerson, S. (1994), Project Management: Engineering, Technology, and Implementation, Prentice-Hall, NJ.

Proceedings of the ACI-KC First International Conference & Fourth Exhibition. September 29-October 1, 2003, Kuwait — ***Concreting and High Performance Concrete in Hot Weather.***

SHEAR TESTS OF BEAMS WITH VARIABLE CONCRETE COVER

Khaldoun N. Rahal
Associate Professor, Department of Civil Engineering, Kuwait University

ABSTRACT:

A study was conducted to investigate the effects of increasing the thickness of the concrete cover on the shear behavior of four reinforced concrete beams. Three of the four beams had two test regions, and hence, a total of seven test results are reported. The thickness of the concrete cover ranged from 5 mm to 75 mm for the four tests with target concrete strength of 25 MPa and from 25 mm to 75 mm for the three tests with target concrete strength of 40 MPa. All the beams were reinforced in the transverse and longitudinal directions. The main objective of the experiments is to study the shear behavior of beams with variable concrete cover, with emphasis on spalling of the concrete cover, and crack pattern and spacing.

INTRODUCTION

Building codes around the world require relatively large thickness of the concrete cover to protect the reinforcement from the threats of corrosion and fire.

The increase in the thickness of the concrete cover affects the behavior of sections subjected to shear. Figure 1 shows a corner of a section subjected to shearing stresses. The compressive diagonal stresses, which contribute in resisting the applied shear force, changes direction near the corners. This creates tensile stresses in the direction perpendicular to the direction of the compressive stress. If these tensile stresses exceed the resistance of the concrete, splitting will take place, causing spalling in the cover. A similar phenomenon takes places in sections subjected to torsion.

Arbesman (1974) tested a beam specimen in a predominant flexural shear loading. The beam had two test regions with zero and 40-mm covers to the reinforcement on the vertical sides. The region with larger cover suffered from spalling and resisted a load smaller than that with zero cover.

Rahal and Collins (1995) tested seven specimens to study the effects of concrete cover on the shear-torsion interaction. The steel cages of the specimens were similar, but had either 22.5 or 42.5 mm cover thickness. The experiments showed that the shear specimens with small and large concrete cover failed at about the same load level, and that was mainly due to the spalling in the specimens with larger cover thickness.

This paper reports the results of an experimental programme in which four beams were tested under a four-point loading setup. These beams were reinforced with transverse and longitudinal steel and three of them had two test regions. Hence a total of seven test results are reported. The main objective is to study the effect of variable thickness of concrete cover on the general shear behavior, with emphasis on the increased potential of cover spalling and on the crack pattern and spacing.

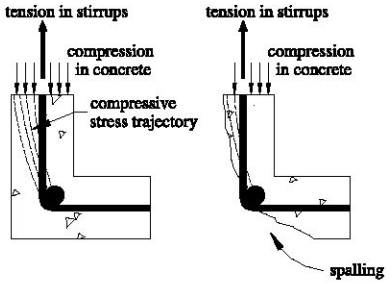

Figure 1: Spalling of concrete cover in sections subjected to shear

Figure 2 and Table 1 show the test set-up and give details of the four specimens. The seven test specimens were divided into two series I and II. Series I consisted of 4 test-regions, identified as S1-25-00, S2-25-25, S3-25-45 and S4-25-75. Series II consisted of the remaining three test regions, identified as S2-40-25, S3-40-45 and S4-40-75. The difference between the test regions of the same series is the thickness of the concrete cover. The difference between specimens of series I and II was the target concrete strength, which was 25 and 40 MPa respectively.

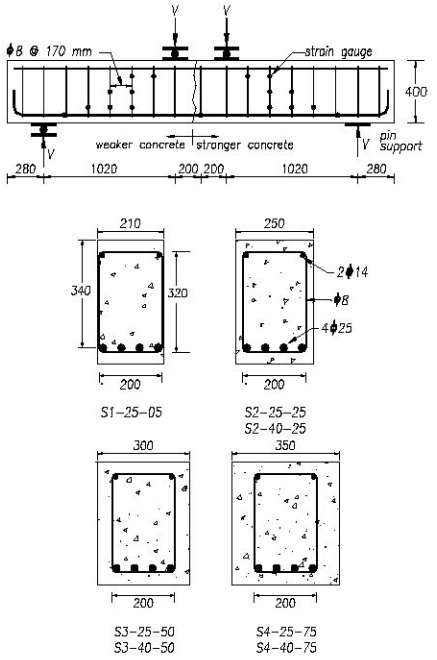

Figure 2: Details of beams and test set-up

The name of the specimen reflects its properties. For example, in specimen S3-25-75, S3 is for specimen number 3, 25 is the target compressive strength in MPa, and 75 is the thickness of the concrete cover in mm. The first specimen was cast using 25 MPa concrete and had a clear cover of about 5 mm on the vertical stirrups. Each of the remaining three specimens had two test regions, which were cast using two different concrete mixes. The two concrete mixes were designed to attain a target compressive strength of 25 and 40 MPa. The cover thickness in these three specimens was 25, 50, and 75 mm. The interface between the two concrete materials in the specimens was near mid-span as shown in Figure 2.

All the beam specimens were 3 m long, 250 mm wide, 400 mm deep and were tested at a shear span to depth ratio a/d = 3. The beams had similar reinforcement in the transverse and longitudinal direction, and the outer dimensions of the steel cage were 200 x 320 mm. The longitudinal reinforcement consisted of 4-ϕ25 bars in the tension zone and 2-ϕ14 in the compression zone. The transverse reinforcement consisted of closed ϕ8 stirrups spaced at 170-mm centers. This spacing is equal to about half the effective depth.

Table 1: Details of specimens

Series	Beam	b mm	cover (mm)	f'_c MPa	$\rho_v f_y$ *(MPa)*	V_{exp} *(kN)*
I	S1-25-05	210	5	24.3	1.20	165
	S2-25-25	250	25	25.3	1.00	192.5
	S3-25-50	300	50	27.3	0.84	197.5
	S4-25-75	350	75	25.3	0.72	242.5
II	S2-40-25	250	25	43.1	1.00	255.5
	S3-40-50	300	50	41.6	0.84	259.5
	S4-40-75	350	75	42.2	0.72	262.5

Concrete– Ordinary Portland cement was used along with two sizes of quartzite coarse aggregates (1/2 and 3/8 inch). The fine aggregate was natural sand. To obtain a measure of the compressive strength of the concrete, standard 102 x 305 mm (6 x 12 in.) cylinders were cast from the concrete used in the beams. These samples were cured in the same conditions as the beams, and were tested on the same day of testing the beams. Table 1 shows the experimental strength values of the concrete. The target compressive strength was achieved within an acceptable tolerance.

Reinforcing steel–Deformed bars with 14 and 25 mm diameters were used to reinforce the beams in the longitudinal direction as shown in Figure 2. Deformed bars, with 8 mm diameter were used to manufacture of the closed stirrups. Table 2 shows the properties of the reinforcing bars.

Table 2: Properties of reinforcing bars

Bar	*Area* mm^2	f_y MPa	f_u (MPa)
$\phi 8$	48	445	700
$\phi 14$	151	480	717
$\phi 25$	475	440	681

BEAM PREPARATION AND TESTING PROCEDURE

Fourteen strain gauges were attached to the transverse steel and three gauges to the longitudinal steel as shown in Figure 2. The ends of the longitudinal steel bars were bent to provide better development of the bars beyond the support.

The concrete was compacted using mechanical vibrators. The beam and the control cubes and cylinders were moist-cured using wet hessian. The curing stopped about two to three days before testing to allow for painting and placement of the beam on the loading frame.

The loading and support arrangement of the specimens is shown in Figure 2. The load was applied using a hydraulic jack on a spreader beam to give two equal loads 400 mm apart. Four 160 x 360 x 25 mm steel plates were used at the support and loading locations. One support location was restrained from movement in the longitudinal direction using a pin-type support, while the remaining plates were provided with roller-type supports to allow free longitudinal elongation of the beam.

The load was applied in increments of 50 kN at early stages of loading. The increments were subsequently reduced to 10 to 25 kN at later stages near ultimate conditions. After every load stage, the load was held constant for about ten minutes to allow marking the cracks, taking photographs of the beams, strain gauge reading, and checking for spalling.

Spalling is typically initiated by the separation of the cover from the concrete confined within the stirrups. Initial spalling is not necessarily accompanied by falling off of pieces of concrete and hence, the separation was checked by knocking on the concrete surface with a steel hammer and listening to the sound. A "hollow" sound indicates that separation have taken place.

EXPERIMENTAL RESULTS

All beams failed in shear before signs of yielding in any of the strain gauges attached to the longitudinal steel. The observed ultimate capacities of the tested beams are shown in Table 1.

Crack patterns and spalling

Figure 3 shows the final conditions of the four 25 MPa concrete specimens with cover thickness of 5, 25, 50 and 75 mm. The cracking pattern in all four specimens was typical for the type of shear test conducted. Flexural cracks appeared first at the bottom face of the beams. At larger loads, these cracks in the shear zone developed into diagonal flexural-shear cracks. The shear failure took place along one major diagonal crack.

Specimen S1-25-05 had a 5-mm thick clear cover and did not suffer from any spalling as shown in Fig. 3. Near ultimate conditions, very limited areas of the cover fell off. At this relatively small cover thickness, a large number of diagonal cracks developed.

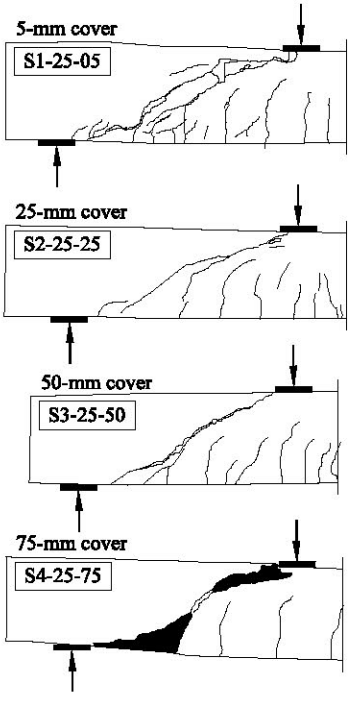

Figure 3: Crack pattern in beams with 25 MPa concrete target strength

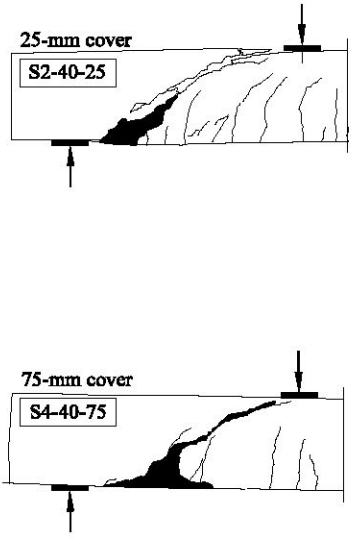

Figure 4: Crack pattern in beams with 40 MPa concrete target strength

Specimen S1-25-25 had a 25-mm thick clear cover did not suffer from spalling. Figure 3 also shows a smaller number of diagonal cracks in the 25-mm cover specimen compared to the 5-mm cover specimen. Specimen S1-25-50, which had a 50-mm clear cover, did not suffer from spalling.

Specimen S1-25-75 had the largest cover (75 mm) and suffered from spalling in areas near the lower parts of the failure diagonal crack as shown in Fig. 3. This spalling was observed simultaneously with the ultimate load. Knocking at the surface of the concrete at the load stage taken at 97% of the ultimate load did not reveal any signs of spalling. At the lower end of the crack, all the concrete cover outside the stirrups spalled off. Meanwhile, spalling near the upper end of the crack was limited in width, with wider spalling near the surface compared to that deeper in the section near the stirrups. Near the bottom part of the beam, the depth of spalling reached the steel near the corners. Considerable spalling affected the lower 40% of the section, but decreased in spread in higher areas as shown in Fig. 3. The concrete across the full width at the bottom of the beam spalled off. Figure 3 shows a consistent decrease in the number of diagonal cracks as the concrete thickness increases.

Figure 4 shows the final conditions of two of the 40 MPa specimens with cover thickness of 25 and 75 mm. Photos of the final load stages of the specimen with 50 mm cover were not available due to technical difficulties. The cracking pattern was similar to that of the specimens of the 25 MPa series of tests. Similar to the observed pattern in Fig. 3, the number of diagonal cracks decreased when the thickness of the concrete cover increased. Specimen S2-40-25 suffered from spalling near the lower end of the major diagonal crack near the support. The bottom side of the specimen did not fully spall, and the depth of the spalling across the width of the section decreased dramatically along the height of the concrete section. Comparing the specimens S2-25-25 and S2-40-25 (which also had 25-mm cover), it is observed that the stronger concrete resisted 33% higher load, but suffered from spalling.

Specimen S3-40-50 suffered from spalling near the lower end of the failure diagonal crack near the support. The intensity of the spalling was comparable to that in specimen S2-40-25.

Specimen S4-40-75 also suffered from spalling near the lower end of the failure diagonal crack near the support as shown in the figure. However, this spalling was not as severe as that in specimen S4-25-75. The bottom side of the specimen did not fully spall, and the depth of the spalling across the width of the section decreased considerably along the height of the section similar to S2-40-25. Comparing the specimens S4-25-75 and S4-40-75, both with a 75-mm thick cover, it is observed that the stronger concrete resisted only 8% higher load, but suffered from a less severe spalling.

Figures 3 and 4 show that spalling affected the behavior of specimens with larger concrete cover. These figures also show that spalling in members subjected to shear is concentrated near the corners of the cross-section, leaving the central part unaffected. A similar trend was observed in the crack pattern of the shear tests reported by Rahal and Collins (1995) in spite of the difference in the test set-up. The spalling observed in Arbesman's (1974) specimen beams was also concentrated near the corners, with relatively less spalling near mid-height of the section.

CONCLUSION

Based on the behavior of the specimens of variable concrete cover, the following conclusions can be made:

1. Increasing the thickness of the concrete cover resulted in a decrease in the number of diagonal shear cracks.
2. Spalling was observed in the specimens with larger concrete cover, but was limited to the corners of the section. A considerable part of the concrete cover on the vertical side remained unspalled.
3. For the 75-mm thick cover, spalling in the specimen with lower concrete strength was more severe than that in the specimen with higher concrete strength. The opposite is true for the specimen with 25 mm cover.

ACKNOWLEDGMENT

The support of Research Administration and the Department of Civil Engineering at Kuwait University is gratefully acknowledged.

NOTATIONS

a	=	shear span
b	=	width of beam cross section
d	=	effective depth of beam cross section
f'_c	=	compressive strength of concrete or cylinder strength
f_y	=	yield stress of reinforcing steel
f_u	=	ultimate strength of reinforcing steel
P	=	applied load on beam
V_{exp}	=	experimental ultimate shear force
ρ_v	=	ratio of transverse reinforcement

REFERENCES

Mitchell, D. and Collins, M.P., *Behavior of Structural Concrete Beams in Pure Torsion.* Publication 74-06, Department of Civil Engineering, University of Toronto, 1974.

Arbesman, B., *Effect of Stirrups Cover and Amount of Reinforcement on Shear Capacity of Reinforced Concrete Beams.* MEng. thesis, University of Toronto, 1975.

Rahal, K.N. and Collins, M.P., "Effect of Concrete Cover on the Shear-Torsion Interaction– An Experimental Investigation." ACI Structural Journal, Vol. 92, No. 3, May-June, 1995, pp. 334-342.

Proceedings of the ACI-KC First International Conference & Fourth Exhibition. September 29-October 1, 2003, Kuwait — ***Concreting and High Performance Concrete in Hot Weather.***

A COMPARISON BETWEEN THE FRACTURE TOUGHNESS OF DIFFERENT TYPES OF CONCRETE

Hisham Abdel-Fattah
Department of Civil Engineering, College of Engineering, University of Sharjah, P.O. Box 27272, Sharjah, United Arab Emirates.

ABSTRACT

The fracture behavior of concrete, in general, plays an important role in the overall assessment of the structural performance of the building. One important fracture parameter is the fracture toughness K_{IC} (also known as the Mode I Stress Intensity Factor) which is defined as the ability of the concrete material to absorb energy in the presence of cracks. The higher the fracture toughness, the better the performance and the durability of the concrete. The Fracture toughness is obtained experimentally by testing pre-notched concrete beams up to failure under four point bending. In this study, the fracture toughness of two types of concrete used in construction in the Arabian Gulf are investigated. The two types are Polymer Portland Cement Concrete (PPCC), and Autoclaved Aerated Concrete (AAC). The first type is also used as repair material for deteriorated concrete. A comparison is made between the experimental results of the two types together with the fracture toughness of the conventional Ordinary Portland Cement Concrete (OPCC). Environmental conditions such as temperature and exposure to sea water are also included in the study. The results show that adding a polymer such as epoxy to the concrete improves the fracture behavior of the structural member. Also, the environmental conditions are shown to have a great effect on the fracture toughness of concrete.

INTRODUCTION

Tests to determine the fracture toughness (K_{IC}) for concrete were carried out at different temperatures on different sizes and shapes of notched concrete specimens (Cherepanov 1979, Bazant & Prat 1988, Brameshuber 1989, Maturana *et al.* 1990). The tests showed that unlike metals, the value of K_{IC} for concrete decrease at elevated temperatures. The effect of cyclic heating (Abdel-Fattah & Hamoush 1997) showed that the residual fracture toughness decreased considerably after every heating and cooling cycle. Studies on the fracture behavior of epoxy polymer concrete (Vipulanandan & Dharmarajan 1989) concluded that K_{IC} for epoxy polymer concrete increases with the increase in polymer content and decreases with increase in temperature. Different numerical methods were developed to estimate the fracture toughness of concrete beams at different temperatures (Abdel-Fattah & Hamoush 1996, 1998).

The main objective of this study is to determine the fracture toughness experimentally on beams made of the materials used in concrete construction in the Gulf area. The study was made on Ordinary Portland Cement Concrete (OPCC), Polymer Portland Cement Concrete (PPCC), and Autoclaved Aerated Concrete (AAC). The study also aims at determining the effects of the harsh environmental conditions of the Gulf on the fracture toughness.

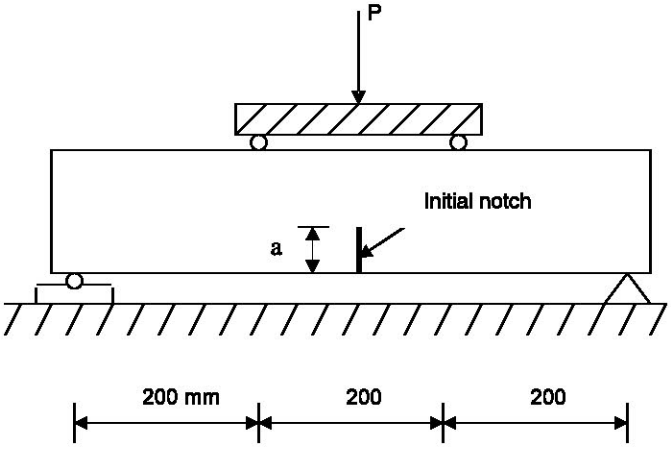

Fig. 1 Test set-up for Fracture Toughness

The Mode I stress intensity factor (K_I) for a concrete beam is obtained by testing the beam under four point bending as shown in Fig. (1). The beam has a total length of 750 mm and cross-sectional dimensions 150x150 mm. The beam is first pre-notched at mid span and then tested to failure. The ratio between the crack length and beam depth is kept constant in all experiments at 1:6. The fracture toughness is then computed as follows (Tada *et al* 1985):

$$K_I = \sigma \sqrt{\pi a}\, F\left(\frac{a}{b}\right) \qquad (1)$$

The stress σ is calculated by:

$$\sigma = \frac{6M}{b^3} \tag{2}$$

where

$$M = \frac{(P)(S)}{6} \tag{3}$$

The function F (a/b) is evaluated as follows:

$$F(\frac{a}{b}) = 1.09 - 1.735(\frac{a}{b}) + 8.2(\frac{a}{b})^2 - 14.18(\frac{a}{b})^3 + 14.56(\frac{a}{b})^4 \tag{4}$$

where a is the crack length (25 mm), b is the beam depth (150 mm), S is the clear span (600 mm) and P is the applied load. The fracture toughness K_{IC} is computed from Eq.(1) after substituting the value of the critical load at failure into Eq.(3) and in this case $K_I = K_{IC}$.

For every beam tested, three control cylinders made of the same concrete and subjected to the same environmental conditions were tested to find the concrete compressive strength (f_c'). The compressive strength tests were carried out on an MTS machine equipped with a moving head platen. The load was applied in increments of 25 KN. The same machine was used for testing the beams and in this case the load was applied in increments of 1 KN. The beam deflections were measured by two LVDTs placed on the two sides of the notch and each located 25 mm away from it. In all the experiments where concrete was exposed to heat, the residual fracture toughness was obtained and the K_{IC} tests were carried out after allowing the concrete to cool off to room temperature.

The notch thickness for all the beams was 2 mm and was made by placing a piece of plexi-glass with the desired crack dimensions into the mold prior to casting. After hardening of concrete and removal of the mold, the plexi-glass piece was removed, thus leaving the desired notch.

ORDINARY PORTLAND CEMENT CONCRETE (OPCC)

In this study, a total of 80 beams were tested using the set-up shown in Fig.(1). The beams were heated by placing them in an oven preheated to the desired temperature. They were kept in the oven for 24 hours and then left to cool in room temperature. This represents one cycle of heating and cooling. The temperatures investigated were 50, 100, 150, 200, 250 and 300 °C. The concrete mix design is shown in Table (1). The mix was designed such that an average compressive strength of 36 MPa is obtained. All specimens were moisture cured in a curing room at 21°C and 95% relative humidity for 28 days.

Table 1. Concrete Mix Design for OPCC

Material	Quantity, Kg/m^3
Cement Type I	421
Fine aggregate (fineness modulus=2.7)	709
Water	190
Coarse aggregate	933

Results of fracture tests on OPCC are shown in Table (2). The table shows that the fracture toughness is greatly influenced by temperature even after cooling. The decrease in fracture toughness becomes more significant at temperatures greater than 50 °C. At a temperature of 300°C, the concrete looses about 60% of its compressive strength and about 30% of its fracture toughness.

Table 2. Experimental values for K_{IC} for OPCC

Temperature °C	F_C' N/mm^2	K_{IC} $N/mm^{3/2}$	K_{IC}/F_C' $mm^{1/2}$
22	36	28	0.78
50	35	27	0.77
100	33	26	0.79
150	28	24.5	0.88
200	27	23	0.85
250	26	21	0.81
300	22	20	0.90

POLYMER PORTLAND CEMENT CONCRETE (PPCC)

Polymer Portland Cement Concrete (PPCC) mixtures are normal portland concrete mixtures to which a polymer has been added during the mixing process. In epoxy modified mixtures, the polymer is formed after the components of the epoxy (base + hardener) are added to the concrete mix where the polymerization process occurs concurrently with the hydration of the cement. Polymer-modified portland-cement concretes and mortars exhibit improved strength properties such as flexural strength, tensile strength and abrasion resistance over similar unmodified concretes and mortars. PPCC applications include overlays of bridge decks, precast members, patching, industrial floors and floors of parking decks.

A total of 40 beams were tested in this study using the set-up shown in Fig.(1). For each beam, three control cylinders of 100 mm in diameter and 200 mm in height were tested to determine the concrete compressive strength (f_c').

The different mixes used in this study are summarized in Table 3. All mixes had a water cement ratio of 0.5. Sand of fineness modulus of 2.6 and quartzite coarse aggregate of maximum aggregate size ¾ inch (19 mm) were used. The sand and the coarse aggregates

were washed and dried before mixing. Type I cement was used and the polymer content in the mix was added as a partial replacement of the cement. The polymer used was an epoxy recommended for grouting and is widely used in the gulf region. Polyamine hardener was used with the epoxy.

All beams and cylinders were cast vertically in steel molds. During casting, the concrete was first hand compacted with a rod and the molds were then put on a shaking table for 2-3 minutes. The molds were removed after twenty-four hours and all specimens were moist cured in a curing room at 21 °C and 95% relative humidity for 28 days. The beams were heated by placing them in an oven preheated to the desired temperature. Each beam was kept in the oven for twenty-four hours and then removed and left to cool in room temperature for another twenty-four hours before testing. The temperatures investigated were 22 (room temperature), 50, 100, 150 and 200°C. Two beams and three cylinders were prepared from each mix. For each test, the cylinders were subjected to the same heating conditions as the beams.

Table 3. Concrete Mix Design for PPCC

Material	Quantity, Kg/m^3
Cement Type I	400
Fine aggregate (fineness modulus=2.6)	594
Water	200
Coarse aggregate:	1108
• ¾ in (19 mm)	465
• ½ in (12 mm)	421
• 3/8 in (10 mm)	222
Epoxy content:	-
• 0 %	40
• 10 %	60
• 15 %	80
• 20 %	

The experimental results for PPCC are summarized in Table (4). The results show that while the increase in temperature decreases the fracture toughness, the addition of epoxy greatly enhances the fracture behavior of the concrete beams. For all mixes, the residual fracture toughness decreased by an average value of 21% when heated to 200 °C.

The loss in residual K_{IC} for PPCC was higher than that of Ordinary Portland Cement Concrete. This is due to the fact that the epoxy properties are affected by the high temperatures and as a result, part of the bond between the aggregates was lost.

Table 4. Experimental values for K_{IC} for PPCC

Percent Epoxy	Temperature °C	F_C' N/mm^2	K_{IC} $N/mm^{3/2}$	K_{IC}/F_C' $mm^{1/2}$
0 %	22	20	14.77	0.738
	50	19	14.51	0.764
	100	17.8	13.82	0.776
	150	17.1	13.47	0.788
	200	14.3	11.73	0.820
10 %	22	21.4	15.87	0.742
	50	21.1	15.72	0.745
	100	19.6	14.86	0.758
	150	19	14.51	0.764
	200	15.6	11.95	0.766
15 %	22	23.4	17.01	0.727
	50	22	16.22	0.737
	100	21.4	15.87	0.742
	150	20.1	15.18	0.755
	200	17.5	13.63	0.779
20 %	22	27.3	19.07	0.700
	50	25.3	17.96	0.710
	100	23.3	16.92	0.726
	150	20.5	15.37	0.750
	200	19.6	14.86	0.758

AUTOCLAVED AERATED CONCRETE (AAC)

Lightweight concrete is widely used as a construction material all over the world due to its desirable properties such as the good quality of the product, good sound absorption, reduced echo effect in empty rooms and improved insulating properties which saves in both heating and air conditioning.

The use of lightweight concrete also results in a reduction in the overall weight of the building and that results into more economical cross sections. The lightweight of the concrete could be achieved either by using lightweight aggregate (Lightweight Aggregate Concrete) or by using additives that react with the constituents of the concrete mix and produce air bubbles (Lightweight Aerated Concrete). Aerated concrete blocks are in general advantageous over the normal concrete blocks.

AAC concrete is used for producing masonary blocks as well as structural elements such as lintels. The reinforcement used is usually protected against corrosion for increased durability. However, since accidental overload conditions may happen and cracks may appear, the issue of fracture toughness of AAC concrete becomes important. Fracture tests on AAC have shown a decrease in the fracture toughness with the increase in autoclaving time (Norifumi 1994). Experiments also showed a similarity between AAC and structural concrete in terms of fracture mechanisms and that the fracture energy G_f is dependent on the specimen size (Bruhwiller et al, 1990). The durability of AAC, however, still needs to be examined in more detail. Carbonation of AAC was investigated (Henecka et al 1997). During the long-term investigation of the physical properties of AAC in the indoor environment with changing

relative humidity and temperature, a significant increase of the AAC density was detected. The increase in density was found to be a consequence of the carbonation process.

In this study, the strength of AAC cubes as well as the fracture toughness behavior of AAC beams under both temperature and exposure to sea water were examined. A total of 20 beams were tested and for each beam, four control specimens (cubes) were used to determine the concrete compressive strength. Each control specimen was subjected to the same environmental conditions as the tested beam. The specimens were tested after being submerged in seawater obtained from one of the beaches of Kuwait City.

Water was kept in two basins, one stored under an average room temperature of 22°C while the other was kept in an oven with the temperature kept constant at 70°C. The specimens were stored for time durations of 1,7,28,56 and 90 days prior to testing. The 70°C temperature was chosen since its common that concrete reaches this temperature in the Gulf states during daytime. In Kuwait City, for example, the temperature in the shade may reach 52°C (125 °F) during the months of July and August.

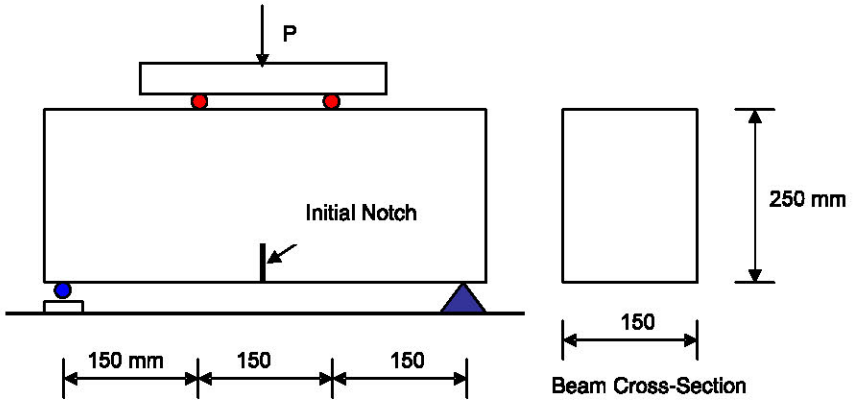

Fig. 2 Set-up for the Fracture Toughness Tests for AAC

The test specimens were ordered from a local plant in Kuwait that produces Autoclaved Aerated Concrete. All the specimens where made from the same concrete batch at the plant. The concrete had an average compressive strength of 4.0 MPa and a modulus of elasticity of 1750 MPa.

The compressive strength tests were carried out on cubes of dimensions 100 x 100 x 100 mm. For all beams, the cross-sectional dimensions were 150 x 250 mm and the length was 625

mm. Those are standard dimensions produced by the concrete plant. Beams for the fracture tests were tested under four point bending with a clear span of 450 mm. For this type of concrete, a diamond saw was used to precrack the beams at midspan. The resulting through crack was 2 mm wide and 50 mm long. The test set-up is shown in Fig. 2.

The results for AAC tests are shown in Table (5). From table one concludes that AAC looses 20% of its fracture toughness and 40% of its cube strength when submerged in sea water for 90 days. Thus, the issue of durability could be a problem for buildings that use AAC. In this case the concrete should be provided with a very effective waterproofing system. Also, the concrete should be well insulated to avoid been subjected to excessive temperatures.

Table 5. Experimental values for K_{IC} for AAC

Temp. °C	Duration in Seawater (Days)	f_C' N/mm^2	K_{IC} $N/mm^{3/2}$	K_{IC}/f_C' $mm^{1/2}$
22	0	3.12	2.06	0.66
	10	2.81	2.02	0.72
	30	2.65	1.94	0.73
	50	2.26	1.85	0.82
	90	1.87	1.71	0.91

CONCLUSIONS

The paper evaluates experimentally the fracture toughness of Ordinary Portland Cement Concrete (OPCC), Polymer Portland Cement Concrete (PPCC) and Autoclaved Aerated Concrete (AAC). Evaluating the experimental results and comparing them together results into the following conclusions:

1. For the wide range of concrete tested, the ratio of the fracture toughness K_{IC} to the concrete compressive strength f_C' ranges between 0.7 and 0.9 for OPCC and PPCC. For AAC, this ratio is between 0.66 and 0.91.
2. The fracture toughness of PPCC increases with the increase of polymer content and decreases with the increase in temperature but at a lower rate than that of the compressive strength.
3. Heating PPCC up to 50°C decreases its residual fracture toughness by a very small amount, but heating above 50°C decreases the fracture toughness considerably. For a temperature of 100°C, the fracture toughness for PPCC is decreases by almost 21%.
4. The effect of elevated temperatures on Polymer Portland Cement Concrete is greater than that on Ordinary Portland Cement Concrete.
5. The fracture toughness (K_{IC}) of AAC is noticed to be decreased by about 12% when submerged for one day in sea water under a temperature of 70°C. The reduction in K_{IC} becomes about 40% after 90 days under the same conditions.

REFERENCES

Abdel-Fattah, H. and Hamoush S. A. (1997), "Variation of the Fracture Toughness of Concrete with Temperature". Construction and Building Materials, Vol. 11 (2), 105-108.

Bazant, Z. P. and Prat, P. C. (1988), "Effect of Temperature and Humidity on Fracture Energy of Concrete". ACI Materials Journal Vol. 84, 262-271.

Brameshuber, W. (1989), "Discussion of effect of Temperature and Humidity on Fracture Energy of Concrete". ACI Materials Journal, Vol. 86, 330-331.

Cherepanov, G. P. (1979), Mechanics of Brittle Fracture. McGraw-Hill, New York.

Hamoush, S. A. and Abdel-Fattah, H. (1996), "The Fracture Toughness of Concrete". Engineering Fracture Mechanics Vol. 53(3), 425-432.

Bruhwiller, E., Wang, J. and Wittmann, H. (1990), "Fracture of AAC Influenced by Specimen Dimension and Moisture", Journal of Materials in Civil Engineering, Vol. 2 (3), 139-146.

Hamoush, S. A., Abdel-Fattah, H., and McGinley M. (1998), "Residual Fracture Toughness of Concrete Exposed to Elevated Temperature". ACI Structural Journal, Vol. 95 (6).

Isu, N., Sasaki, K., Ishida, H., and Mitsuda, T., (1994) "Mechanical Property Evolution During Autoclaving Process of Aerated Concrete using Slag [(i) Tobermorite Formation and Reaction Behavior of Slag]", Journal of the American Cement Society, Vol. 77 (8), 2088-2092.

Isu, N., Sasaki, K., Ishida, H., and Mitsuda, T., (1994), "Mechanical Property Evolution During Autoclaving Process of Aerated Concrete using Slag [(ii) Fracture Toughness and Microstructure]", Journal of the American Cement Society, Vol. 77 (8), (1994) 2088-2092.

Hanecka, K., Koronthalyova, O. and Matiasovsky, P. (1997), "The Carbonation of Autoclaved Aerated Concrete in Conjunction with its Physical Properties", Cement and Concrete Research, Vol. 27 (4), 589-599.

Maturana, P., Planas, J. and Elices, M. (1990), "Evaluation of Fracture Behavior of Saturated Concrete in the Low Temperature Range". Journal of Engineering Fracture Mechanics, Vol. 35, 827-834.

Tada, H., Paris, P. C. and Irwin, G. R. (1985). The Stress Analysis of Cracks Handbook, 2nd Edition, Paris Productions, St. Louis.

Vipulanandan, C. and Dharmarajan, N. (1996), "Analysis of Fracture Parameters of Epoxy Polymer Concrete". ACI Materials Journal Vol. 86(4), 383-393.

Proceedings of the ACI-KC First International Conference & Fourth Exhibition. September 29-October 1, 2003, Kuwait — ***Concreting and High Performance Concrete in Hot Weather.***

FRACTURE BEHAVIOR OF STEEL FIBER REINFORCED CONCRETE

S.S.E. Ahmad, E.M.Y. Abdin, Faculty of Engineering, Zagazig Univ., Egypt
H.Abdel-Raouf Faculty of Engineering, Zagazig Univ., Egypt
A.T.Atwa, Faculty of Engineering, Zagazig Univ., Egypt

ABSTRACT

In the present work, the effect of coarse aggregate type and area of steel bars reinforcement on the fracture behavior of concrete beams reinforced with and without steel fiber was investigated. The fiber volume fraction was 1.0%. The steel bars reinforcement areas were equivalent to 2 Ø 6 mm and 2 Ø 8 mm. Two different types of coarse aggregate were used in the mix, dolomite and gravel. Concrete beams of 6 x 15 x 65 cm in dimensions with crack / depth ratios of 0.1, 0.3, and 0.5 were used to measure the fracture toughness parameters. The flexural strength of un-notched beams of the same dimensions, splitting tensile strength of standard cylinders (15 cm x 30 cm) and compressive strength of standard cubes (15x15x15 cm) were, also, measured.

It was found that by adding steel fibers to plain concrete, the corresponding properties and fracture toughness were enhanced. Furthermore, adding steel fibers to plain concrete increases crack propagation resistance. It was found, also, there is no single value for plane strain fracture toughness of concrete and it appears to change with crack size. In addition, the presence of steel bars reinforcement creates a closing effect. Such closing effect due to the local compressive stress field around steel bars inhibits ability for crack extension. The value of the local compressive stresses increases with increasing the area of steel bars reinforcement, which gives higher values for the apparent fracture toughness. Moreover, using the dolomite as coarse aggregate gives good results more than when using the gravel as coarse aggregate.

INTRODUCTION

Fibers have been introduced in both research and industry fields to strengthen the concrete and cement mortar. However, of all the fibers currently used to reinforce mortar and concrete, galvanized steel fibers are the only fibers that can be used for long-term load-carrying properties. The relative ductility of steel fiber reinforced concrete renders such a material valuable properties for military purpose such as building and underground safety structure against bombing and shelling. It may prove to be useful for structures subjected to earthquakes where higher bond strength and ductility are important. Many practical applications for fiber reinforced concrete have already been utilized in the piling industry, parking garages, airport taxi strips and runways (ACI Committee 544, 1986).

Plain concrete may be considered as a composite material composed of coarse granular material (aggregate) embedded in hard matrix cement, which fills the space between the aggregate particles and glues them together. So the failure of concrete may occur by, failure of the cement paste, failure of the aggregate, failure of the bond between cement paste and aggregate, or any combination of these mechanisms. All these failures often occur suddenly in a brittle manner (Strange and Bryant 1979, Seleem and Ahmad 1997). The fracture toughness of plain concrete measured by energy method i.e. area under the load – deflection curve, is strongly influenced by mix variables. It increases with increasing maximum aggregate size and decreases significantly with increasing water / cement ratio. Furthermore, using large aggregate particles having coarse texture in a concrete mix improves its fracture toughness (Nallathambi et al 1984). Similar results have been also found in (Petersson 1980). They reported that the fracture toughness of concrete increased significantly with increasing the volume percentage of coarse aggregates and was independent of the water / cement ratio.

Owing to the higher compressive strength and lower tensile strength of concrete, its use in members subjected to axial tension or members subjected to bending is generally not possible. To overcome this difficulty, steel, which has a relatively high tensile strength, is used to reinforce the concrete, mainly in the tension zones; otherwise the small tensile strength of the concrete would limit the carrying capacity of the member. Although steel reinforcement is added to concrete to overcome the deficiency in the tensile strength of concrete, it does not prevent cracking completely. It prevents, however, crack propagation to some extent. The ability of steel reinforcement to control crack initiation and propagation depends on many factors such as, area and diameter of main steel, the distribution and number of steel bars, and the interfacial bond between concrete and steel especially when smooth bars are used.

The function of the reinforcement can be viewed as a restraining force, which tends to close the crack opened by an external moment, and thereby increasing the demand of energy input for crack growth. The apparent stress intensity factor, K_Q, of reinforced concrete was found to be increased with the increasing in the area of steel for different initial notch depths and 0.4 w/c ratio (Azad et al 1987) Generally, the fracture stability of the reinforced concrete beams increases with the increase of the beam depth and the area of steel reinforcement (Carbinteri 1984).

The important properties of steel fiber concrete are its relative resistance to cracking and crack propagation. As a result of its ability to arrest cracks, fiber composites posses higher extensibility and tensile strength, both at crack starting and at ultimate flexural loading. The effect of fiber content, V_f, and fiber aspect ratio, L/ϕ, on the fracture toughness of steel fiber reinforced concrete SFRC have been studied (Sameer et al 1991). It was found that the

fracture toughness of concrete, K_Q, increased by adding steel fibers. Also the fracture toughness of concrete, K_Q, was found to increase with increasing L/ϕ ratio except for $V_f = 2.0$ % where fracture toughness of concrete decreased at $L/\phi = 60$ or higher. Fracture criterion of concrete in terms of K_{IC} was measured by using notched beams and tested under four - point bending for plain concrete and a set of seven different steel fiber concretes whose fibers were having a rectangular cross - section and of contents ranging from 0.23% to 2% (by volume). It was argued that the value of K_{IC} for plain concrete was 90.73 kg cm $^{-3/2}$ and increased to 100.75, 110.09 and 136.27 kg cm $^{-3/2}$ with the use of steel fiber volume fractions of 0.23, 1.06, and 2% respectively (Zaki 1989).

The effect of fiber volume fraction on peak load, P_{max}, the energy absorption, the trend of load-crack mouth opening displacement, CMOD, curves and load-deflection curves was studied in reference (Shah and Jenq 1985). The results argued that the strength of FRC beams with fiber volume fraction 2.5% was twice the strength of un-reinforced matrix. It can be noticed that the energy absorption ability for beams with $V_f = 2.5$ % was about 30 times that of un-reinforced matrix. Also, the experimental results of load-CMOD curves and load-deflection curves for beams made with different fiber volume fractions illustrate that as the fiber volume fraction increases, the area under the curve increases too.

The primary interest of the present work deals with this class of random discontinuous fiber reinforced composites. The fracture toughness (measured in terms of critical stress intensity factor, K_Q) of concrete reinforced by steel bars and steel fibers is studied by testing notched beams subjected to flexure under three-point loading. Flexural, indirect tensile and compressive strengths are also measured for both plain as well as fibrous concrete.

EXPERIMENTAL PROGRAM

The experimental work was divided into four groups of experiments. The first group was to investigate the effect of the coarse aggregate type and steel fibers on compressive, indirect and flexural strength of plain concrete. The second group was to investigate the effect of coarse aggregate type and steel fibers on the flexural strength of reinforced concrete beams. The third group was to investigate the effect of coarse aggregate type and presence of steel fibers on the fracture toughness of plain concrete. The fourth group was to investigate the effect of coarse aggregate type, steel fibers, area of steel reinforcement, and crack / depth ratio on the fracture toughness of reinforced concrete.

The fine aggregate used in this work is ordinary siliceous sand with 100% passing ASTM sieve No. 4. The properties of the used sand are shown in Table (1). Natural gravel and dolomite with properties as in Table (1) and maximum aggregate size of 14 mm is used as coarse aggregate. The coarse aggregate, gravel or dolomite, was washed carefully and dried before mixing to remove any impurities and organic matter, which may weaken its bond with the cement paste. Ordinary Portland cement of Suez factory was used in this work. The properties of the used cement are given in Table (2).

The water used in all mixes was ordinary tap water. The water-cement ratio was kept constant in all mixes. The steel reinforcing bars used in this investigation were mild steel and produced locally. The bars diameters used were 3, 6, and 8 mm. The tension test was carried out on the used bars. The results of the test are summarized in Table (3). The used steel fibers were galvanized with 0.7 mm diameter and fiber aspect ratio, $L/\varnothing$, = 60. The ACI method of mix design was used to determine the required quantities for the used mix in this research.

Table (1): Properties of coarse aggregates

Property	Measured value		
	Sand	Gravel	Dolomite
Compacted Density	1750 Kg / m^3	1720 Kg / m^3	1735 Kg / m^3
Loose Density	1600 Kg /m^3	1650 Kg /m^3	1670 Kg /m^3
Specific Gravity	2. 45	2. 65	2. 66

Materials of the specified mix were weighted first, and then mixed in dry state. The required amount of water was then added. For fibrous concrete, the required amount of steel fibers was dispersed after rotating the constituents of the mix for two minutes through a 1. 18 mm sieve while the mixer was rotating in order to provide a uniform distribution of fibers in the mix. The whole batch was remixed again by using a trowel until uniform mix was attained. The slump test was performed to measure the workability of concrete mix. The slump was maintained approximately equal to 3 cm for all mixes by using variable dosage of a water-reducing additive.

Table (2): Properties of the cement.

Property	Measured value
Specific gravity	3.15
Setting Time:	
Initial, min.	60
Final, hr.	5.0
Fineness cm^2 / gm	2871
Soundness cm	1.00
Crushing strength:	
• After 3 days	145.7 kg / cm^2
• After 7 days	282.0 kg / cm^2
• After 28 days	371.6 kg / cm^2

Table (3): Mechanical properties of steel bars.

Bar Diameter	3 mm	6 mm	8 mm
Strength, MPa			
Yield Strength	310	293	279.8
Ultimate tensile Strength	457.5	450	444.1

The batch was casted in the oiled steel moulds immediately after mixing. The moulds (standard cubes of 15x15x15 cm, cylinders of 15x30 cm and steel forms for beams of 6 x 15 x 65 cm overall dimensions) were filled in three layers and compacted mechanically on a vibrating table. The notches were performed in pre-notched beams by locating a thin steel

plate of 0.3 mm thickness at the center of the mould and fixed by steel grips. Top surfaces were trawled smoothly. After 24 hours the specimens were removed from the moulds and immersed in clean water at room temperature for another 27 days. All mechanical tests were carried out on a universal testing machine, AVERY- DENSION, of maximum capacity 1000 KN.

RESULTS AND DISCUSSION

Compressive, Splitting and Flexural Strengths:

Table (4) shows the results of the compressive strength, σ_c, in MPa for fiber volume fractions, V_f, = 0 and 1.0 % and for two types of coarse aggregate, dolomite and gravel. It can be seen that the compressive strength has been improved by the addition of steel fiber and by using the dolomite as coarse aggregate. For example, at V_f = 1.0%, the σ_c = 52.8 MPa when using the dolomite and σ_c = 38.6 MPa when using the gravel i.e. increasing by about 36.90 %. In the case of dolomite by increasing the fiber volume fraction from 0 % to1.0 % the σ_c increased from 46.1 MPa to 52.8 MPa, i.e. increasing by about 14.49 %.

The mode of failure for all compression test specimens containing fibers are completely different from plain concrete ones. For the latter specimens, failure was either by crushing or splitting of the specimen. But in the case of fiber reinforced specimens, the mode of failures mainly occurs by excessive cracking pattern. For fiber concrete specimens, no splitting, crushing or spalling was noticed. This may be due to the effect of the randomly distributed fibers in restricting the lateral deformation and inhibiting micro-cracks growth. This may lead to higher pre-cracking as well as post-cracking strengths.

From Table (4) it is clear that the splitting tensile strength of concrete increased by the addition of steel fiber and when using dolomite as coarse aggregate. For example, when using dolomite as coarse aggregate at V_f = 0, σ_t = 3.44 MPa and at V_f = 1.0 %, σ_t = 3.62 MPa. That's means increasing in splitting strength by about 5.2%. By comparing the mixes of dolomite and gravel at the same conditions, it was found that at V_f = 0, σ_t = 3.44 and 1.96 MPa respectively. That's means increasing by 75.3 % when using the dolomite as coarse aggregate. The mode of failure of splitting tension test specimen is affected by the presence of fibers. Inspection of the test specimens indicated that neither complete splitting nor separation was observed before failure has taken place.

Table (4) Test results of compressive, indirect tensile and flexural strengths

V_f %	0 %		1 %	
Coarse aggregate	**Dolomite**	**Gravel**	**Dolomite**	**Gravel**
Compressive strength, σ_c, MPa	46.1	32.1	52.8	38.6
Indirect tensile strength, σ_t, MPa	3.44	1.96	3.62	2.31
Flexural strength,σ_f, A_s = 0	4.1	3.1	5.37	4.42
Flexural strength,σ_f, A_s=2Ø6 mm	13.8	13.5	19.6	16.3
Flexural strength,σ_f, A_s=2Ø8 mm	21.4	18.9	22.9	20.26

Table (4) gives the results of the flexural strength, σ_f, in MPa, for fiber volume fractions, V_f = 0 and 1.0 %, steel reinforcement area, A_s, equivalent to 2Ø 6 mm and 2 Ø 8 mm and for two types of coarse aggregate, dolomite and gravel. It is clear that the ultimate flexural strength generally increased with the increase of both fiber volume fraction and steel area. For example, when using the dolomite as coarse aggregate, at $V_f = 0$, $\sigma_f = 4.1$ MPa and at $V_f = 1.0$ %, $\sigma_f = 5.4$ MPa, that's means increasing in flexural strength by 31.6 %. At $V_f = 0$, $A_s = 2Ø6$ $\sigma_f = 13.8$ MPa and at $V_f = 1.0$ %, $A_s = 2Ø6$, $\sigma_f = 19.6$ MPa. That's means increasing in flexural strength by 41.8 %.

By comparing the flexural strength when using dolomite and gravel at the same condition, i.e. at $V_f = 0$, $A_s = 0$ we find that $\sigma_f = 4.1$ and 3.1 MPa respectively, that's means increasing in flexural strength of mix with dolomite by 33.3 %. That's increasing may be related to the rough texture of dolomite particles and sharpness of its edges which lead to good cohesion of the particles with each other and with other components of the mix, consequently, improving the mechanical properties. The mode of failure of flexural test specimens having the steel fiber reinforcement is not the common brittle type of failure but is mainly due to excessive cracking without complete separation. This behavior may be due to the linking action of the randomly distributed fibers. It is noticed that, the load carrying capacity increases by increasing the fiber volume fraction, area of steel reinforcement and by using the dolomite as coarse aggregate. These results agree with that in (Leug and Chi 1995, Bazant and Cedolin, 1980).

Regarding the three measure, flexural, splitting tensile and compressive strengths of fibrous concrete one can notice that the steel fibers generally improved the mechanical properties of concrete and all failure modes. This is can be related to the strengthening mechanism of the fibers which involves the transfer of stresses from the matrix to the fibers by interfacial shear, or by interlock between the fibers and the matrix. The most important variables governing the properties of steel fibers reinforced concrete are fiber content and fiber aspect ratio. The stresses are shared by the fibers and the matrix in tension until the matrix cracks, and then the total stress is progressively transferred to the fibers. Therefore, it can be said that the mechanical properties of the fibrous concrete are improved with the addition of steel fiber by 1% and with using the dolomite as coarse aggregate.

Fracture Toughness of Plain Concrete

Notched plain concrete beams with fiber volume fractions, V_f, = 0 and 1.0 %, different crack /depth ratios, (ao/w = 0.1, 0.3, and 0.5) and two types of coarse aggregates, dolomite and gravel are tested in three-point bending. The apparent fracture toughness, K_Q, is equal to K_I at maximum moment. Each value of K_Q is the mean value of three beams. The influence of fiber content upon the apparent fracture toughness is evident from Table (5). The data show an increase in K_Q with the addition of fiber for all crack depth ratio and for the two types of coarse aggregate. In the case of dolomite and at crack depth ratio equals 0.1, as an example, the apparent fracture toughness increased by about 17.30 % with the increasing in the fiber content from 0 to 1.0 %. In the case of gravel and at crack depth ratio equals 0.1 the apparent fracture toughness increased by about 28.60% with the increasing in the fiber content from 0 to 1.0%.

The effect of coarse aggregate types (dolomite and gravel) on the apparent fracture toughness (K_Q) at different crack /depth ratios is shown in Fig. (1) for $V_f = 0$ and $V_f = 1.0$ %. By comparing the effect of dolomite and gravel on K_Q at ao/w = 0.1 and $V_f = 0$, it was found

that, K_Q increased by about 31.4 % when using dolomite as a coarse aggregate. Also, K_Q increases by about 26% and 10 % at crack-depth ratios 0.3 and 0.50 respectively at the same conditions. The data in Fig. (1) clearly indicate that the K_Q decreases with the increase in the crack-depth ratio, ao/w. Moreover the effect of aggregate type and fiber content also decreases with the increase in ao/w.

During the observation of the crack path at any load level from the two sides of any tested beam, it is noticed that the crack length observed on one beam face is at times longer and at other times shorter than its length taken from the other face. This indicates that there is non-uniform crack propagation through the beam thickness due to the inhomogenity of the tested material. It is agreed with results in (Bazant and Cedolin 1980).

Table (5) Test results of K_Q for plain concrete in terms of MPa $mm^{0.5}$

V_f %	0 %		1 %	
ao/w	Dolomite	Gravel	Dolomite	Gravel
0.1	22.4	17.03	26.29	21.89
0.3	20.5	16.27	22.61	20.54
0.5	17.12	15.57	18.1	16.9

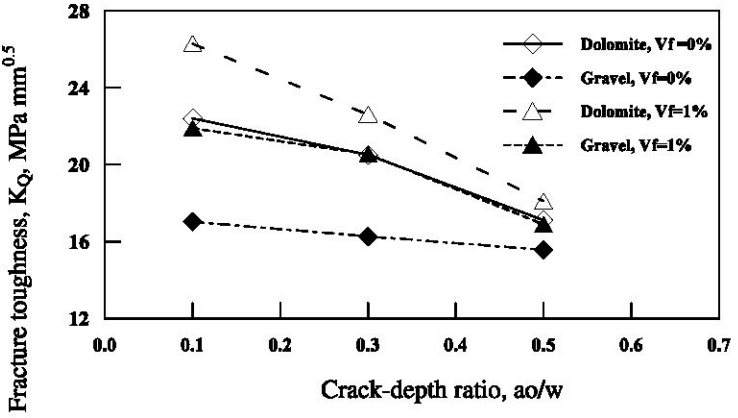

Fig. (1) Variation of K_Q with crack-depth ratio for plain concrete

Fracture Toughness of Reinforced Concrete Beams

The dependence of fracture toughness of the notched beams upon the fiber content, type of coarse aggregate in the mix, area of steel reinforcement in the cross section and crack-depth ratio are shown in Table (6). These results were obtained from tests on beams reinforced by two steel bars, A_s equivalent to 2Ø6 mm and 2Ø8 mm as main reinforcement in fiber concrete with fiber contents = 0 and 1.0 %. The values of initial crack-depths ratio were 0.1, 0.3, and 0.5. From Table (6) we notice that when increasing the fiber volume fraction from 0 % to 1.0 % at ao/w = 0.1, 0.3 and 0.5, K_Q increases by about 6.9%, 6.10% and 4.70% respectively when using dolomite as coarse aggregate.

Also from Table, at V_f = 1.0 %, $A_s = 2\ \phi\ 6$ mm, by increasing the crack / depth ratio from 0.1 to 0.3, K_Q increases by about 50.9 % and increases by about 60.6% when ao/w increases from 0.3 to 0.5 for dolomite concrete. Therefore, it can be concluded that as the steel fiber volume fraction increases, the fracture toughness was improved for all notch depths and for two types of coarse aggregate. Also, similar trend was found at $A_s = 2\phi 8$ mm.

Table (6) Test results of K_Q for reinforced concrete in terms of MPa $mm^{0.5}$

As	2 Ø 6 mm				2 Ø 8 mm			
V_f	0%		1%		0%		1%	
ao/w	Dolomite	Gravel	Dolomite	Gravel	Dolomite	Gravel	Dolomite	Gravel
0.1	102.5	90.6	109.7	95	134	127.8	140.7	133
0.3	156	144	165.6	165	231	222	238.7	230.9
0.5	254	222	266	255.7	361	353.7	377	368.3

This behavior may be explained as follows: the stress field due to loading is localized at tip of the initial crack and the crack initiation is expected to originate at that tip, then it propagates in the concrete beam till it causes failure. The initiation and propagation of the crack is a result of the net stress intensity factor acting on the tip of the crack. The presence of the fibers in the zone ahead of the notch contributes in carrying the load, which can be attained to a local reduction in the stress intensity factor, and this means that a higher load is needed to initiate and propagate the crack. Furthermore, the apparent stress intensity factor can be expressed as:

$$K_Q = K_S + K_{FC}$$

Where:
K_S is the stress intensity factor of the steel bars and K_{FC} is the stress intensity of the fiber reinforced concrete and equal to:

$$K_{FC} = K_{PC} + K_F$$

Where:
K_{PC} is the stress intensity factor of the plain concrete, and K_F is the stress intensity factor of the steel fibers. Taking into consideration that K_S and K_F are stress intensity factors that applied on the crack but in the closing direction therefore:

$$K_Q = K_S + K_{PC} + K_F$$

Hence, the initiation and propagation of the crack is taking place when the net stress intensity factor (K_Q- (K_S+K_F)) reaches the value of the critical stress intensity factor for plain concrete, K_{PC}. In the case of concrete beams reinforced by constant area of steel bar reinforcement and varying steel fiber contents, K_S remains constant and K_F varies. This means that only K_F increases with increasing in V_f, therefore, in order to reach a certain critical value of K_{PC}, K_Q must be increased, i.e., the element becomes of higher fracture toughness value. The above explanation is also valid in the case of concrete reinforced by fibers only. The only difference is that the value of K_S will be equal to zero.

From Table (6) it can be observed that the increase in the fracture toughness due to the increase in fiber volume fraction is more pronounced when the area of steel bar reinforcement

is small. As example, for concrete beams with ao/w = 0.1 and with dolomite as coarse aggregate, K_Q increased by about 6.9% when V_f increased from 0 % to 1.0% in the case of beams reinforced by 2ϕ6 mm. On the other hand K_Q increased by about 5% in the case of beams reinforced by 2ϕ8 mm. Also K_Q increased by about 20% in the case of beams reinforced by steel fibers only. This is may be due to the fact that the presence of larger area of steel bar reinforcement may mainly control the behavior of concrete and therefore obscure significantly the sharing role of the fibers. As the steel bar reinforcement area decreases, the sharing role of the fibers becomes more sensible. In the absence of the steel bar reinforcement, the behavior of the concrete member may be mainly controlled by the fibers.

The relationship between K_Q and the crack-depth ratio, ao/w, is shown in Fig. (2a, b). From these figures it can be noticed that: as the crack depth increased, the fracture toughness, K_Q, increased although the load carrying capacity of the beam decreased. This may be attributed to the increase in the resisting moment provided by steel bars. In the case of plain concrete beams, as the crack depth increases, the load carrying capacity and the fracture toughness are decreased as shown in Fig (1). Such behavior is typical for concrete as indicated in experimental results shown in (Carbinteri 1984).

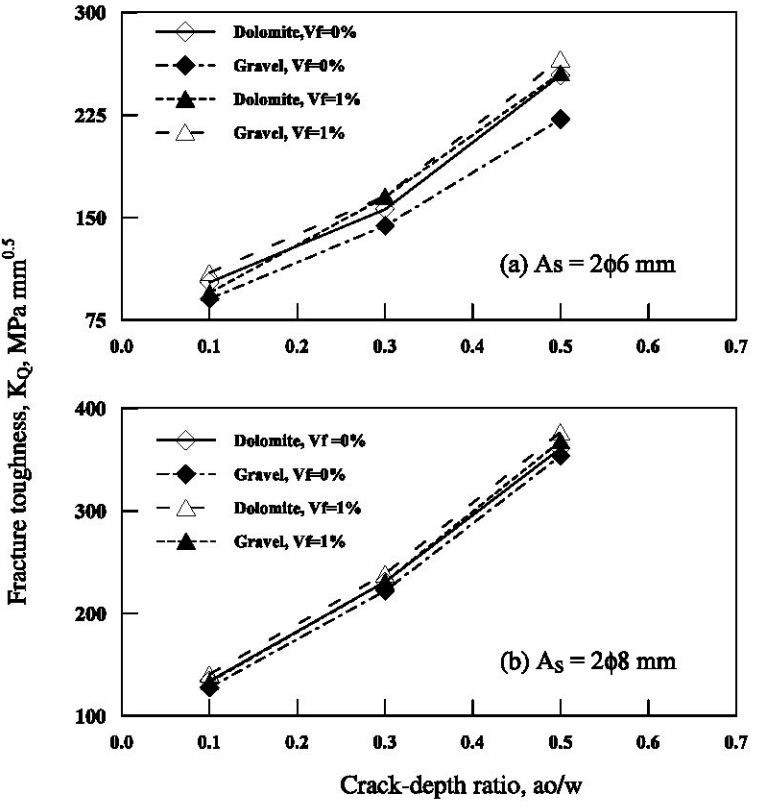

Fig. (2) Variation of K_Q for reinforced concrete against crack-depth ratio at (a) A_S = 2ϕ6 mm and (b) A_S = 2ϕ8 mm

The steel bar reinforcement has a noticeable effect upon the fracture toughness of concrete beams. From figures (2a, b) we notice that at V_f = 1% and for dolomite, K_Q increased by about 28.5 %, 44.4 % and 41.7 % at ao/w = 0.1, 0.3 and 0.5 cm respectively as the area of steel bar reinforcement increases from 2ϕ6 mm to 2 ϕ 8 mm. Also under the same conditions but the only difference is the fiber content, V_f = 0%, the fracture toughness increased by about 30.3 %, 48.1 % and 42.1 % respectively.

The above results may be analyzed as follows: the presence of steel bar reinforcement creates a closing effect on the initial crack. This closing effect due to the local compressive stress field around steel bars inhibits ability for crack extension. The values of the local compressive stresses increase with the increasing in the area of steel bar reinforcement. Consequently the closing stress intensity factor, K_S, increases due to the increase in area of steel bar reinforcement, which leads to an increase in K_Q of the specimen.

We can notice, also, from Figures (2a and b) that the using of dolomite as coarse aggregate in the mix improves the fracture toughness of reinforced concrete relative to using gravel. That's due to rough texture and sharp edges of dolomite particles, which lead to good bond between the matrix, steel fibers and steel bars reinforcement and consequently leads to durable mix.

CONCLUSIONS

The results of the present work reveal the following conclusions:

1-Adding steel fibers to plain concrete improves its mechanical properties, but the relative gain in the flexural strength is more pronounced than the gain in the splitting tensile strength and compressive strength.

2-Adding steel fibers to steel bars reinforced concrete improves its fracture toughness, K_Q, but with different levels according to area of steel bar reinforcement.

3–The beneficial effects of fiber addition on the fracture toughness of concrete were increased for under-reinforced concrete members.

4-When the initial crack-depth ratio, a_o/w, increased, the fracture toughness was increased in the case of reinforced concrete and decreased in the case of plain concrete.

5-When the area of reinforcing steel bars increased; the fracture toughness of concrete was increased.

6- Using dolomite as a coarse aggregate improved the fracture toughness of plain and reinforced concrete.

REFERENCES

ACI Committee 544, (1986), " State-of-the-Art Report on Fiber Reinforced Concrete", ACI 544. IR-82, ACI Manual of Concrete practice, Part 5, ACI, Detroite, 1986.

Azad, A.K., Baluch, M.H. and Zirab, Y., (1987), 'Fracture characterization of reinforced concrete beams", International Conference on Fracture of Concrete and Rock, Texas, June, pp. 443-446.

Bazant, Z.P. and Cedolin, L., (1980), " Fracture Mechanics of reinforced concrete", Journal of the Structural Engineering Division, ASCE, V.106, pp. 1287-1306.

Carbinteri, A., (1984), " Stability of fracturing process in reinforced concrete beams", Journal of the Structural Engineering Division, ASCE, V.110, No. 3, March, pp. 544-558.

Leug, C.K.Y. and Chi, J. (1995), " Crack bridging force in random ductile fiber brittle matrix composites", J. Engrg. Mech., ASCE, 121 (12), 1315-1324.

Nallathambi P., Karihaloo B.L. and Heaton B.S., (1984) "Effect of Specimen and Crack Sizes, Water-Cement Ratio and Coarse Aggregate Texture Upon Fracture Toughness of Concrete", Magazine of concrete Research, V. 36, No. 129, pp. 227-236.

Petersson P.E., (1980), "Fracture Energy of Concrete, Practical Performance and Experimental Results", Cement and Concrete Research, V. 10, No. 1, pp. 91-101.

Sameer, A.H., Reza Salami, M., and Abu-Saba, E.G., (1991), "Fracture model to predict stress intensity in fiber reinforced concrete", ACI Materials Journal, V. 88, No. 5, pp. 504-519.

Seleem, M.H. and Ahmad, S.S.E., (1997), "Fracture behavior of concrete made with non conventional coarse aggregate types", 3rd Conference in Structural and Geotechnical Engineering, Alexandria University, Egypt, pp.312-320.

Shah, S.P., and Jenq, Y.S., (1985), " Fracture resistance of steel fiber reinforced concrete", Steel fiber concrete, US-SWEDEN JOINT SEMINAR, Stockholm, 3-5 June, pp. 273-297.

Strange P.C. and Bryant A.H., (1979), "The role of Aggregate in the Fracture of Concrete", Journal of Materials Science, V. 14, pp. 1863-1868.

Zaki, Y.L., (1989), " Fracture in fiber reinforced concrete", M.Sc. Thesis, Faculty of Engineering, Zagazig University, Zagazig.

Proceedings of the ACI-KC First International Conference & Fourth Exhibition. September 29-October 1, 2003, Kuwait — ***Concreting and High Performance Concrete in Hot Weather.***

ON THE RETROFITTING OF RC BEAMS USING FRP FABRICS

M. El-Hawary[1], S. Fereig[2], J. Al-Duaij[3], H. Al-Khaiat[4]

ABSTRACT

The use of Fiber Reinforced Polymers FRP in repair and rehabilitation of reinforced concrete structures is gaining a worldwide acceptance due to their numerous advantages over other repair materials. In this paper, the structural behavior of reinforced concrete beams repaired using Carbon Fiber Reinforced Polymer (CFRP) and Glass Fiber Reinforced Polymer (GFRP) fabrics, was investigated. Five beams of 300x100x1100 mm were designed to assure shear failure, cast, cured and then loaded to failure. Ultimate load, load- deflection relation and crack pattern were recorded for each beam. Beams were then repaired using either CFRP or GFRP. Wraps were epoxy bonded on both sides of beams, except for one beam where the bottom was also wrapped for comparison. Repaired beams were then loaded to failure. Ultimate load and ductility were compared.

It was concluded that the use of either GFRP or CFRP wraps restores and improves both the load carrying capacity and the ductility of tested beams. GFRP repaired beams demonstrated better results than the CFRP repaired ones. The beam repaired on both sides and bottom showed better load carrying capacity than those where wraps were applied on sides only. Failure of rehabilitated beams was found to be due to debonding and peeling of FRP wraps. The repair method was found to be easy, efficient and less time consuming compared to other conventional repair methods.

[1] Research Scientist, Kuwait Institute for Scientific Research, Kuwait

[2] Professor of Civil Eng., Kuwait University, Kuwait

[3] Associate Professor of Civil Eng., Kuwait University, Kuwait

[4] Professor of Civil Eng., Kuwait University, Kuwait

INTRODUCTION

Due to deterioration, overloading, accidents or other reasons, structural members may require some kind of repair to restore and enhance their structural behavior and loading carrying capacity. Structural members may also require rehabilitation due to change in the required type of service, architectural changes that require alteration to the structural system or just to prolong the service life of the structures. Many techniques and materials are available for repair and rehabilitation. The of some type of plates or sheets have found special favor with engineers, specially for heavily damaged beams. The strengthening by steel plate bonding has been done since 1970. Glass fiber plates were also used for repair and were either bonded using epoxy, bolted or both to prevent peeling [1]. The use of plates was then mostly replaced by FRP laminates which are manufactured as sheets or strips by pultrusion, in which fiber strands are impregnated in an epoxy resin bath and are shaped by being pulled through a die. Afterwards they are hardened in oven. The used fibers are commonly Carbon or Glass fibers. The glass fibers have a tensile strength of 2-4 G Pa while the tensile strength of carbon fibers is about 3 GPa, which is higher than that of steel (0.5 –2), along with a comparable Modulus of Elasticity to that of steel. The resulting sheets possess many advantages such as:

- Easy to handle, they strips may be up to 500m long and can be rolled up.
- Light weight, they can be fixed in place by hand or very light equipment and don't affect the structure's dead weight.
- High tensile strength, CFRP laminates have a tensile strength in the range of 3000 N/mm^2.
- Excellent resistance to fatigue
- Resistance to chemicals and corrosion.
- Thin sheets, they don't alter the overall dimensions of the concrete members.
- Clean application, there is no need to close the structure, bridge or tunnel completely for the repair work to take place.

The only disadvantage of FRP laminates sheets or strips is that they are unidirectional and that the interlaminary strength is much less than that in the fiber direction. This problem, however, was overcome by the introduction of FRP fabrics or textile which possess the same strength in both directions. The research work on FRP laminates includes that on ductility of strengthened beams [2,3]; importance of adequate anchorage system [2,4]; effect of CFRP on concrete confinement [4,5]. ACI 440 report [6] contains also some details regarding the use of FRP in concrete structures. FRP laminates may also be prestressed to help in arresting and reducing existing cracks [7], in which case mechanical fixation should be used along with epoxy bonding.

FRP may also be used as strands for internal reinforcement replacing steel bars in reinforced concrete structures [8].

The use of bidirectional CFRP and GFRP fabrics is rather new and the related research is still limited. More research is needed to shed the light on the actual behavior of structural members repaired using FRP fabrics along with the verification of the effectiveness and advantages of this repair method. The main objective of this paper is to investigate the structural behavior and ductility of reinforced concrete beams failed in shear and subsequently repaired using two different types of FRP fabrics and two different repair techniques.

TEST BEAMS

Five beams were utilized for the experimental study. The beams were designed to fail in shear before they reach their flexural capacity. The beam dimensions are 300x100x1100 mm. The used reinforcement is two 14mm diameter bars in bottom , two 8 mm in top and 6 mm stirrups at 120 mm spacings, making the steel ratio equal 0.0123 . The geometry, reinforcement and loading set up of the beams are shown in Figure 1.

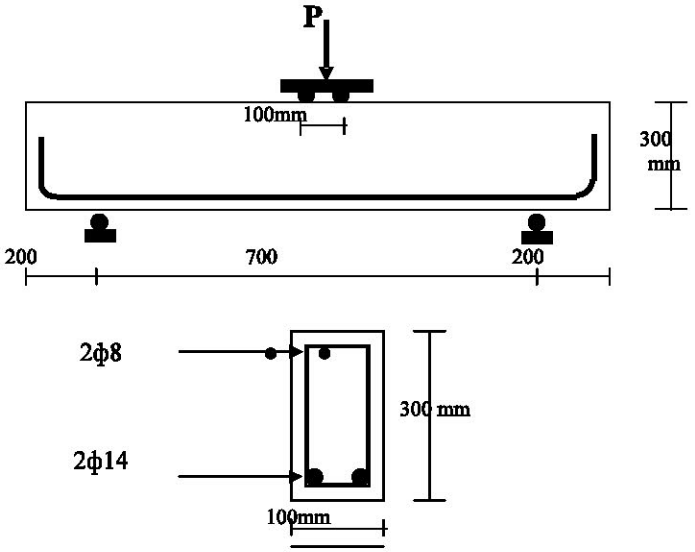

Figure 1: Beam dimensions, reinforcement and set up

MATERIALS

The proportions of the concrete constituent materials are shown in Table 1. Ordinary Portland cement and natural sand were used in this rich mix, along with two different sizes of quartzite coarse aggregates. The GFRP and CFRP fabrics used for repair are single layer FiberBond® (E-glass/Epoxy and Carbon/Epoxy systems, respectively).

Table 1: Concrete Mix Design Proportions

Material	Weight kg/m^3
OPC	330
Water	198
Sand	720
Coarse Agg. 3/8 in.	380.25
Coarse Agg. 1/2 in.	770.25
Superplasticizers	2.25 liters

The material used for bonding the repair fabrics is a multi-purpose adhesive based on solvent free epoxy resin. It is supplied as two-pack material. It is waterproof, chemical resistant and has a cure time of 10 hours at 20°C.

EXPERIMENTAL PROGRAM AND TESTING PROCEDURE

Five reinforced concrete beams were utilised in this experimental program. All beams have the same reinforcement as mentioned before. Steel reinforcement was placed in forms and then concrete was mixed, poured and compacted. Forms were removed the second day and beams were cured in laboratory for 28 days using wet burlap, before being tested. Beams were loaded in flexure according to the four-point loading set up as shown in Figures 1 and 2. Loads were increased in 10kN intervals till failure. Mid span deflection was measured and recorded at each loading interval using a dial gauge, as shown in Figure 2. Crack patterns and propagation were also recorded, Figure 3.

The five beams were then repaired using either GFRP or CFRP fabrics. The beams were divided into three groups. The first group consists of beams B1 and B2. Beams in this group were repaired using GFRP fabrics applied in both sides, while the second group consists of beams B3 and B4 and was repaired using CFRP on both sides. The last group contains beam B5, which was repaired using CFRP applied on the bottom of the beam in addition to the two sides. The beams details and method of repair is given in Table 2.

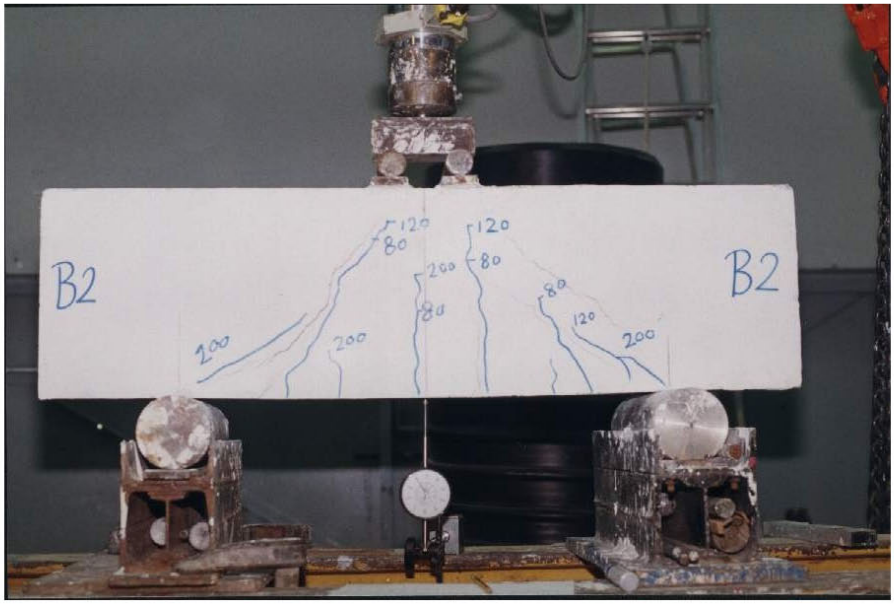

Figure 2: Beam B2 during testing

Table 2: Details of test beams

Group / Beam	Bottom steel	Top steel	Stirrups	Repair material	Application zones
Group 1 (B1, B2)	2Φ14	2Φ8	Φ6@ 120mm	GFRP	Two sides
Group 2 (B3, B4)	2Φ14	2Φ8	Φ6@ 120mm	CFRP	Two sides
Group 3 (B5)	2Φ14	2Φ8	Φ6@ 120mm	CFRP	Bottom & two sides

The fabrics were cut to the required sizes. The resin and the hardener of the epoxy adhesive material were mixed and the repair fabric was soaked in the epoxy before being applied to the repair surface. The fabric was squeezed using a trawler to get rid of trapped air in order to assure homogeneous bond. Excess epoxy was removed. A full size fabric was used in each face of repair without splicing. In beam B2, however, two separate pieces were used for each face and a splice of 100mm was used to assure the continuity of the repair material (Figure 4). The repaired beams were tested in four-point loading flexure set-up, as before. The load was applied at 10kN intervals at which mid span displacement was measured. The load-displacement relationship, the ultimate loads and the type of failure were determined for each beam .

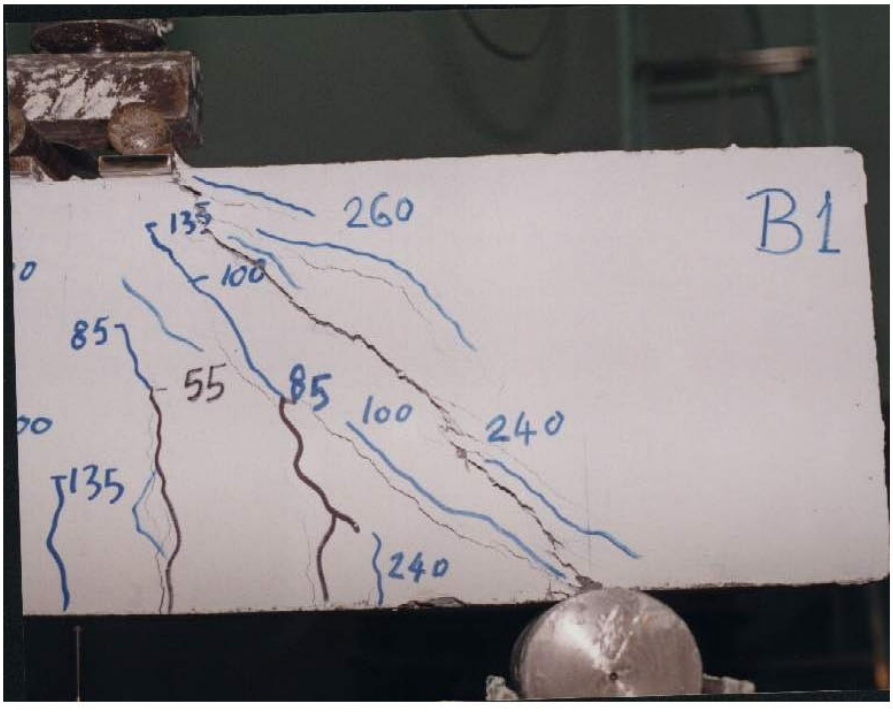

Figure 3: Crack pattern

The concrete mix was designed to have a compressive strength of 35 N/mm^2. In order to verify the compressive strength of the actual beams, three cores were cut off the first three beams and tested in compression according to ASTM C-42 specifications. The average cylinder compressive strength was found to be 34.7 N/mm^2. The details of the test are shown in Table 3.

Figure 4: Application of CFRP fabrics

Table 3: Compressive strength of concrete cores

	Specimen 1	Specimen 2	Specimen 3
Average diameter	68.12	68.12	68.12
Density (kg/m^3)	2426	2436	2422
Length before capping (mm)	101.8	100.7	101.8
Length before capping (mm)	101.8	100.7	101.8
Method of preparation	Sawing and capping		
Duration in water	40 hours		
Length / diameter after capping	1.49	1.48	1.49
Direction of applied load	Vertical	vertical	vertical
Maximum load at failure (kN)	124.5	136.4	123.0
Cross-sectional area (mm^2)	3644.51	3644.51	3644.51
Measured compressive strength (N/mm^2)	34.2	37.4	33.7
Strength correction factor	0.986	0.980	1.0
Cylinder compressive strength	33.7	36.7	33.7
Average cylinder comp. Strength (N/mm^2)	34.7		

RESULTS AND DISCUSSION

All five beams failed in shear, as designed. After each load increment, the load was held constant for few minutes to allow for crack measuring. The crack patterns and directions were recorded for each beam. Typical shear behaviour was observed, as flexural crack first appeared at the bottom surface of the tested beam in the middle where the bending moment is maximum. This was followed by other flexural cracks along the bottom, which propagated along the height of the beam and shifted direction to become diagonal shear cracks. Those cracks propagated closer to the loading plate and the support and their width increased quickly, just before failure. A typical cracked beam is shown in figure 3. For the repaired beams the repair fabrics prevented the observation of crack patterns and propagation. All repaired beams, however, failed by debonding and peeling of the repair fabrics.
The mid-span displacement was also measured at each loading increment before and after repair. The load-displacement relationships for all five beams are shown in Figures 5-9. It is clear in all cases that beams did not only retain their load carrying capacity in shear that were lost after failure, but also an obvious increase in those capacities were observed. The increase in the load carrying capacity depends on the material and method of repair. The increase in the load carrying capacity was calculated in two methods. The first I_1 was calculated in reference to the individual load carrying capacity of each beam before the first failure, while the second I_2 was calculated in reference to the average load carrying capacities of all five beams. Both indices, along with the load carrying capacities of each beam, before and after repair, are shown in Table 4. The second index I_2 is more meaningful, as beams were already cracked before repair and the difference between the individual load carrying capacities of each beam, which is mainly due to concrete strength, will not contribute to the load carrying capacity of the repaired beams. The increase in the case of repairing sides only was found to be 43.4% for the GFRP repaired beams and 18% for the CFRP ones (average of B3 and B4). The use of separate pieces of fabrics for repair reduced the increase in the load carrying capacity by 47.2%, from 43.4% to 22.9% and the application of the repair fabrics on the bottom in addition to the sides, increased the load carrying capacity by 106.1%, from 18% to 37.1%.

Table 4: Experimental results for the tested beams

Beam	P_{max} (kN)		I_1	I_2	Ductility Index		I_3
	Original	Repaired			Original	Repaired	
B1	240	317	32.1	43.4	1	6	1.14
B2	255	271.5	6.47	22.9	3.4	4.6	0.89
B3	215	270	25.6	22.2	8	3.6	0.69
B4	210	251.3	19.7	13.7	6	3.5	0.67
B5	185	303	63.8	37.1	3.6	6.9	1.31

Ductility of reinforced concrete members represents their ability to sustain excessive energy and/or deflection after the steel reach its yield stress. High ductility is essential to assure that the structure can withstand the effects of earthquakes, vibrations, impact or wind and that there is enough warning before its collapse. Three types of ductilities may be used; deflection ductility, curvature ductility and energy ductility. The first was utilised in this work.
Deflection ductility index is defined as:

$$\text{Ductility Index} = \Delta_u / \Delta_y \qquad (1)$$

Where Δ_u is the midspan deflection at ultimate load and Δ_y is the midspan deflection at tension steel yielding.
The ductility indexes for the original and repaired beams are shown in table 4. The value of the ductility index for B1 before repair is obviously an error in measurement, where the post yield increase in deflection was not included. As discussed before, the average ductility index for the original beams was used as basis for comparison between the ductility of original and repaired beams. The factor I_3, in table 4, represents the ratio between the ductility indexes of the repaired beams to the average ductility index for the original beams. Only two beams showed improvement in ductility over original unrepaired beams. The highest ductility, I_3 , was for Beam 5, which was repaired on the sides and bottom followed by Beam 1, which was repaired on the sides only using GFRP. All other beams experienced a reduction in ductility due to the use of FRP fabrics. The use of full repair sheets resulted in better ductility than the use of separate repair fabric pieces.

CONCLUSIONS

Five full scale reinforced concrete beams, designed to fail in shear, were tested in flexure till failure and then repaired using either GFRP or CFRP, before being tested again. GFRP fabrics were applied on the beam sides either as full layer or as separate pieces on each side. CFRP fabrics were applied either on both sides only or on sides and bottom. Crack pattern, mode of failure, load-displacement relationships, ultimate load carrying capacity and displacement ductility were determined and evaluated. The following were concluded:

- Application of FRP laminates in repair is easy and does not require special equipment.
- Both GFRP and CFRP may be used in repairing flexural members failed in shear.
- All five tested repaired beams showed an increase in their load carrying capacity compared to those of the original beams, regardless of the repair material and method of repair. The increase varied between 13.7% to 43.4%.
- All repaired beams failed by debonding and peeling of the repair fabric.
- Although ductility is a common problem in FRP repaired beams [3], the beam repaired using CFRP on both sides and bottom and the one repaired using GFRP showed some increase in ductility, while other three beams experienced some reduction in ductility compared to original beams.
- In general GFRP repaired beams showed better results in both the load carrying capacity and ductility compared to those repaired using CFRP.
- Application of the CFRP on the bottom in addition to the two sides improved the ultimate load and the ductility of the repaired beam.
- The application of separate pieces of GFRP, although 100mm splice was used, resulted in a reduction in both the load carrying capacity and the ductility of the repaired beam.
- The utilization of FRP fabrics in repair seems superior to all other repair methods. Its only drawback is the cost. This, however, is expected to decrease with time as most other new technologies.
- More work is still needed in order to fully understand the structural behavior of the repaired beam and to achieve a systematic design method. Work is also needed on the use of FRP laminates as external reinforcement, fully or partially replacing steel reinforcement.

REFERENCES

1- Kamal,H. "Strengthening of Loaded Concrete Beams Using FRP Plates", MS thesis, Kuwait University, 1996.

2- Bencardino,F.; Spadea,G. and Swamy,R.N. "Strength and Ductility of Reinforced Concrete Beams Externally Reinforced with Carbon Fiber Fabric", ACI Structural Journal, Vol.99, No. 2, 2002.

3- Spadea,G.; Bencardino,F. and Swamy,R.N. "Structural Behavior of Composite RC Beams with Externally Bonded CFRP", Journal of Composites for Construction, ASCE, Vol.2, No. 3, 1998.

4- Spadea,G.; Bencardino,F. and Swamy,R.N. "Optimizing the Performance Characteristics of Beams Strengthened with bonded CFRP Laminates", Materials and Structures, Vol.33, 2000.

5- Swamy,R.N. and Mukhopadhyaya,P. "Debonding of Carbon-Fiber-Reinforced Polymer Plate from Concrete Beams", Structures and Buildings, Vol.134, 1999.

6- ACI Committee 440, "State of the Art Report on FRP for Concrete Structures", ACI440R-96, Manual of Concrete Practice, American Concrete Institute, MI, 1996.

7- Deuring,M. "Strengthening Reinforced Concrete with Prestressed Composite Fibre Materials", EMPA research report No. 224, 1993.

8- Hamid,A.;Issa,M.;Sabouni,A.R. and Mukhtar,A. "Use of Fiber Reinforced Plastics in Reinforced Concrete Slabs", Proceedings of the Sixth Arab Structural Engineering Conference, Damascus University, Damascus, Syria,1995.

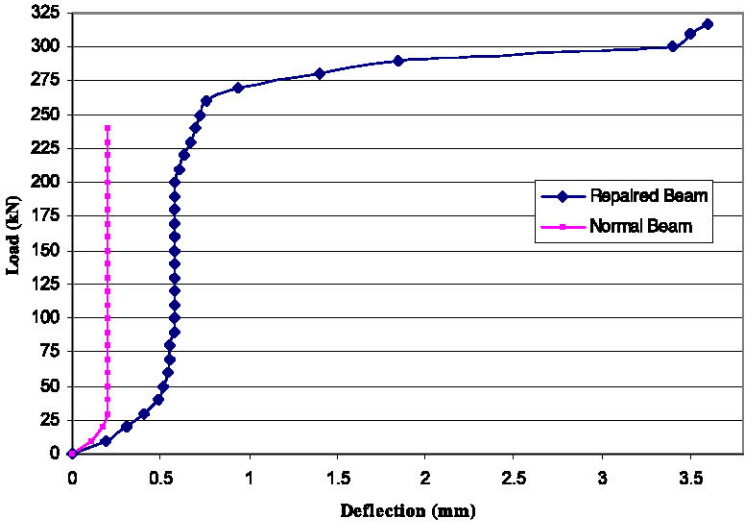

Figure 5: Load-Deflection Relationship, Beam 1

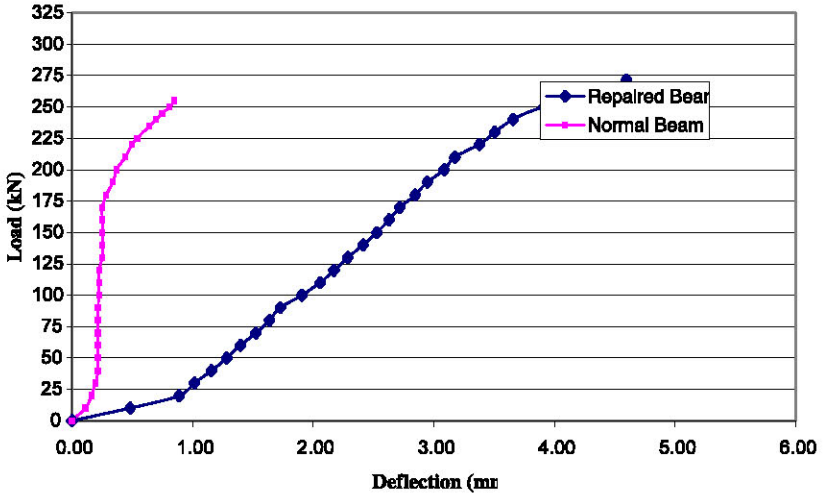

Figure 6: Load-Deflection Relationship, Beam 2

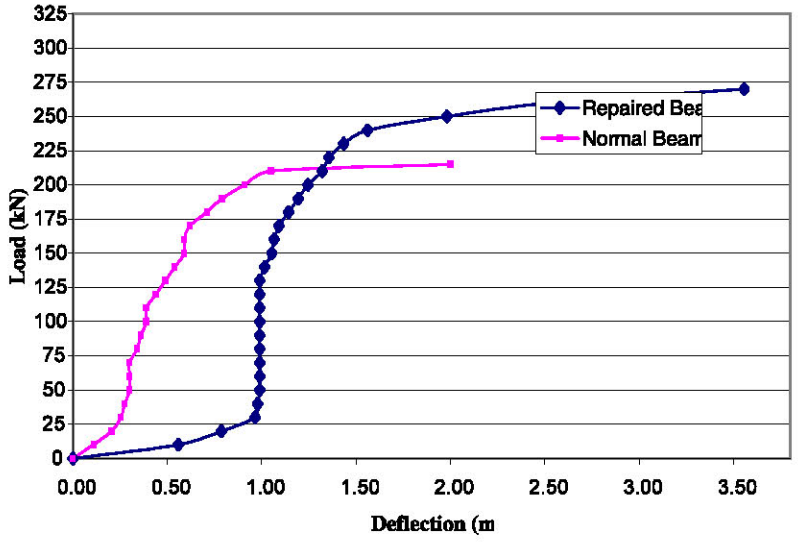

Figure 7: Load-Deflection Relationship, Beam 3

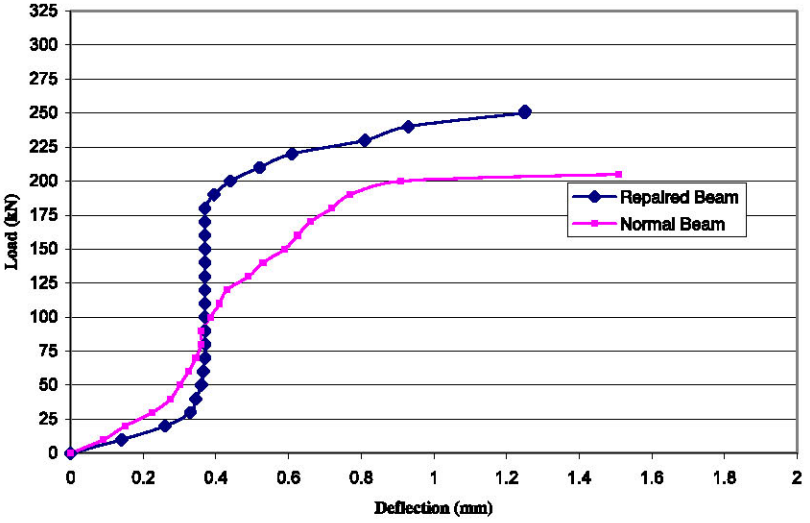

Figure 8: Load-Deflection Relationship, Beam 4

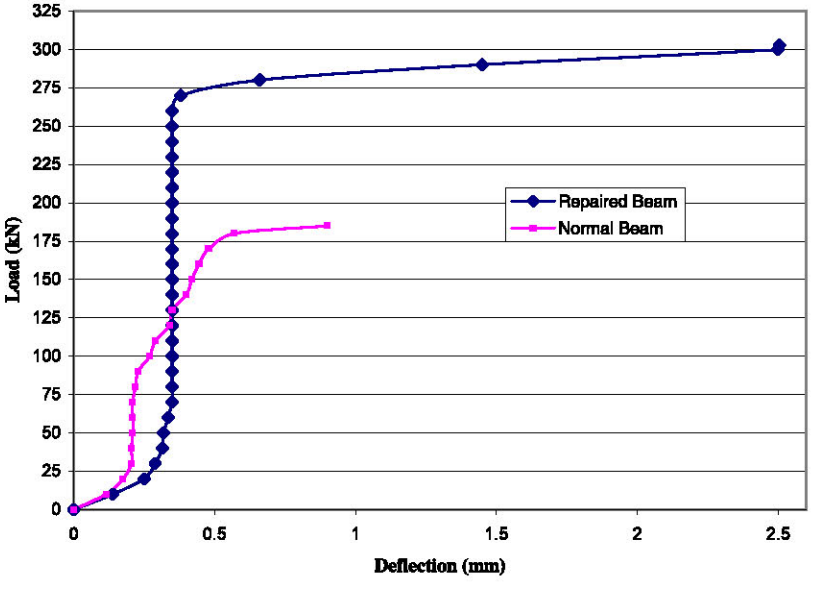

Figure 9: Load-Deflection Relationship, Beam 5

Proceedings of the ACI-KC First International Conference & Fourth Exhibition. September 29-October 1, 2003, Kuwait — ***Concreting and High Performance Concrete in Hot Weather.***

MODELING CONCRETE CRACKING CAUSED BY ALKALI AGGREGATE REACTION

Dr. Guemmadi Z'hor, University Mentouri Constantine, Algeria
Dr. Toumi Belkacem, University Farhat Abbas Setif, Algeria
Dr. Houari Hacene, University Mentouri Constantine, Algeria

ABSTRACT

The causes of concrete deterioration are multiple. Concrete degradation caused by physical agents are well controlled but internal degradation of concrete remains yet to be studied.

One of the factors that cause internal damage in concrete is alkalis-aggregate reactions. The degradations caused by these reactions are mainly inflation of mass and cracking. There are no methods that predict the level of the degradation caused by these reactions but numerical simulation based on experimental study provides a clear idea on the state of stress and resulting cracks.

Keywords
Concrete, Cracking, Alkali Aggregate Reactions, Experimental, Numerical Simulation.

INTRODUCTION

Hydraulic concrete is an artificial conglomerate formed by aggregate dispersed in a bending phase. In due course, the bending phase may be degraded by physical or chemical agents, internal or external. Microscopic cracks may often appear within the interface paste-aggregates, where there is a pore water film. Consequencely, this interface constitutes a zone of weakness and hence concrete may be represented as a multi-fissured media starting from the finest layer of the CSH of paste (some nanometers) up to the largest stones (a few centimeters).

One of the causes of internal degradation of the concrete was due to the reaction of the alkalis aggregates, the effect of the chemical and mineralogical factors that exist in the components of the concrete. The alkali-aggregate reaction materializes with a mosaic of crack and an exudation of gel. The reactions are obvious at the end of 4 to 10 years and are spread out over a large period of time. For the plane structural elements, such as the plates and the retaining walls, cracking occurs once the stress of expansion exceeds the working stress of traction. Nishibaya Shiet et al. [1] have reported that in Japan some plane structure affected by the alkali aggregate reactions had fissure of 8mm of 20 cm opening profundity.

In this study, a simulation of the kinetics of the crack development caused by the alkali aggregates reaction is proposed.

Although these parameters exist almost in all the concretes, they cannot be harmful if they preexist at the same time with a certain rate.

ALKALIS AGGREGATES REACTIONS IN CONCRETE

The reactions of alkalis aggregates in concrete appear for a long period and largely affect the durability of concrete. This problem may be described as "the internal corrosion of the concrete" and recently it has been noted that many concrete structures are affected by these reactions. In 1983, Poole [2] provided several cases of this phenomenon over the world (Figure 1). Undoubtedly, this problem is mainly due to some reactive aggregates. According to Grattan-Bellew [3] the aggregates cannot be studied without cement since the concrete comprises aggregates, cement, water and sometimes additives. Therefore the alkali reaction problem is not specific to some aggregate, however it must be studied in relation to cement-aggregates.

Taking into account the phenomenon complexity, professionals in the concrete industry are seriously worried at this problem while considering the following factors:

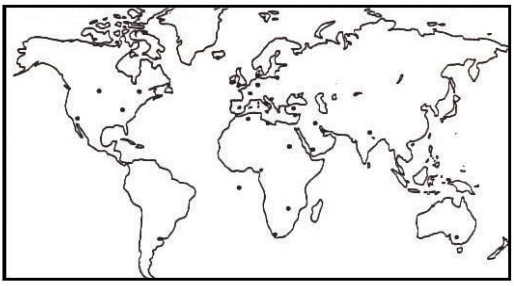

Fig.1: Recanted case of AAR phenomenon over the world

- Importance of the phenomenon affecting the massive works: dams, bridges, airports, and buildings.
- The increased use of new layers of the aggregates, particularly in developing countries.
- The complexity of the phenomenon because of the composition of cement: slag, fly ashes, and fillers.

The common factors affecting concrete degradation:

- **The presence of alkaline in cement:**

The chemical analysis of cement shows the existence of alkalis in the aggregates and in the additives. The maximal alkaline content is not yet defined. This limit of alkaline content varies from one researcher to another; however, the value retained by ASTM standards is of 0.6% Na_2O in cement.

- **Reactivity of the aggregates to alkalis:**

Researchers realized that sands containing not only reactivates of silica but poly-phased siliceous aggregates could also be quite as reactive. These aggregates contain cryptocrystalline quartz, feldspars, and micas. The reactivity of the aggregates can be related to their origin: the vitreous volcanic rocks have properties more constant than the sedimentary rocks (limestone), they are more stable than the metamorphic rocks (gneiss) having undergone stresses of pressure and temperature during their geological history. Another parameter concerning the reactive aggregates is that of their granularity and their quantity.

- **The presence of moisture:**

The critical values of relative moisture favorable to the alkali reaction range between 80 and 85%. The water/cement ratio has also a considerable role for the reason that an expansion can occur without external contribution, if water in the concrete is sufficient for the formation of an inflating gel. Desiccation-humidification cycles seem also dangerous as well as the relative humidity like the case of the Capetown dolosses where the emerged zone was more fissured than those immersed in sea water.

Other factors include time and the temperature, which accelerate the chemical reactions. The cracking of the concrete can be inoffensive as long as there are no water inhibitions.

The disorders appear after prolonged period of time. Following are some of the warning signs:

- **Cracking**: The fissures are evolutionary; their opening increase by 0.5mm every year
- **An exudation of gel**: White exudations consist of calcite. There are several types of gel. Regourd - Moranville [4] have classed them in three categories: Massive gel, Gel in the process of crystallization and Crystallized gel.
- **Pustules or craters**: pustules occur in the shape of small cones, due to the reaction of superficial coarse aggregates, which are invisible in the bottom of the bursting craters.

- **Movements and deformations**: A rising of the peak can be detected in dams, 1 to 2mm per year.
- **Coloration or discolorations**: A dark coloring along the fissures can be observed on piles of bridge or retaining walls.

Chemical mechanism of the alkalis aggregates reactions

The most significant and the most frequent reactions are the alkali-silica reactions. The process of these reactions [5] includes three phases:

- Attack of siliceous aggregates by setting the silica in solution in the interstitial solution.
  $S_i\text{-}OH + OH^- \longrightarrow S_i\text{-}O^- + H_2O$ (1)
- Gel creation by transformations of undissolved residual silica into gel.
  $S_i\text{-}O\text{-}S_i + 2OH^- \longrightarrow S_i\text{-}O^- + O^- - S_i + H_2O$ (2)
- Deteriorating expansion by the gel swelling.

DESCRIPTION OF THE MECHANISMS OF FAILURE

The reactions of hydration are not immediate, and for a long time the cement paste evolves. Its mechanical properties change all through the time, increasing gradually, but more and more slowly. It is usual to measure these properties at 28 days. It is also important to remember that there remains water inside the pores, adsorbed on their surface in the liquid or vapor state.

Each fissure corresponds to a critical stress of propagation, which may be superimposed by three modes (see Figure 2):

Mode I: a displacement only if Oy axis corresponds to a particular plane problem, indicated by Mode I. This mode is, generally, the most dangerous.

Mode II: it is generated by a shearing in the plane of the fissure and parallel with Ox axis.

Mode III: it is produced by an opposing-plane shearing, located in the fissure plane Oxz and is parallel with axis Oz. This last mode is solved by a representation 2d anti-plane, while the two precedents are solved by an opposing-plane analysis in plane stress or in plane deformation.

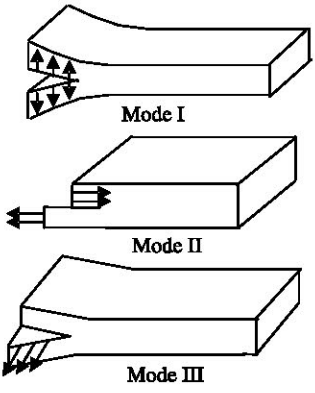

Fig.2: The modes of failure

During the loading (swelling), the most critical fissures start to be propagated. Subjected to a normal stress, they would be unstable. The critical fissures are propagating in the concrete in mode I, i.e. perpendicular to the direction of the normal stress [6].

Criteria of Rupture of MOHR-COULOMB

In the space of the principal deformations, this criterion takes the shape of an irregular hexagonal cone. This irregularity with the stress σ_2 is not taken into account. To describe the criterion by using the invariants of the stresses tensor, it is enough to express the main stress according to the invariants (Eq.3) and try to substitute in the expression of the MOHR circle (Eq. 4)

$$\sigma_1=\sigma_m+\sqrt{\frac{2}{3}}\,\bar{\sigma}\sin\left(\theta-\frac{2\pi}{3}\right)$$

$$\sigma_2=\sigma_m+\sqrt{\frac{2}{3}}\,\bar{\sigma}\sin(\theta) \qquad (3)$$

$$\sigma_3=\sigma_m+\sqrt{\frac{2}{3}}\,\bar{\sigma}\sin\left(\theta+\frac{2\pi}{3}\right)$$

$$\frac{\sigma_1+\sigma_3}{2}\sin(\varphi)\frac{\sigma_1-\sigma_3}{2}-c\cos(\varphi)=0 \qquad (4)$$

Consequently, the MOHR-COULOMB law is stated as follow:

$$F=\sigma_m\sin(\varphi)+\sigma\left(\frac{\cos(\varphi)}{\sqrt{3}}-\frac{\sin(\varphi)\sin(\theta)}{3}\right)-c\cos(\varphi) \qquad (5)$$

SIMULATION BY NUMERICAL MODEL

The study of the mechanical concrete behavior of the structures under internal stress due to the alkali reaction was not recently approached with the angle of numerical modeling by the finite element method which uses a simple approximation of the unknown variables to transform the partial derivative equations into algebraic equations. The principle of the finite element method is defined as a mathematical approach of a physical system characterized by one or more variables or functions recognized as exact which are represented by algebraic functions.

Assumption of the model:

The properties of the concrete always depend on the levels of degradation that reign in its mass. Among the factors that appear in the mass of the concrete and generate its progressive degradation we find the alkali-aggregate reactions. This reaction appears mainly in the interface binding aggregates and results in a swelling of the gel, which results from these chemical reactions. This swelling exerts compression on the reactive grains of aggregate and traction in the paste.

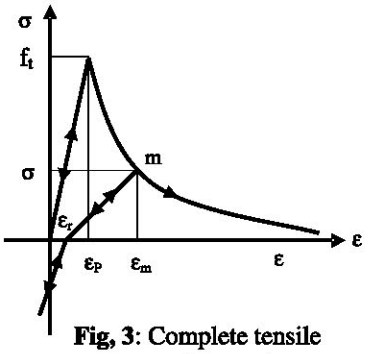

Fig, 3: Complete tensile curve of concrete

Concrete is a composite material tree physic (aggregates, paste and interface). Since the swelling appears in the interface and the compressive strength of the aggregates is much higher than the tensile strength of the paste, we modeled only the paste, therefore the homogeneous media. The non-linearity of material (Figure 3) was taken into account by the complete tensile law [7]:

$$\begin{aligned} \sigma &= E\,\varepsilon && \varepsilon \le \varepsilon_P \\ \sigma &= f_t\left(1 - \frac{\varepsilon - \varepsilon_P}{\varepsilon_U - \varepsilon_P}\right) && \varepsilon_P \le \varepsilon \le \varepsilon_U \\ \sigma &= 0 && \varepsilon \le \varepsilon_P \end{aligned} \qquad (6)$$

The material degradation according to time due to the reaction was calculated on the basis of experimental results [8]

Description of the Program and the Stages of Calculation Used

With an aim of simulating the evolution of the fissures caused by the alkali-aggregates reaction, we developed a program, which uses four nodes isoperimetric finite elements.

Calculation progresses by steps of loading of low amplitude starting with a null initial value and up to the value of 9 Mpa [9] after each step; the calculated stresses are compared with the Mohr criterion of ruptures. If the rupture is not reached, the program continues with the following step and by taking the new constants of the material (degradation of the concrete by alkali-aggregates according to time).

RESULTS AND DISCUSSION

The observation of the curves, point out:

Expansive gel evolution:

The expansive evolution of the gel (Figure 4) according to time follows an approximately linear variation. The interpolation function is of the form:

$$P = 0.0034T + 0.037 \qquad (7)$$

P: expansion of the gel
T: time in days

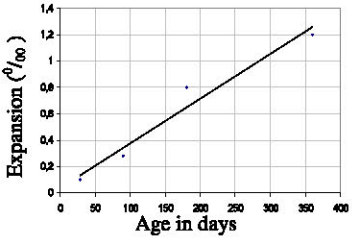

Fig.4 Gel expansion as function of time

Compressive Strength Variation as Function of Time:

The variation of the compressive strength according to time (Figure 5) increases quickly until certain limit, and beyond this limit, it decreases by environs 25% then it is stabilized.
The same observation was made for the tensile strength.

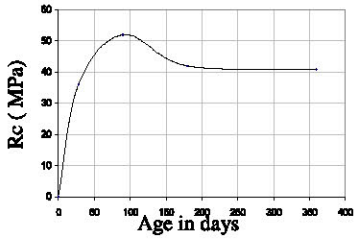

Fig.5 Compressive strength as function of time

Evolution Of The Modulus Of Elasticity:

The evolution of the modulus of elasticity, according to time (Figure 6), signifies 3 zones:

- A fast increase during the first twenty eight days;
- Between 28 and 175 days a quasi-linear reduction is observed;
- Beyond 175 days a weak increase in the modulus of elasticity is noted.

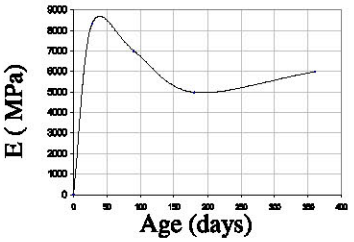

Fig.6: Elasticity of modulus as function of time

By plotting the curve of material degradation as function of time (Figure 7), we note that it is done in three phases:

- Until 28 days, the materials remain virgin and that explains why all the properties of materials increase with time.
- From 28 to 175 days, the value of damage factor increases linear up to the value of 0,4. During this increase all off the concrete properties show a reduction (damage).
- Beyond 175 days, the damage factor starts to decrease more or less linearly [10] and the various concrete properties increase slightly.

Fig. 7: Degradation Factor as function of time

Propagation of Cracks:

Figure 8, shows the fissures propagation. This occurs according to mode I under the action of tensile stresses (zones framed). The tensile stresses concentration is more marked around the assemblage points of the two lips of the fissure.

CONCLUSION

Although the calculation program is in course of development, the first simulation results compared with previously existing experimental results, have provided very encouraging deformations results. The numerical simulation of concrete expansion, taking into account the change of the mechanical characteristics as function of time, contributes to a better comprehension of the damage level and a better insight to the solutions of prevention and repair of the structures affected by this phenomenon.

This study highlights the importance of the phenomena related to the alkalis-aggregates and makes it possible to follow the evolution and the propagation of the fissures caused by this phenomenon.

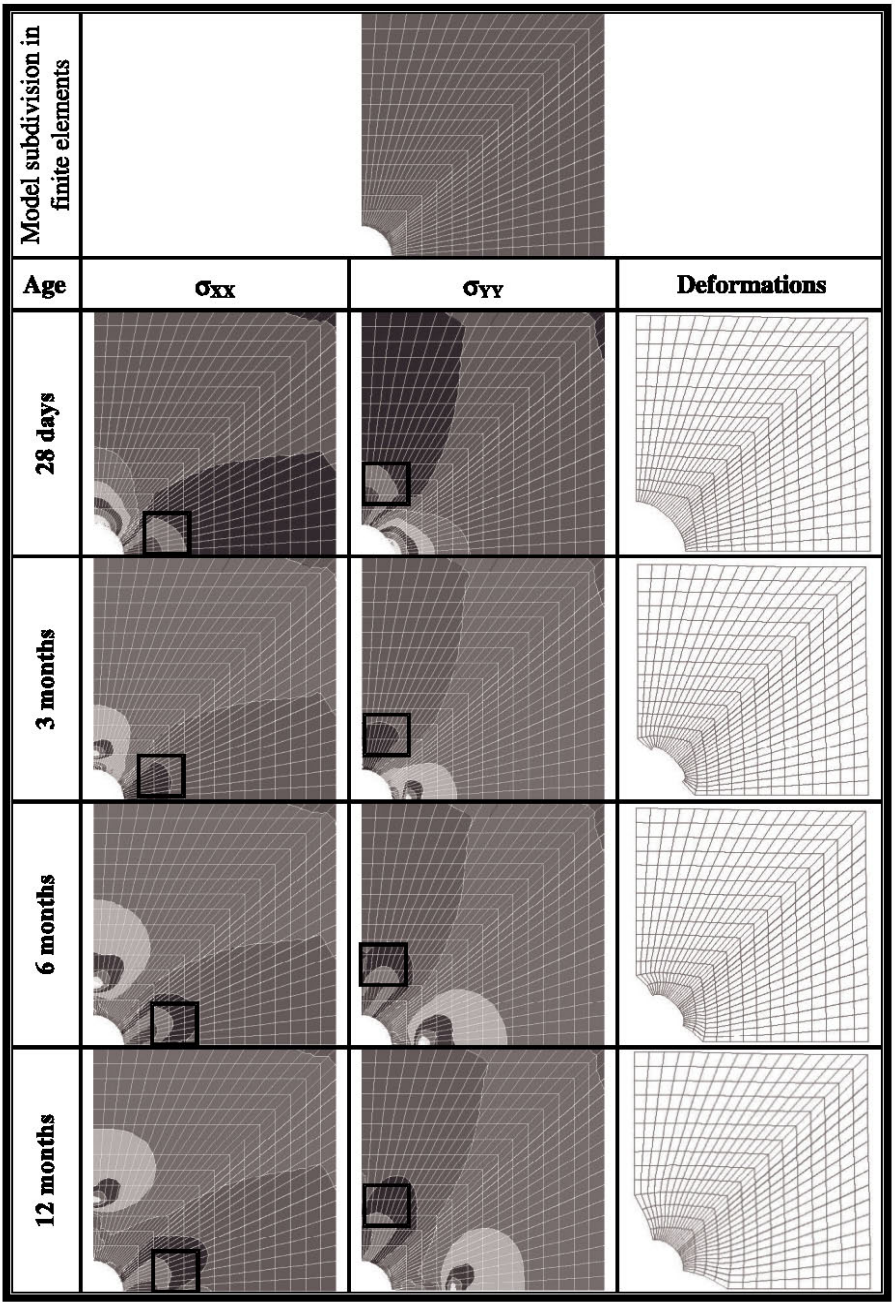

Fig. 8 Evolutions and propagation of the fissures according to the expansion and time.

REFERENCES:

1. Nishibaya Shiet and Al: A rapid method of determining the alkali-aggrergate reaction in concrete by autoclave.Proceeding of 7th International Conference of AAR in concrete, Ottawa, Canada, 1986, p.299-303.

2. Poole: Diagnosis- Working-Party, The diagnosis of alkali-silica reaction.British cement Assocation, England,1988.

3. Grattan-Bellew, P.E., A review of test methods for alkali expansivity of concrete aggregates. Proceedings of the Conference on Alkali-aggregate reaction in concrete, Cape Town, South Africa, 1981.

4. Regourd-Moranville, M., Products of reaction and petrographie examination. Proceegings of the 8th International Conference on Alkali-Aggregate Reaction, Kyoto, Japan,1989, p.445-456.

5. Diamond, S., On the physics and chemistry of ASR. Proceeding of the Conference on Alkali-aggregate reaction in concrete, Cape Town, South Africa,1981.

6. Domenica, Francois, Andre Pineau and André Zaoui, Matériaux Viscoplasticity, Damage, Contact mechanics p115-118, Editions Hermes1995.

7. Microphone mechanical modeling of concrete response under static loading – part1: model development and validation Ashraf Reguab Mohamed and Will Hansen; ACI FLIGHT 96 N°2 MARSH/APRIL 1999

8. Habita, M.F, Contribution to the study of the incidence of the alkali reaction on the mechanical behavior of the concrete beams arms. These of Doctorate in Civil Engineering.

9. Guettache, B, Behavior of minerals in hyper-alkaline medium. Application to the forecast of degradation intern concretes by tests and modeling, Thèse of Doctorate in geology, Mars 1993.

10. Habita, M.F, Brouxel. M and Prin.D, Structural AAR effects: an experimental study. Proceedings of the 9th International Conference one Alkali-aggregate Reaction in Concrete, London, UK, 1992. p.403-410.

11. D.W. Expansion of concrete due to alkali-Silica reaction – year explanation. Magazine of Concrete Research, 1978, v.30, p.215-221

Proceeding of the ACI-KC First International Conference & Fourth Exhibition. September 29-October 1, 2003, Kuwait — ***Concreting and High Performance Concrete in Hot Weather.***

مواصفات البيتون في الجو الحار والجاف

د. عبدالخالق طالب

مقدمة

إن دراسة العوامل المناخية عند تصميم الخلطة البيتونية في مجال المنشآت الهندسية ضرورية جداً لما لها من إنعكاس سلبي على المنشأة، كما أن المعرفة الدقيقة للبيانات المناخية في موقع العمل تلعب دوراً أساسياً في التصميم الهندسي ككل وبالتالي تلعب دوراً أساسياً في الحسابات الهندسية.

إن أخذ الظروف المناخية بالحسبان وتأثيرها على مواصفات البيتون في البلدان العربية أمر محدود وهذا يعود في الغالب إلى عدم التقدير الصحيح لتأثير هذه العوامل عل المنشآت الهندسية.

وتعتبر ظاهرة التشقق في البيتون الطري من أخطر الظواهر السلبية التي تواجه البيتون المصبوب حديثاً خلال الساعات الأولى من الصب حيث يكون البيتون لم يمتلك بعد المقاومة الكافية لمواجهتها والحد من تأثيرها.

ويهدف هذا البحث إلى دراسة تأثير العوامل المناخية على تقلص وتشقق البيتون الطري وإمكانية تقليل هذه التشققات.

١ ــ تبخر الماء من البيتون الطري:

عندما يحصل تماس بين الماء وذرات الأسمنت فإن التفاعل الكيميائي يأخذ مجراه مباشرة والذي يستمر ما بين **40-120 min** بعد ذلك تبدأ مرحلة السكون والإستقرار في البيتون وظهور الماء على سطحه (الإنزياح) [٢,٦].

يستمر ظهور الماء على سطح البيتون الطري (الإنزياح) بمعدل كبير حوالي **15-30 min** وبعد ذلك يبدأ بالتناقص حتى يبلغ الصفر خلال ساعة ونصف تقريباً.

إن التبخر هو إنتقال للماء من مرحلة السائل إلى مرحلة البخار وهو يحدث عندما يتعرض الماء لتأثير العوامل المناخية. وفي حالة البيتون الطري فإن الماء المتجمع على سطحه والناتج عن عملية الإنزياح

هو المعرض للتبخر. في الحقيقة يعد تبخر الماء من البيتون الطري من دون تواجد ما الإنزياح على سطحه السبب الرئيسي لحدوث التقلص.

تمر عملية تبخر الماء من البيتون الطري بثلاث مراحل :

ـ **المرحلة الأولى** وتتضمن تبخر الماء المتجمع على سطح البيتون والناتج عن الإنزياح.

ـ **المرحلة الثانية** والتي تبدأ بعد تبخر الماء المتواجد على سطح البيتون حيث يحصل تبخر ضمن سطح البيتون الرطب والتي تنتهي بجفافه.

ـ **المرحلة الثالثة** وتتضمن تبخر الماء من داخل البيتون.

يتأثر معدل تبخر الماء من البيتون الطري بعدد من العوامل مثل درجة حرارة الجو المحيط ـ درجة حرارة البيتون ـ درجة الرطوبة ـ سرعة الهواء ...

إن كلاً من هذه العوامل ذو تأثير خاص على معدل التبخر والذي يزداد عندما تتجمع هذه العوامل معاً ، الشكل ١.

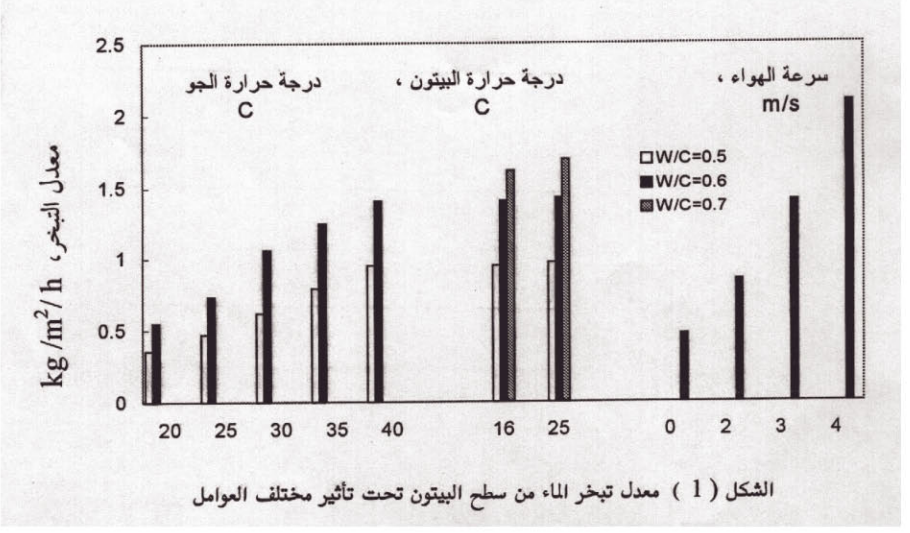

الشكل (1) معدل تبخر الماء من سطح البيتون تحت تأثير مختلف العوامل

إن تخفيض معدل التبخر من سطح البيتون هو من الأهمية ليس فقط من حيث أن معدل التبخر المنخفض سوف يزيد من مقاومة البيتون وإنما أيضاً سوف يقلل من إحتمال تشقق البيتون الطري.

٢ ـ التشقق في البيتون الطري:

يمكن أن يحدث على سطح البيتون الطري نوعان من التشقق [٧] :

١-٢ ــ التشقق الناجم عن التقلص اللدن :

عندما تبدأ المرحلة الثانية من تبخر الماء من البيتون فإن الماء ما بين ذرات الأسمنت والحصى والقريب من الأسطح يشكل أسطحاً هلالية ذات أشكال معقدة والتي تؤدي إلى تكون الضغط الشعري ضمن القسم السائل من البيتون والذي يبدأ بالإزدياد ببطء عند بدء عملية جفاف سطح البيتون.

يتطور الضغط الشعري ضمن البيتون خلال مرحلتين :

حيث يزداد الضغط الشعري بشكل حاد خلال المرحلة الأولى حتى يصل إلى مرحلة إستقرار ويتناسب الضغط الشعري خلال هذه المرحلة مع معدل تبخر الماء المتجمع على سطح البيتون. في المرحلة الثانية يتابع الضغط الشعري الإزدياد حتى يصل إلى الذروة والتي توافق جفاف سطح البيتون.

يحدث التقلص اللدن في البيتون الطري بعد فترة قصيرة من بدء تشكل الضغط الشعري وإمتلاكه كمية كافية لحدوث تقلــص في البيتون الطري والذي يزداد مع الضغط الشعري الأعظمي ، الشكل ٢ .

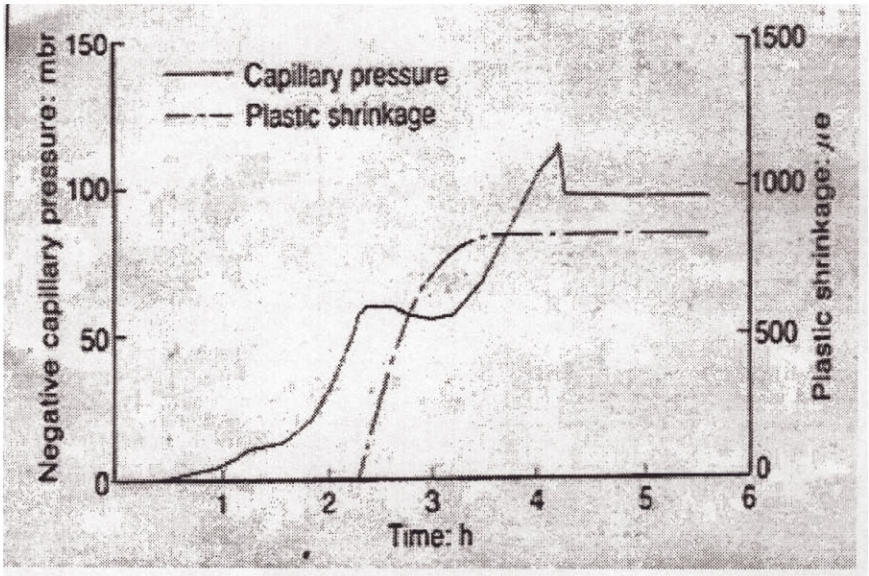

الشكل (2) الضغط الشعري و التقلص اللدن ضمن البيتون الطري

ـــــــ الضغط الشعري ـــــ ـ ـــــ التقلص اللدن

يتعلق حدوث التقلص اللدن في البيتون الطري مباشرة بزمن وصول الضغط الشعري إلى مرحلة الإستقرار الأولى والذي يتأثر بالظروف التي يتم فيها صب البيتون وكذلك بمواصفاته.

نتيجة لعملية التقلص فإنه تظهر إجهادات شد ضمن البيتون والتي تبدأ بالتطور بدءاً من سطح البيتون. في حال زيادة إجهادات الشد عن الإجهادات المسموحة فإن البيتون سوف يتشقق وتسمى هذه التشققات (التشقق الناتج عن التقلص اللدن في البيتون الطري). وهذه التشققات غير مرغوبة وخاصة عندما تكون مرئية بالعين المجردة وطويلة وتعتبر غير عادية وخاصة في البلاطات البيتونية وذلك لأن هذه التشققات تستمر بالتوسع مع الزمن ويتراوح عرض التشقق الناجم عن التلقص ما بين **0.1-3 mm** ويمكن أن يصل طوله حتى **1m**. إن السبب الرئيسي الذي يؤدي لحدوث هذه التشققات هو نسبة التبخر العالية من سطح البيتون وصغر معدل إنزياح الماء من داخله لتعويض كمية الماء المتبخر إن هذا الأمر يزيد من إحتمال تشقق البيتون الطري وخاصة عندما يزيد معدل التبخر عن **1000 gr/m^2/h**.

٢-٢ ــ التشقق الناتج عن إستقرار البيتون الطري :

يحدث هذا النوع من التشقق نتيجة للهبوط المتفاوت للبيتون الطري بسبب تواجد حبات بحص كبيرة ويمكن تفادي هذا النوع من التشقق بإستخدام بيتون أقل طراوة وبالرص الجيد. تظهر هذه التشققات بعد حوالي **10 min** بعد الصب وتستمر لمدة **3 hours** تقريباً.

يمكن أن يحدث هذا التشقق في درجة الحرارة الطبيعية غير أنه في الجو الحار فإنه يمكن حدوث كلا النوعين من التشقق معاً بحيث يدعم أحدهما الآخر.

٣ ــ التقلص اللدن في البيتون الطري:

إن التقلص اللدن هو التقلص الذي يحدث في البيتون المصبوب حديثاً وخلال عدة ساعات بعد بدء صبه حيث يكون البيتون في المرحلة اللدنة. إن هذه المرحلة قصيرة وتبدأ بفقدان اللمعان من سطح البيتون وتنتهي بإستقراره. يتعلق التقلص اللدن بشكل أساسي بتبخر الماء وبالتالي يتأثر بنفس العوامل المؤثرة على تبخر الماء من سطح البيتون.

يتم حساب التقلص اللدن في البيتون الطري من خلال صب البيتون ضمن قالب ذو أبعاد **700x150x150 mm** وذلك عن طريق قياس تحرك المسبر المغروس في سطح البيتون وبعمق **20 mm** والمتصل بجهاز قياس تغير الحركة **LVDT** والموصول بدوره إلى جهاز الكمبيوتر لتحليل القراءات، الشكل ٣، الجدول ١.

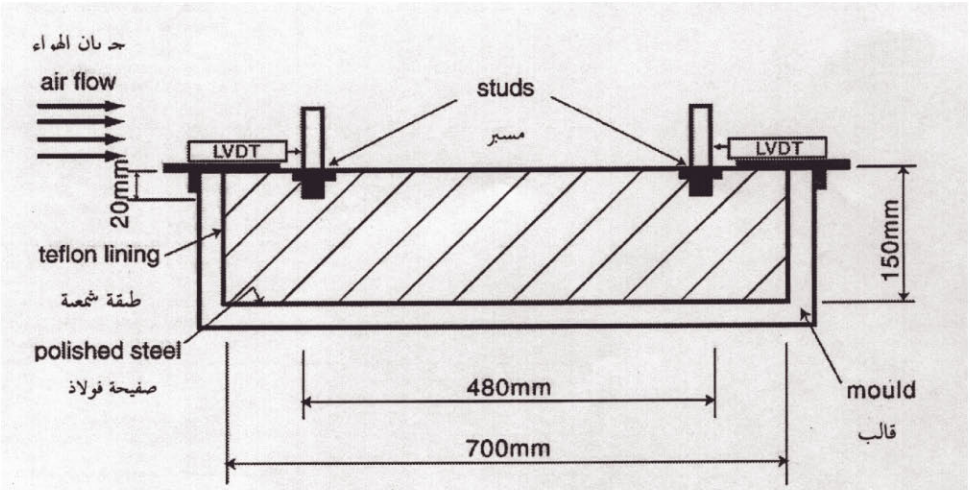

الشكل (3) جهاز قياس التقلص اللدن في البيتون الطري

الجدول (١) تقلص البيتون الطري تحت تأثير مختلف العوامل :

التقلص 10^{-3} x mm/m	زمن بدء التقلص min	W/C	درجة حرارة البيتون ، C	درجة حرارة الجو ، C	سرعة الهواء m/s
1.42	48	0.5	16	40	3
2.61	72	0.7	16	40	3
3.53	108	0.6	16	40	1
1.04	74	0.5	25	40	3
2.06	89	0.6	25	40	3
2.55	116	0.7	25	40	3
1.3	49	0.5	16	35	3
2.06	85	0.6	16	30	3
1.11	59	0.5	16	35	0
1.78	93	0.6	16	30	3
1.01	75.6	0.5	16	25	3
1.6	114.5	0.6	16	25	3
0.98	88	0.5	16	20	3
1.35	159	0.6	16	20	3
0.65	104	0.6	16	40	0
1.35	87	0.6	16	40	2
2.61	72	0.6	16	40	3
4.02	48	0.6	16	40	4

يظهر الشكل ٤ تغير التقلص اللدن في البيتون الطري بإختلاف W/C ودرجة حرارة البيتون.

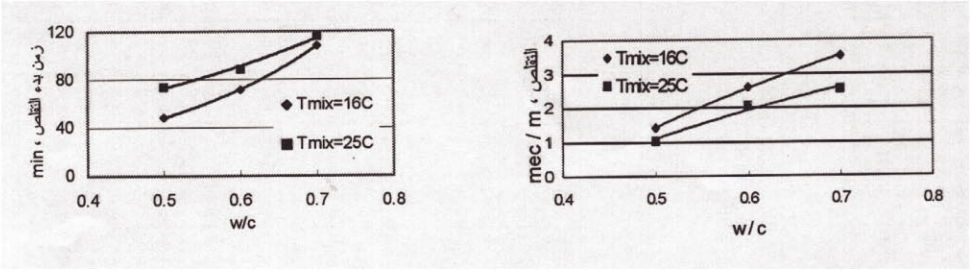

الشكل (٤) تأثير مواصفات البيتون على التقلص اللدن

الشكل (٥) تأثير مواصفات البيتون على زمن بدء التقلص اللدن

يتعلق التقلص بـــ W/C بشكل مباشر وذلك لأن W/C يحدد كمية الماء المتبخر من البيتون لذلك فإن إزدياد W/C سوف يؤدي إلى إزدياد نسبة التبخر من سطح البيتون وبالتالي زيادة التقلص اللدن. وفي نفس الوقت فإن إزدياد W/C سوف تزيد كمية إنزياح الماء من داخل البيتون وبالتالي فإن سطح البيتون سوف يحتاج إلى زمن أطول للوصول إلى اللحظة التي يكون فيها نسبة تبخر الماء أكبر من نسبة الإنزياح أي يحتاج لزمن أطول لبدء حدوث التقلص اللدن، الشكل ٥.

من جهة أخرى عندما تزداد درجة حرارة البيتون فإن التفاعلات الكيميائية بين الماء والأسمنت ضمن البيتون سوف تزداد وهذا يؤدي إلى زيادة المقاومة الأولية للبيتون خلال الساعات الأولى وبالتالي تقليل التقلص اللدن. إن إمتلاك البيتون الطري للمقاومة بشكل أسرع عندما تزداد درجة حرارته سوف تؤدي إلى تأخر بدء حدوث التقلص اللدن الشكل ٥.

تؤثر درجة حرارة الجو المحيط على تقلص البيتون الطري ولكن بنسب مختلفة حسب درجة الحرارة حيث إن إزدياد درجة حرارة الجو المحيط ستزيد من نسبة تبخر الماء من سطح البيتون وهذا ما يتطلب زيادة نسبة إنزياح الماء من داخل البيتون وبالتالي زيادة التقلص اللدن، الشكل ٦.

على سبيل المثال من أجل W/C=0.6 فإن التقلص اللدن سوف يزداد بنسبة ٢٠٠% تقريباً في حال تغير درجة حرارة الجو المحيط من 30 C إلى 40 C وذلك بالمقارنة مع تغير درجة حرارة الجو المحيط من 20 C إلى 30 C .

كذلك الأمر فإن زيادة سرعة الهواء المحيط سوف تزيد من نسبة التبخر من سطح البيتون وبالتالي زيادة التقلص اللدن، على سبيل المثال إن التقلص اللدن في حال T concrete=40 C وسرعة الهواء

0 m/s سوف يكون $0.65x10^{-3}$ mm/m وفي حال سرعة الهواء 4 m/s فسوف يكون $4.02x10^{-3}$ mm/m.

أما بالنسبة لزمن بدء التقلص اللدن فإن زيادة درجة حرارة الجو المحيط أو إزياد سرعة الهواء المحيط سوف تسرع من زمن بدء تقلص البيتون، الشكل ٧.

على سبيل المثال في حال T concrete=16C,W/C=0.6 فإن إزدياد درجة حرارة الجو المحيط من 20 C إلى 40 C سوف تنقص زمن بدء التقلص اللدن بشكل كبير من 159 min إلى 72 min.

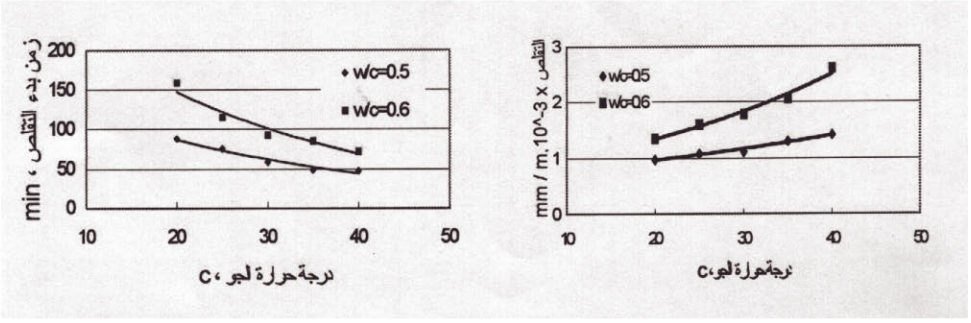

الشكل (٦) تأثير العوامل المناخية على التقلص اللدن في البيتون الطري الشكل (٧) تأثير العوامل المناخية على زمن بدء التقلص اللدن

وفي حال إزدياد سرعة الهواء من 0 m/s إلى 4 m/s فإن زمن بدء التقلص اللدن سوف يتناقص من 104 min إلى 48 min ، وتشير الأرقام السابقة وبوضوح إلى التأثير الكبير للعوامل المناخية القاسية على تقلص البيتون الطري.

٤ ــ تشقق البيتون الطري:

يشكل ظهور التشقق على سطح البيتون الطري المرحلة التي تلي حدوث التقلص وذلك عندما يستمر تعريض البيتون الطري لنفس العوامل ولمدة أطول أي أن التقلص هو السبب الرئيسي لظهور التشقق على سطح البيتون الطري ، لذلك فإنه يمكن القول إن شدة وكثافة التشقق تتأثر بنفس العوامل التي تؤثر على التقلص مثل خواص البيتون الطري والعوامل المناخية المؤثرة عليه.

يتم قياس كثافة التشقق على سطح البيتون الطري في بلاطات بيتونية رقيقة أبعادها 600x900 mm وبسماكة 20 mm حيث يتم صب بلاطتين بنفس الطريقة ومن ثم يتم تعريضهم لظروف مخبرية متشابهة (درجة حرارة الجو ــ سرعة الهواء ...) الشكل ٨.

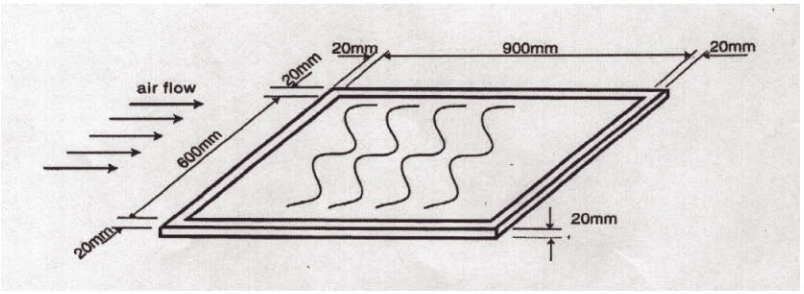

الشكل (٨) دراسة التشقق على سطح البيتون الطري

إن إستخدام البيتون الذي يحتوي على حصى يصل قطرها حتى **20 mm** للصب في هذا القالب هو غير عملي ويحتوي على إنقطاعات كثيرة وثغرات ومن أجل ذلك فقد تم إستخدام البيتون ذو المواد الحصوية الصغيرة (**micro concrete**) لصب البلاطات. إن التشققات التي ظهرت على سطح البلاطات في كافة التجارب كانت موازية للبعد الأصغر للقالب (العرض) الشكل ٩ ، وقد تم إستخدام المجهر لقياس عرض التشققات وكثافتها.

الشكل (٩) تشقق سطح البلاطات البيتونية تحت تأثير مختلف العوامل

١-٤ ــ تأثير مواصفات البيتون على التشقق :

إن إزدياد **W/C** سوف تؤدي إلى زيادة كثافة التشقق على السطح وذلك بسبب إزدياد إجهادات الشد المتولدة على السطح والناجمة عن التقلص اللدن للبيتون وبسبب إنخفاض مقاومة البيتون بنفس الوقت. الشكل ١٠ ، الجدول ٢.

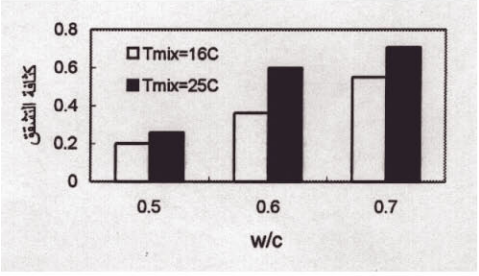

الشكل (١٠) تأثير مواصفات البيتون على كثافة التشقق

نلاحظ من الجدول أنه من أجل درجة حرارة الجو 40 C وسرعة الهواء 3 m/s فإن زيادة w/c من 0.5 إلى 0.7 ستزيد كثافة التشقق من 0.2 إلى 0.55 وزيادة عدد التشققات من 7 إلى 12 تشقق.

وبالنسبة لبدء ظهور التشققات فإن إزدياد W/C سوف يزيد من زمن بدء ظهور التشققات وذلك لأن البيتون الأكثر ميوعة يملك إمكانية أكبر للحركة وبشكل متوافق مع التقلص الحجمي وذلك بالمقارنة مع البيتون الأقل ميوعة.

عند إزدياد درجة حرارة البيتون فإن كثافة التشقق وعدد التشققات على السطح سوف تزداد بسبب إزدياد إجهادات الشد الناجمة عن التقلص اللدن للبيتون.

على سبيل المثال من أجل **W/C=0.6** عندما تزداد درجة حرارة البيتون من **16 C** إلى **25 C** فإن كثافة التشقق سوف تزداد من ٠,٣٦ إلى ٠,٥٩ أي تزداد بنسبة ١٦٤%. إن إزدياد مقاومة البيتون الطري خلال الساعات الأولى للصب نتيجة لإزدياد درجة حرارته ستؤدي إلى بعض التأخير في ظهور التشققات على السطح وذلك بالمقارنة مع البيتون ذو درجة الحرارة الطبيعية ، الشكل ١١.

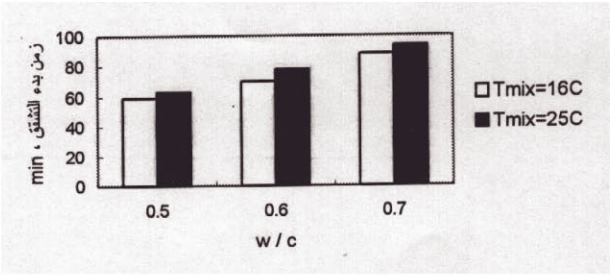

الشكل (١١) تأثير مواصفات البيتون على زمن بدء ظهور التشققات على السطح

٢-٤ ــ تأثير العوامل المناخية على تشقق البيتون الطري :

تؤثر العوامل المناخية على تشقق البيتون الطري بشكل فعال وكبير حيث أن إزدياد كل من درجة حرارة الجو المحيط أو سرعة الهواء ستزيد النقلص في البيتون وبالتالي التشقق (كثافة التشقق ــ عرض وعدد التشققات) على سبيل المثال من أجل **W/C=0.6** إن زيادة درجة حرارة الجو من **20 C** إلى **40 C** ستزيد عدد التشققات على السطح من ٣ إلى ٨ تشقق ، أما إزدياد سرعة الهواء من **0 m/s** إلى **4 m/s** فقد أدت إلى إزدياد كثافة التشقق بنسبة **١١٥٠%** وعدد التشققات من ٢ إلى ١٢ تشقق.

إن هذا التأثير الكبير للعوامل المناخية على تشقق البيتون سببه الرئيسي هو نسبة التبخر العالية من البيتون وسرعة جفافه ، الجدول ٢ ، الشكل ١٢.

كذلك الأمر فإن إزدياد سرعة التبخر من سطح البيتون الطري نتيجة لحرارة الجو المرتفعة أو السرعة العالية للهواء سوف تؤدي إلى تسريع ظهور التشققات على السطح وزيادة عددها وعرضها ، الشكل ١٣.

الجدول (2) تشقق البيتون الطري تحت تأثير مختلف العوامل :

سرعة الهواء m/s	درجة حرارة الجو ، C	درجة حرارة البيتون ، C	W/C	كثافة التشقق	زمن بدء حدوث التشقق ، min	عرض التشقق mm	عدد التشققات
3	40	16	0.5	0.2	89	0–1.2	7
3	40	16	0.6	0.36	100	0.15–1.8	8
3	40	16	0.7	0.55	118	0.2–1.6	12
3	40	25	0.5	0.26	93	0.15–1.2	12
3	40	25	0.6	0.59	108	0.2–1.6	14
3	40	25	0.7	0.71	124	0.2–1.8	15
3	35	16	0.5	0.19	99	0.09–1.1	6
3	35	16	0.6	0.31	112	0.1–1.5	7
3	30	16	0.5	0.14	112	0.06–0.69	4
3	30	16	0.6	0.22	135	0.15–1	6
3	25	16	0.5	0.09	137	0.07–0.6	3
3	25	16	0.6	0.17	157	0.08–0.85	3
3	20	16	0.5	0.05	160	0.08–8.45	2
3	20	16	0.6	0.06	188	0.07–0.53	3
0	40	16	0.6	0.06	201	0.05–0.45	2
2	40	16	0.6	0.23	136	0.06–0.5	3
3	40	16	0.6	0.36	100	0.15–1.8	8
4	40	16	0.6	0.69	87	0.3–2.4	12

نلاحظ من الجدول 2 أن إزدياد درجة حرارة الجو من 20 C إلى 40 C أدت إلى تخفيض زمن بدء ظهور التشققات إلى النصف تقريباً.

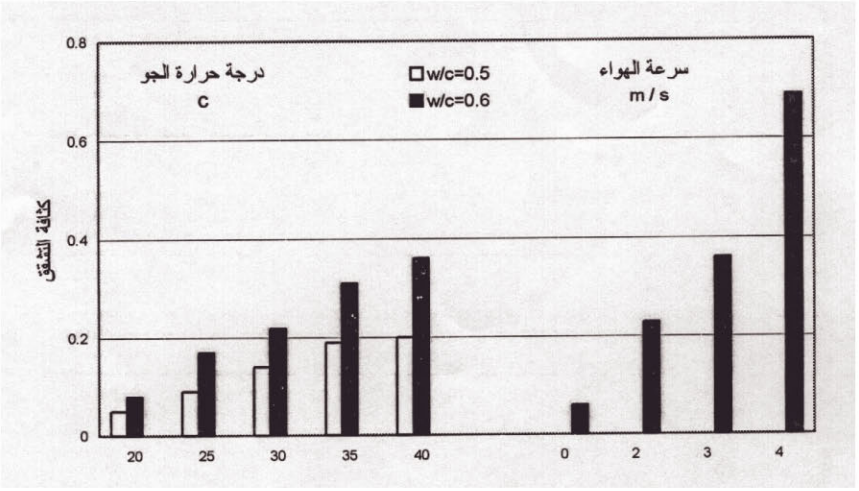

الشكل (١٢) كثافة التشقق في البيتون الطري تحت تأثير مختلف العوامل المناخية

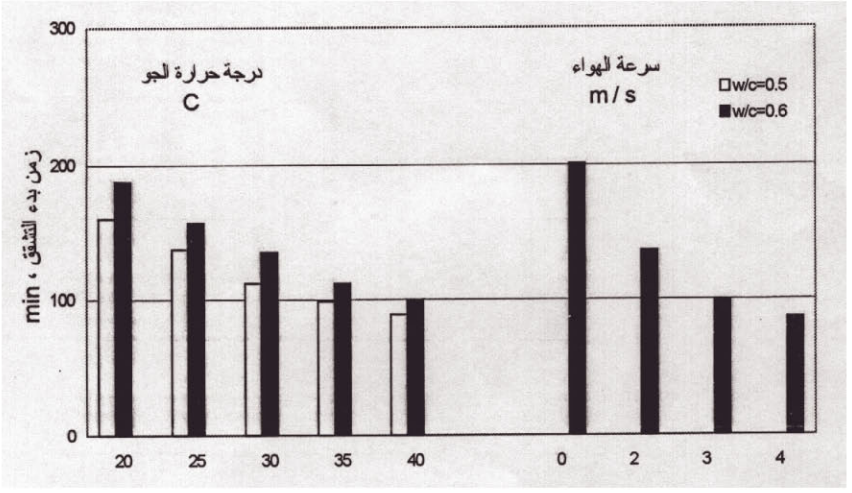

الشكل (١٣) زمن بدء ظهور التشققات على سطح البيتون الطري تحت تأثير مختلف العوامل المناخية

أما إزدياد سرعة الهواء من 0 m/s إلى 4 m/s فقد أدت إلى تخفيض زمن بدء ظهور التشققات أكثر من ٦٠%. من خلال التجارب المخبرية التي تم إجراؤها لدراسة التشقق فقد لوحظ أن فقدان اللمعان من سطح البلاطات البيتونية قد تم بأزمنة مختلفة حسب الظروف المخبرية للتجارب المنفذة ، وهذا

الزمن كان هاماً للتنبؤ بظهور التشققات حيث أن فقدان اللمعان المبكر من سطح البلاطات البيتونية ذات الخواص المتشابة نتيجة للظروف المناخية القاسية (الصعبة) كان يتنبأ بتشققات كبيرة على السطح إذ أن البيتون لم يمتلك المقاومة الكافية لمقاومة الإجهادات الناتجة عن تقلص البيتون الطري لذلك فإن التأخير من زمن بدء فقدان اللمعان من سطح البيتون عن طريق تقليل نسبة التبخر أو تأمين الحماية المباشرة للبيتون بعد الصب سوف تؤدي إلى تقليل التشققات وكثافتها وخاصة إذا بدأ البيتون بإمتلاك المقاومة بشكل أسرع.

يجب أن لا يتجاوز العرض الأعظمي المسموح للتشققات عن 0.15 mm وذلك بالنسبة للبيتون المصبوب في المناطق ذات المناخ القاسي (الصعب)، فإذا نظرنا إلى الجدول ٢ والذي يحدد عرض التشققات تحت تأثير مختلف العوامل نجد التأثير الكبير والخطر لدرجة حرارة الجو المرتفعة وسرعة الهواء على عرض التشققات الأمر الذي يجعلها أكبر من العرض المسموح وبالتالي يجعل من الضروري النظر في ضرورة تقليل عرض هذه التشققات وكثافتها.

٥ ــ تخفيض نسبة التشقق في البيتون الطري :

إن حفظ البيتون مباشرة بعد الصب في جو رطب سوف يلغي التشقق وذلك لأن نسبة التبخر سوف تكون صغيرة إن وجدت ، وفي حال إمكانية حفظ البيتون في جو رطب فإنه توجد عدة طرق لتقليل نسبة التشقق.

وتعتمد طرق تقليل نسبة التشقق اللدن في البيتون الطري على تقليل نسبة التبخر من سطح البيتون أو زيادة مقاومة البيتون خلال الساعات الأولى بعد الصب وهذا يتم تحقيقه من خلال صقل سطح البيتون أو إستخدام الألياف.

٥-١ ــ صقل سطح البيتون :

تتم عملية الصقل للأسطح البيتونية مباشرة بعد إنتهاء الصب والرج وذلك لجعل سطحه أملساً ولإغلاق نسبة كبيرة من الفجوات المتواجدة على سطحه.

إن الأسطح البيتونية المصقولة والملساء سوف تقلل من نسبة التبخر من سطح البيتون ، على سبيل المثال أدت عملية الصقل إلى خفض نسبة التبخر من سطح البيتون من $1.36kg/m^2/h$ إلى $1.06kg/m^2/h$ ضمن نفس الظروف المخبرية وهذا ما أدى إلى تقليل تقلص البيتون بمقدار ٢٥% وذلك بالمقارنة مع العينات البيتونية الغير مصقولة. أما بالنسبة لزمن بدء التقلص فقد إزداد بنسبة ٣٧% بالمقارنة مع نفس العينة.

إن هذا الإنخفاض في تقليص البيتون سوف يرافقه إنخفاض في إجهادات الشد المتولدة على السطح وبالتالي تخفيض نسبة التشقق. يظهر الشكل ٩ تشقق سطح البلاطات الغير مصقولة بينما يظهر الشكل ١٤ تأثير عملية الصقل على تشقق سطح البلاطات ضمن نفس الظروف المخبرية حيث إنخفضت كثافة التشقق في البلاطات المصقولة من 0.36 إلى 0.16 وكذلك الأمر فقد إنخفض عدد التشققات وعرضها.

الشكل (١٤) إنخفاض كثافة تشقق سطح البيتون الطري للبلاطات المصقولة

أما بالنسبة لزمن بدء تشقق سطح البلاطات فقد إزداد من 100min بالنسبة للبلاطات غير المصقولة إلى 132min للبلاطات المصقولة وذلك للسبب نفسه.

٢-٥ ــ إستخدام الألياف :

إن إستخدام الألياف ضمن البيتون من مقاومته لإجهادات الشد المتولدة ضمنه حيث تعمل هذه الألياف مع البيتون في مقاومة الإجهادات الناجمة عن التقلص. وقد تمت دراسة تأثير نسبة الألياف على تقلص البيتون الطري وعلى تشقق سطح البلاطات البيتونية حيث تمت دراسة عينات بيتونية تحتوي على نسب ألياف مختلفة 0.2-0.4-0.6% من حجم البيتون ، وقد إستخدمت الألياف polypropylene fibre في هذه الدراسة.

إن الألياف المتواجدة ضمن البيتون ستزيد من مقاومته خلال الساعات الأولى بعد الصب وذلك في مواجهة إجهادات الشد المتولدة عن عملية التقلص. وقد أدى إستخدام ألياف بنسبة ٠,٢% من حجم

البيتون إلى تخفيض التقلص بنسبة ٤٥% أما إستخدام ألياف بنسبة ٠,٦% فقد أدى إلى تخفيض التقلص بنسبة ٩٥,٧% ، الجدول ٣.

وبنفس الوقت فإن إستخدام الألياف ضمن البيتون قد زاد من زمن بدء التقلص حيث أن إستخدام الألياف بنسبة ٠,٦% ، ٠,٢% من حجم البيتون قد أدى إلى زيادة زمن بدء التقلص بنسبة ١٣٠,٥% ، ٧٥% على التوالي.

الجدول (٣) تخفيض التقلص في البيتون الطري بإستخدام الألياف

نسبة الالياف ،%	0	0.2	0.4	0.6
التقلص 10^{-3} x، mm/m	2.61	1.42	0.23	0.11
زمن بدء التقلص ، min	72	127	145	166

أما بالنسبة لتشقق البيتون فقد أدى إستخدام الألياف بنسبة ٠,٢% من حجم البيتون إلى تخفيض كثافة التشقق بنسبة ٤٠٠% وإلى إزدياد زمن بدء التشقق بنسبة ٢٠٠% تقريباً بينماً لم تظهر أية تشققات على سطح البلاطات عند إستخدام الألياف بنسبة ٠,٤% ، ٠,٦% ، الشكل ١٥.

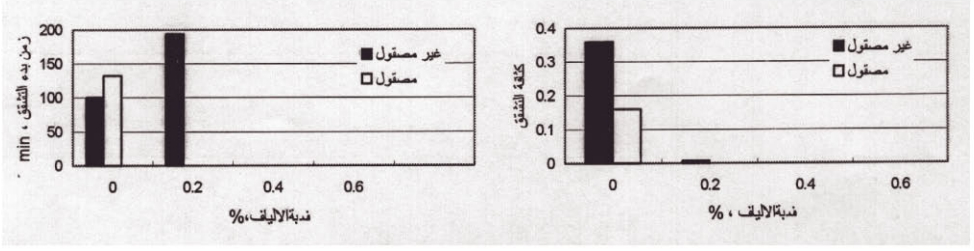

الشكل (١٥) تأثير نسبة الألياف المستخدمة على كثافة وزمن بدء التشقق

إن عملية المزج بين الطريقتين (صقل سطح البيتون ، إستخدام الألياف) ذات فعالية كبيرة حيث أن نسبة التبخر سوف تنخفض من الأسطح البيتونية المصقولة وبنفس الوقت سوف تزداد مقاومة

البيتون حيث أدى إستخدام ألياف بنسبة ٠,٢% ضمن العينات البيتونية المصقولة إلى تقليل التقلص بنسبة ٧٦% وبمضاعفة زمن بدء التقلص تقريباً ، بينما لم تلاحظ أية تشققات على السطح وذلك ضمن درجة حرارة الجو 40 C وسرعة الهواء 3 m/s.

نتائج البحث :

١. يعتبر تبخر الماء من سطح البيتون العامل الرئيسي المؤثر على التقلص اللدن في البيتون الطري وتشققه والذي يتأثر ــ التبخر ــ بخواص البيتون والعوامل المناخية المحيطة والتي يتم صب البيتون فيها. ويزداد معدل تبخر الماء من سطح البيتون بإزدياد درجة حرارة الجو، سرعة الهواء، درجة حرارة البيتون ، w/c. وتكون العلاقة بين معدل التبخر والتقلص اللدن في البيتون الطري أكثر فاعلية عندما يزداد معدل التبخر عن $1000gr/m^2/h$ حيث يزداد التقلص اللدن مع إزدياد معدل التبخر.

٢. إن الفقدان المبكر للمعان من سطح البلاطات البيتونية والمعرضة لمختلف العوامل المناخية سوف يؤدي إلى زيادة كثافة التشقق في البلاطات وذلك لأن البيتون الطري لم يمتلك بعد المقاومة الكافية لمقاومة إجهادات الشد السطحية الناجمة عن التقلص ، وكذلك الأمر فإن الفقدان المبكر للمعان من سطح البلاطات البيتونية والذي يحدث نتيجة للتعرض لظروف مناخية قاسية سوف يتنبأ بظهور تشققات على السطح.

٣. إن زيادة درجة حرارة الجو وسرعة الهواء سوف يزيد وبنسبة كبيرة من تقلص وتشقق البيتون الطري وخاصة وخاصة عندما تزيد درجة حرارة الجو عن 30 C حيث يجف سطح البيتون بشكل سريع.

٤. إن التشققات التي ظهرت على سطح البلاطات البيتونية في كافة التجارب المنفذة كانت موازية للبعد الأصغر للبلاطة (عرض البلاطة).

٥. إن صقل سطح البيتون مباشرة بعد الصب سوف يخفض من معدل التبخر والذي بدوره سيخفض من التقلص اللدن والتشقق في البيتون الطري ويؤخر ظهور التشققات على السطح حيث أن صقل سطح البيتون الطري قد خفض التقلص اللدن بنسبة ٢٥% وكثافة التقلص بنسبة ٥٥% وزاد من زمن بدء التقلص بنسبة ٣٧% وذلك بالمقارنة مع العينات الغير مصقولة. أما إستخدام الألياف ضمن البيتون فإنها تزيد من مقاومته وهذا ما يؤدي إلى خفض التقلص اللدن في البيتون الطري وتأخير ظهور التشققات أو إلغاؤها ، حيث أن إستخدام ألياف بنسبة ٠,٦% ، ٠,٤% ضمن البيتون المعرض لظروف مناخية قاسية (درجة حرارة الجو مرتفعة ــ سرعة الهواء كبيرة) قد خفض من التقلص اللدن بنسبة ٩٥,٧% ، ٩١,١% على التوالي وهذا ما أدى إلى عدم ظهور أية تشققات على سطح البيتون.

أما إضافة ألياف بنسبة ٠,٢% إلى عينات بيتونية ذات سطح مصقول فقد أدى إلى خفض التقلص اللدن بنسبة ٧٦% وبمضاعفة زمن بدء التقلص تقريباً وبالنتيجة عدم ظهور أية تشققات على سطح البلاطات البيتونية.

٦. يمكن تعميم نتائج الدراسات حول تشقق البيتون الطري (ميكرو بيتون) تحت تأثير مختلف العوامل المناخية لفهم سلوك البيتون الطري العادي وذلك عندما يكون مقاس حبات البحص صغيرة بالنسبة لسماكة البلاطة أو عند إستخدام حبات بحص ذات مقاس صغير.

Proceedings of the ACI-KC First International Conference & Fourth Exhibition. September 29-October 1, 2003, Kuwait — ***Concreting and High Performance Concrete in Hot Weather.***

الجدوى الفنية والاقتصادية من الإضافات الكيميائية السائلة والمعدنية الصلبة في البيتون

المهندس الدكتور بسام مخائيل حنا
أستاذ مواد البناء و رئيس قسم المواصلات والنقل
كلية الهندسة المدنية ــ جامعة البعث ــ سورية

ملخص البحث *

يهدف هذا البحث إلى دراسة تقنية استخدام الإضافات في البيتون الإسمنتي، التي نميز بين نوعين منها: إضافات كيميائية (Chemical Admixtures) وإضافات معدنية صلبة (Mineral Additives) وبرغم الاختلاف في آلية عمل كل منهما في البيتون فإن عملهما يهدف إلى تخفيض كمية ماء الجبل في البيتون وذلك من خلال إملاء الفراغات المتبقية بين حبات الاسمنت نتيجة عمل الإضافات الكيميائية في منع تكتل الحبيبات الناعمة سواء أكانت حبيبات اسمنت أو حبيبات صلبة معدنية عند ملامستها الماء والعمل على تشتيتها وتوزيعها داخل الفراغات المتبقية بين حبات الاسمنت مما يسهم في زيادة اكتناز البيتون وتخفيض درجة مساميته، وبالتالي إلى رفع مقاومته ، تلك الآلية التي بينها الباحث Bache [4] عام 1981 في الشكل التالي :

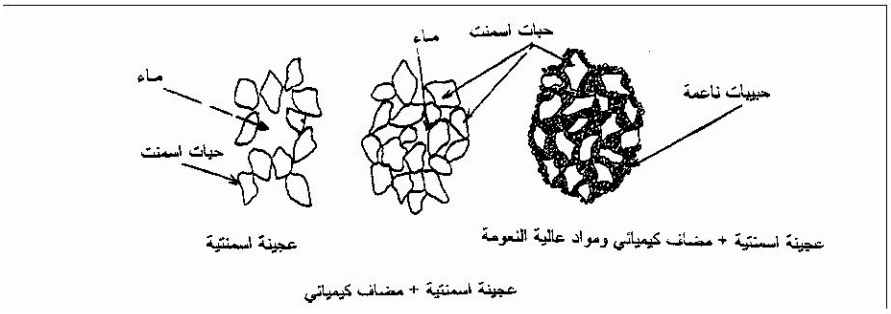

وبرغم الانتشار العملي الواسع لهذه التقنية لاتزال محط اهتمام بعض الباحثين في مجال تكنولوجيا البيتون خصوصاً بعد وجود البيتون العالي المقاومة والاهتمام في ديمومة البيتون ولأهمية هذا الموضوع تركز اهتمامنا في التعرف على معظم الإضافات المتوفرة محلياً ومن خلال وضع منهجية دقيقة واضحة لهذا البحث تم الوصول إلى نتائج تجريبية تبين بوضوح الجدوى الفنية والاقتصادية من هذه الإضافات وقد توصل البحث إلى أن استخدام الإضافات في البيتون ، بغية تحسين مواصفاته، أمر حتمي ليتمكن هذا البيتون من تلبية حاجة المنشآت الهندسية المتطورة والنوعية.

١-مقدمـــــة:

نميز بين نوعين من الإضافات: إضافات كيميائية تعرف بالإنكليزية (Chemical Admixtures) وبالفرنسية(Adiuvants Chimiques) وإضافات معدنية تعرف بالإنكليزية (Mineral Additives) وبالفرنسية (Additions Minirales).

الإضافات الكيميائية :

هي مواد تكون إما بشكل بودرة سريعة الذوبان في الماء أو بشكل سائل، تضاف إلى البيتون بنسب صغيرة من وزن الاسمنت. عرفت الإضافات الكيميائية في البيتون منذ عام 1936 ولأول مرة عندما استخدم المهندس (H:.L.Kennedy) بعض الأملاح الحامضية الكبريتية كمشتت في البيتون [4]، وبقي استخدام هذه الإضافات محدوداً في مجال الصناعة إلى أن قامت هيئات المواصفات والمقاييس في العالم باعتمادها خلال الدراسات التجريبية البحتة التي قام بها العاملون في هذا المجال، فوضع لها توصيف وتصنيف وطرق اختبار واضحة وأيضاً طرق للاستخدام في البيتون، ففي المواصفات الأمريكية ASTM توصف هذه الإضافات وفق المواصفة ASTM C49. وتصنف إلى سبعة أصناف أو نماذج (A,B,C,D,E,F,G) لكل صنف عمله الخاص [1].

- الصنف A : مخفض لكمية ماء الجبل (Water Reducing) .
- الصنف B: مؤخر تجمد (Retarding) .
- الصنف C : مسرع تجمد (Accelerating) .
- الصنف D : مخفض كمية ماء الجبل ومؤخر تجمد (Water Reducing + Retarding).
- الصنف E : مخفض كمية ماء الجبل ومسرع تجمد (Water Reducing + Accelerating).
- الصنف F : مضاف عالي الجودة ومخفض لكمية ماء الجبل (Water Reducing, High range admixtures) .
- الصنف G : مضاف عالي الجودة ، مخفض لكمية ماء الجبل ومؤخر تجمد . (Water Reducing, High range and Retarding Admixtures)

يقوم مبدأ عمل الإضافات الكيميائية في تشكيل فيلم رقيق من جزيئات المضاف الكيميائي حول حبيبات الاسمنت وشحنها بشحنات مختلفة تمنع تكتلها وتعمل على تشتيتها وتوزيعها في الفراغات المتبقية بين حبات الاسمنت الكبيرة وبالتالي بدلاً من أن تمتلىء هذه الفراغات في الماء فتمتلىء بحبيبات الاسمنت الصغيرة فيؤدي ذلك إلى تخفيض كمية ماء الجبل. ويتوقف عمل الإضافات الكيميائية في البيتون على [13]: ــ نوع وتركيب المضاف الكيميائي ــ كمية المضاف ــ وجود مضاف كيميائي آخر ــ نوع وطبيعة وتركيب الاسمنت المستعمل (فاعلية المضاف الكيميائي أكبر مع الاسمنت الذي يحوي نسبة C3A أقل) ــ كمية ماء الجبل البدائية أو النسبة (W/C) البدائية ــ تركيب البيتون (نوع وطبيعة المواد الحصوية المستعملة، التدرج الحبي، نسبة النواعم...) ــ قابلية التشغيل البدائية (الهبوط البدائي بمخروط أبرامز مثلاً) ــ درجة حرارة الوسط المحيط.

الإضافات المعدنية الصلبة :

عبارة عن مواد ناعمة كالبودرة (Filler)، يمكن أن تكون طبيعية كالبوزولانا أو صناعية ناتجة عن طحن بعض الصخور النقية (الكلسية او السيليسية) أو مخلفات صناعية كالرماد الطائر (Fly ash) أو خبث الأفران العالية (Slag) أو هباب السيليس [11]. يقوم مبدأ عمل هذه الإضافات على إملاء الفراغات المتبقية بين حبات الاسمنت الكبيرة إذ بسبب اختلافها عن الاسمنت بنشاطها الكيميائي ونسيجها السطحي تعمل على إملاء الفراغات المتبقية بين حبات الاسمنت وتسهم بشكل جيد في زيادة درجة اكتناز العجينة الإسمنتية وتخفيض مساميتها [2] وتكون فاعليتها عالية عند استعمال مضاف كيميائي ملائم [2] ، [5] ، [6] [9] تضاف هذه المواد في البيتون للأغراض التالية:

١- تخفيض كمية الاسمنت المستهلكة في البيتون بغية تخفيض كلفته.

٢- تخفيض كمية الحرارة المنتشرة عن تميه مركبات الاسمنت.
٣- تحسين قابلية تشغيل البيتون ولزوجته.
٤- توقع مقاومة عالية أو مماثلة لمقاومة البيتون المنفذ بدون إضافات على عمر متأخر.
٥- تحسين مقاومة البيتون ونفوذيته وديمومته عند استعمالها مع إضافات كيميائية.
وتضاف هذه الإضافات إما باستبدال جزئي لكمية من الاسمنت أو باستبدال جزئي للرمل حسب نوع هذه المواد وطبيعتها ونعومتها [11] .
غدت تقنية استعمال الإضافات في البيتون مع نهاية القرن الماضي إحدى التقنيات الهامة التي تهدف إلى تحسين مواصفات البيتون الإسمنتي لسهولتها ولقلة التكاليف المترتبة عليها بالإضافة إلى هدفها السامي في التخلص من المخلفات الصناعية التي أخذت تشكل خطراً كبيراً على البيئة في مواقع وجودها . ومع التقدم الكبير الذي عرفته هذه التقنية في البلدان المتطورة في مجال صناعة البيتون وخصوصاً بعد وجود البيتون العالي المقاومة لاتزال هذه التقنية محط اهتمام الكثير من الباحثين في مجال تكنولوجيا البيتون ، في حين أن معرفتنا بها في القطر لاتزال سطحية جداً وغير صحيحة ومن أجل ذلك تركز اهتمامنا في هذا البحث بإلقاء الضوء على هذه التقنية الهامة من خلال دراسات تجريبية تم تنفيذها باستعمال بعض الإضافات الكيميائية المستوردة والمتوفرة محلياً إلى جانب بعض الإضافات المعدنية المحلية أو المستوردة لتنفيذ بعض الأعمال النوعية في القطر (هباب السيليس) وبما أن الاقتصاد من المهام الأولى التي يسعى إليها المهندس انصب اهتمامنا في تبيان الجدوى الاقتصادية من استعمال هذه الإضافات في البيتون خصوصاً الكيميائي منها آملين أن نخصص للجدوى الاقتصادية من الإضافات المعدنية بحثاً آخر أكثر شمولية وتعمقاً فيها.

٢- المواد المستخدمة في الدراسة :

٢-١- مواد حصوية : تتألف المواد الحصوية المستعملة في الدراسة من ثلاثة أصناف من النوع المكسر ذات منشأ دولوميتي كلسي، مستخرجة من مقالع حسياء في منطقة حمص هي:
- بحص خشن يعرف محلياً باسم (البحص الفولي).
- بحص أكثر نعومة يعرف محلياً باسم (البحص العدسي).
- رمل مكسر يعرف محلياً باسم (الزرادة أو السرادة).
- يضاف إلى هذه الأصناف الثلاثة رمل طبيعي، سيليسي المنشأ، يجمع من مجاري السيول في منطقة القريتين يعرف محلياً باسم الرمل القرواني.

يبين الجدول (1) بعض الخواص الهندسية للمواد الحصوية المستعملة في الدراسة:

الصنف	التدرج الحبي (mm)	الوزن الحجمي (g/cm3)	الوزن النوعي (%)	درجة التشرب (%)	قرينة الاهتراء (%)	المار من No 200
بحص خشن	10-25	1,445	2,705	0,5	21,5	0.3
بحص ناعم	5-12,5	1,450	2,705	0.8	21,5	0.5
رمل مكسر	0-10	1,475	2,685	1.1	-	5,5
رمل طبيعي	0-1	1,505	2,65	1.3	-	1,5

الجدول (1) : بعض الخواص الهندسية للمواد الحصوية المستعملة

يبين الجدول (1) تطابق مواصفات المواد الحصوية المستعملة في الدراسة مع المواصفات (ASTM C33) للمواد الحصوية المستعملة في البيتون الإسمنتي.

٢-٢- اسمنت : الاسمنت المستعمل في الدراسة هو اسمنت بورتلاندي عادي يصنع وفق المواصفة السورية (S.N.S 1887-1997)، صنع بعض معامل القطر (الرستن، حماه، طرطوس) لكون الدراسة نفذت خلال مدة زمنية طويلة مابين عام 1995 وعام 2002 .

٢-٣- الإضافات السائلة : تم استعمال ثلاثة أنواع من الملدنات عالية الجودة Super plasticizer وفق المواصفـــات الأمريكية ASTM C494 – Type F يبين الجدول /1/ بعض المواصفات العامة لهذه الملدنات:

اسم المضاف	الشركة الصانعة	الوصف العام	الكثلة الحجمية g/cm3	المادة الصلبة %	نسبة الإضافة من وزن الاسمنت %
Hydra Flow 40	هدرة الهندسية	سائل بني اللون	1.2	38	0.6 – 1.2
Rheobuild	MBT	سائل بني اللون	1.2	40	0.6 – 1.5
Sikament S 20	SIKA	سائل بني اللون	1.18	40	0.6 – 1.5

الجدول(1): بعض مواصفات الإضافات السائلة المستعملة

٢-٤- الإضافات الصلبة : تم استعمال الإضافات الصلبة التالية:

- بودرة حجر كلسي شبه نقي مصدرها خان السبل التابعة لمحافظة ادلب، نعومتها تعادل نعومة الاسمنت تقريباً.
- بودرة خبث بركاني تعرف في معامل الاسمنت بالبوزولانا وتضاف أحياناً إلى الاسمنت في بعض المعامل تم طحنها حتى أصبحت بنعومة تعادل نعومة الاسمنت.
- هباب السيليس يعرف بالفرنسية (Fumee de silice) وفي الإنكليزية (Silicafume) تم الحصول عليها من شركة التشييد السريع بحمص وهي بودرة ناعمة جداً وأنعم من الاسمنت بعدة مرات [11]، مستوردة من بلجيكا لبعض الأعمال البيتونية النوعية في الشركة. يبين الجدول (2) بعض الخواص الهندسية لهذه الإضافات:

نوع البودرة	التدرج الحبي mm	الوزن الحجمي g/cm3	الوزن النوعي	المتبقي على المنخل 0.090 mm	السطح النوعي cm2/g	I.P
بودرة حجر كلسي	0 – 150	1.10	2.9	3.5	3350	3
بوزولانا طبيعية	0 – 150	1.205	2.97	6.5	3100	-
هباب السيليس	0 – 10	0.6	2.8	0.0	-	-

الجدول (2): بعض الخواص الهندسية للإضافات الصلبة المستعملة.

٢- ٥- الماء المستعمل: هو ماء الشرب في مدينة حمص.

٣- المنهجية التجريبية المتبعة في الدراسة:

تم في هذه الدراسة إتباع المنهجية التالية:

- تحضير كمية كبيرة من الحصويات تكفي لكافة الخلطات المقترحة ضمن المخطط العام الموضوع للبحث لتلافي تأثير الحصويات في سلوكية البيتون.
- استعمال جبالة واحدة باستطاعة معينة (100L).
- تنفيذ بيتون سائل بهبوط (25cm) يتلاءم مع البيتون المنفذ في معظم الورش المنفذة للبيتون في القطاع الخاص.
- تم تشكيل خلطة مرجعية دون أية إضافات بعيار اسمنت (350 kg/m3) يتلاءم مع العيار المعتمد في معظم الورش في القطر وقد تم إضافة الماء حتى الوصول إلى هبوط (25cm)، فقد بلغت نسبة الماء للاسمنت (W/C = 0,75).
- تم اعتماد عينات مكعبية نظامية (15x15x15cm) لسهولة التعامل معها.
- تم اعتماد عدد عينات الاختبار (15) عينة لاختبارها على الأعمار(1 , 2 , 7 , 28) وتعيين مقاومتها على الضغط وتعيين نفوذيتها ودرجة تشربها على (28) يوما.
- تم حفظ العينات في الماء بعد(24 h) أي بعد فك القوالب مباشرة وحتى عمر الاختبار المحدد إذ ترفع العينات من الماء وتنشف سطوحها بقطعة قماش جافة وتختبر على الضغط عملاً بمواصفات (ASTM)

ـ تم اعتماد توصيات الكود العربي السوري للخرسانة في تقييم نتائج الاختبار.
ـ نفذت هذه الدراسة خلال فترة مابين 2002 – 1995 وتم خلالها استعمال اسمنت مأخوذ من عدة مصادر بالإضافة إلى الملدنات الثلاثة المستعملة.
ـ ومن أجل دراسة العوامل المؤثرة في تركيب الخلطة البيتونية تم تشكيل عدة مجموعات من الخلطات البيتونية بحيث تم دراسة معظم العوامل المؤثرة في سلوكية البيتون.

٤- عرض وتحليل النتائج:

٤-١- تأثير المضاف الكيميائي في النسبة (W/C) والمقاومة على الضغط من أجل هبوط بمخروط أبرامز ثابت: يبين الشكل (1) تغير كل من W/C والمقاومة المكعبية على الضغط تبعاً لنسبة المضاف لمجموعة العينات المشكلة بعيار اسمنت ثابت 350 kg/m3 وهبوط ثابت.

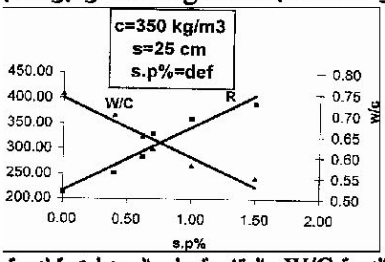

الشكل (1) : تغير النسبة W/C والمقاومة على الضغط تبعاً لنسبة المضاف الكيميائي.

من الشكل (1): نستخلص الآتي:

– تنخفض النسبة W/C تدريجياً بزيادة نسبة المضاف الكيميائي وتبلغ نسبة نقصان هذه النسبة عند إضافة نسبة (1,5 %) من المضاف الكيميائي حوالي (26,5 %). تختلف هذه النسبة عن النسبة المبينة في نشرات الشركات الصانعة لهذه الإضافات ربما يعود ذلك إلى نوع وطبيعة الخلطة البيتونية المعتمدة والمواد الأولية الداخلة في تركيبها.

– تزداد المقاومة على الضغط تدريجياً مع تزايد نسبة المضاف الكيميائي وتصل نسبة الزيادة في المقاومة إلى (83%) عند نسبة الإضافة (1,5 %) من المضاف الكيميائي.

٤-٢- تأثير كمية ماء الجبل أو النسبة W/C في قابلية تشغيل البيتون ومقاومته على الضغط مع وبدون المضاف الكيميائي: يبين الشكل (2) تغير كل من قابلية تشغيل البيتون مقاسة بمخروط أبرامز والمقاومة على الضغط تبعاً للنسبة W/C لمجموعتين من العينات: المجموعة الأولى مشكلة بعيار اسمنت ثابت (350 kg/m3) دون إضافات كيميائية وبالتالي فهي منفذة بهبوط مختلف. المجموعة الثانية مشكلة بنفس العيار من الاسمنت وبنسب مختلفة من الإضافات الكيميائية عملت على تنفيذ هذه المجموعة بهبوط ثابت.

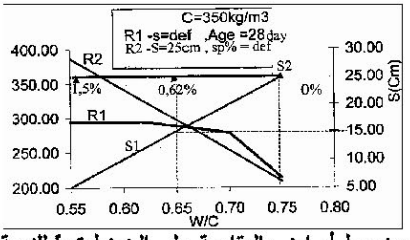

الشكل (2) : تغير كل من الهبوط بمخروط أبرامز والمقاومة على الضغط تبعاً للنسبة W/C مع وبدون مضاف كيميائي

من الشكل (2) نستخلص :

– تغير المقاومة على الضغط تبعاً لـ W/C في حال استعمال مضاف كيميائي مختلف عن مثيله في حال عدم وجود المضاف الكيميائي، إذ إن تغير المقاومة مع النسبة W/C خطّي في حال وجود مضاف كيميائي وهذا التغير مختلف في حال عدم وجود المضاف الكيميائي.

- يسهم المضاف الكيميائي في تحسين كل من قابلية تشغيل البيتون ومقاومته على الضغط عندما تكون W/C < 0,65 الموافقة لهبوط بمخروط أبرامز أقل من 15cm في حين يقتصر عمل المضاف الكيميائي على تحسين قابلية التشغيل فقط عندما تكون W/C ≥ 0,65 .

٤-٣- تأثير الزمن ودرجة حرارة الوسط المحيط في قابلية تشغيل البيتون : يبين الشكل (3) تغير قابلية تشغيل البيتون مقاسة بمخروط أبرامز تبعاً للزمن لبيتون منفذ مع W/C = 0.75 وبثلاث درجات حرارة مختلفة 10 - 20 – 30 C° وقد تم إضافة نسبة 0.4 % من الملدن عند الوصول إلى بيتون جامد (Slump = 3 – 5 cm).

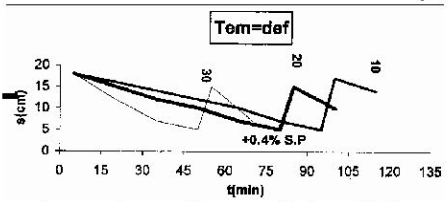

الشكل (3) : تغير قابلية تشغيل البيتون مع الزمن وبثلاث درجات حرارة مختلفة

من الشكل (3) نستخلص:

تتناقص قابلية تشغيل البيتون مع الزمن ويعود سبب هذا التناقص لامتصاص الحصويات لماء الجبل والبدء في تميه مركبات الاسمنت كالجبس وC3A

١- يزداد مقدار التناقص في قابلية التشغيل كلما ارتفعت درجة الحرارة.

٢- إن إضافة الملدن بنسبة 0.4 % من وزن الاسمنت أي ما يعادل($1\ell/m^3$) إلى البيتون بعد انخفاض قابلية تشغيله تسهم في إعادة قابلية تشغيله إلى حالة تسمح بصب البيتون بشكل جيد وهذا يدل على كفاءة الملدن في زيادة زمن نقل البيتون إلى مسافة أكبر شريطة توفر وسائط نقل البيتون المناسبة.

وعلى الرغم من تناقص الهبوط مع الزمن فإن مقاومة البيتون لا تتناقص بل قد تتزايد قليلاً خصوصاً بعد إضافة تلك النسبة من الملدن وهذا ما يبينه الشـكل (4) الذي يظهر تغير كل من الهبوط والمقاومـــــة تبعاً للزمن لبيتون منفذ معW\C = 0.75 بدون ملدن.

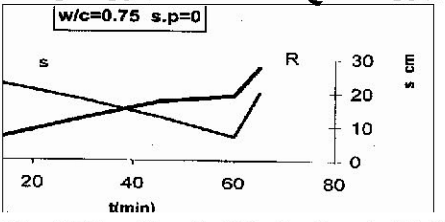

الشكل (4): تغير الهبوط والمقاومة مع الزمن W/C = 0.75

٤-٤- تأثير عيار الاسمنت في النسبة W/C والمقاومة على الضغط مع وبدون مضاف كيميائي من أجل هبوط بمخروط أبرامز ثابت : يبين الشكل (5) تغير كل من W/C والمقاومة على الضغط تبعاً لعيار الاسمنت لمجموعة بيتونات منفذة بعيارات اسمنت مختلفة (250 – 500 kg/m3) وبهبوط ثابت S = 25 cm دون إضافات.

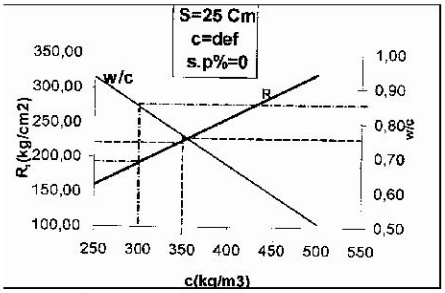

الشكل (5): تغير كل من W/C والمقاومة على الضغط تبعاً لعيار الاسمنت

من الشكل (5) نستخلص الآتي :

- تتناقص W/C تدريجياً وبشكل شبه خطي مع تزايد عيار الاسمنت .
- تتزايد المقاومة على الضغط تدريجياً وبشكل شبه خطي أيضاً مع تزايد عيار الاسمنت.
- إن تناقص w/c وتزايد المقاومة على الضغط مع تزايد عيار الاسمنت مماثل لحالة استعمال ملدنات عالية الجودة وبالتالي بمقارنة الشكل (1) الذي يبين تأثير المضاف الكيميائي في كل من W/C والمقاومة على الضغط مع الشكل (5) الذي يبين تأثير عيار الاسمنت في كل من W/C والمقاومة على الضغط من أجل هبوط ثابت نستخلص الآتي:
- تبدو فاعلية المضاف الكيميائي في تخفيض W/C وزيادة المقاومة على الضغط أكبر في حال استعمال المضاف الكيميائي في البيتون مقارنة بزيادة عيار الاسمنت.
- من أجل إضافة 1,5% من المضاف الكيميائي (الشكل 1) تم تخفيض النسبة W/C من 0,75 إلى 0,55 أي بنسبة % 26,5 وزيادة المقاومة 213,5 kg/cm2 إلى 390kg/cm2 أي بنسبة 83,5% .
- من أجل تخفيض نفس النسبة من W/C الشكل (5) بزيادة عيار الاسمنت يلزم الانتقال من عيار اسمنت 350 kg/m3 إلى عيار اسمنت 500 kg/m3 أي بكمية اسمنت إضافية 150kg/m3 أو بنسبة إضافية من الاسمنت مقدارها (43%) في حين أن المقاومة لم ترتفع أكثر من (50%). من هذه المقارنة نصل إلى استنتاج واضح في تبيان فاعلية المضاف الكيميائي في تخفيض W/C وزيادة المقاومة وهذا طبعاً يحقق وفراً في استهلاك الاسمنت في البيتون.

عرض آخر لهذه النتائج نبينها على الشكلين (6) و(7) إذ يظهر الشكل (6) تأثير كل من عيار الإسمنت ونسبة المضاف الكيميائي (Hydra Flow 40) في النسبة W/C والشكل (7) يبين تأثير كل من عيار الاسمنت ونسبة المضاف الكيميائي في المقاومة على الضغط.

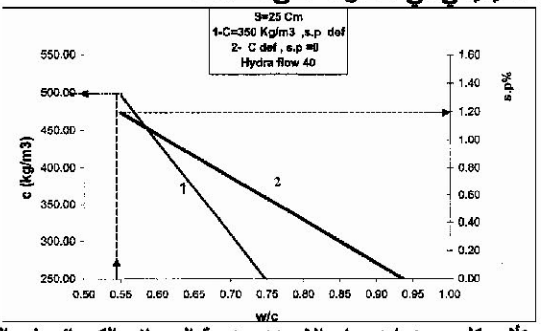

الشكل (6) : تأثير كل من زيادة عيار الاسمنت ونسبة المضاف الكيميائي في النسبة W/C

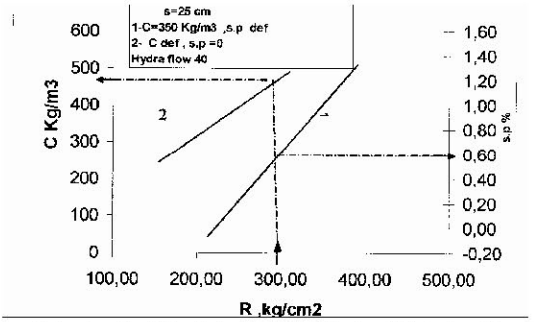

الشكل (7) :تغير كل من زيادة عيار الاسمنت والمضاف الكيميائي في المقاومة على الضغط

من الشكلين (6) و (7) نستخلص الآتي:

- تسهم كل من زيادة عيار الاسمنت وإضافة المضاف الكيميائي إلى تخفيض النسبة W/C وزيادة المقاومة على الضغط.
- إن زيادة عيار الاسمنت من350 kg/m3 إلى 500 kg/m3 تسهم في تخفيض النسبة W/C من 0,75 إلى 0,55 أي بنسبة % 26,5 وإن إضافة % 1,5 من المضاف الكيميائي للبيتون المنفذ بعيار اسمنت 350 kg/m3 تسهم في تخفيض نفس النسبة من W/C.
- إن زيادة عيار الاسمنت من 350 kg/m3 إلى 500 kg/m3 تسهم في زيادة المقاومة على الضغط من 213,3 kg/cm2 إلى 325 kg/cm2 أي بنسبة زيادة مقدارها 52,5% في حين إن إضافة % 1,5 من المضاف الكيميائي إلى البيتون المنفذ بعيار اسمنت 350 kg/m3 تسهم في زيادة المقاومة من 213,3 kg/cm2 إلى 300 kg/cm2 أي بنسبة مقدارها 83%

دراسة مشابهة تماماً نفذت في العام الدراسي 2000 - 1999 لكن باستعمال اسمنت طرطوس ومضاف كيميائي آخر يعرف تجارياً باسم (Rheobuild 1100) وتم الحصول على نتائج مماثلة.

في العام الدراسي 1996 - 1995 تم تنفيذ دراسة أخرى باستعمال اسمنت طرطوس ومضاف كيميائي آخر يعرف تجارياً باسم (Sikament 520) وقد نفذت هذه الدراسة على مجموعتين من الخلطات: الأولى بعيارات اسمنت مختلفة دون استعمال المضاف الكيميائي والثانية بنفس العيارات من الاسمنت لكن بإضافة (1,5%) من المضاف الكيميائي المذكور لكل منها وقد تم صب العينات البيتونية عند هبوط (10 cm) أي بعد مضي حوالي ثلث ساعة من إضافة الماء للخلطة البيتونية .يبين الشكل (8) تغير المقاومة مع عيار الاسمنت للمجموعتين المذكورتين.

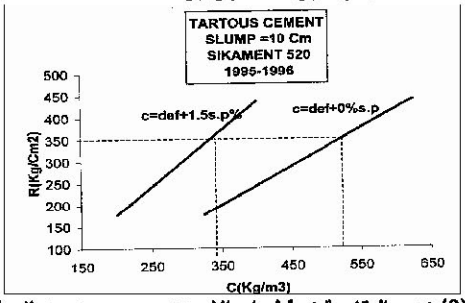

الشكل (8) تغير المقاومة تبعاً لعيار الاسمنت مع وبدون مضاف كيميائي

من الشكل (8) نستخلص الآتي:

- تزداد المقاومة مع عيار الاسمنت في المجموعتين من الخلطات مع وبدون مضاف كيميائي.
- إن استخدام المضاف الكيميائي في البيتون يحقق وفراً في استهلاك الاسمنت يزيد عن % 30 من أجل الوصول إلى مقاومة ثابتة.

٤-٥- تأثير المضاف الكيميائي في نفاذية البيتون :

يبين الشكل (9) تغير عامل النفاذية للبيتون تبعاً لـ W/C ولمجموعتين من العينات منفذتين بعيار اسمنت ثابت مع وبدون مضاف كيميائي مقاس وفق المواصفات الألمانية (DIN – 1048) وبالاعتماد على العلاقة التجريبية التالية: $K = 0.03\frac{L^2}{2TH}$ حيث:

L : طول خط تسرب الماء داخل العينة. T : زمن التجربة (Sec). H : ارتفاع العينة المختبرة(cm).

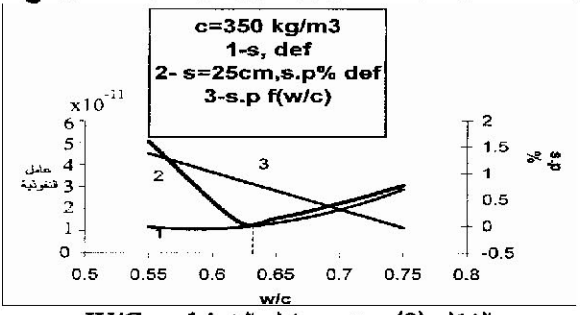

الشكل (9) : تغير عامل النفوذية مع W/C

من الشكل (9) نستخلص الآتي :

-يتزايد عامل النفوذية بتزايد النسبة (W/C) في الخلطات المنفذة مع مضاف كيميائي وهذا أمر طبيعي

-يلاحظ سلوك مختلف لعامل النفاذية في الخلطات المنفذة بدون مضاف كيميائي إذ يتناقص عامل النفاذية مع تزايد (W/C) حتى (W/C = 0,65) وبعدها يأخذ بالتزايد وهنا تظهر جلياً كفاءة المضاف الكيميائي في تأثيره في عامل النفاذية.

٥- تأثير الإضافات الصلبة في النسبة W/C للخلطات البيتونية ومقاومتها على الضغط مع أو بدون مضاف كيميائي:

من أجل تنفيذ هذه الدراسة وبسبب عدم توفر كمية كبيرة من بودرة هباب السيليس تم اعتماد نسبة (10%) من وزن الاسمنت من الإضافات الصلبة المستخدمة في الدراسة وبعدها تم دراسة تأثير هذه النسبة من الإضافات الصلبة في النسبة W/C والمقاومة على الضغط لمجموعتين من الخلطات: الأولى مشكلة مع النسبة W/C = 0,75 دون مضاف كيميائي والثانية مشكلة مع النسبة W/C = 0,55 مع 1,5 % من المضاف الكيميائي (Hydra Flow 40) ، وقد تم تشكيل هاتين المجموعتين من الخلطات بهبوط ثابت بمخروط أبرامز (25cm) وبعيار اسمنت ثابت (350kg/m3) ومن كل خلطة من الخلطات المنفذة في كل مجموعة تم أخذ عينات مكعبية نظامية وكسرها على الأعمار (1 , 2 , 7 , 28 days). تبين الاشكال (10)، (11) تغير المقاومة تبعاً للزمن للخلطات المنفذة مع الإضافات الصلبة (هباب السيليس) بودرة الحجر الكلسي.

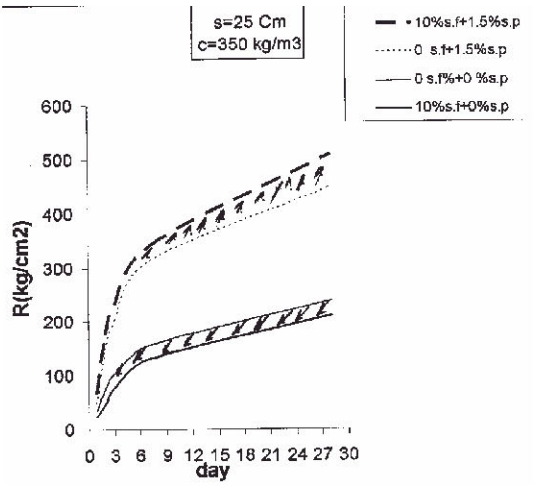

الشكل (10) : تغير المقاومة تبعاً للزمن للخلطات المنفذة مع هباب السيليس

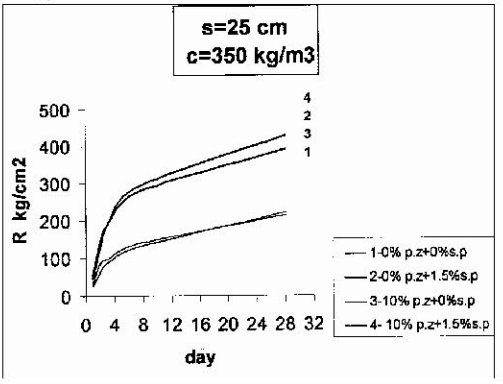

الشكل (11) : تغير المقاومة مع الزمن للخلطات المنفذة مع بودرة الحجر الكلسي

من الشكلين (10)، (11) نستخلص الآتي:

- تسهم الإضافات الصلبة في زيادة النسبة W/C وفي نقصان المقاومة لجميع الخلطات المنفذة مع الإضافات الصلبة بدون إضافات كيميائية مقارنة بالخلطة المرجعية، وهذا يعود إلى شراهة هذه الإضافات لامتصاص الماء ولتكتلها أثناء ملامستها الماء وبالتالي يكون دورها ضعيفاً في إملاء الفراغات المتبقية بين حبات الاسمنت.
- تسهم الإضافات الصلبة في تخفيض W/C وزيادة المقاومة في الخلطات المنفذة مع الإضافات الصلبة بوجود المضاف الكيميائي مقارنة مع الخلطات المنفذة دون إضافات صلبة، لكن منفذة مع مضافة كيميائي بنسبة (1.5 %) منه من وزن الاسمنت أي الإضافات الصلبة تعمل عمل الملدن بوجود المضاف الكيميائي وهذا يعود إلى دور المضاف الكيميائي في تشتيت حبيبات الإضافات الصلبة ومنع تكتلها والعمل على توزيعها داخل الفراغات المتبقية بين حبات الاسمنت مما يؤدي إلى

زيادة اكتناز هذه الخلطات وتحسين مقاومتها بالإضافة إلى وجود بعض التفاعلات الكيميائية التي تقوم بها هذه الإضافات مع مركبات الاسمنت المائية (التفاعل البوزولاني) الذي يتم بين عنصر السيليس الموجود في هباب السيليس او بودرة البوزولانا مع Ca (OH)2 الذي يدعى بالبورتلانديت وتشكيل جيل يدعى سليكات الكالسيوم الذي يحسن من مقاومة البيتون [11] [13] [12]. وأيضاً تفاعل عنصر الكلس مع مركبات الاسمنت الألومينية وتشكيل مركب ألومينى جديد يكون بشكل جيل يحسن من مقاومة البيتون على الضغط [13] يدعى هذا المركب الجديد بـ ($C3A\ CaCO_3\ 10H_2O$).

٦- الجدوى الفنية والاقتصادية من الإضافات ونتائج عامة:

إن تحديد الجدوى الفنية أو الاقتصادية من الإضافات في البيتون بدقة يتطلب دراسة أكثر شمولية وتفصيلاً لكن بدراسة معمقة لمجموعة النتائج التي حصلنا عليها يمكن أن نصل إلى الاستنتاجات التالية: ١- تتوقف كفاءة وفاعلية المضاف الكيميائي في البيتون على كمية ماء الجبل أو (W/C) البدائية وقابلية تشغيل البيتون البدائية فالشكل (2) يبين بوضوح كفاءة المضاف الكيميائي في تحسين قابلية تشغيل البيتون مقاسة بمخروط أبرامز ومقاومته على الضغط عندما $W/C \leq 0,65$ و $S = 15\ cm$ في حين يقتصر عمله على تحسين قابلية تشغيل البيتون عندما $W/C > 0,65$.

٢- يبدو بوضوح أن فاعلية المضاف الكيميائي في تخفيض (W/C) وزيادة مقاومة البيتون أكبر من تأثير زيادة عيار الاسمنت في تخفيض (W/C) وزيادة المقاومة.

٣- تتوقف فاعلية واستعمال الإضافات الصلبة في البيتون على نوع وطبيعة الإضافات الصلبة ووجود مضاف كيميائي ملائم يعمل على تشتيت حبيبات هذه الإضافات وتوزيعها بشكل منتظم داخل الفراغات المتبقية بين حبات الاسمنت الكبيرة.

٤- بمقارنة كلفة الرابط المستعمل في البيتون مع إضافات كيميائية (ASTM C494,Type F,G) مع كلفة الرابط دون إضافات من أجل مقاومة ثابتة أو W/C ثابتة من خلال النتائج المبينة على الأشكال (8),(7),(6) تبين أن كلفة الرابط مع إضافات كيميائية أقل من كلفته بدون إضافات بنسبة تصل حتى 30% من أجل الوصول إلى مقاومة ثابتة و 15 % من أجل الوصول إلى W/C ثابتة وهذا ما يبينه الشكلان (12) و (13)، حيث يبين الشكل (12) تغير نسبة كلفة الرابط مع مضاف كيميائي إلى كلفته دون مضاف تبعاً لمقاومة البيتون والشكل (13) يبين تغير هذه النسبة مع W/C:

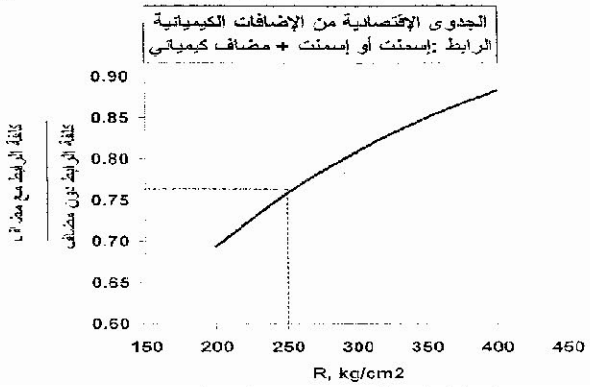

الشكل (12) : تغير نسبة كلفة الرابط مع مضاف إلى كلفته بدون مضاف مع مقاومة البيتون

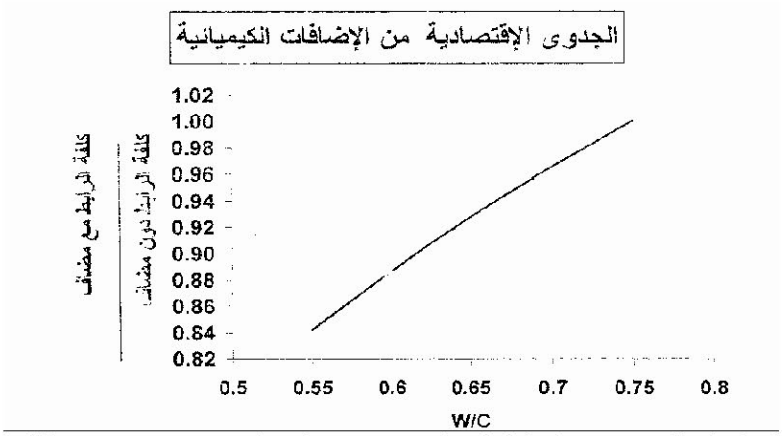

الشكل (13) : تغير نسبة كلفة الرابط مع مضاف إلى كلفته بدون مضاف مع W/C

ملاحظة: يقصد بالرابط هنا الاسمنت أو الاسمنت مع إضافات كيميائية في حال استعمال إضافات كيميائية وقد تم حساب الكلفة على أساس أن سعر الكيلو غرام الواحد من الاسمنت (3,5) ليرة سورية حسب تسعير مؤسسة العمران وسعر الكيلو غرام من المضاف الكيميائي (60) ليرة سورية حسب السوق المحلية.

References

1- ASTM, American Standards for testing Materials 1994 .
2- P.C.ATTCIN. Optimization of the composition of High Performance Concrete, ACI, 1994.
3- P.C, ATTCIN, ESSAIS et Contrale des Betons, Universite de sherbrocke CANADA, 1984
4- H.H. BACHE, Densificd Cement, Ultra fine Particules based material, 2nd, int, cont, Superplasticizers in concrete, Ottawa CANADA , 1981
5- J.J.BEAUDOIN and al , Ideal structural model for very low porosity Cementitious Systems, C.C.R, 1993.
6- J.P.BOMBLED et al , Mecanismes d'action des Fluidifiants CERILH, 1987 , PARIS.
7- M.BUIL. Qulelques Techniques recentes d'obtention de pate de ciment, Bulletin de liaison des LPC , 1984, PARIS .
8- M.BUIL and al , Utilisation des Fillers ultra fins dans les Betons, Bulletin de AIGI , PARIS 1984
9- F.DELARRARD, Ultra fine particles for the making of very high strength concrete , C.C.R, 1989.
10- G.DREUX, Guide pratique du Beton, CEBTP, 1984 FRANCE .
11- V.M.MALHOTRA , Materiaux Complementaires en Cimentation Pour le Beton , CANMET , CANADA 1987.

12- V.M.MALHOTRA Use of mineral Admixtures for specialized concretes, concrete , International . 1984 .
13- M.VENLIAT , Adjuvants et traitements en Beton, Iere edition 1984, PARIS.

• تم إنجاز هذا البحث في مخابر كلية الهندسة المدنية ــ بجامعة البعث ــ سورية

Proceedings of the ACI-KC First International Conference & Fourth Exhibition. September 29-October 1, 2003, Kuwait — ***Concreting and High Performance Concrete in Hot Weather.***

التأثير الداخلي والخارجي لكلوريدات الصوديوم على الخرسانة

د. مختار معمر أبو راوي
أستاذ مساعد في الهندسة المدنية
قسم الهندسة المدنية/جامعة المرقب

الملخص

من خلال الدراسات الميدانية لعدد من المنشآت الخرسانية التي تعرضت في الآونة الأخيرة لبعض التصدعات بسبب مهاجمة الكلوريدات للغطاء الخرساني وما ترتب عليه من تآكل لحديد التسليح وضعف هذه المنشآت لمقاومة الأحمال التصميمية، تستعرض هذه الدراسة التأثير الخارجي والداخلي معاً لكلوريدات الصوديوم الدائبة سواء في المياه المستعملة في خلط الخرسانة أو في المياه المستخدمة للمعالجة بعد الصب، تركزت هذه الدراسة لمعرفة التأثير الداخلي والخارجي لكلوريدات الصوديوم على الخواص الميكانيكية للخرسانة المكونة من الإسمنت البورتلاندى سريع التصلد مضافاً إليه نسبة ٦٥% خبث الأفران العالية من الوزن الكلى للإسمنت، تم تحضير ٢٥٢ عينة لهذه الدراسة من خلطات خرسانية مختلفة، المياه المستعملة في خلط العينات يصل درجة تركيزها الملحي إلى ٦% من وزن الأسمنت، والنتائج الأولية بينت عدم جدوى استخدام الإسمنت سريع التصلد لزيادة المقاومة المبكرة للخلطات الخرسانية التي تحتوى نسبة عالية من إسمنت خبث الأفران، نتيجة لتأثير ترسبات الأملاح وتبلرها خلال حالات التجفيف، وهذا بخلاف العينات التي تمت معالجتها في المياه العادية حيث أظهرت بعض التحسن في قيم المقاومة، ربما يرجع ذلك الى استعمال المياه العادية عند المعالجة في تخفيف درجة التركيز الملحي للأملاح الدائبة والموجودة بالعينات.

مقدمة

سيشهد القرن الحالي وفي اغلب مناطق العالم نقص شديد في المياه الصالحة للشرب والمستعملة أيضا في صناعة الخرسانة ذات الجودة العالية لخلوها من الأملاح الضارة، كما ان انخفاض منسوب المياه الجوفية ساهم أيضا في زيادة ملوحتها، ولما يشكله محتوى الكلوريدات من خطورة عالية وبالغة في تآكل حديد التسليح في الخرسانة بالإضافة إلى تفاعلها مع العجينة الإسمنتية حيث تشارك أيونات الكلوريدات في تفاعلات كيميائية ينتج عنها الكلوروالومينات المتأثرت (المائي) الذي يسبب هشاشة للخرسانة، كما إن وجود الأيونات السالبة لكلوريدات الصوديوم وغيرها من ضمن مكونات الخرسانة على سبيل المثال الركام الغير نظيف أو وجودها في الوسط المحيط بالخرسانة كما هو الحال بالنسبة للأرصفة البحرية والمنشآت المتاخمة لشواطئ البحر أو الرذاذ المحمل بالأملاح أو الرطوبة العالية في المناطق الساحلية وخزانات مياه التحلية وكذلك الخزانات الخرسانية لمعالجة مياه الصرف الصحي، واثر ذلك على تفتت الخرسانة والإسراع في تآكل حديد التسليح، وحيث أن أقصى نسبة للأملاح المسموح بها في المياه سواء لخلط أو معالجة الخرسانة بعد الصب لا تزيد عن 4% من وزن الإسمنت حسب المواصفات الأمريكية وإذا ما تعدت هذه النسبة ستتعرض الخرسانة المسلحة للانهيار، وعلى الرغم من توفر بعض البدائل التي تستخدم كإضافات تعمل على تحسين جودة الخرسانة ومقاومتها

للبيئة المحيطة بها، وبالإضافة إلى ذلك حماية اوجه الخرسانات بطلائها بأنواع خاصة، واستخدام أنواع أخرى من حديد التسليح الأكثر مقاومة للتآكل، إلا أن هذه البدائل لم تستخدم بشكل واسع وخاصة في معظم الدول النامية نتيجة لارتفاع تكلفتها وعدم توفر التقنية اللازمة محلياً وصعوبة التنفيذ.
المياه المالحة سواء المستخدمة في خلط مكونات الخرسانة أو في معالجتها بعد الصب وخاصة عندما يكون تأثيرها داخليا وخارجيا في نفس الوقت سيكون التأثير كبير جداً على ديمومة المنشآت الخرسانية، وللتغلب على هذه مشكلة يجب اتخاذ بعض الإجراءات التحفظية التي من شأنها يمكن تقليل خطر مهاجمة هذه الأملاح على المنشآت الخرسانية والمحافظة عليها من الانهيار التدريجي المبكر، ولتحسين خواص الخرسانة في المستقبل لابد من استخدام مواد إضافية أخرى، على سبيل المثال إضافة إسمنت خبث الأفران والذي يساعد على مقاومة هجوم الكبريتات والكلوريدات وهذه الخاصية نتيجة للحد الأدنى للنفادية بالنسبة للخرسانة التي تحتوى على إسمنت خبث الأفران (BS6699: 1986)، ونسبة ٦٥% من إسمنت خبث الأفران كان لها التأثير الفعال على تقليل حجم الفرغات الكبيرة عند ٢٨ يوم من المعالجة مما ساهم في زيادة انخفاض النفادية (Bamforth 1994, Aburawi 2002)، إضافة إلى ذلك فأن معدلات تطور المقاومة لخرسانة إسمنت خبث الأفران تتأثر بحساسية عالية بعمر الخرسانة ومدى نعومة الخبث المستخدم (Lim 2000)، ولذلك يعد إسمنت خبث الأفران المطحون ذو فائدة كبيرة في إنتاج الخرسانة العالية المقاومة في المناطق الصحراوية الحارة لما يتميز به في تقليل حرارة التفاعل عند اماهة الإسمنت والتي تعد مشكلة كبيرة عند إنتاج الخرسانة العالية المقاومة ذات المحتوى الإسمنتي العالي وما ينتج عن ذلك من تشققات حرارية داخلية (Sanjayan 2000). ولتحقيق الجدوى الاقتصادية ومستويات عالية من الجودة في مجالات البناء والتشييد يتطلب الأمر دراسة استخدام المواد الإضافية وتأثيرها على الخواص الطبيعية والكيميائية والميكانيكية للخرسانة وذلك لغرض استحداث مواصفات فنية دقيقة تتلاءم مع البيئة المحيطة وخاصة في المناطق الحارة

أهداف الدراسة:

المعلومات المتوفرة غير كافية لإنتاج خرسانة عالية المقاومة للعوامل البيئية المحيطة وخاصة عندما تكون المكونات الأساسية للخرسانة ملوثة بكلوريدات الصوديوم ناهيك عن الهجوم الخارجي لهذه الأملاح. تهدف هذه الدراسة لمعرفة تأثير أملاح الكلوريدات على الخواص الهندسية للخرسانة التي تحتوى على نسبة ٦٥% من إسمنت خبث الأفران وخاصة عندما يكون هذا التأثير نتيجة لتلوث المواد المكونة للخرسانة بما في ذلك المياه المستعملة في الخلط أو المعالجة أو كلاهما، بالإضافة إلى ذلك دراسة هذا التأثير المزدوج على الديمومة (durability) والبنية الدقيقة (microstructure) لخرسانات إسمنت خبث الأفران.

البرنامج العملي:

المواد المستخدمة:

خلال هذه الدراسة تم استخدام الإسمنت البورتلاندى العادي وسريع التصلد، إنتاج شركة القلعة المحدودة للاسمنت، لنكشير ببريطانيا، وإسمنت خبث الأفران المستخدم في هذه الاختبارات مورد بواسطة شركة فرودنجهام للإسمنت المحدودة، سكنتورب بريطانيا. كما تم استخدام كسر الأحجار الناعمة أقصى حجم ٥مم بوزن نوعي ٢,٥٧ ونسبة امتصاص ٢,١%، والخشنة أقصى حجم ١٠مم بوزن نوعي ٢,٦١ ونسبة امتصاص ٠,٣%، والموردة من محاجر فيننجلى في شمال نتونجهامشير بريطانيا، وتم استخدام المضاف فائق اللدونة الذي يتكون من (sulphonated melamine-formaldehyde) لتحسين التشغيلية وانتاج خرسانة صالحة للصب بالمضخة الخرسانية ذاتية الدمك.

تحضير العينات ومعالجتها:

تم تحضير واختبار عدد ٢٥٢ عينة مقاس ١٠٠×١٠٠×٥٠٠مم، بواقع ثلاثة عينات لكل خاصية وذلك لاحتساب المتوسط للحصول على افضل النتائج، أربعة خلطات خرسانية تم اعتمادها لهذه الدراسة مكوناتها مبينة في الجدول رقم ١، نسبة الماء للإسمنت (W/C) كانت ثابتة في كل الخلطات وللمحافظة على درجة تشغيلية عالية للخرسانة استخدمت الملدنات الفائقة، تمت معالجة العينات بعد فكها من القوالب في حالات المعالجة المبينة بالتفصيل في الجدول رقم ٢.

جدول رقم ١: نسب ومكونات الخلطات الخرسانية.

المكونات		M1	M2	M3	M4
الأسمنت البورتلاندى العادي	كج/م٣	١٦٠	١٦٠	٤٥٠	–
الأسمنت البورتلاندى سريع التصلد	كج/م٣	–	–	–	١٦٠
أسمنت خبث الأفران العالية	كج/م٣	٢٩٠	٢٩٠	–	٢٩٠
الكمية الكلية للإسمنت	كج/م٣	٤٥٠	١٥٠	٤٥٠	٤٥٠
المياه المستعملة في الخلط	كج/م٣	١٦٢	١٦٢	١٦٢	١٦٢
نسبة الماء للكمية الكلية للإسمنت		٠,٣٦	٠,٣٦	٠,٣٦	٠,٣٦
كسر الأحجار	كج/م٣	١٠١١	١٠١١	١٠١١	١٠١١
الرمل	كج/م٣	٧٠٠	٧٠٠	٧٠٠	٧٠٠
صوديوم كلورايد % من الكمية الكلية للإسمنت		–	٠,٦	٠,٦	٠,٦
الملدنات الفائقة *SP6		١,٤٠–١,٦٠% من الكمية الكلية للإسمنت			
اختبار الهبوط		٩٠–١٤٠مم			

* SP6= ملدنات فائقة وعالية الفاعلية للتقليل من المياه المستعملة في الخلط.

جدول رقم ٢: حالات المعالجة للعينات.

حالة المعالجة	وصف حالة المعالجة
C1	٣ أيام غمر في مياه عادية وبعد ذلك ٤ أيام في الهواء وبشكل دوري
C2	٧ أيام غمر في مياه عادية وبعد ذلك ترك العينة في الهواء بشكل دائم
C3	٣ أيام غمر في مياه مالحة وبعد ذلك ٤ أيام في الهواء وبشكل دوري
C4	٧ أيام غمر في مياه مالحة وبعد ذلك ترك العينة في الهواء بشكل دائم

* المياه المالحة تركيزها الملحي ٤% صوديوم كلورايد (NaCl)

الاختبارات المعملية:

أجريت عدد من الاختبارات المعملية لتحديد الخواص الهندسية للعينات التي تم تحضيرها وذلك بفحص الضغط والانحناء والامتصاص والانكماش وحد المرونة الديناميكي والموجات فوق الصوتية، ولمعرفة الديمومة والبنية الدقيقة تم فحص الكربنة وتعيين النفاذية باستخدام مقياس النفاذية المصمم بواسطة كبريرا (Cabrera 1988)، الأشعة الحيادية (XRD) استعملت لحساب كمية الكلوريدات في العينات ولدراسة بعض الأطوار في الخلطات الخرسانية وعلى وجه الخصوص تكوين الكالسيوم كلوروالومينيت (calcium chloroaluminate)، والتحليل الحراري التفاضلي (DTA) استخدم أيضا، ومقياس الحقن الزئبقي للمسامية (Mercury Intrusion Porosimetry) لتحديد المسامية الكلية والتوزيع الحجمي للفراغات، وفي هذه الدراسة نستعرض فقط نتائج مقاومة الانضغاط والانحناء.

النتائج:

الشكل رقم (١) يوضح التأثير الداخلي لكلوريدات الصوديوم على مقاومة الانحناء والضغط، والنتائج تبين انخفاض مبكر لتطور مقاومة خرسانة إسمنت خبث الأفران في الخلطة M1 بينما نلاحظ ان هناك زيادة في تطور المقاومة في الخلطة M2 نتيجة لوجود الأملاح الإضافية التي تعمل على تنشيط تفاعلات مركبات الإسمنت خلال الأيام الأولى والتي تقود إلى تعجيل الاماهة وبالتالي زيادة المقاومة المبكرة، إلا إن هذه الزيادة تميل إلى الانخفاض بعد ٧ أيام نتيجة لتأثير ترسبات الأملاح وتبلرها خلال حالات التجفيف، وبما أن مقاومة الانحناء والضغط تعتمد على البنية الدقيقة (microstructure) فأن بعض الدراسات السابقة (Mehta 1986, Figg 1989) تبين إن أملاح الصوديوم المتبلر من الممكن أن تحدث ضغط داخلي مقداره ٦٠٠ ضغط جوى، وهذه الاجهادات يمكن أن تسبب تشققات دقيقة للعينات الخرسانية.

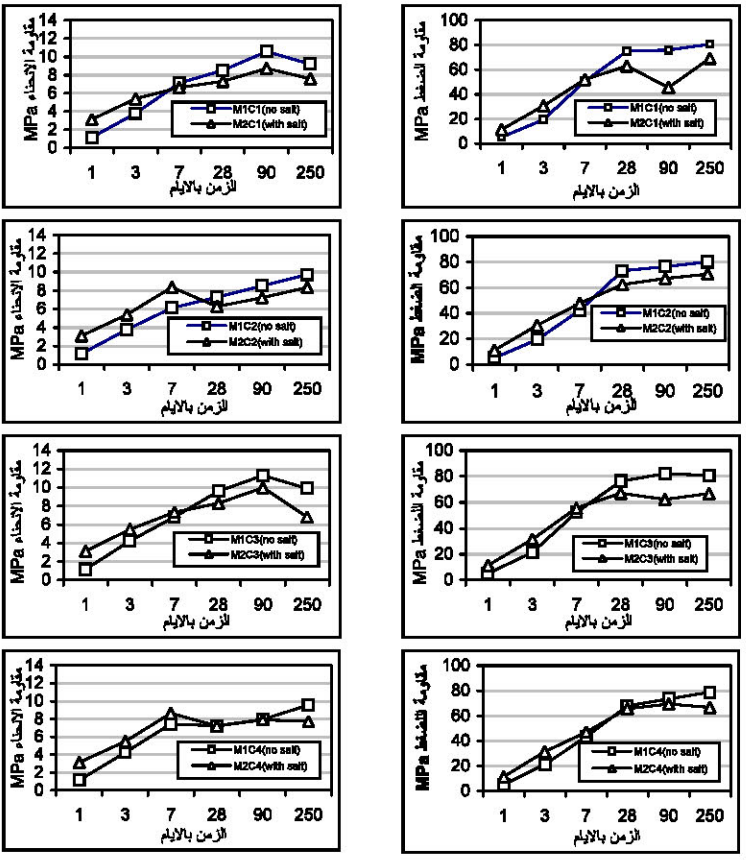

الشكل رقم ١: التأثير الداخلي والخارجي للكلوريدات على مقاومة الانحناء والضغط

الشكل رقم (٢) يوضح تأثير بعض الأنواع الأخرى من الإسمنت على خواص المقاومة، حيث لوحظ ان الكمية المضافة من إسمنت خبث الأفران سببت في انخفاض المقاومة في الخلطة M2 في الأيام المبكرة مقارنة بالخلطة M3 والتي تحتوى على نفس الكمية من الإسمنت البورتلاندى فقط، كلا

الخلطتين مع الزمن يصلا تقريبا لنفس المقاومة عندما تكون المعالجة بشكل دوري سواء كانت في المياه العادية او المالحة (C1)،(C3) . نتائج مقاومة الانحناء في الخلطة M2 كانت منخفضة بشكل ملحوظ عن الخلطة M3، وهذا الانخفاض كان متوقع خلال الأيام الأولى نتيجة لانخفاض معدل الاماهة، بينما كان غير متوقع في الخلطة M4 التي تحتوى على نفس الكمية من إسمنت خبث الأفران المضاف إلى الإسمنت سريع التصلد RHPC الذي من المفترض ان يزيد في المقاومة المبكرة لخرسانات إسمنت خبث الأفران (Hooton 1986)، أو ربما يرجع ذلك إلى وجود الأملاح في الخلطتين M3(OPC) و(RHPC) M4. زيادة كمية المساحة السطحية لجزيئات الإسمنت تعنى زيادة نسبة كلورايد/الإسمنت أو ربما تكون نفس نسبة الماء/الإسمنت، وتكون هذه النسبة غير كافية لتنشيط كل جزيئات الإسمنت. وبشكل عام نلاحظ أن هناك تقارب كبير في قيم المقاومة مع زيادة فترة المعالجة لكل حالات المعالجة المصممة لهذه الدراسة، وخاصة عند استخدام إسمنت خبث الأفران مع الإسمنت سريع التصلد في الخلطات التي تحتوى على الأملاح سواء الملوثة لمكونات الخلطة أو الدائبة في المياه المستعملة في الخلط، كما بينت النتائج تحسن في قيم المقاومة للخلطة M4 عند معالجة العينات في الماء العادي (C1 , C2)، والتي تجاوزت القيمة المستهدفة لهذه الدراسة 50MPa عند ٢٨ يوم وفي دراسات أخرى أنجزت هذه القيمة عند ٢٨ يوم (Swamy 1990)، وفي هذه الدراسة تم الحصول على هذه القيمة فقط خلال ٧ ايام الاولى من المعالجة في المياه العادية.

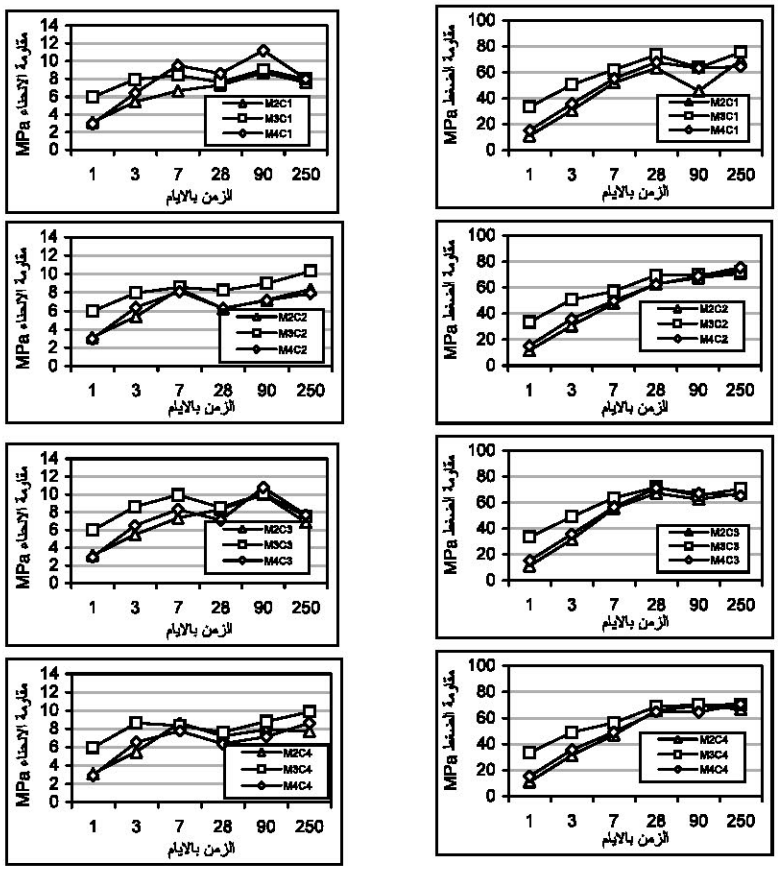

الشكل رقم ٢: تأثير المحتوى الإسمنتي على مقاومة الانحناء والضغط في جميع حالات المعالجة

العلاقة بين معامل التمزق ومقاومة الضغط:

معادلة التراجع الخطية الآتية تم الحصول عليها من تحليل النتائج لمعامل التمزق ومقاومة الضغط لكل الخلطات التي تم تحضيرها ومعالجتها في كل الحالات واختبارها والشكل رقم (٣) يوضح العلاقة بين معامل التمزق ومقاومة الضغط، وهذه النتائج بينت إن معامل الترابط r^2=0.95.

$$F_{cu} = -6.03 + 8.19\ (f_t)$$

عندما f_{cu} مقاومة الضغط

f_t معامل التمزق

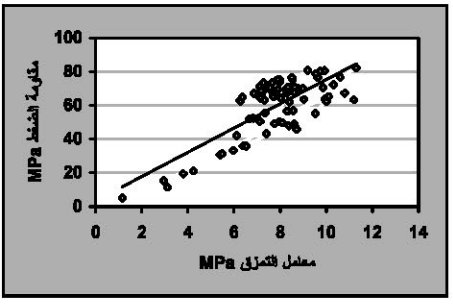

الشكل رقم ٣: العلاقة بين معامل التمزق ومقاومة الضغط للعينات في كل حالات المعالجة

الخلاصة:

بناءا على نتائج الاختبارات التي تمت على العينات يمكن استخلاص النقاط التالية

١. للمحافظة على نفس معدل التشغيلية للخرسانة نحتاج لإضافة كمية اكثر من الملدنات للخرسانة التي تحتوى على الإسمنت سريع التصلد، ويرجع ذلك لزيادة المساحة السطحية وارتفاع معدل الاماهة في الساعات الأولى لتفاعل الإسمنت مع الماء.

٢. مقاومة خرسانة إسمنت خبث الأفران تصل في اليوم الأول إلى 15MPa نتيجة لوجود الكلوريدات في الخلطة، وفيما بعد ٢٨ يوم تميل إلى الانخفاض بسبب التأثير الداخلي والخارجي للكلوريدات.

٣. حققت خرسانة إسمنت خبث الأفران مقاومة ضغط قدرها 50MPa خلال ٧ أيام في حالات المعالجة الدورية.

٤. استخدام الإسمنت سريع التصلد مع إسمنت خبث الأفران لانتاج خرسانة عالية المقاومة المبكرة لم يحقق النتائج المتوقعة بسبب تلوث مكوناتها بنسبة عالية من الكلوريدات.

٥. زيادة مستوى تأثير كلوريدات الصوديوم على الخرسانة مع زيادة المساحة السطحية للإسمنت.

٦. النتائج بينت ان هناك علاقة خطية بين معامل التمزق ومقاومة الضغط لخرسانة إسمنت خبث الأفران من الممكن استخدامها.

المراجع:

1. BS6600: (1986),Granulated ground blast furnace slag concrete for used with Portland cement, British Standards Institution, London.
2. Bamforth, P. (1994), "Reinforcement in marine structures", Concrete, January/February, 33-36.
3. Aburawi, M.M. (2002), " Durable concrete in salt weathering environment" Proceedings of 6ICCT, Amman, Jordan.
4. Lim, S.N. and Wee, T.H. (2000), "Autogenous shrinkage of ground-granulated blast-furnace slag concrete", ACI Material Journal, Vol. 97(4), 587-592.
5. Sanjayan, J.G. and Sioulas, B. (2000), "Strength of Slag-cement concrete cured in place and other conditions", ACI Material Journal, Vol. 97(4), 603-611.
6. Cabrera, J.G. and Lynsdale, C.J. (1988), "A new gas permeameter for measuring the permeability of mortar and concrete", Magazine of Concrete Research, Vol. 40(144), 177-182.
7. Mehta, P.K. (1986), "Concrete: structure, properties, and materials" Prentice-Hall, Englewood Cliffs, NJ.
8. Figg, J. (1989), "Salt, sulfate, rust and other chemical effects" Proceedings Gerwick symposium on durability of concrete in marine environment, Berkely.
9. Hooton, R.D. (1986), " Permeability and pore structure of cement pastes containing fly ash, slag and silica fume, blended cements" ASTM STP897.
10. Swamy, R.N. and Bouikni, A. (1990), " Some engineering properties of slag concrete as influenced by mix proportioning and curing" ACI Materials Journal, Vol. 87(3), 210-220.

Proceedings of the ACI-KC First International Conference & Fourth Exhibition. September 29-October 1, 2003, Kuwait — ***Concreting and High Performance Concrete in Hot Weather.***

SUPERPLASTICIZED RICE HUSK ASH POZZOLANIC PORTLAND CEMENT

Magdy A. Abd El.Aziz, Faculty of Engineering,
Cairo University-Fayoum Branch, Egypt
Saleh M. Abd El.Aleem, Faculty of Science,
Cairo University-Fayoum Branch, Egypt
Hamdy El. Didamony, Faculty of Science,
Zagazig University, Egypt

ABSTRACT

Rice husk ash (RHA) is an active artificial pozzolana and can be used as a cement replacement material. Superplasticizers have been found beneficial in offsetting some of the undesirable characteristics of concrete. This research has been undertaken to study the effect of rice husk ash with and without superplasticizer on the chemical and physico-mechanical characteristics of ordinary portland cement. Therefore, different mixes were made from OPC with 4,8,12, and 16 Wt., % rice hush ash fired at 450 °C for 2.0 hours. The hydration behavior as well as the physico-mechanical characteristics were studied with curing time up to 90 days. The results have shown that, the water of consistency increases with RHA content which adversely affects the mechanical properties, especially at a high RHA, % (above 8.0 Wt., %). Also, the free lime content of blended cement pastes decreases with curing time and RHA contents. In order to improve the physico-mechanical properties of OPC-RHA pozzolanic cement, different blends were made from OPC with 8 Wt., % RHA and various doses of water reducer (0.5, 1.0, 1.5, 2.0, 2.5 Wt., %). The different blends were hydrated for 3,7,28 and 90 days. The hydration behavior was followed and the physico-mechanical characteristics were studied. The results show that, the mix containing OPC with 8.0 Wt., % RHA and 1.5-2.0 Wt., % superplasticizer is the suitable mix which gives a good mechanical properties.

Keywords
Pozzolanic cements; rice husk ash; superplasticizers; hydration behavior; physico-mechanical properties.

1. INTRODUCTION

Rice husk is a challenging problem for each country grows rice to dispose or utilize this by-product, because of the tough, woody, abrasive nature of the husks, their low nutritive properties, resistance to weathering, great bulk and high ash content. Also, the burning of rice husk in open fields constitutes a great source of environmental pollution. Rice husk under controlled burning and if sufficiently ground leaves a whitish fluffy voluminous ash which is known to be mainly silica in an amorphous phase with high surface area[1].

The constituents of rice husks are both organic and inorganic compounds. The organic compounds present in husk are generally lygnin, cutin, carbohydrates and nitrogen compounds. The inorganic constituents comprises about 13.29 Wt., % of the husk. The predominant compound of RHA is silica. Other elements are also present such as Na, K, Ca, Mg, Fe, Al, Mn, P and Cu. The silica of the ash is described to be in a hydrated form like silica gel[2].

In the last few years, a considerable attention has been directed towards the utilization of rice husk ash in portland cement concrete, especially in countries of south east Asia, and Egypt. Reaction of lime with husk ash may be regarded as a reaction of a base with acidic oxide. The reaction proceeds with intimate contact in presence of water as in the system $CaO\text{-}SiO_2\text{-}H_2O$. Therefore, the formation of this binder is more quick as compared to conventional lime-pozzolana reaction.

Differential thermal analysis (DTA) curves of 7, 28 and 300 days water-cured samples of RHA-lime–H_2O binder clearly indicate the nature of hardened paste[3] similar to the products in silica-lime–water system. The main hydration product is calcium silicate hydrates (CSH). Also, Differential thermogravimetry (DTG) and X–ray data confirm this observation.

Rice husk ash with known physical and chemical characteristics has been reacted with lime and water[4]. The product of the reaction has been shown to be CSH by a combination of thermal analysis and X- ray diffraction. Alkalies act as catalysts in the formation of calcium silicate from lime and RHA. This might be due to the formation of sodium silicate which further reacts with $Ca(OH)_2$ to form CSH. Presumably NaOH released in this reaction would react again with silica and thus continue the cycle.

Superplasticizers have been found beneficial in offsetting some of the undesirable characteristics of concrete, especially in hot climate[5,6]. The advantages of these chemical admixtures are reducing the mixing water, retarding the initial and final setting, enhancing the strength and decreasing the drying shrinkage or the permeability. Therefore, superplasticizers are widely used in concrete industry.

The commonly used superplasticizers are polycarboxylic acids and sulphonated naphthalene or melamine formaldehyde condensates. These chemical admixtures have essentially the same dispersing mechanism. The polymer's chains adsorb to the surface of the cement particles; the cement particles become negatively charged. Consequently, electrostatic repulsion occurs between them leading to better dispersion and fluidity. During the last few decades, the use of both mineral and chemical admixtures has drawn increasing attention[7] because they play an important role in changing the physical and chemical properties of concrete matrix.

The aim of the present work is to study the effect of partial replacement of OPC by RHA with and without superplacticizer on its the chemical and physico- mechanical characteristics.

2. EXPERIMENTAL TECHNIQUES.

The starting materials employed in this work were ordinary portland cement provided from Beni-Swif cement company, rice husk from Fayoum area and polycarboxylate superplasticizer (Conplast SP 610) provided from Fosroc Company, 6 October, Egypt. The superplasticizer used is opaque light yellow liquid, with density 1.08 g/ml and chloride content < 0.1 Wt.,%. The chemical analysis of OPC and RHA is shown in Table (1). The surface area of OPC was 3000 ± 50 cm^2 /g.

Rice husk was boiled for one hour, then washed with distilled water and dried at 110 °C for 24 hours. The washed and dried rice husk with grain size 0.5 mm was burnt at 450 °C for 2.0 hours in muffle furnace in an oxidizing atmosphere at low rate of heating (10 °C/min) to facilitate the burning and the decarbonization of the organic material. From the economic point of view the burning for 2 hrs in this work is more economic and give better RHA than that fired for long times in closed atmosphere. The produced ash was sufficiently ground to pass through 90 μm sieve. The surface area of RHA as determined by the adsorption of nitrogen gas reaches 200 m^2/gm[8].

Rice husk ash pozzolanic cement pastes were prepared by mixing OPC with RHA (Table 2). The ingredients of each mix were blended in a porcelain ball mill for one hour using a mechanical roller mill to ensure complete homogeneity. The spuerplasticizer was added with mixing water. The water of consistency and setting times for each mix were determined according to ASTM specifications[9,10]. The dry blends were mixed with the water of consistency for 3 minutes then pelletized and put in humidity chamber for 24 hrs. The pellets were cured under tap water up to 90 days.

The compressive and flexural strengths were measured on cement mortars according to ASTM specifications[11,12]. The mortars were prepared by mixing one part of cement and 2.75 parts of sand proportion by weighing with the water content which sufficient to obtain a flow of 110 ± 5 with 25 drops of the flow table. 50 mm cubes and 40×40× 160 mm prisms were used for compression and flexural tests respectively. The specimens were cured in a humidity chamber at 23±1 °C for 24 hours, then demolded and immersed in tap water until tested. The result of each test is the average of three specimens that were taken from a single batch of mortar and tested at the same curing time.

For estimation of free as well as combined water and free lime contents at any time of hydration, a weight of the saturated sample was ignited at 1000 °C for one hour to determine the total water content (Wt., %). After the predetermined curing time, the hydration of the cement paste was stopped on another sample. About 5 gm of hydrated samples was ground for 5 minutes in a matrix of acetone and methyl 1:1 by volume. A ground paste was filtered through glass funnel (G.4) and then washed 3 times with acetone and methyl. Finally the solid material was dried at 70 C for 2 hours then kept in air tight bottles[13]. The combined water content (W_n %) was determined from the ignition loss of the dried cement paste on the ignited weight basis. The free water content (W_e %) was calculated as :

$$W_e\ \% = (W_t - W_n)\ \%$$

Free lime and free silica contents were determined after any time of hydration as described elsewhere[14]. The total pore volume is calculated as 0.99 W_e.%

3. RESULTS AND DISCUSSION

3.1 Effect of RHA replacement.

The artificial pozzolanic cement was prepared by blending 4,8,12 and 16 Wt., % of RHA and OPC. Figure (1) shows the water of consistency and setting times of the different cement pastes as a function of RHA content. The results show that, the water of consistency of the blended cement is higher than that of only OPC. Also, as the ash replacement increases, the water of consistency increases. This may be due to the relatively higher surface area of RHA compared with that of OPC[15]. The setting times of the cement pastes behave in the same way of water of consistency. The blended cement pastes have longer setting times than those of only OPC. Also, as the ash content increase, the setting times are elongated due to the increase of water demand and the increase of the open poresfrom the free water. Also, the ash and the early hydrated product form coating layer on the cement clinker particles which delay further hydration. Therefore, the setting times are elongated. Superplasticizers should be used when RHA is added as a pozzolanic material to decrease the water of consistency which affects the mechanical properties.

The values of total pore volume of the hydrated samples are graphically represented as a function of curing time in Fig.(2). It is clear that, the total pore volume of the all cements pastes decrease with curing time. This is mainly due to the progress of hydration with curing time. The hydration products fill up the open pores, thus increasing the bulk density and decreasing the total pore volume. As the ash content increases, the total pore volume increases due to the high water of consistency.

The free lime contents of the hydrated pastes are plotted as function of curing time in Fig.(3). The results show that, the free lime contents increase with curing time for OPC pastes. This is mainly due to the continuous hydration of the main cement clinker phases liberating free lime. On the other side, free lime contents decrease with curing time for blended mixes and as the ash content increases, the free lime decreases. This is due to the decrease of cement content, which liberates Ca $(OH)_2$ and due to the reaction of RHA with liberated lime forming CSH.

The degree of hydration is measured from the combined water content .The results of combined water contents (W_n %) of the hydrated mixes are plotted in relation to curing time in Fig. (4). It can be observed that, the combined water content increases with curing time. This is mainly attributed to the continuous hydration of cement clinker phases as well as RHA with free lime. At a given time, the blended cement has higher combined water contents than OPC. Also, as the amount of RHA is increased, the combined water content enhances due to the high reactivity of RHA with the liberated Ca $(OH)_2$ forming CSH[16].

The free silica contents of the hydrated samples are graphically represented in Fig. (5). It can be seen that, free silica contents decrease with curing time and increase with the ash content for all investigated blends. This is mainly due to that, RHA is highly reactive microsilica and reacts with the liberated lime producing CSH. The following reaction sequence might explain this.

C_3S or C_2S (portland cement) + H_2O $\longrightarrow$ CSH + Ca $(OH)_2$

SiO_2 (RHA) + $Ca(OH)_2$ + H_2O $\longrightarrow$ CSH + SiO_2 (residual unreacted silica)

Figures (6,7) show the compressive and flexural strengths of the investigated mortars. The compressive and flexural strengths increase with curing time for all hardened mortars. This is attributed to the increase of the hydrated products with the time, especially tobermorite gel (the main source of strength). These products accumulate in water filled pores to from a more compact body. At a given time the strengths of RHA- OPC blends are lower than that of only OPC. The results also show that, the strengths decrease with the increase of ash content. This is mainly due to that, the water of consistency increases with the ash content leading to increase of the total pore volume as shown in Fig.(2) and consequently decrease of the ultimate strength.

3.2 Effect of Superplasticizer.

The artificial pozzolanic cement was prepared by blending a mixture of OPC and 8.0 Wt., % RHA, with water of consistency. Different doses of superplasticizer namely, 0.5, 1.0, 1.5, 2.0 and 2.5 Wt., % of cement were thoroughly mixed with water just prior its addition to cement powder. The prepared pastes were tested for their normal consistency at each dose.

The water of consistency and setting times of the investigated pastes are plotted in Fig. (8). The results show that, the water of consistency decreases with the superplasticizer content. This may be due to the formation of superplasticized thin film around cement grains or/and early formed hydration products which adversely affects the hydration process and modifies the microstructure of the hydrated phases[17]. Also, polycarbxylate superplasticizer is anionic surfactant and when adsorbed on cement particles become negatively charged causing repulsive effect with each other, consequently the fluidity of cement particles increase. Therefore, the water demand decreases. The setting times are elongated with the addition of superplasticizer. This may be attributed to the electrostatic repulsion among the negatively charged superplasticied cement particles causing better dispersion and fluidity. Also the superplasticizer is from the type of retarding which delay the setting and reduce the w/c.

The values of total pore volume of the investigated mixes are graphically represented in Fig.(9). As the superplasticizer dose increases, the total pore volume decreases due to the decrease of water of consistency with the increase of superplasticizer dose. But above 2.0 Wt., % superplasticizer the rate of the decrease of total pore volume diminishes. Therefore, 2.0, % is the suitable dose of admixture. This may be attributed to the fact that, the admixture does not react with cement compounds to from new crystal types[18].

The values of free lime and free silica are graphically represented in Figs. (10,11). It can be seen that, free lime and silica contents decrease with curing time. This is due to the pozzolanic reaction of RHA with the liberated lime. The addition of superplasticizer decreases free lime and silica contents. This is mainly due to the decrease of mixing water and total pore volume. Both of them positively affect the efficiency of the pozzolanic reaction by approaching the RHA particles from the liberated lime leading to more consumption of the lime and formation of CSH.

The variation of combined water contents of the hydrated blends with curing time is shown in Fig (12). It is clear that, as the superplasticizer dose increases, the combined water contents are reduced. This may be attributed to the reduction of mixing water with the addition of superplasticizer, which affects the rate of hydration of cement components.

Figure (13) illustrates the variation of compressive strength of the tested mortars with curing time. It is clear that, the compressive strength increases with curing time and superplasticizer dose up to 2.0 Wt., %. This is attributed to the decrease of mixing water as well as the total pore volume. Therefore, the compressive strength enhances. The higher superplasticizer dose (above 2.0 Wt., %) shows slight effect on the compressive strength because, the admixture doesn't react with cement compounds to from new crystal types[18].

The results of flexural strength of the blended cement mortars are shown in Fig (14). It can be observed that, the flexural strength increases with curing time and superplasticizer dose. This is owing to that, the polymer admixture acts as a binder for the sand particles leading to the improvement of the degree of compaction. The results of compressive and flexural strengths are in a good agreement with those of free lime, free silica and total pore volume.

4. CONCLUSION

From above findings ،it can be concluded that :

1- Addition of RHA to OPC, increases the water of mixing, total pore volume and setting times which negatively affect the mechanical properties, especially at higher RHA content (above 8.0 Wt., %). Therefore superplasticizer should be used with RHA-OPC pozzolanic cement.
2- The free lime content of RHA-OPC pastes decreases with the RHA content due to the reaction of RHA with the lime forming CSH which is the main source of compressive strength.
3- Addition of superplasticizer up to dose (2.0 Wt., %) to RHA-OPC pozzolanic cement enhances the mechanical properties. Above 2.0 Wt., %, superplasticizer the compressive strength shows slight increase, therefore 2.0 % admixture is the suitable dose. In contrast, flexural strength increases with superplasticizer dose. The mix containing OPC + 8.0 Wt., % RHA and 1.5-2.0 Wt., % superplasticizer is the suitable mix which gives a good mechanical properties.

5. REFERENCES

(1) Galal, A.F., Taha, A.S., Helmy, I.M. and EL-Didamony, H., (1990), " Rice husk in blended cements'' Sil. Ind., 55, PP. 55-58

(2) Patel, M., karera, A. Prasanna ,P., (1987), J. Mat .Sci., 22, P. 2457

(3) Masood, I. and Melhotra, S.P., (1981).Res. Ind. 26 (1), P. 4

(4) James, J. and Rao, S.M., (1986), " Reactivity of rice husk ash" Cem. Concr. Res., 16(1) P.67

(5) ACI Committee 305 (1991)., Hot Weather Concrete, ACI Mater. J., 88(4 ،PP. 417- 436

(6) Aitcin, P.C and Mao, B. Proc. (1992), 2nd Int. Conf. High Performance Concrete, Taipei, P.91

(7) Collepardi, M. and Ramachandran, V.S., (1992). "Effect of admixtures Part : I, "Effect of superplasticizer on the physico-mechanical characteristics of cement " 9th Int. Conf. On Cem. Chem. New Delhi, India.

(8) Hanafi, S., Abo-El-Enein, S.A., Ibrahim D.M. and El-Hemaly S.A. (1980) ,"Surface properties of silica as produced by thermal treatment of rice husk ash" Thermochimical Acta, 37, PP. 137-143

(9) ASTM Standards , (1992). "Standard Test Method for Normal Consistency of Hydraulic Cement". ASTM. , C 187-86 .

(10) ASTM Standards، (1992). " Standard Test Method for Setting of Hydraulic Cement by Vicat Needle", ASTM Designation, C 191-92

(11) ASTM Standards ،(1992),"Standard Test Method for Compressive Strength of Hydraulic Cement Mortars", ASTM Designation, C 109 -92

(12) ASTM Standards ،(1992)," Standard Test Method for Flexural Strength of Hydraulic Cement Mortars", ASTM Designation, C 348-92

(13) El-Didamony, H., Haggag, M.Y. and Abo El-Enein, S.A., (1978), " Hydration kinetics,surface properties and microstructures" Cem. Concr. Res., 8, PP. 351-358

(14) Kondo, R., Abo El-Enein, S.A., and Daimon, M, (1975), "Kinetics and mechanisms of hydrothermal reaction of granulated blast furance slag" Bull. Chem. Soc., Japan, 48, PP. 222-226

(15) Al-Wakeel, E.I., El-Korashy, S.A., (1996).,"J. Mat. Sci.", 31, P. 1909

(16) Amer A.A., El-Didamony, H., El-Hemaly, S.A.S., and El-Alfi S., (1997)," Rice husk ash pozzolanic cement" Sil. Ind., 62(7-8), PP. 141-147

(17) Sarker, S.L. and Amin, X., (1992).," Cem. Concr. Res.", 22, PP. 605-608

(18) Sweetland, D ،.(1976), " Flowing Concrete" Civil Engineering , P. 33

خواص الأسمنت البورتلاندى العادى المخلوط برماد سرس الأرز والأضافات فائقة التخفيض للماء

ان العديد من بلدانِ العالم تجرى المحاولات للاستفادة من المخلفات الزراعية إما بإضافتها كما هى أو بمعالجتها قبل الإضافة . وقشةُ الأرّزّ واحدة من مثل هذه المواد عند حرقها عند درجة حرارة من ٤٥٠ – ٧٠٠ م يتخلف عنها رماد يتكون أساسا من سليكا نشطة ووجود هذه السليكا فى وسط تفاعل الأسمنت يحسن كثيرا من الخواص الكيميائية و الخصائص الميكانيكية للإسمنتِ البورتلاندى ولاسيما فى حالة وجود إضافات فائقة التخفيض للماء نظرا لأن رماد سرس الأرز يحتاج لكميات كبيرة من ماء الخلط للحصول على درجة تشغيل مناسبة .

وفى هذا البحث تم دراسة تأثير خلط رماد سرس الأرز بنسب مختلفة على الخواص الكيميائية والفيزيقوميكانيكية للإسمنتِ البورتلاندى العادى فى حالة وجود إضافات فائقة التخفيض للماء وبدونه وتم استخلاص النسب المناسبة التى تحسن خواص الأسمنت .

Table(1) : Chemical analysis of ordinary portland cement and rice husk ash, Wt% ..

Oxides	OPC	RHA
SiO_2	٢٠,٥٠	٩٤,٤٧
Al_2O_3	٥,٥٠	٢,٠٣
Fe_2O_3	٢,٨٩	٠,٤١
CaO	٦٢,٠٠	١,١٥
MgO	٢,٠٧	٠,٨٨
SO_3	٢,٤٢	–
Na_2O, K_2O	٠,٥٢	١,٥٢
L.O.I	٣,١١	–

Table (2) : Mix composition of the prepared pozzolanic cements, Wt., %

Mix No.	OPC	RHA	Superplasticize
M_0	١٠٠	٠	–
M_1	٩٦	٤	–
M_2	٩٢	٨	–
M_3	٨٨	١٢	–
M_4	٨٤	١٦	–
M_5	٩٢	٨	٠,٥
M_6	٩٢	٨	١,٠
M_7	٩٢	٨	١,٥
M_8	٩٢	٨	٢,٠
M_9	٩٢	٨	٢,٥

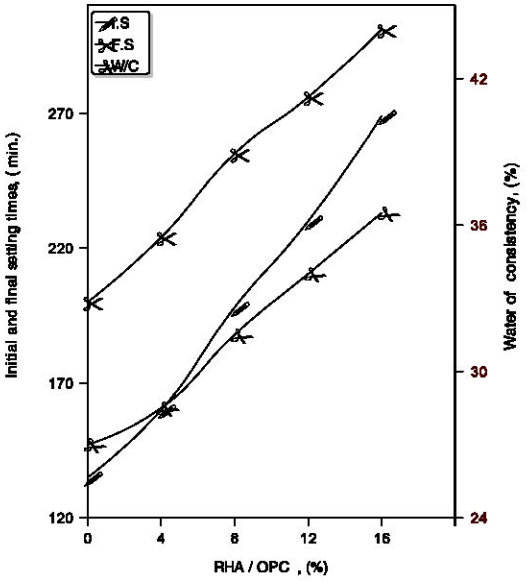

Fig. (1) : Water of consistency and setting times of different blended cement pastes and various proportions of RHA.

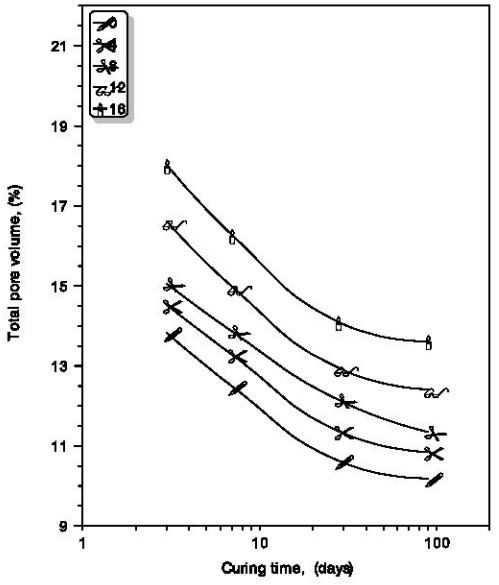

Fig. (2) : Total pore volume of different blended cement pastes and various proportion of RHA as a function of curing time.

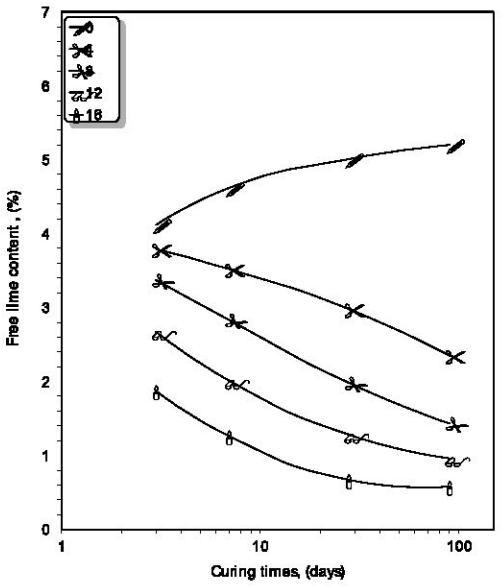

Fig. (3) : Free lime contents of different blended cement pastes and various proportions of RHA as a function of curing time.

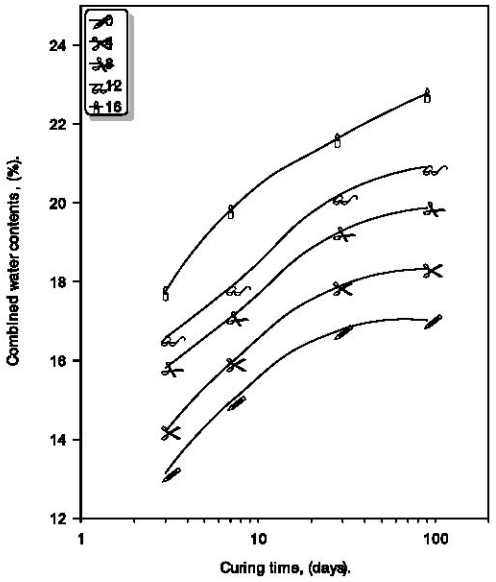

Fig. (4) : Combined water contents of different blended cement pastes and various proportions of RHA as a function of curing time

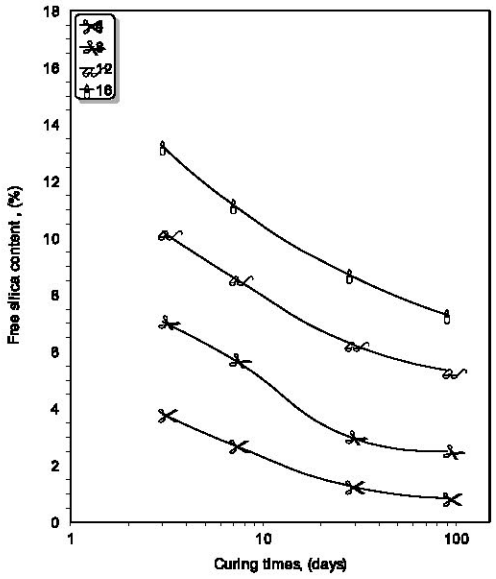

Fig. (5): Free silica contents of different blended cement pastes and various proportions of RHA as a function of curing time.

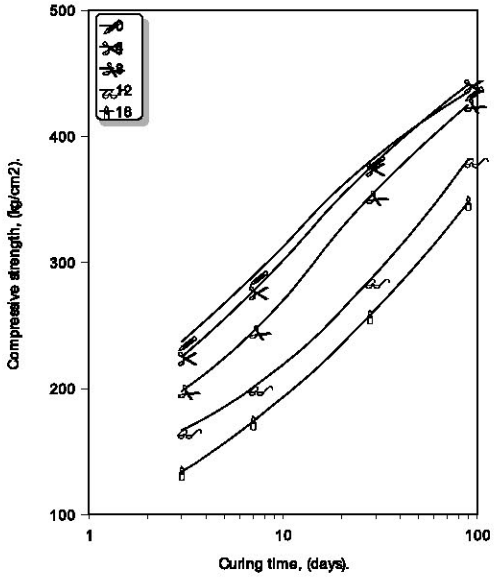

Fig. (6): Compressive strength of different blended cement mortars and various proportions of RHA as a function of curing time.

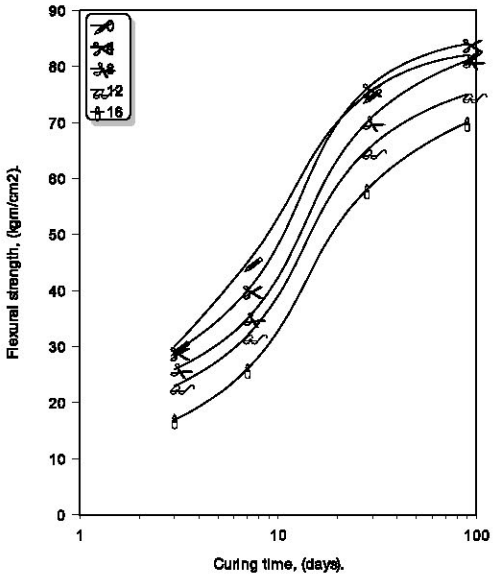

Fig. (7) : Flexural strength of different blended cement mortars and various proportions of RHA as a function of curing time.

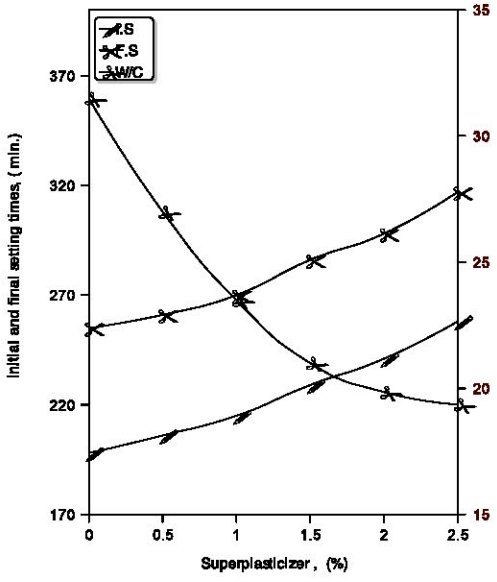

Fig. (8) : Water of consistency and setting times of blended cement pastes and various superplasticizer doses.

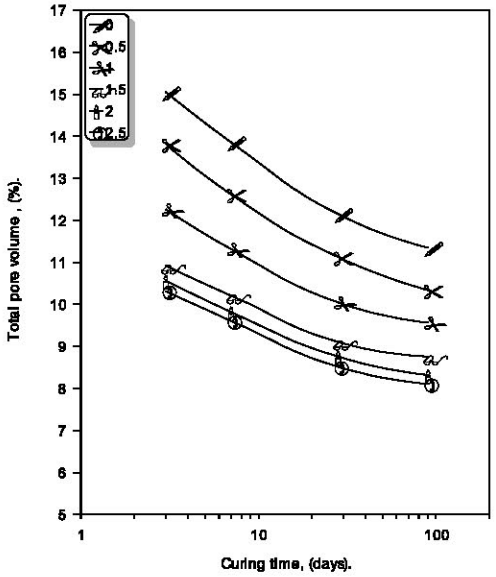

Fig. (9) : Total pore volume of cement pastes containing 8 % RHA and various superplasticizer doses as a function of curing time.

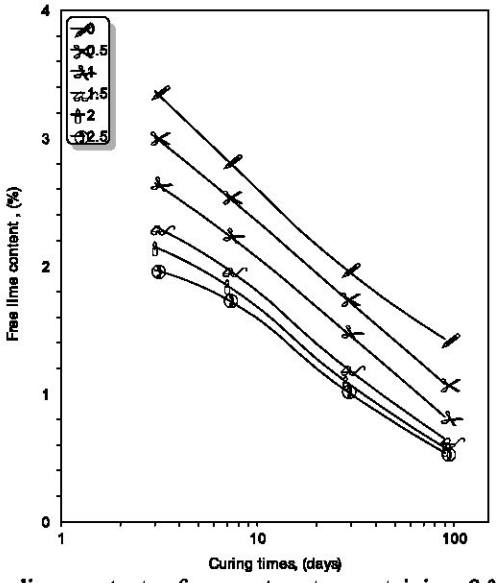

Fig. (10) : Free lime contents of cement pastes containing 8 % RHA and various superplasticizer doses as a function of curing time.

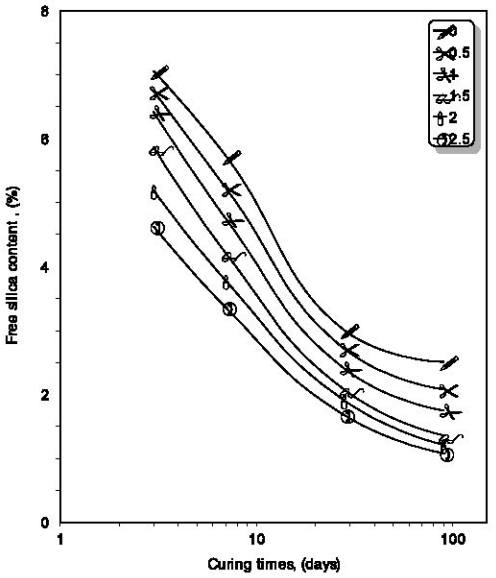

Fig. (11) : Free silica contents of cement pastes containing 8 % RHA and various superplasticizer doses as a function of curing time.

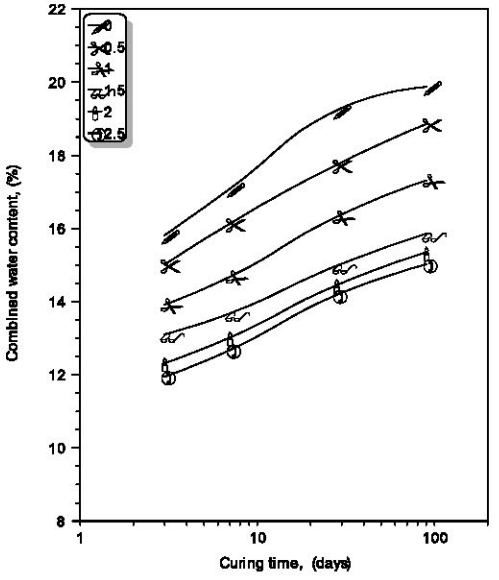

Fig. (12) : Combined water contents of cement pastes containing 8 % RHA and various superplasticizer doses as a function of curing time.

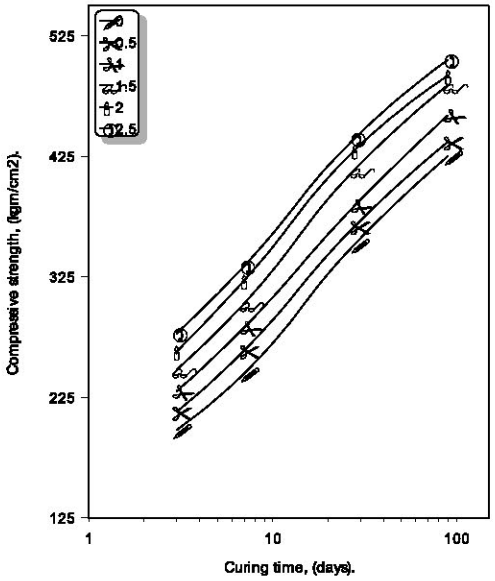

Fig. (13) : Compressive strength of cement mortars containing 8 % RHA and various superplasticizer doses as a function of curing time.

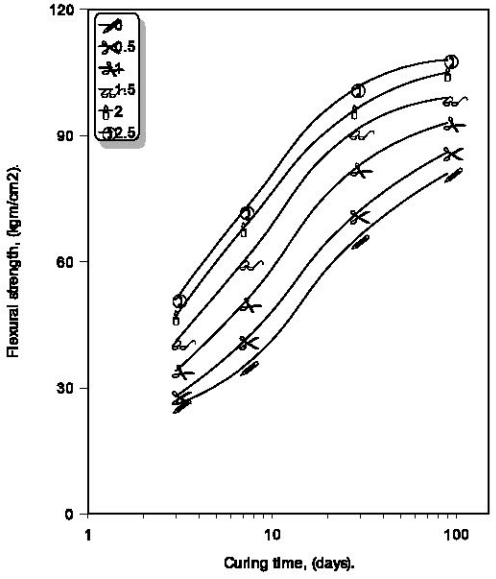

Fig. (14) : Flexural strength of cement mortars containing 8 % RHA and various superplasticizer doses as a function of curing time.

Proceedings of the ACI-KC First International Conference & Fourth Exhibition. September 29-October 1, 2003, Kuwait — ***Concreting and High Performance Concrete in Hot Weather.***

PERFORMANCE OF CONCRETE MADE WITH CRUSHED BRICKS AS COARSE AGGREGATE

Dr. Guemmadi Z'hor, University Mentouri Constantine, Algeria
Dr. Toumi Belkacem, University Farhat Abbas Setif, Algeria
Dr. Houari Hacene, University Mentouri Constantine, Algeria

ABSTRACT:

Every year, during clay brick manufacturing, certain quantities of bricks are discarded due to breakage or nonconformity to specific standards. The percentage of discarded bricks may reach 3 to 5%, this represents about 1.2 million bricks per year. As this could pose an environmental hazard, it is essential to consider recycling the material.

The present study aims to discuss the possibility of including the crushed bricks as coarse aggregate.

The obtained results indicate that the substitution of crushed bricks in concrete as coarse aggregate led to satisfactory performance, comparable to those of ordinary concrete.

The results indicate that concrete based on crushed bricks as coarse aggregate has compressive strength comparable to the strength obtained with a conventional concrete and a higher tensile strength. The shrinkage of concrete using crushed bricks as coarse aggregate is lower than that of conventional concrete.

Keywords:

Concrete, Performance, Crushed Bricks, Coarse Aggregate, Compressive Strength, Tensile Strength, Shrinkage.

INTRODUCTION

The growing rate of the population in Algeria gave rise to demand for buildings and hence for local building materials to construct buildings.

Each year, several million tons of bricks are rejected by industrial units due to damages or nonconformity to the standards. A brick factory approximately produces two million bricks per month of which an average of 12% are rejected, accounting for 2.9 million bricks per year, thus constituting a very significant number.

Currently, for the environment and other reasons related to urbanization, solid brick bit valorization has exceeded the stage of experimentation throughout the world and is recognized as a rather significant development with a recycling rate of more than 80%. This can constitute, even in the areas where aggregate resources are superabundant, a good re-use of solid waste in order to reduce the crucial problem of global ecology.

The principal objective of this study is to contribute to the valorization of the brick bits and their re-use as aggregates for hydraulic concrete and thus make it possible to preserve the environment and to help to solve some problems linked to the need for aggregate.

TEST PROGRAM

Two concrete mixes are designated by OC for ordinary aggregate concrete and BC for crushed aggregate brick, which have been formulated using the Dreux and Gorisse method[1]. The workability was kept constant (8 to 10 cm measured on standard cone instantaneously after mixing) by adjusting the amount of free water. The cement content was also kept constant. The flakiness index for the two types of aggregate was approximately 0.44.

Table 1. Dosages of concrete constituents

Constituents		Dosage en Kg/m^3	
		OC	BC
Sand 0/3		435.9	405.1
Gravel	3/8	133.2	123.0
	8/15	400.5	380.1
	15/25	805.3	737.5
Cement		350.0	350
Water		192.0	201.6
W/C		0.55	0.57
Slump		11 cm	10.5
Density		2317.5	2197.3

Characteristics of constituent

Aggregates: aggregates that form the skeleton of the concrete are of two types; the first one is constituted by ordinary crushed aggregates obtained from Ain Smara. The granular classes used are 0/3, 3/8, 8/15 and 15/25. The second type is obtained first by crushing the hollow brick that comes from a local factory and then sieved to reconstruct granular grade similar to those of ordinary aggregates. The gradations of aggregates are mentioned in Table 2.

Table 2. Gradation of aggregate *(standard NA 2607*								
Sieve size	0/3		3 / 8		8 / 15		15/ 25	
	Usual	Brick	Usual	Brick	Usual	Brick	Usual	Brick
0.08	14	7						
0.16	18	15						
0.315	27	29						
0.63	39	40						
1.25	56	54	0	0				
2.5	85	86	5	6				
5	100	100	54	55	0	0		
6.3			85	87	12	13		
8			100	100	37	37		
10			100	100	76	77	0	0
12.5					99	100	2	3
16					100	100	25	23
20							71	70
25							100	100
31.5							100	100

Table 3. Physical properties of aggregates				
Aggregates Grading	Sand		Aggregate	
	Usual	Brick	Usual	Brick
Density (Kg/m^3)				
▪ Absolute	2.73	2.39	2.57	2.28
▪ Apparent	1.44	1.36	1.36	1.27
Equivalent of sand	78	84	/	/
Water Absorption	1.20	4.10	1.60	5.90
Teneur en $CaCO_3$ (%)	56	24	58	29

Cement: The cement type is CPJ 45. It comes from the ERCE factory and conforms to Algerian norms (NA 442). Mineralogical and chemical compositions of cement clinker are reported in Table 4.

Table 4. Portland clinker characteristics (%)								
Mineralogical composition								
C_3S		C_2S		C_3A		C_4AF		
56.60		22.98		9.78		8.25		
Chemical composition								
SiO_2	Al_2O_3	Fe_2O_3	CaO	MgO	SO_3	Na_2O	K_2O	Other.
27.83	6.21	3.12	57.22	0.94	2.02	/	/	2.28

Water: The water used for concrete mixture is the drinking water. The chemical composition of this water is shown in Table 5.

Table 5. Chemical composition of water								
Ca	Mg	Na	K	Cl	SO_4	CO_3	NO_3	Insoluble
116	36	80	3	140	170	305	5	786

Preparation of test tubes:

The two types of aggregates were kept in water for 24 hours and then dried in air to a saturate surface before mixing. The exact water content needed to keep a constant workability was determined by progressive adjustment during the concrete mixture. The test specimens were caste in steel moulds and then compacted by a vibrating table. After 24 hours they were remolded and cured in water at the temperature of 20°C until the testing time except for the specimen which were meant for shrinkage. They were then kept inside the laboratory in the open air (19 to 30°C and 50 to 70 RH).

Tests carried:

For each one of the two concrete mixes, fifty-four test tubes were prepared, twenty-four cylinder 16x32 cm to determine the compressive strength, twenty-four prisms 7x7x28 cm to determine the tensile strength and six specimen to undergo shrinkage from day one to ninety days. These test tubes were submitted to test for 3, 7, 28 and 90 days.

Test results:

Water content:

Results of water contents needed to keep a constant workability are presented in Table 1. These results show that crushed brick aggregates need more water than those of ordinary aggregates for a desired workability, this may be explained by the sharpness index in reality; this parameter is more marked for crushed brick aggregates than for naturally crushed aggregates.

Compressive strength:

As shown in Figure 1, the compressive strength of concrete based on crushed brick aggregate is higher than the concrete made with naturally crushed aggregates and this remains true except after 7 days when the compressive strength of concrete made with natural aggregate is lower.

After 28 days, the compressive strength of brick-concrete (34 MPa) is approximately 14 percent more important than the compressive strength of conventional concretes (34 MPa). Same results are also reported by Akhtaruzzaman and Hasnat[2], Mohamed Mansur, T.H Wee and Lee Soo Cheran[3].

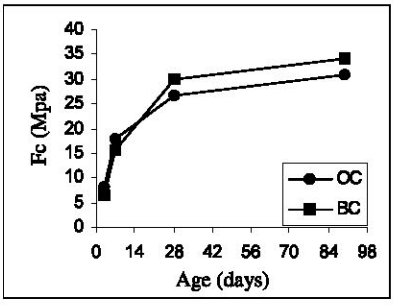

Fig 1. Variation of compressive strength with time

The relatively high strength of brick-concrete compared to those of conventional concrete is mainly due to surface texture of brick-aggregate which occupy a large area due to their shape and high specific density. According to Ozol [4], the most important aggregate properties that influence the concrete strength are the surface texture, the modulus of elasticity and the shape.

Tensile strength:

The tensile strength evolution over a period of time is comparable to the compressive strength evolution (see figure 2).

For tensile strength the crushed brick aggregate also yield higher strengths than those from natural aggregate by approximately 12 to 14 percent.

This improvement in brick-concrete is also due to surface texture of brick-aggregate which occupy a large area, according to their shape and specific high density of brick.

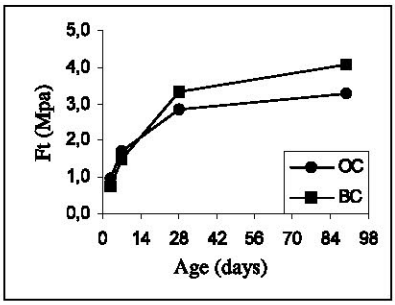

Fig 2. Variation of tensile strength with time

Drying shrinkage

As it may be seen in figure 3, the shrinkage of concrete made with brick aggregate is less important than the shrinkage of the concrete made with conventional aggregate. This is true at all ages and it also reported by Mohamed Mansur, T.H Wee, Lee Soo Cheran[3] and Hansen [5].

According to Hansen, the drying shrinkage of brick-aggregate concrete is delayed by continued hydration due to the presence of internal moisture in the aggregate, and experimental period of more than a year is necessary to eliminate this effect.

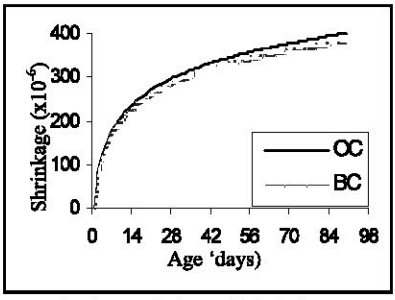

Fig 3. Variation of shrinkage with time

CONCLUSION:

This experimental study has shown that with an equivalent brick aggregate (having identical mix proportion and bulk volume as conventional aggregate) the following occur:

- ✓ The obtained concrete had a higher compressive and tensile strength than the concrete made with conventional aggregate.
- ✓ For equal workability, the quantity of water needed by brick aggregate concrete is higher than the quantity needed for conventional aggregate concrete.
- ✓ The density of brick aggregate concrete is about 70% of the conventional aggregate concrete.
- ✓ The drying shrinkage of brick aggregate concrete is lower than the conventional aggregate concrete.

REFERENCES:

1. DREUX . G. & FIESTA. J , Nouveau guide du béton, septième édition, EYROLES, 1995

2. AKHTARUZZAMAN A. A. and HASNAT A., Properties of concrete using crushed brick as aggregate, Concrete International, Vol 5, No 2, February 1985, pp 58-63

3. MOHAMED A. MANSUR, T.H WEE and LEE SOO CHERAN, Crushed Brick as Coarse Aggregate for Concrete, ACI Materials Journal, Vol 96, No 4, July-August 1999, pp 478-484.

4. Ozol M. A., Significance of Tests and Properties Concrete and Concrete making Materials, ASTM Special Technical Publication No169B, pp 685-628

5. HANSEN I. A., Recycling of Demolished Concrete and Masonry, RILEM, Report No 6, 1992, pp 161-245.

Proceedings of the ACI-KC First International Conference & Fourth Exhibition. September 29-October 1, 2003, Kuwait — ***Concreting and High Performance Concrete in Hot Weather.***

DESTRUCTIVE AND NON-DESTRUCTIVE TESTS OF CONCRETE IN KUWAIT: A COMPATIBILITY ANALYSIS

PA Koushki, H Kabir, A Al-Khaleefi & S Philipose
Department of Civil Engineering, Kuwait University

ABSTRACT

This paper examines the compatibility between the non-destructive test (NDT) (Schmidt rebound hammer), and the conventional destructive (cylinder) testing (DT) of concrete structures in Kuwait. A total of 206 NDT, and 46 DT of concrete strength results are statistically examined and compared. Cumulative frequency distributions of the two test results are performed, and correlation coefficients between the sample NDT and DT results of concrete strength are developed. Linear and quadratic regression models between the destructive and non-destructive tests of concrete strength measures are calibrated. The result of the comparison between DT and NDT for column structures are reported herein. Findings point to the existence of a close compatibility and agreements between the two strength test results.

INTRODUCTION

The specific objective of this paper is to present the result of a study aimed at the examination of compatibility between the conventional destructive test (cylinder), and the non-destructive test (Schmidt Hammer) measures of concrete strength for a sample of structural components in Kuwait.

With concrete being a key construction material, worldwide, its quality and strength are vitally important in the performance of any structure. Non-destructive (insitu) testing of concrete structures is gaining increasing acceptance as a means of evaluating the strength, durability, uniformity and other properties of existing structures.

Non-destructive (NDT) testing of concrete structures are of significant value in a number of situations which include the following: quality control of precast construction, compliance with specifications, assessment of uniformity, location of cracks and voids, monitoring strength development, assessment of reinforcement condition, identifying the location of suspected deteriorated concrete, and providing strength data for structural capacity analysis and integrity surveys (Guirguis 1987). Its obvious advantages over the destructive testing option are savings in time and money.

It is also important to note the limitations of NDT of concrete structures. The measured strength result of the NDT of concrete are usually affected by a number of variables including the aggregate type and size, the moisture content of concrete mix, the mix proportions, and the structure's age.

In general, the basic premise of the NDT of concrete structures relies on the fact that certain physical properties of concrete can be related to strength and can be measured by non-destructive methods. Such properties include hardness, resistance to penetration by projectiles, rebound capacity and ability to transmit ultrasonic pulses (Jones & Facaoaru 1969; Malhotra 1976); Feldman 2000).

The most frequently used method for non-destructive testing of concrete and structural components is the Schmidt Hammer Test (Concrete Test Hammer 2002). The rebound hammer is a surface hardness tester for which an empirical correlation has been established between strength and rebound number. The test instrument consists of a spring-controlled hammer mass that slides on a plunger within a tabular housing (Durham GEO 2002). The hammer is used to determine the in-place compressive strength of concrete within a range of 1500 to 8000 (psi). The hammer is placed on the concrete test surface and impact force is released. The rebound value is noted and compared to a correlated strength value. The test surface can be horizontal, vertical or at any angle however the instrument must also be calibrated in the same position.

THE DATA

The test samples were taken from concrete structural components (columns, beams, and slabs), of six government buildings in Kuwait City. The NDT samples measurements were made on the same structural components where the DT sample cores were taken for laboratory analysis. The structural components were systematic-randomly chosen for test samples. A total of 206 NDT samples (102, 53 and 51 on columns, beams, and slabs, respectively), and 46 DT cores (19, 17 and 12, respectively, from columns, beams and slabs), were included in the database.

DATA ANALYSIS

Distributional characteristics, mean traits and confidence intervals, correlation analysis, and regression statistics were all utilized to examine and evaluate the NDT and the DT measurements of concrete strength. These are presented below.

The cumulative frequency distributions of the NDT and the DT samples are shown in Figure 1. The cumulative distributions indicate that the non-destructive test measures of the sample concrete columns' strengths were higher than those of the destructive test samples

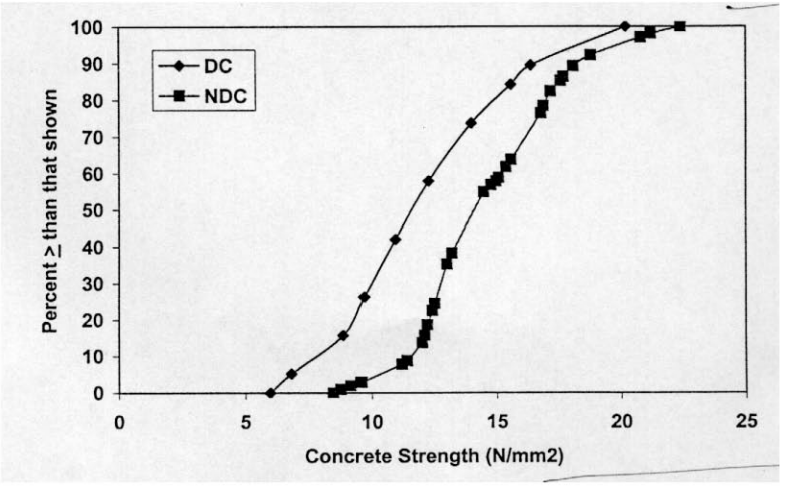

Figure 1. Cumulative Frequency Distribution of Concrete Column Strength: ND & D Tests

along the entire curve. For example, the fifty percentile strength of the destructive tests was 12.5 (N/mm^2), as compared to around 14 (N/mm^2), for the NDT samples. The gap between the two cumulative distribution curves however narrows for higher values of concrete strengths.

The measured values of the sample concrete strength were also utilized to compute the sampling error (e) associated with the NDT and the DT measurements. The computed errors were then employed to construct confidence intervals for the two test results. As shown in Figure 2, the true mean strength value of concrete is within the range of $X \pm e$ which for the NDT samples, is within 14.7 ± 0.35 (N/mm^2), or from 14.4 (N/mm^2) to 15.1 (N/mm^2), with 95% confidence. The same for the DT samples will be located within the 10.1 to 14.7 (N/mm^2) range. The variations in concrete properties such as aggregate type and size, mix proportions, quality control, compaction, etc. are mainly responsible for variations in the sample mean strength values (larger standard deviations) of the destructive test samples. The NDT results on the other hand are mainly affected by concrete surface hardness, and thus the properties stated above do not affect the test result significantly.

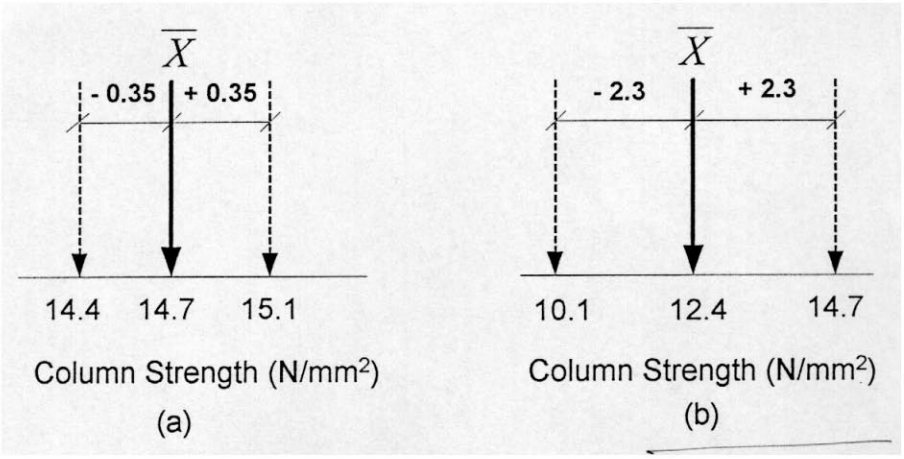

Figure 2. Confidence Intervals for Concrete Strength Means:
(a) NDT, and (b) DT Samples

REGRESSION MODELS

A correlation analysis was performed on the test data in order to measure the strength of the linear relationship between the NDT and DT sample results. If the measurement result of one test (e.g. NDT) could be expressed exactly as a linear function of the measured result of the destructive test, then a correlation coefficient of 1 or -1, depending on whether the two test results are directly related or inversely related. A correlation coefficient of zero between the two test results means that each test result has no linear predictive ability for the other.

The true Pearson correlation is defined as follows (Draper & Smith 1966):

$$\rho_{xy} = \frac{\operatorname{cov}(x, y)}{\sqrt{\operatorname{var}(x) \times \operatorname{var}(y)}} \qquad (1)$$

The sample correlation estimates the true correlation, which in the case of Pearson product-moment is computed as follows:

$$\rho_{xy} = \frac{\sum_{i=1}^{n} (X_i - \overline{X})(y_i - \overline{y})}{\sqrt{\sum_{i=1}^{n} (X_i - \overline{X})^2 \times \sum_{i=1}^{n} (y_i - \overline{y})^2}} \qquad (2)$$

The computed correlation coefficient between the NDT and DT results was:

	Destructive Strengths
Non-Destructive Strength	0.9631
	$p < 0.0001$

The computed coefficient indicates that the two test results are nearly exactly a linear function of each other, and for all practical purposes, one can substitute the other. The probability value of 0.0001, confirms the non-zero value of the coefficient of correlation (i.e. there is 1 in 10,000 chance that the computed correlation coefficient is in fact equal zero).

To develop the exact form of the linear relationship between the NOT and DI results, a regression analysis was performed on the data. The linear model form was:

$$DTC = \alpha_0 + \alpha_1 NDTC + \varepsilon_i \quad (3)$$

where:

DTC = destructive test of column strength (N/mm2)
α_0, α_1 = Model parameters
NDTC = non-destructive test of column strength (N/mm2)
ε_i = model error

The result is shown in the analysis of variance below:

Source	Sum of Squares	Degree of Freedom	Mean Square	F Value
Model	188.896	1	188.896	220.04
Error	14.594	17	0.858	$p < 0.0001$
Total	203.490	18		
		R-Square = 92.4%		
		Parameter Estimates		
Variable	Estimate	t-value	$p > \|t\|$	
Intercept, α_0	–23.923	–9.74	<0.0001	
NDTC, α_1	1.884	14.83	<0.0001	

The calibrated mode form is as follows:

$$DTC = -23.923 + 1.884\ NDTC \quad (4)$$
$$R^2 = 92.4\%$$

The R^2 — the coefficient of determination — is the "goodness of model fit". It indicates that 92.4 percent of variation in DTC strength measures is explained by the NDTC strength measures. The remaining 7.6% of the variations in DTC measures are explained by factors absent from the model. In addition, both the F—test and the T—test results statistically confirmed the appropriateness of the NDTC as an independent variable in the model as well as the significance of its parameter, respectively. The quadratic model form increased the predictive ability of the model by only 1.8 percent — not significant enough to justify the additional input requirement.

The calibrated regression model (Eq. #4), was then used to predict the DTC as a function of the NDTC strength measures. The result of the model—predicted and those of the actual measurements of DTC strengths are shown in Figure 3. A rather close fit is observed between the actual and the model—predicted values of column strengths.

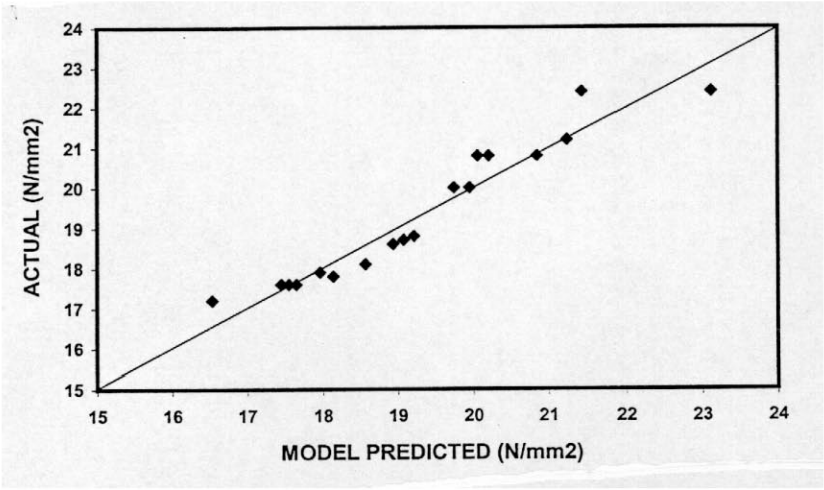

Figure 3. Relationship between the Actual and Model Predicted Non-destructive Strength Tests of Concrete Columns

CONCLUSIONS

The aim of the paper was to examine and evaluate the compatibility between the conventional destructive and the non-destructive tests of concrete strengths. The strength measurement result of 102 non-destructive, and 19 destructive samples of concrete column structures in Kuwait were subjected to a number of statistical analyses. These included the distributional traits, analysis of correlations, and regression statistics. Findings all pointed favorably to the existence of a close linear relationship between the two test sample results. While the measured column strength values of the non-destructive test samples were generally higher than those of the core samples, a regression model relating the destructive strength measures to the corresponding non-destructive strength values proved highly accurate. The calibrated model demonstrated a predictive accuracy level of more than 92 percent, and was thus judged appropriate.

REFERENCES

Concrete Test Hammer (2002),~ "Schmidt concrete test hammer", www. concretendt.com/OO2.htm, accessed: December 14, 2002.

Draper, N. and Smith, H. (1966), Applied Regression Analysis, John Wiley & Sons, Inc., New York, USA.

Durham GEO (2002), "Nondestructive tests", www.durhamgeo.com/cgi-bin/softcart.exe/testing.htm, accessed: December 14, 2002.

Feldman, R. (2002), "Non-destructive testing of concrete", Canadian Building Digest, CBD-187, 1-5.

Guirguis, S. (1987), "Insitu testing of concrete — a review". Concrete Institute of Australia, NSW, No. 22, 1-7.

Jones, R. and Facaoaru, I. (1969), "Testing of concrete by the ultrasonic pulse method". Materials and structures, Vol. 2, (10), 253-661.

Malhotra, V. (1984), "Insitu/non-destructive testing of concrete: a global review". American Concrete Institute (ACI), SP-82, 1-16.

Proceedings of the ACI-KC First International Conference & Fourth Exhibition. September 29-October 1, 2003, Kuwait — ***Concreting and High Performance Concrete in Hot Weather.***

PERFORMANCE EVALUATION OF AN EIGHT-STORY RC OFFICE BUILDING LOCATED IN HOT, AGGRESSIVE AND SEISMIC ENVIRONMENT OF BANDAR-ABBAS

Dr. Ali R. Khaloo, Civil Engineering Department,
Sharif Univ. of Technology, Tehran
Email: khaloo@sharif.edu
N. Asadpoor, Yadman Sazeh Consulting Eng., Tehran

ABSTRACT

The objective of this paper is to present the steps taken by the authors to evaluate the vulnerability of an eight-story RC office building located in hot, aggressive and seismic environment of Bandar-Abbas. The steps considered were: (1) Evaluation of materials and general condition, (2) seismic analysis of the building, (3) performance evaluation, (4) proposing strengthening method, and (5) decision making. Based on the field observations and NDT, and also results of the analysis, considerable deficiencies in structural components were present. A reasonable method was proposed to strengthen the building; however the general critical condition of the structure provided the basis for proposing the destruction of the building.

GENERAL INFORMATION (FIELD OBSERVATIONS AND NDT)

Bandar-Abbas is located in Northern region of the Persian Gulf. This region is humid, contains chloride ion in the air and is in high-risk seismic zone. The performance of structures in areas with both hot-aggressive climate and seismic activities, especially due to loss of bond characteristics of reinforcing steel in concrete caused by corrosion should be given considerable attention. The objective of this paper is to present the performance of an eight story RC structure, built in 1974, considering gravity and seismic loads and also durability condition. The structure is an office building of electrical company of Hormozgan province located in Bandar-Abbas city. The building is composed of RC frames and shear walls in N-S direction, and in E-W direction composed of only one wall which may be considered as flexural frame. The floor slabs are designed using a local joist and block system spanning 5.5 m and 8 m. During the last six years, at different times, some noticeable signs of degradation and distress of the structure have been observed, such as extensive cracking and separation of slabs concrete cover, and corrosion of steel reinforcement. Heavy partition walls were constructed in almost all the floors. This has imposed considerable gravity load on the building. The four shear walls in N-S direction were used to control displacements of the building.

The field observations indicated that the strength of concrete in beams and columns with porous state was less than that specified in design. Some of the steel reinforcements were corroded by the presence of chloride ion and humidity in the air. Also, some of the steel bars in the RC ceiling were corroded and the original diameter was reduced by over 50%.

In order to analyze the building, it was required to know the concrete strength in the structure. The strength was determined using Schmidt hammer, ultrasonic and core test methods. The hammer test was conducted on over 25% of columns and beams of all stories. Also, hammer strength of walls and a few single footings were measured. The compressive strength varied considerably according to hammer test, and ranged between as low as 8.8 MPa to a maximum strength of 20 MPa.

Core was taken from numerous points in the columns and beams, and then the cores were used for strength determination using ultrasonic test. The strength ranged between 9.5 Mpa and 19.8 MPa according to ultrasonic test, and varied between 10.5 MPa and 18.6 Mpa according to core test. Even the maximum available strength based on the three test methods was lower than the design strength of 25 MPa. In recently taken cores specimens, the strength of concrete was not higher than 22 MPa. The compressive strength was assumed 15 MPa for analysis of the structure.

There was no data regarding the properties of reinforcing steel. Reinforcing steel was assumed to have yield strength of 300 MPa. The area reduction due to corrosion of some of steel reinforcements was not included in the analysis.

SEISMIC ANALYSIS AND DESIGN

Codes

The codes consisted of loading and design codes. The gravity loading of the structure followed the 519 Loading Code (1), and earthquake loading followed the 2800 Seismic Code (2). For design and performance evaluation of structural components and the structure, ACI-318-99 Code was utilized (3).

Loading and analysis

Dead load of roof and floors was 7.7 KN/m2 and 6.0 KN/m2, respectively. The interior and exterior walls weighed 1.6 KN/m2 and 2.1 KN/m2, respectively. For the office building, floor live load was 2.5 KN/m2, roof live load 1.5 KN/m2 and corridor was 3.5 KN/m2.

Different methods may be used to apply equivalent earthquake load on structures, among them are equivalent static method which is used for low-rise and regular in plan and in height structures, and spectrum analysis method which is used for irregularity in plan and/or height.

Total dead load, including floor, interior and exterior walls, beams and columns, and 20% of live load were considered for lateral distribution of earthquake load. Bandar-Abbas is located in high-risk seismic zone (region coefficient = 0.3) according to 2800 Seismic Code. Behavior coefficient for ductility was Rx = 5 for bending frame system, and for frame and shear wall in N-S direction Ry = 7. The periods in X and Y directions were 0.69 sec and 0.62 sec, respectively. Based on the 2800 Code, the structure is not regular in height, due to over 50% difference in mass in the highest story as compared to the one below. Moreover, presence of half story in the first two stories, made the structure irregular in both plan and height. This made the dynamic analysis of the structure necessary; however, spectral time-history was used for analysis. At first modal analysis was performed and the first 20 modes were determined. First period of the building in E-W direction was 1.01 sec, and period of second mode was 0.81 sec in the N-S direction. Accidental torsion was also included in the analysis. The difference between dynamic and static lateral load distribution is shown in **Figure 1**.

Structural modeling was carried out using SAP90 software (4). For accurate modeling, shear walls were modeled by SHELL elements (**Figure 2**). The first, second and third modes of the structure are shown in **Figures 3a**, **3b** and **3c**. Maximum displacement in X direction (E-W) was 6.4 cm with a drift of 0.0022, and in Y direction (N-S) was 3.6 cm with a drift of 0.0012. Based on the 2800 Code, the allowable values are 0.006 and 0.004, respectively, which indicates the structure does not have any problem with lateral displacement.

PERFORMANCE EVALUATION

Design evaluation of the structure was performed by the results obtained from SAPCON software. ACI-318-99 was used for loading combinations and to control the design of the structure. Concrete strength and yield strength of steel were assumed 15 MPa and 300 MPa, respectively, however, due to low structural strength most of members were unable to resist the loads and consequently, the software could not execute the analysis. Based on the available safety margin, concrete strength and yield strength were changed to 20 MPa and 400 MPa, respectively, in order to perform the analysis.

Columns

Reinforcement of some columns was lower than minimum required (i.e., 1%). The cross sectional area and steel reinforcement were inputted in SAPCON file. The columns strength were divided into three categories; (1) those that with available section area and steel resisted the loads, (2) those that the available section area was not sufficient, and (3) those that demand/capacity ratio was less than one.

Most of columns in all stories were weak, especially in the first story; all the columns are weak (**Figure 4**). In numerous cases the column section is not adequate for gravity loads. It is concluded that, presence of relatively thick partition walls has prevented failure of columns.

Beams

Only cross-sectional area was inputted in SAPCON file. The beams strength was divided into three categories; (1) those that the available section area and steel were able resist loads, (2) those that with available section area, even with maximum allowable steel were not adequate in strength, and (3) those that available steel in the sections was not adequate. The major beams in all stories were also weak (**Figure 5**). Also, arrangement of steel reinforcements in beams did not comply with that for seismic design. These structural weaknesses in addition to materials deficiencies such as corrosion of some steel reinforcement, and general durability related problems, provided the bases for proposing strengthening of the structure at this stage.

STRENGTHENING FEASIBILITY STUDY

Existing condition

floor slabs

The joist and block floor slabs contained reinforcements with corrosion in such a way that concrete cover has spalled in most cases and swelled in other locations. The corrosion is caused by excessive deflection of approximately simply supported beams spanning 8 m and consequence cracking and later by being exposed to the air containing chloride ions. Some parts of concrete floors were totally failed.

beams

It was assumed in the analysis that reinforcements in beams were not corroded, however, this was not the case, and moreover, most of them were incapable of carrying the load (**Table 1**).

Table 1- Condition of beams in different stories

Story No.	Weak beams	No. of beams with inadequate cross sectional area
1	Almost all the beams	9
2	Almost all the beams	16
3	Almost all the girders	31
4	Almost all the girders	26
5	Almost all the girders	17
6	Almost all the girders	8
7	Almost 50% of the girders	5
8	Almost 20% of the beams	-

It should be noted that in some beams, even with maximum steel reinforcement, the cross-sectional area is not adequate to carry the loads (**Table 1**). Moreover, the beams reinforcements in negative moment region were not designed to carry cyclic earthquake loads.

columns

A summary of strength of columns is given in **Table 2**. It should be noted that in some cases, the present cross-sectional area is not adequate for carrying the loads. Also, most of the weak columns are boundary columns of shear-walls.

Table 2- Condition of columns in different stories

Story No.	Weak columns	No. of columns with inadequate cross sectional area
1	All the columns	30
2	21 out of 48	11
3	16 out of 43	9
4	Almost all the columns	5
5	Almost all the columns	2
6	29 out of 43	4
7	Almost all the columns	7
8	Almost all the columns	3

Feasibility study

floor slabs

Based on the available data, it is required to remove almost all the floor slabs. This makes the strengthening procedure very expensive.

beams

Most of the beams required strengthening. Also, for strengthening, the RC repair system should be connected to the present beams. As mentioned earlier, the concrete strength in the present beams is low, and can not act as composite with the repairing system. Moreover, the repair should economically match the remaining useful life of the structure.

If shear-walls are added in the X and Y directions, based on the analysis, they will compensate for the weak performance of most of the beams. However, still some of the beams will be weak. Moreover, the construction of additional shear-walls required; (1) removal of several facing walls, (2) compatibility with architecture of the building, (3) proper connection with beams, columns and foundations for monolithic response, while it is known that the present concrete is not sound enough.

columns

Addition of new shear-walls improves the gravity and lateral resistance of the structure, however; still some of the columns (specially in the first 3 stories) need upgrading, based on the analysis. Although there are some methods for strengthening the RC columns, due to weak material strength and steel bond, these methods were not found appropriate.

DECISION MAKING

This structure is over 28 years old, and a good portion of its useful life time in very aggressive and humid environment of the region has elapsed. Additional resisting and upgrading systems can not be properly connected to the existing structural elements (with average concrete strength of 15 MPa), with confidence.

Economic consideration included:

1) Foundation: Based on the overall condition of the structure, it is strongly expected to have weaknesses; such as concrete strength, steel corrosion and inadequate bond.
2) Beams: As mentioned earlier, even with addition of four shear-walls, there are still many weak beams, which require expensive strengthening.

3) Columns: As mentioned earlier, even with addition of four shear-walls, the columns in the first three stories are still weak, which is not possible to strengthen them due to inadequate strength in existing columns.
4) Floor slabs: Almost all the concrete floors should be removed and replaced with new flooring system.
5) Removal of floor slabs, and some of the beams and girders, will damage or requires replacing architectural ceiling, walls and floors. Moreover, electrical, piping, heating and cooling systems of the structure will be also heavily damaged.

Based on the overall technical and economical analysis of the structure, including NDT tests, field observations, gravity and earthquake analysis, and considerable strengthening requirements in the building, it is concluded to destroy the structure. In other words, the construction cost of upgrading can be equivalent to a new similar building. It should be noted that the client is also convinced, and has planned to destroy the structure.

CONCLUSIONS

An eight-story RC building located in hot, aggressive and seismic environment has been studied for materials and general strength condition. Based on the study the following conclusions are reached:

1) Concrete strength in beams and columns are considerably lower than required. Most of the steel bars in floor slabs were corroded. Corrosion in beams and columns could have been also possible.
2) Seismic analysis indicated that most of the beams and columns are incapable to carry the gravity and seismic loads. Full bond between concrete and steel was assumed in the analysis.
3) A realistic strengthening method was proposed, which included addition of shear walls in the X and Y directions. However, still some of the beams and most of the columns in the first 3 stories need upgrading.
4) Due to the inadequacy in present concrete strength, any additional resisting and upgrading systems can not be properly connected to the existing structural elements.
5) Economical analysis indicated that any strengthening method will be too expensive, and may equal construction of a new similar building, in the long term.
6) The final decision was to destroy the building, which is also accepted by the client.

ACKNOWLEDGEMENT

The authors greatly appreciate the supports provided by Sharif University of Technology and Electrical Company of Hormozgan.

REFERENCES

1) Minimum Design Loads in Buildings and Other Structures, Standard 519, 2000.
2) Iranian Code of Practice for Seismic Resistant Design of Buildings, Standard No. 2800, 1999.
3) ACI Committee 318, Building Code Requirements for Structural Concrete (ACI 318-99) and Commentary, American Concrete Institute, Farmington Hills, MI, 1999.
4) Habibullah, A., and Wilson, E. L., SAP90-Structural Analysis Program, Berkeley, CA.

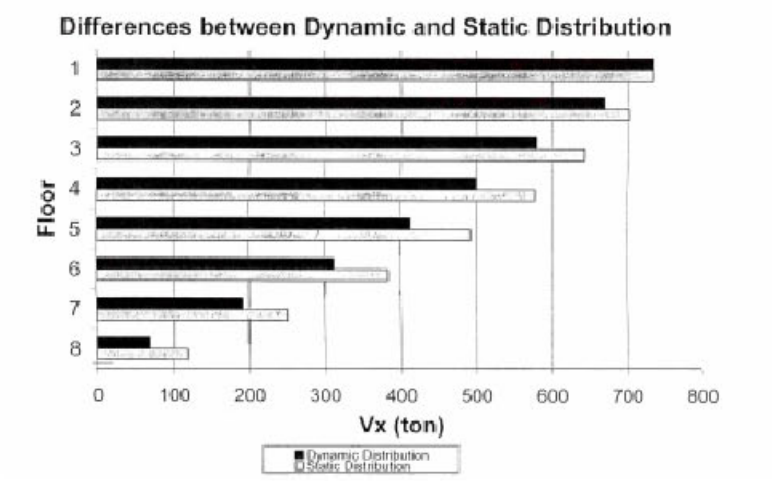

Figure 1. Comparison between lateral load distribution over height based on equivalent static and dynamic methods.

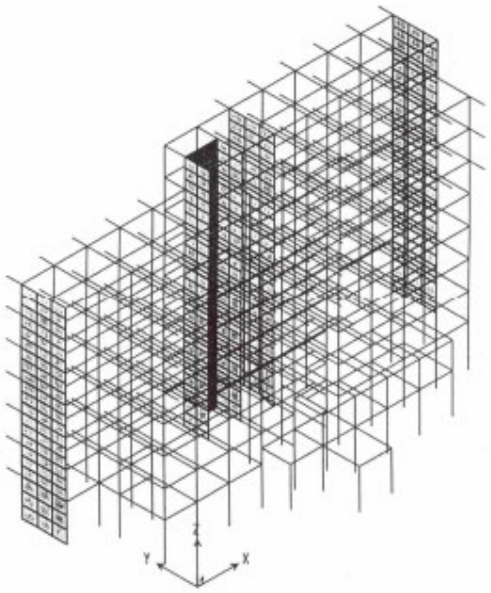

Figure 2. A view of the modeled structure.

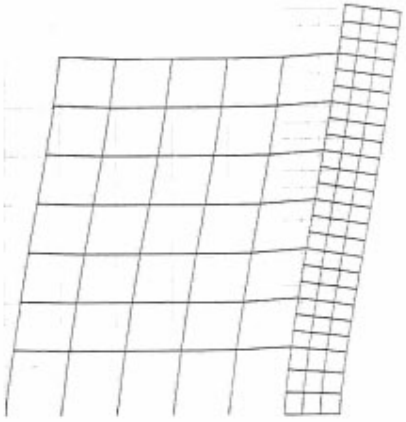

Figure 3a. First mode of a typical frame.

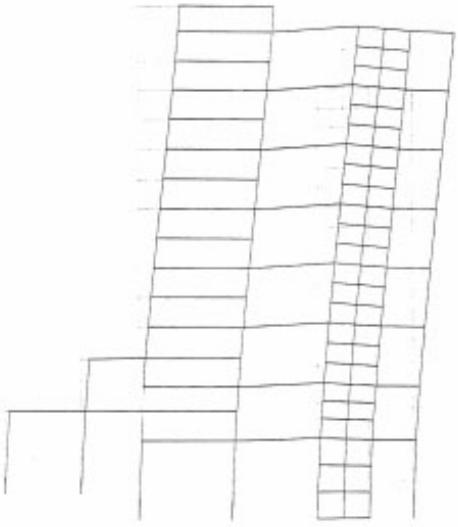

Figure 3b. Second mode of a typical frame.

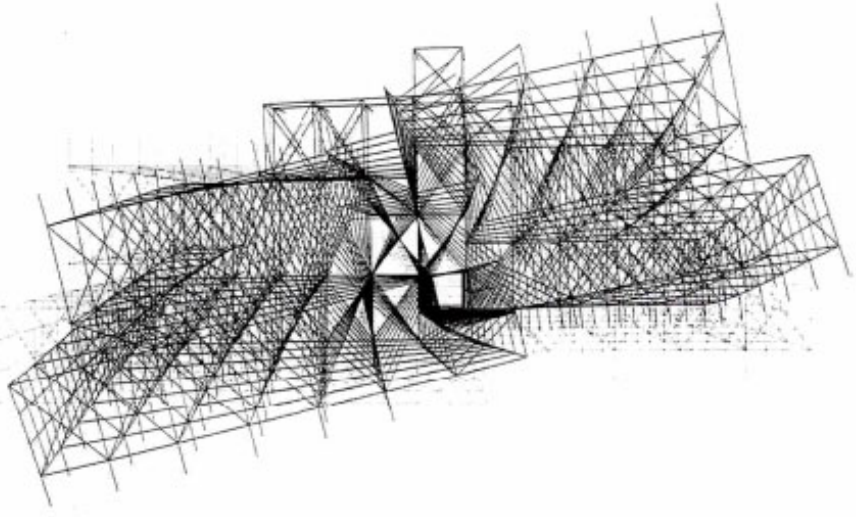

Figure 3c. Thirl mode (torsional) of the structure.

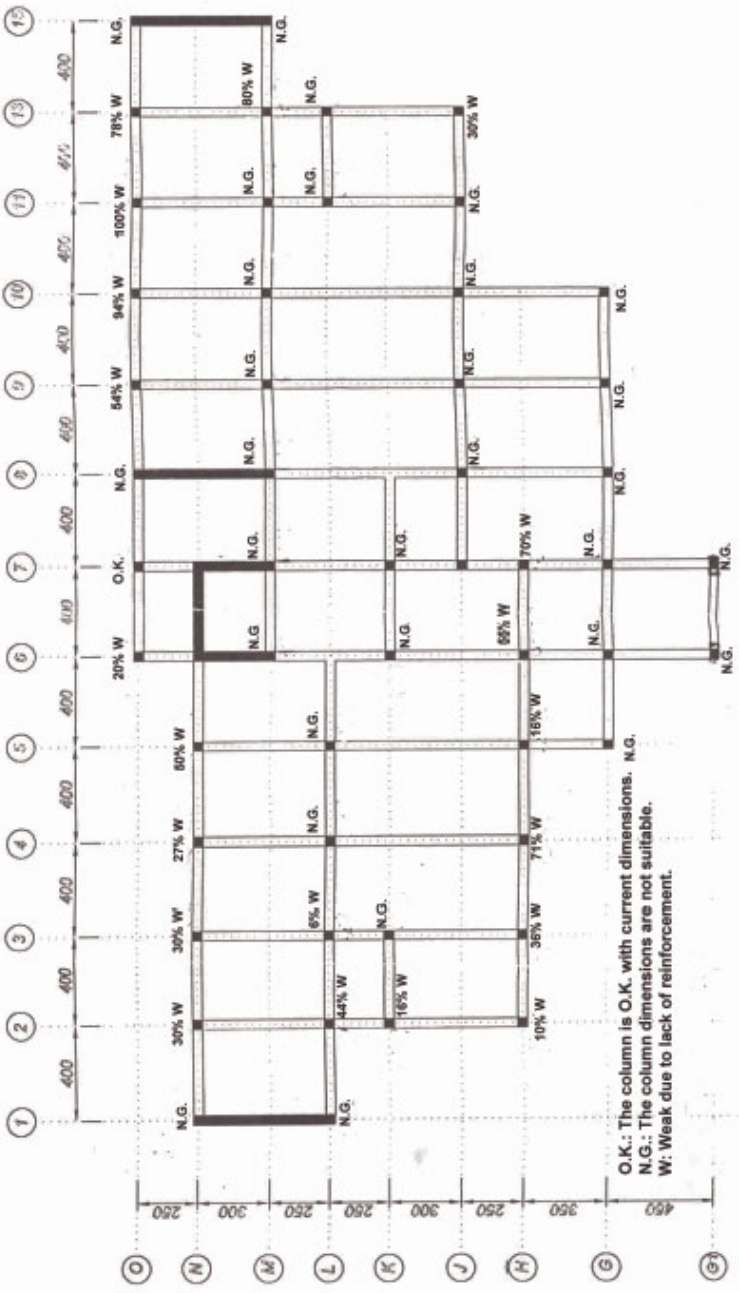

Figure 4. Present condition of 1st floor columns.

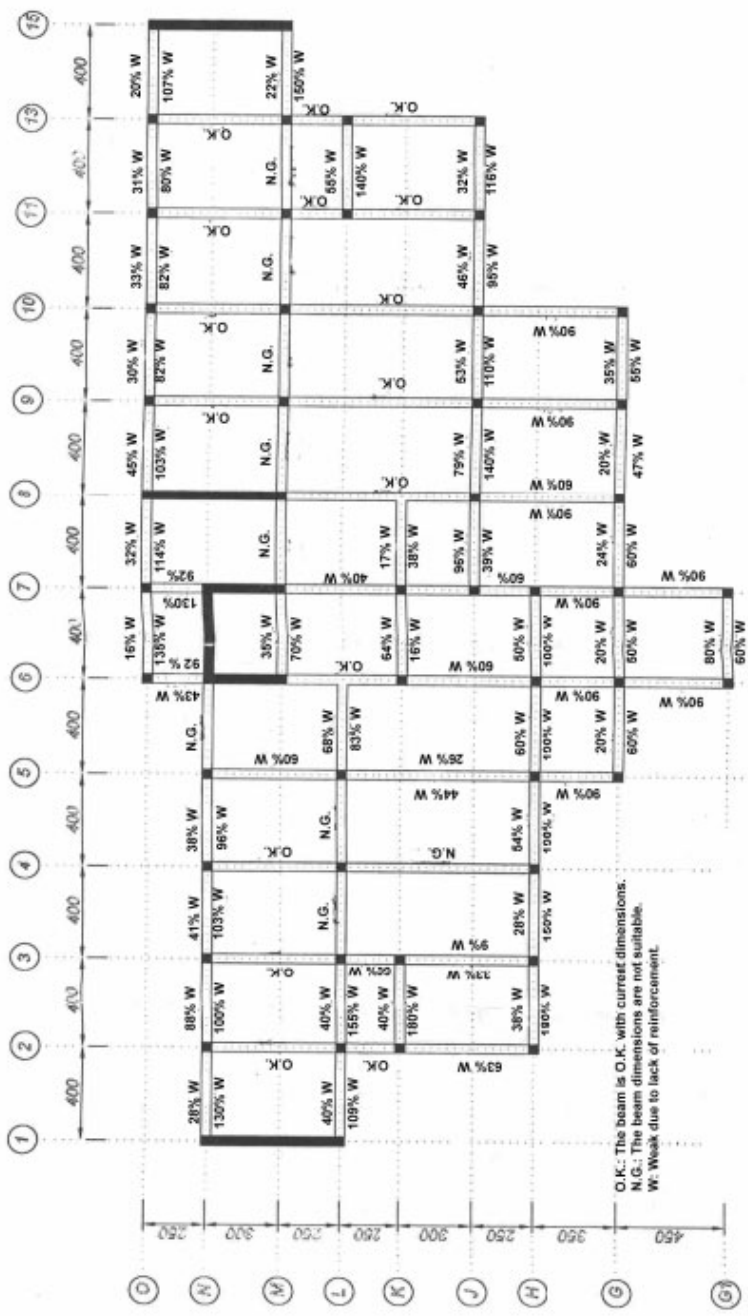

Figure 5. Present condition of 1st floor beams.

Proceedings of the ACI-KC First International Conference & Fourth Exhibition. September 29-October 1, 2003, Kuwait — ***Concreting and High Performance Concrete in Hot Weather.***

ROLLER-COMPACTED CONCRETE: A NEW TECHNIQUE IN ALGERIAN DAM CONSTRUCTION

Dr. Toumi Belkacem, University Farhat Abbas Setif, Algeria
Dr. Guemmadi Z'hor, University Mentouri Constantine, Algeria
Dr. Houari Hacene, University Mentouri Constantine, Algeria

ABSTRACT

Roller-compacted concrete is a new developing technique in Algeria applied to dam construction. The Beni Haroun dam constructed in Wilaya, Mila is one of the biggest dams in Africa and one of the first dam construction projects to use roller compacted concrete (RCC).

This present paper describes the different steps of the concrete formulation, from fabrication and control to the completion of the product.

This new technique is expected to reduce the time and cost of dam construction, while also ensuring safety of structures. Further, it will be of great benefit to Algeria, taking into account water problems and its limited availability in the region.

Keywords:

RCC, Dam, Cost, Formulation, Control, security

1. INTRODUCTION

Advancements in agriculture, industry, tourism and economy have necessitated the development of a system to conserve and supply water for the purpose of irrigation, drinking and industries.

It is within this framework that the Algerian state decided to erect the Beni Haroune dam located in North East of Algeria, forty kilometers off the entrance of the Mediterranean and 350 kilometers east of Algiers.

This dam, completed in 2001, allows water conservation for the meadows extending to one billion m^3 and constitutes an important project for the irrigation of the high plateaus which extend from Telegma, Chamoura, Tafouna and Batna. An area which is spread out more than 200 kilometres South of the dam is approximately 33600 ha extending to Wilaya in Milla, Constantine, Batna, Khanchela and Oum El Bouaghi.

The cost of this important project was about one billion US$ and has been an object of several studies by researchers.

The decision to build the dam using the technique of the roller compacted concrete (RCC) results first from the large quantities of explosives disposed in several sites during the troubled period which prevailed in Algeria and one needed meadows for 3000 tons of ripraps generated and 10 million m^3 for the embankments of the dam (solution retained in 1985). Secondly, the technique stemmed from the technical and economic interests and benefits this method would create.

The advantages of the roller-compacted concrete (RCC) are many and may be summarized as follows:

- reduced cost of materials
- shorter duration in construction
- possibility of substituting a rock-fill dam by a dam in RCC (like the case of the Beni Haroun dam).

2. CONSIDERATIONS OF BENI HAROUNE DAM

The Beni Haroune dam is weight rectilinear type, constructed using roller compacted concrete - the rollers are pressed on a calcareous rock foundation (figure 1).

The crest gate surface is of the type called 'free threshold' and is integrated into the body of the dam in the central part. Its length of 124 meters is divided into six ways and

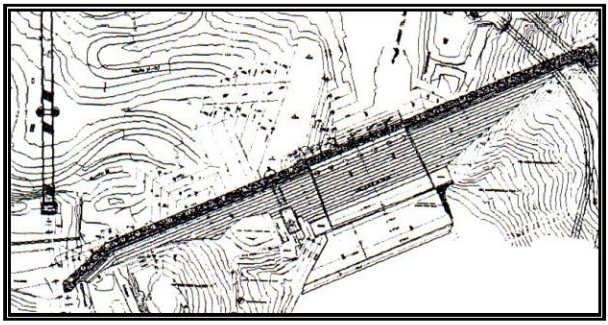

Fig.1: The Beni Haroun Dam

assembled by a bridge road. At the threshold of the exit, a dispatch rider connects to a ski-jump fixed at the top of high waters (figure 2). The capacity of the crest gate is of 137 m^3/S. The draining is at the bottom of the crest gate, out of right bank. It makes it possible to drain out a flow of 700 m^3/s under normal selected level.

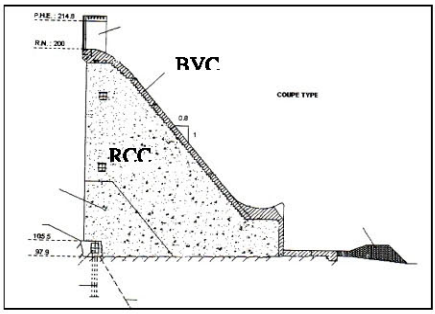

Fig. 2: Right section of the dam

The dam has a maximum height of 120m from foundation and 710 m length in peak. At the peak of the dam a length of 8 m is levelled at the coast 216.30 m, 1.5 m above high waters.

The upstream face of the dam is vertical, whereas the downstream face presents a constant slope of 0.8H for 1V. This slope makes it possible to eliminate the stress concentrations (seismic zone) and simplify the building work. Above the coast 196 m the face downstream changes slope, which facilitates the execution of the peak and allows the installation of a lane.

Three galleries are fixed respectively at the coasts of 100, 140 and 175 m (figure 3) and located near the upstream face of the dam. They will allow the control of flow operations. These galleries are placed at a distance varying from 70 to 150 m.

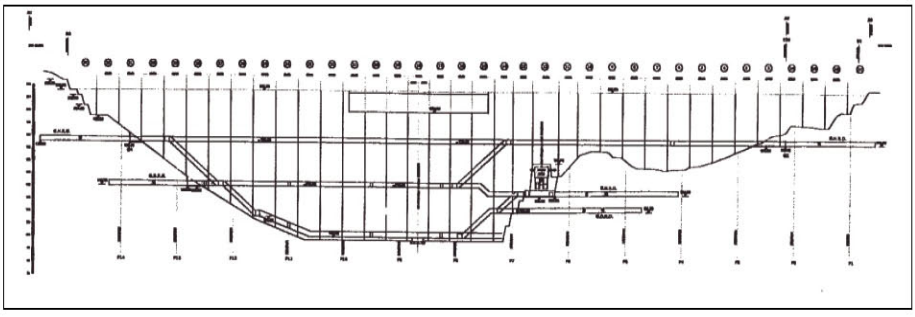

Fig. 3: Disposition of the galleries in the body of the dam

The system of galleries described above will enhance the water flow from the body of the dam, right from the foundations and the supports and it will also allow necessary repair and maintenance work to be carried out under the dam, the impervious diaphragm consists of a grout curtain multifilaire (3 files a depth of 60 with 100 m).

Injections of consolidations of the rock of foundations are carried out on the entire dam at a depth of 8 m and with a square mesh of 4 m on the coast.

During work, the derivation of the river supported by derivations of two galleries visualizes the basic riprap solution.

The design of the dam focused on the following:

- To minimize the quantities of conventional concrete.
- To guarantee a good continuity of RCC building site.
- To concentrate, as much as possible, the work requiring the use of a conventional concrete.

The total volume of the concrete of the work was close to 1700 000 m^3:

- 1400 000 m^3 of roller concrete was compacted.
- 300 000 m^3 of conventional concrete was used.

3. MATERIALS AND DOSAGE

Taking into account the characteristics of the dams (H=120m) and construction in seismic zone (earthquake of 0.17g and exceptional earthquake 0.3g), the RCC solution was considered. The roller compacted concrete (RCC) requires a mixture which will not pack in an excessive way without the effect of a vibrating roller or others but which will have a granulometry and a volume of paste so that a satisfactory consolidation is done without related problems.

The basic criteria which guides the definition of the compositions of a concrete compacted with roller (RCC) are as follows:

- Choices of a granulometry suitable to minimize the segregation.
- Dosage of water supporting the compaction.
- Minimal dosages of bind guaranteeing the necessary mechanical characteristics.

3.1 Aggregates: The choice of the aggregates and the control of granulometry are significant to maintain the quality and regular properties of RCC. The variation of the aggregates during work affects to a significant degree the requirements of cement and water, on which depend the resistance. The compressive strength and the connection between layers with the construction joints must thus be taken into account when it is a question of defining the specifications of the aggregates to be used.

The zones of loans are located at the junction of Oued Rhumel and Oued Endja, approximately 4 km with the upstream of the dam. The aggregates are produced near the upstream of the dam with a capacity of 500 T/h. The materials produced are washed and ready to use. The size ranges produced by the station are: 0/5, 5/15, 15/25 and 25/63.

The granulometric analyses of the various classes are present in Table 1 and figure 3. The results of the analyses of sand are presented in Tables 2 and 3 respectively.

Table 1. Granulometric analysis of the aggregates

Sieve	0,08	0,145	0,297	0,59	1,19	2,38	4,76	8	9,5	12,5	16	19	25	32	38	50	63
0/5	5	14	27	47	63	79	96	100									
5/15						0,6	1,7	27,2	45,5	85,9	96,8	100					
15/25								0,5	0,9	2,4	16,8	27,2	73,3	99,5	100		
25/63										1	1,1	1,7	2,5	11,8	30,8	82,7	100

Table. 2 Sand equivalent (%)

Fraction	Visuel ES	Piston ES
0/5	86	79

Table. 3 Cleanliness of the aggregates (%)

Fraction	Source	P '%)
5/15	Station of sifting	0.6
15/25	Station of sifting	0.8
25/63	Station of sifting	0.15

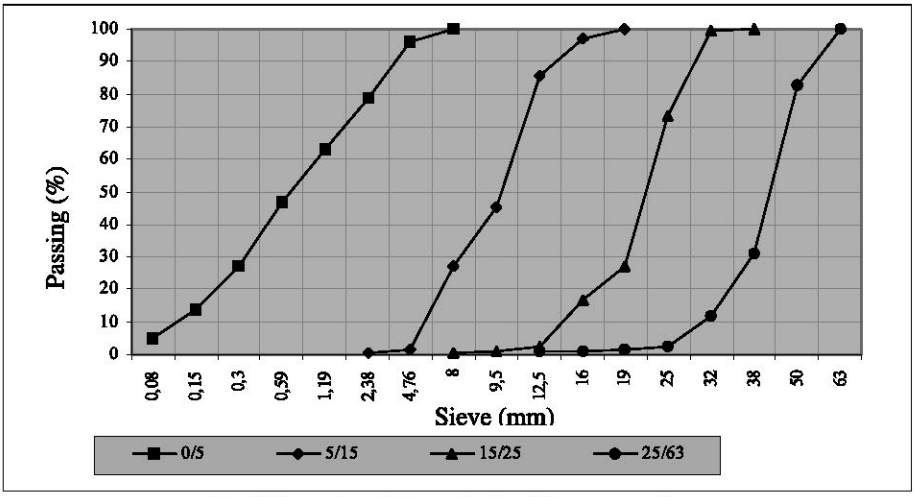

Fig. 3 Granulometric analysis of the aggregates

Before the starting of the RCC the station produced more than 1/3 of the consumption planned for the execution of the dam.

3.2. Cement: HRS cement that is used has low hydration heat. The chemical, physical and mechanical characteristics obtained according to the standard ONE 80 303/96, are presented in Tables 4, 5 and 6.

Table. 4 Chemical composition of cement

Component	Value	Specification
Loss on the ignition	2.95	5% max
SO_3	2.72	4% max
Insolubles	0.99	5% max
CL^-	0.01	0.1% max
C_3A	0.44	<55%
C_3A+C_4AF	15.46	<22%

Table. 5 Physical characteristic of cement

	Value	Specification
Beginning of seting time	146	> 60 minutes
End of seting time	216	<840 minutes

Table. 6 Mechanical characteristic of cement

Compressive strength	Value	Specification
2 days	28	> 20 N/mm^2
28 days	51	> 42 N/mm^2 <62.5 N/mm^2

3.3. Fly-Ashes: The choice of an ash is guided by the standards or corresponding specifications, by its behavior in the concrete and its availability on the building site. The principal characteristics of the fly-ashes are given according to standards UNE 83 431, UNE 83 432, UNE 83 433. The results are in Table 7.

Table. 7 Characteristics of fly-ashes

	Value	Specification
Loss on the ignition	3.3	6% max
SO_3	0.52	4.5% max
Moisture	0.05	1.5% max

3.4 Water: The results of analyzed chemical of mixing water are in Table 8

Table. 8 Chemical composition of water

Echantillion	N°1	N°2	Aggressiveness
Matter in suspention	Traces	Traces	Null
SO_4^{--}	343.43	311.35	Weak
PH	8.9 at 12°C	8.9 at 12°C	Weak
Mg^{-}	72	81.6	Weak

3.5 Admixture: The advantages that we obtain by using admixture are increasing handiness and delaying the setting time of the concrete, in order to keep 'alive' the mass of concrete and to avoid the dry joints, especially in hot weather. The admixtures used for the RCC were: air entraining, water reducers and retarder.

4. FORMULATION OF RCC

On the whole, 31 different mixtures were prepared using the formula of HUSOY DUNSTAN and tested on an experimental solid mass. This solid mass has a total volume of 4000 m^3, which corresponds to 12 layers of RCC, the selected formula which reaches the most contractual characteristic resistance to 28 days (14 MPa), is presented in table 9.

Table. 9 Ponderal composition of the RCC

0/5	760 Kg/m^3
5/15	416 Kg/m^3
15/25	520 Kg/m^3
25/63	396 Kg/m^3
Cement	82 Kg/m^3
Fly-Ashes	147 Kg/m^3
Water	100 – 110 L/m^3
Density of the RCC	2.42 t/m^3

5. QUALITY CONTROL

A continuous assessment was carried out with each operation of concreting and on all the production line, up to the hardened concrete.

5.1. Binder Control: Each batch was submitted for various testing. A card of obligatory homologation accompanied the batch.

5.2. Aggregates Control: Tests of granulometry and cleanliness were done each day at the power station.

5.3. Freshly Mixed Concrete Control: Each week tests were carried out on freshly mixed concrete to check the mixture.

5.4. Density And Water Content Control: The densities were obtained directly by gamma densimeter; the density of reference was of: 2.40 T/m3. The average density obtained by densimeter was 99% of 2.40 T/m3. The water content varied from 5.5 to 8%.

5.5. Vébé Test Control: Every half-hour a vébé test was carried out, vébé used varied on average between 8 and 15 seconds. The influence of temperature and winds were checked when the RCC arrived at the implementation with 6 to 7 seconds and vébé was measured at the level of RCC power station.

5.6. Strength Check:

On Test-Tube: Each layer was prone to a taking away of 9 test tubes for the ages of 7, 28 and 90 days. Each week, 9 test tubes were taken for cylinder splitting tests (28 and 90 days) and tests of compression at 365 days.

The influence of the temperature was also noticed on the level of the compressive strengths obtained where the maximum were obtained during the hot seasons.

On Cores: Cores were taken for resistance tests, the compression of the cylinder splitting tests and direct tensile tests. The results obtained were lower by 15 to 20% per contribution with those of the test tubes.

6. CONCLUSION

The current technique, which prevails in dam constructions, is roller compacted concrete (RCC). This relatively new process of construction uses the combined techniques of traditional concrete and earthworks.

RCC is manufactured in a concrete batching and mixing plant then transported and spread in horizontal layers with null depression and compacted with vibrating rollers. The advantages of this technique are the speed of execution and the economy of the project

Experiments on this type of construction in Algeria are still not much. Tichi – Haf dam was one of the first building sites to use this technique before it was used for the Benni Haroun dam.

7. REFERENCES

1. Agence national des barrages (2000). « Les techniques du béton compacté au rouleau » journée technique du 7 juin 2000 barrage Benni Haroun.
2. Agence national des barrages (1999). « Projet barrage Benni Haroun » Rapport de synthèse mois de février et mars 1999.
3. Bourioune M. (2001). « Le béton compacté au rouleau, une voie nouvelle au services des barrages » LTPEst Constantine.

4. Commission internationale des grandes barrages « Béton compacté au rouleau pour barrages poids » Techique actuelle. 151 Boulevard Haussmann 75008 Paris-France.

5. Lajeat A. P. Orth J. (1961). « Le barrage de Roselend, Conduite et contrôle du bétonnage étanchéisation de la roche de fondation » Travaux mai 1961.

List of Authors

A. Al Khaleefi

Department of Civil Engineering, Kuwait University, Kuwait.

A.T.Atwa

Faculty of Engineering, Zagazig University, Zagazig, Egypt.

Abdel Khalek Taleb

Al Baath University, Syria.

Tel: 963 314 26707
Email: A-taleb@scs-net.org

Adel Husain

Building and Energy Technologies Department, Kuwait Institute for Scientific Research, Kuwait.

PO BOX 24885- Safat 13109, Kuwait
Email: xhusain@yahoo.com

Ali R. Khaloo

Sharif Univ. of Technology, Tehran, Iran.

Email: khaloo@sharif.edu

A.W. Sadek

Building and Energy Technologies Department, Kuwait Institute for Scientific Research, Kuwait.

Email: asadeq@safat.kisr.edu.kw

Bassam M. Hanna

Al Baath University, Syria.

Tel: +963 314 88982

David Wilson

Max Frank GmbH, Germany.

Tel: 0044 796 8298439,
Email: djwilson@orange.net

Davison, N.

Fosroc GroupDevelopment, Tamwork, UK

E.M.Y. Abdin

Faculty of Engineering, Zagazig University, Zagazig, Egypt.

Guemmadi Z'hor

University Mentouri Constantine, Algeria.

Tel: 00213 319 66392,
Email: zguemmadi@yahoo.fr

H. Al-Khaiat

Department of Civil Engineering, Kuwait University, Kuwait.

H. Kabir,

Department of Civil Engineering, Kuwait University, Kuwait.

H.Abdel-Raouf

Faculty of Engineering, Zagazig University, Zagazig, Egypt.

Haboubi, L

Fosroc International Ltd, Dubai, UAE

Hamdy El. Didamony

Faculty of Science Zagazig University, Zagazig, Egypt.

Hasan J. Karam

Building and Energy Technologies Department, Kuwait Institute for Scientific Research, Kuwait.

Hasan Kamal

Building and Energy Technologies Department, Kuwait Institute for Scientific Research, Kuwait.

Tel: +965 483 6100 ext: 4561,
Email: hkamal@kisr.edu.kw

Hisham Abdel-Fattah

Department of Civil Engineering, College of Engineering, University of Sharjah, UAE.

P.O. Box 27272, Sharjah, United Arab Emirates.
Email: hibrahim@sharjah.ac.ae

Houari Hacene

University Mentouri Constantine, Algeria

J. Al-Duaij

Department of Civil Engineering, Kuwait University, Kuwait.

Khaldoun N. Rahal

Department of Civil Engineering, Kuwait University, Kuwait.

Tel: +965 481 1188 ext: 5734, P.O. Box 5969, Safat 13060, Kuwait.
Email: rahal@kuc01.kuniv.edu.kw

Khaled Al-Rasheed

Civil Engineering Department, Kuwait University. Kuwait.

PO Box 5969 Safat,
13060 Kuwait, Tel: (965) 4811188 Ex. 5742,
Fax: (965) 4817524,
khaled@civil.kuniv.edu.kw

M. El Hawary

Building and Energy Technologies Department, Kuwait Institute for Scientific Research, Kuwait.

Tel: +965 483 6100 ext: 4558,
Email: mhawary@safat.kisr.edu.kw

M. N. Haque

Department of Civil Engineering, Kuwait University, Kuwait.

Tel: +965 481 1188 ext: 5762, P.O. Box 5969, Safat 13060, Kuwait.

Magdy A. Abd El Aziz

Faculty of Engineering Cairo University Fayoum Branch, Egypt.

Michael Nemeth

Al Gurg Fosroc LLC, Dubai, UAE.

Tel: +9714 2858606,
Email: MichaelNemeth@JMHFZCO.com

Muktar M. AbuRawi

Al Marqab University, Libya

Tel: 0021 831 621585

Mustafa K. Badrah

Department of Civil Engineering & Member at the Unit of Construction and Technology for Engineering & Consultancy University of Aleppo, Aleppo, Syria.

Email: mkbadrah@popmail.com

N. Al-Mutairi

Kuwait Institute for Scientific Research, Kuwait.
Kuwait Foundation for the Advancement of Sciences (KFAS), Kuwait.

N. Asadpoor

Yadman Sazeh Consulting Eng., Tehran

Omar S.B. Al-Amoudi

Department of Civil Engineering, King Fahd University of Petroleum And Minerals Dhahran, Saudi Arabia.

Tel: +966 557 58489,
Email amoudi@kfupm.edu.sa

P.A. Koushki

Department of Civil Engineering, Kuwait University, Kuwait.

Tel: +965 481 1188 ext: 5738,
Email: parviz@civil.kuniv.edu.kw

S. Al-Fadala

Building and Energy Technologies Department, Kuwait Institute for Scientific Research, Kuwait.

S. Fereig

Kuwait University, Kuwait

S. Phillipose

Department Of Civil Engineering, Kuwait University, Kuwait.

Safa Abdul-Salam

Building and Energy Technologies Department, Kuwait Institute for Scientific Research, Kuwait.

Saleh M. Abd El.Aleem

Faculty of Science Cairo University Fayoum Branch, Egypt.

Seleem.S.E. Ahmad

Faculty of Engineering, Zagazig University, Zagazig, Egypt.

Tel: +20 105 153282,
Email: sse_ahmadh@hotmail.com\

Shakeel Ahmad

Rezayat Trading Company Ltd., Kuwait

Suad Al-Bahar

Building and Energy Technologies Department, Kuwait Institute for Scientific Research, Kuwait.

Tel: +965 483 6100 ext: 4520
Email: sbahar@safat.kisr.edu.kw

Toumi Belkacem

University Farhat Abbas Setif, Algeria.

Tel: +213 319 66392 Email:
Toumi@imel.org